UNIVERSITY OF SOUTHAMPTON

Faculty of Engineering and Physical Sciences
School of Engineering

Assessment of Offshore Wind Energy Potential in the Middle East: Case Studies Egypt, Arabian Peninsula

Mostafa Mahdy

A thesis submitted for the degree of
Doctor of Philosophy

June 2020

UNIVERSITY OF SOUTHAMPTON

Abstract

Faculty of Engineering and Physical Sciences
School of Engineering

Thesis for the degree of Doctor of Philosophy

Assessment of Offshore Wind Energy Potential in the Middle East: Case Studies Egypt, Arabian Peninsula

Mostafa Youness Mosad Mahdy

Offshore wind energy is highlighted as one of the most important resources to be exploited for electrical power production. This is due to the higher wind speed availability and minimal visual impacts compared with onshore wind energy sites. Currently, there is a lack of clear systematic assessment methodology for offshore wind energy potential. A methodology is proposed here addressing this gap and providing global applicability for offshore wind energy exploitation. It is based on the Analytical Hierarchy Process (AHP) and pairwise comparison methods linked to site spatial assessment in a Geographical Information System (GIS). The method is applied to Egypt and then extended to the Arabian Peninsula countries. In 2014, Egypt had plans to scale renewable energy capacity from 1 GW to 7.5 GW by 2020, which was likely to be through solar, onshore wind, and offshore wind energies. Hence, this work will contribute to the proposed Egyptian target and provide seminal outcomes to quantify the offshore wind energy potential and its contribution to the Arabian Peninsula's countries renewable energy ambitions.

The applicability of spatial analysis based on multi-criteria decision analysis was introduced to provide accurate estimates of the offshore wind energy from suitable locations in Egypt where in-depth further analysis of these sites where also carried out. Three suitable high wind areas around the Red Sea in Egypt were identified with minimum restrictions that can provide around 33 GW of installed wind power capacity. The results for Arabian Peninsula countries indicate that by installing 35GW of offshore wind capacity, 25.7 of their electrical demands can be met. Suitability maps are also included providing a blueprint for the development of wind farms at these sites. Sensitivity analyses was undertaken for the Egypt case study to support the robustness of the proposed methodology assumptions and data quality. An economic analysis of sites, defined as the Representative Cost Ratio RCR approach was undertaken was validated using UK site data. The overall results presented for both case studies indicate that the proposed methodology is applicable for local and regional scales. The developed methodology is generalised and is applicable globally to produce offshore wind energy suitability maps for appropriate offshore wind farm locations.

The second phase of this research is to provide full wind farm turbine layout and piling design of the sites in Egypt. This included the choice of the appropriate foundations and farm (array) planning for the chosen sites. From a review and analysis of the different available foundation technologies and their suitability in terms soil conditions and of available infrastructure needed for deployment, it was found that a monopile foundation system is most appropriate for the sites. The final monopile dimensions are with 8 cm wall thickness, 6 m diameter, and insertion depth of either 20 m or 24 m. This size will support a 5 MW offshore wind turbine for the identified soil types of the three different proposed locations in Egypt.

The final analysis undertaken covers overall cost reductions for the Egyptian sites through optimising the farm layout. This included a study of the port feasibility and environmental impacts of deploying offshore wind turbines in these locations. The layout optimisation designs showed that the optimum layout has a spacing of five times the turbine rotor diameter in both directions. The port feasibility analysis showed that "Distance between port and wind farm location" was the highest weighting factor. In addition, (East Port Said port) is highly recommended to install the first 500MW offshore farm in Egypt for three different locations, predominantly due to proximity to farm site. Finally, the environmental investigation confirmed that deploying offshore wind farms in Egypt is predicted to have minimum impacts on the surrounding ecosystems and other minor impacts are easily mitigated with proper measures.

Author Declaration

Print Name: Mostafa Mahdy

Title of thesis: Assessment of Offshore Wind Energy Potential in the Middle East: Case Studies Egypt, Arabian Peninsula

I declare that this thesis and the work presented in it are my own and has been generated by me as the result of my own original research.

I confirm that:

1. This work was done wholly or mainly while in candidature for a research degree at this University;

2. Where any part of this thesis has previously been submitted for a degree or any other qualification at this University or any other institution, this has been clearly stated;

3. Where I have consulted the published work of others, this is always clearly attributed;

4. Where I have quoted from the work of others, the source is always given. With the exception of such quotations, this thesis is entirely my own work;

5. I have acknowledged all main sources of help;

6. Where the thesis is based on work done by myself jointly with others, I have made clear exactly what was done by others and what I have contributed myself;

7. Either none of this work has been published before submission, or parts of this work have been published as:

- Mahdy, M. and Bahaj, A.S., 2018. Multi criteria decision analysis for offshore wind energy potential in Egypt. Renewable energy, 118, pp.278-289.
- Mahdy, M., Bahaj, A.S. and Richards, D., 2017. Selection and Design of Offshore Wind Turbine Foundations for the Red Sea Area – Egypt. Proceedings of the 16th International Conference on Sustainable Energy Technologies.

- Mahdy, M., Bahaj, A.S. and Alghamdi, A.S., 2017. Offshore Wind Energy Potential around the East Coast of the Red Sea, KSA. Proceedings of the ISES Solar World Congress 2017.
- Mahdy, M., Bahaj, A.S. and Richards, D., 2018. Port Feasibility Study to Support Offshore Wind Farms around Egypt. Proceedings of the International Conference on Renewable Energy ICREN.
- Mahdy, M., Bahaj, A.S. and Richards, D., 2019. Offshore Wind Farm Layout Optimisation for High Resources Sites in Egypt Red Sea. Proceedings of the International Conference on Renewable Energy ICREN.
- Bahaj, A.S., Mahdy, M., Alghamdi, A.S. and Richards, D.J., 2020. New approach to determine the Importance Index for developing offshore wind energy potential sites: Supported by UK and Arabian Peninsula case studies. Renewable Energy, 152, pp.441-457.

Signature: Date:

Acknowledgment

Firstly, I would like to express my sincere gratitude to my advisor Professor AbuBakr Bahaj for his incessant support to finish my PhD study and related papers, for his tolerance, motivation, and immense knowledge. His guidance helped me in all the time of research and writing this thesis. I want also to thank him for the hard questions he asked, which drive me to widen my research from various perspectives. I could not have imagined having a better advisor and mentor for my PhD study. Besides my advisor, I would like to thank my second supervisor, Professor David Richards, for his insightful comments and encouragement.

My sincere thanks also go to Abdulsalam Alghamdi (Associate Professor at King Abdulaziz University), who helped me in the Arabian Peninsula, Ahmed Abd-el-Kader (Lecturer at Port aid University), who give some valuable recommendations for the foundation part, and my colleagues in Civil Engineering department of Port Said University for providing me with some of the data I needed for the Egypt case study part.

Last but not the least, I would like to thank my family: my three little daughters, my wife, my mother, and my brother for supporting me spiritually throughout this thesis and my life in general.

Table of Contents

List of Tables

List of Figures

Definitions and Abbreviations

A	Wind speed probability Weibull distribution factor
AHP	Analytical Hierarchy Process
BEIS	Department for Business, Energy and Industrial Strategy, UK
BODC	British Oceanographic Data Centre, UK
C.F	Capacity factor of an offshore wind farm
CFD	Contract for Difference
CI	Consistency index
C_j	Constraint j (Boolean Mask j)
CR	Consistency Ratio
C_t	Thrust coefficient (obtained from the wind turbine manufacturer)
d	Average water depth
D	Rotor diameter
D_{10}	Effective diameter
E_a	Actual energy yield for a turbine "t"
E_c	Calculated net energy yield for a turbine "t"
EEAA	Egyptian Environmental Affairs Agency
EGAS	Egyptian Natural Gas Holding Company
EIA	Environmental Impact Assessment ()
EMA	Egyptian Meteorological Authority
E_s	Young's modulus / modulus of elasticity
Es	Spring stiffness

ESIS	Egypt State Information Service
f_y	Yield stress
g	Gravitational acceleration
GAFRD	General Authority for Fish Resources Development, Egypt
GCC	Gulf Cooperation Council
GDP	Gross Domestic Product
GIS	Geographical information system
GIS-MCDA	Multi-criteria decision analysis GIS based
H_s	Max significate wave height
HSD	Hydro Sound Dampers
I	Intensity of Importance.
INDCs	Intended Nationally Determined Contributions.
k_v	Von Karman constant and equal to 0.4
k_w	Wake decay constant
K	Directional probability Weibull distribution factor
L	Wave length
ℓ	Number of constraints
L_c	Offshore wind array cross wind spacing.
LCOE	Levelised cost of electricity
L_d	Offshore wind array downwind spacing.
MaRS	The Marine Resource System, database programme developed by The Crown State, UK
MCDA	Multi-criteria decision analysis
MDMP	Ministry of Defence and Military Production, Egypt
MEEE	Ministry of Electricity and Energy of Egypt
MPMR	Ministry of Petroleum and Mineral Resources, Egypt
MSEA	Minister of State for Environmental Affairs, Egypt
MSL	Mean sea water level

n	Number of factors
NAT	National Authority for Tunnels, Egypt
NREA	New and Renewable Energy Authority, Egypt
OWF	Offshore wind farm
OWT	Offshore wind turbine
P	Pressure at any distance below the fluid surface
p	Pile lateral load
P.W.D	Prevailing wind direction
R	Representative Cost Ration
R_d	Rotor diameter.
RI	Random consistency index
S	Offshore wind turbine footprint area.
S_t	Wind speed sensitivity in the energy yield for a turbine "t"
$S_{terrain}$	Terrain wind speed-up factor and
T	Mean wave time period
U_f	Friction velocity
U_i	Wind speed just before pathing the rotor
U_z	Wind speed in a surface layer
w_i	Weight assigned to factor i
WLC	Weighted Linear Combination
W_t	Relative weighting factor for turbine "t"
X	Distance between the two turbines
X_i	Criterion score of factor i
y	Pile lateral displacement
YPL	Yearly Peak Load
z	Water depth below the MSL
Z_w	Wind speed height, where the wind speed (U_z) is calculated

Z_0	Aerodynamic roughness length
γ_{sub}	Submerged unit weight
Δz	Difference of altitude in meter for terrains with slip less than three degrees.
θ	Principal (central) direction for the spectrum measured counter clockwise from the principal wave direction
λ_{max}	Principal Eigen value
ν	Poisson's ratio
Π	Product of constraints
ρ	Mass density of salt water
φ	Friction angle
ψ	Dilation angle
ULS	The ultimate limit state loads
SLS	Serviceability Steady State Loads

Chapter 1: Introduction

Offshore wind energy is now considered a mature technology with over 12 GW capacity already installed globally (Council, 2016); hence it is highly applicable in the study areas. In addition, the UK's Department for Business, Energy and Industrial Strategy (BEIS) recently announced the new Contract for Difference (CfD) for the round two offshore wind energy projects in the UK, which showed halving the cost per MWh to from £114.39 (2015) to £57.5 (2017) (Simon Virley CB, 2017). Finally, the new CfD for 2019 even lower at £39.65/MWh (Woodman and Fitch-Roy, 2019), which reduced it by more than 30%.

Most of onshore wind farms are located in the best resource areas. The exploitation of further land-based onshore areas in many countries is currently impeded due to visual impacts, threats to birdlife, public acceptance, noise, land use conflicts, and local reluctance to generate electricity for use elsewhere (Green and Vasilakos, 2011, Kahlert et al., 2004, Harper et al., 2019). All these conflicts are likely to hinder future development of onshore wind farm deployment (Esteban et al., 2011b, Kaldellis and Kapsali, 2013, Kaldellis et al., 2012). Hence, most major developments worldwide are now shifted towards offshore wind energy where the resource is high, and development is less likely to be affected by the drawbacks of land-based wind farms mentioned earlier. Furthermore, scaling up is likely to result in cost reductions propelling offshore wind energy on a trajectory that will be on par with that of the onshore in the future (Bilgili et al., 2011).

To the author's knowledge, previous studies that evaluated the offshore wind energy potentials in certain areas tend to use one or two factors to identify the suitable areas, which is not accurate and need further investigations. In addition, other studies used only restrictions to identify candidate development areas, which is not enough to identify the most suitable locations. Restriction analysis is only suitable for small-scale study areas.

However, to the author's knowledge, there is no general and systematic approach to assess offshore wind energy resources accurately. This work presents a new methodology to address this lack of knowledge, which has global applicability for offshore wind energy exploitation.

Multi-criteria decision analysis coupled with the Analytic Hierarchy Process (AHP) are well known techniques in engineering to solve complex problems including the spatial planning for siting renewable energy projects – such as offshore wind farms (Saaty, 1977, Saaty, 2008, Siddiqui et al., 1996). AHP is a structured technique for organising and analysing complex decisions, based on mathematics and psychology. This work utilises AHP for siting offshore wind farms promoting a new approach developed to support coherent analysis, which circumvent the current processes, which have reduced accuracy and are time consuming.

To formally, select suitable offshore wind turbine sites, a number of analytical tools have been combined to form an analytical hierarchy process (AHP). This process provides organised process to generate weighted factors to divide the decision-making procedure into a few simple steps and pairwise comparison methods linked to site spatial assessment in a Geographical Information System (GIS). GIS-based multi-criteria decision analysis (MCDA) is an effective method for spatial siting of wind farms (Jiang and Eastman, 2000). GIS-MCDA is a technique used to inform decisions for spatial problems that have many criteria and data layers. GIS-MCDA is widely used in spatial planning and siting of onshore wind farms. GIS is used to put different geographical data in separate layers to display, analyse and manipulate, to produce new data layers and or provide appropriate land allocation decisions (DeMers, 2008). The MCDA method is used to assess suitability by comparing the developed criteria of the alternatives (Yoon and Hwang, 1995). The alternatives are usually a group of cells that divide the study area into an equally dimensioned grid. The most popular and practical method to deploy MCDA is the Analytical Hierarchy Process (AHP). AHP was defined as an organised process to generate weighted factors to divide the decision making procedure into a few simple steps (Saaty, 2008). Each criterion could be a factor or a constraint. A factor is a criterion that increases or decreases the suitability of the alternatives, while a constraint approves or neglects the alternative as a possible solution. AHP has two main steps: "Pairwise" comparison and Weighted Linear Combination (WLC). Pairwise comparison method is used to weight the different factors that are used to compare the alternatives (Saaty, 2008) while WLC is the final stage in AHP evaluating the alternatives (Eastman et al., 1998).

Identifying the most suitable locations for offshore wind energy around a region is a spatial siting decision problem. Spatial problems comprise the analysis of a large number of suitable alternatives and a multiple criteria that will need appropriate evaluation. Once these criteria are chosen, they are evaluated and weighted by experts - stakeholders, and/or scholars. The evaluation is normally based on knowledge and experience of the appraisers concerning the specific problem to be

solved, and the region under consideration (Estoque, 2011). In such cases, AHP is used to identify the problem criteria, to weight them, and then to evaluate each alternative (Eastman et al., 1998, Eastman, 1999). For example (Hansen, 2005, Jiang and Eastman, 2000, Lesslie, 2012, Dodgson et al., 2009, Dell'Ovo et al., 2018) indicates that such *spatial decision problems* are complex and require innovation. This is because the techniques typically involve a large set of feasible alternatives and multiple evaluation criteria, which are often conflicting.

The GIS-based constraints analyses limited to only restrictions, such as government regulations, are not enough to identify the most suitable locations, for offshore wind energy development. In essence, such analysis is only suitable for small-scale study areas as evidenced in the studies (Ntoka, 2013, Mahdy et al., 2017, Farhan and Murray, 2008, Jäger et al., 2016, Siyal et al., 2015, Schallenberg-Rodríguez and Montesdeoca, 2018). To make it widely and fully applicable, one need to produce suitability maps which requires an AHP analysis to produce factor weights to score the available areas on the maps to *high*, *moderate* and *not suitable* grades. For example, in the UK, the available areas for offshore wind energy are vast, so, stakeholders and investors do not need just the locations of the available areas only; they need to know the most suitable locations. Hence, appropriate analyses will need to create a descending score of the available areas from the highest to the lowest suitability (i.e. suitability maps). Such suitability maps assist stakeholders in targeting investments by exploiting the most suitable areas first and then the moderate areas and so on.

In essence, currently published work needs to find a robust way to compare factor pairs. As indicated earlier, alternatives and criteria are often evaluated by a number of individuals (decision-makers, managers, stakeholders, interest groups) who most of the time, have conflicting ideas, preferences, objectives, etc. This current practice, which is based on expert surveys and their subsequent analysis, is a long-winded process, requiring:

(a) The generation of appropriate succinct questions to be addressed,

(b) Ethics approval for data collection,

(c) Identifying a cohort of experts,

(d) Once identified pooling them with the survey questionnaires and hoping to get robust sample return for the cohort

(e) Analysis for providing judgment and agreement between experts.

This could take 6 months or more, (Lirn et al., 2004, Stević et al., 2015, Dalalah et al., 2011, Aruldoss et al., 2013, Martin et al., 2013, Lozano-Minguez et al., 2011, Akbari et al., 2017). In addition, most studies only mentions the Importance Index (I) parameter without a clear explanation on how they arrive at the outcomes (The Crown Estate, 2012b, Ntoka, 2013, Aydin et al., 2010, Hansen, 2005, Wang et al., 2009, Mostafaeipour, 2010, Flood, 2012, Kim et al., 2016).

Egypt and the Arabian Peninsula were chosen as case studies to apply the site assessment methodology as they are surrounded by sea and hence a large scope for offshore wind energy potential. In addition to funding this work, Egypt is in need of increasing its renewable energy electricity fraction to reduce its dependence on imported fossil fuels, to support the ever-increasing need for power due to population increases and to achieve its set renewables targets. Countries in the Arabian Peninsula mainly depend on fossil fuels and have set out future renewable energy targets. More details on consideration of such needs are given in the Literature Review Chapter. Furthermore, in both case studies, offshore wind energy potential has not been investigated in-depth before and this will contribute knowledge for the exploitation of this important resource for power supply.

For the Egypt case study, further in-depth analysis was performed to provide a blue print for site development. For the selected sites, this included investigation of suitable foundation for offshore wind turbines, optimise farm layout, logistics needs (ports, grid, etc.), and a study of the environmental impacts for proposed offshore wind farms.

1.1 Aims and Objectives

The core aim of the thesis is to establish a systematic analysis of all the factors relevant to offshore electricity generation to produce a pathway for exploiting offshore wind energy resources. The approach is to address the paucity of generalised modelling to support the exploitation of offshore wind energy. In order to do this, this work will utilise a countrywide and regional case studies, where the developed methodology will be used to investigate the wind energy potential, specify appropriate locations of high resources with no imposed restrictions, and generate suitability maps for offshore wind energy exploitation. The development methodology will appropriately identify the essential criteria that govern the spatial siting of offshore wind farms. The overall research objectives are as follows:

A. Identify, address, and quantify the criteria that governs offshore wind farm siting.

B. Perform appropriate modelling to establish resource intensities and produce suitability maps of the offshore wind energy in Egypt, and the Arabian Peninsula, then, identify the appropriate sites and their potential for both case studies.

C. Develop a clear understanding of the technologies needed for anchoring such turbines, by assessing typical soil conditions of appropriate sites and then assess the appropriate foundation for the chosen sites as a function of the Egyptian soil and weather condition.

D. Inform the optimized design of the wind farm layout for the chosen sites in Egypt.

E. Create a feasibility study to identify the Egyptian ports available to support the offshore wind turbine installation processes.

F. Provide an initial environmental assessment study for deploying offshore wind farms in Egypt.

1.2 Report Outlines

The overall structure of the thesis is summarised in Figure 1-1. The figure is a flowchart that divides the work into four parts, which are Introduction & Literature Background, Methodology & Data Collection, Analyses, and Result Discussion. Finally, the thesis is concluded in chapter seven. This report consists of seven chapters, which are summarised below:

Chapter 1: introduces a brief research background, which will be extended in the literature chapter. In addition, the research aims and motivations are presented.

Chapter 2: identifies the two case studies locations and their characteristics, energy and renewable energy status, illustrates the potential for offshore wind energy and a MCDA-spatial siting methodology for determining these potentials is presented, reviews relevant research related to both onshore and offshore wind energy spatial siting. Moreover, a background for other thesis objectives is indicated, such as, previous wind studies for both case studies, offshore wind turbine foundations, port feasibility, monopile design, layout optimisation, and environmental impact assessment.

Chapter 3: explains the methodology developed and utilised to fulfil the research objectives and aims.

Chapter 4: describes the process to collect and prepare the relevant data required for different research analyses. In addition to, the data preparation in a form that can be used easily in the next analyses phase using ArcGIS, ABAQUS, and WindFarmer software.

Chapter 5: applies the described AHP methodology discussed in chapter three, using the data prepared in chapter four to produce suitability maps for Egypt and Arabian Peninsula to fulfil the first and second research objectives.

Chapter 6: provides more investigation to study the infrastructure feasibility to establish offshore wind farms in Egypt, this was done through producing:

- Offshore wind foundation type and safe dimensions covering the third objective.
- Optimum offshore wind farm layouts to achieve the fourth objective.
- The most suitable port to install the first offshore wind farm in Egypt to obtain the fifth objective.
- The environmental impact assessment to obtain the last objective.

Chapter 7: concludes the research finding and highlights any future work.

Appendix A: shows the borehole logs to investigate the soil conditions for the major case study (Egypt) chosen sites.

Appendix B: presents the sensitivity validation tables for Figure 5-20.

Appendix C: indicates the attribute tables for the three sets of the UK's offshore wind areas.

Appendix D: includes a copy of the published journal and conference papers that derived from this thesis.

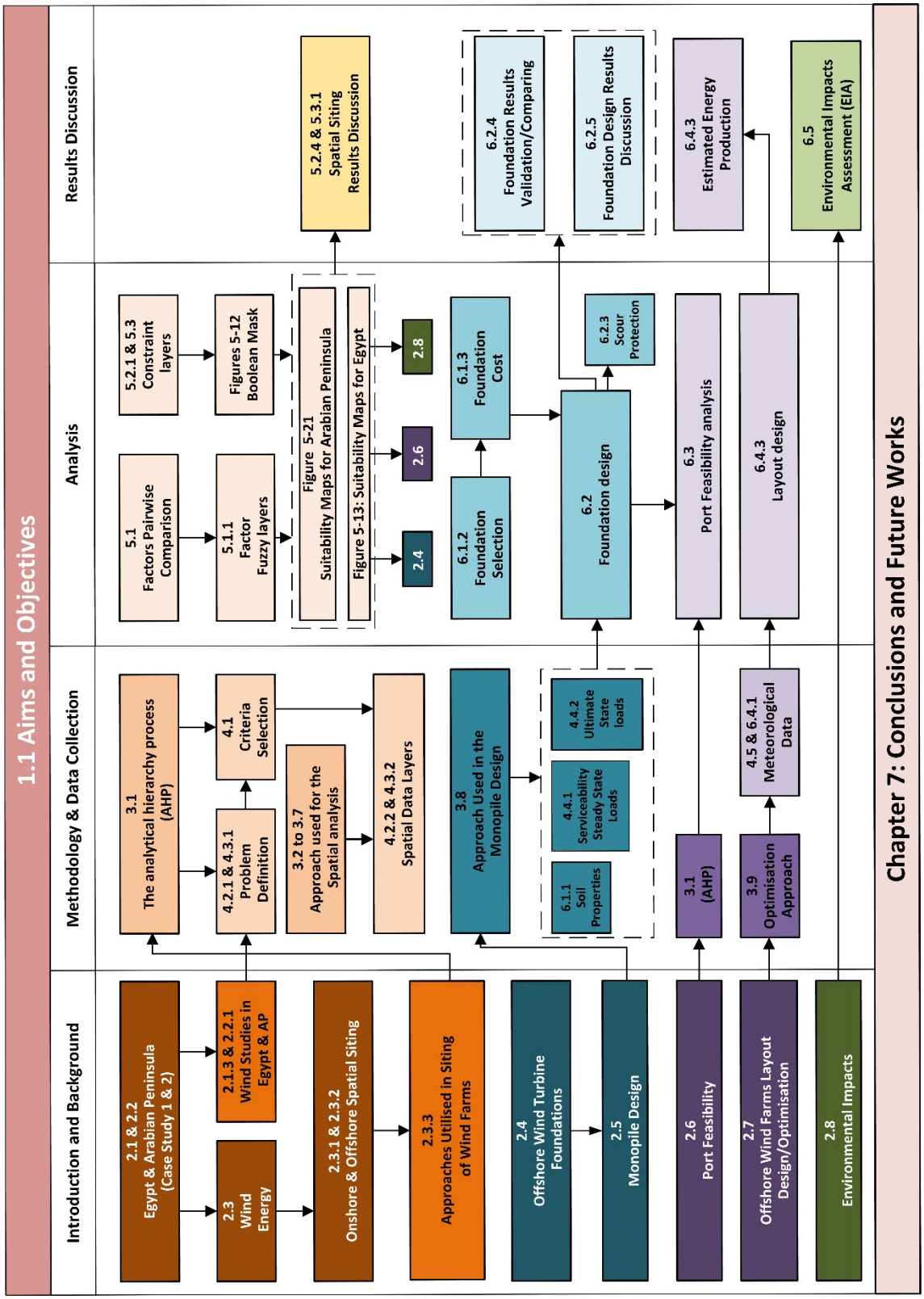

Figure 1-1: The flowchart explains thesis structure.

Chapter 2: Literature Review and Technical Background

The chapter discusses the related literature of the research scope. Egypt and Arabian Peninsula backgrounds are included. In addition, wide and recent studies survey of onshore, offshore wind energy siting, offshore wind turbines anchoring systems, offshore wind farm layout optimisation, and environmental impact are presented.

2.1 Egypt Location and Features

Egypt is located between 24º40`E, 37º23`E and 21º50`N, 31º50`N, and has approximately 3000 km of coastal zones situated on the Mediterranean Sea and the Red Sea, (Figure 2-1). Around 1150 km of the coast is located on the Mediterranean Sea, which extends from El-Salloum in the west to Rafah in the east, whilst 1200 km is situated on the Red Sea which extends from Hurghada in the north to the Hala`ib Triangle in the southeast. The remaining 650 km of the coast is located on the Gulf of Suez and the Gulf of Aqaba (Minister of State for Environmental Affairs, 2016). According to the 2017 census, the population of Egypt is more than 97 million, and 97% of Egypt's population lives permanently on 5.3% of Egypt's one million kilometres square area. this 5.3 % is located mainly beside the banks of the River Nile and its Delta (Egypt State Information Service, 2017). Figure 2-1 is showing the location of the case study 1 (Egypt); the map is highlighting the long stretch of Egypt's shorelines and the position of Gulf of Suez and the Gulf of Aqaba.

The Gulf of Suez has significant offshore wind energy potential, according to Wind Atlas of Egypt, the average wind speed there over the year is more than 11 m/s (measured at 50m above the MSL) blowing from one direction for more than 60% of the year (Mortensen et al., 2006b). Soil conditions and seabed stability are also suitable to deploy offshore wind turbines support structure, especially in the Red Sea and its two gulfs, for instance, sandy soil layers could be found after less than two meters (Roberts and Murray, 1988), which reflect a robust soil conditions for deploying the offshore

wind turbine foundations. In addition, Egypt has more than 55 seaports, twelve of which are suitable for offshore wind farm installing; more analyses are shown in part 5.10.

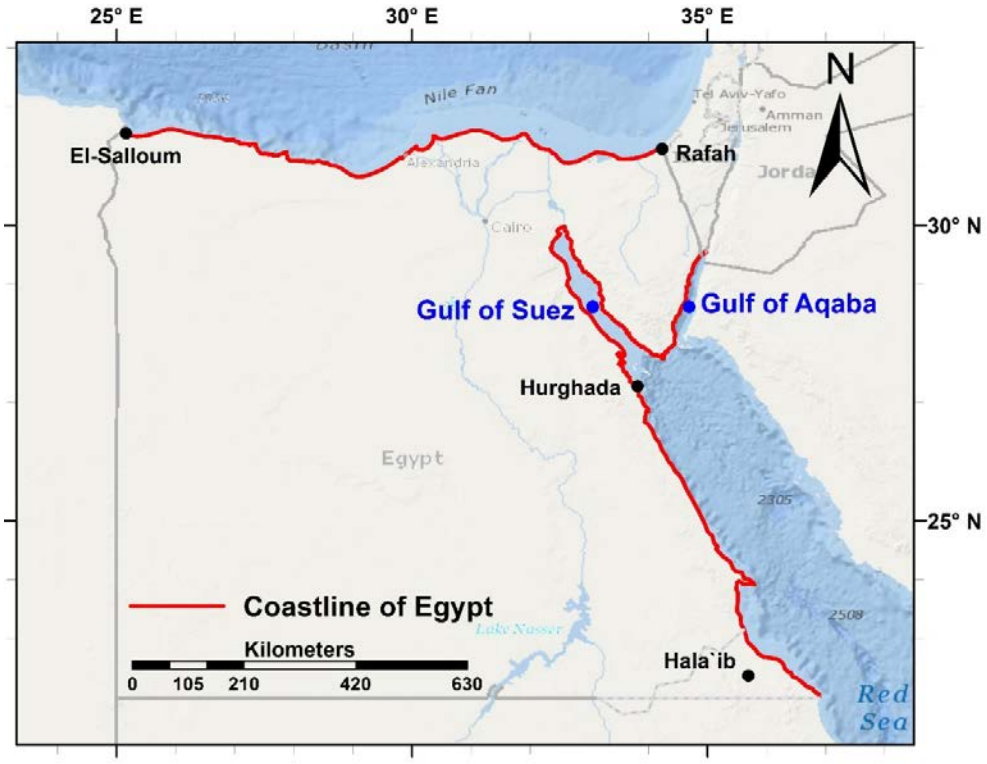

Figure 2-1: Study area map, the map generated and modified using ArcGIS (Esri, 2012).

2.1.1 Egypt Energy Dilemma

Electricity consumption has increased by 45.8% between 2008 and 2016, which was delivered by a 72.1% increase in the installed capacity. The population increased by 18.3% in the same period, see Table 2-1 and Figure 2-2. Until 1990, Egypt was able to generate all its electricity needs from its fossil fuel and hydropower (High Aswan Dam) plants. However, in recent years, due to a combination of population increase and industrial growth, the gap between generation and consumption has widened greatly, forcing the government to import more diesel to fuel its power plants (Bahgat, 2013). The government produces 93% of the total electricity production and the private sector produce the rest (The Ministry of Electricity and Energy of Egypt, 2017), and the private sector is urged to invest more in the renewable energy sector, particularly, wind farms. To meet the accelerated rates of peak load and energy demand, Egypt constructed more thermal power plants to add 13200 MW of installed capacity between 2012 and 2017 (The Ministry of Electricity and Energy of Egypt, 2017). While the total renewable energy contribution to the total electricity

generated decreased from 2.4% to 2.3% between 2012 and 2017 (The Ministry of Electricity and Energy of Egypt, 2017). Table 2-1 presents the main data related to energy status in Egypt, such as electricity demand, installed capacity, population, average temperature, etc., from 2008 to 2016. Figure 2-2 graphs the energy status in Egypt and population.

Table 2-1: Egypt electricity, population, and temperatures statistics (2008-2016), adopted from (The Ministry of Electricity and Energy of Egypt, 2017, The Ministry of Electricity and Energy of Egypt, 2011, Egypt State Information Service, 2017).

Year	2008	2009	2010	2011	2012	2013	2014	2015	2016
Electricity Demand [TWh]	107.2	112.6	120.2	126.9	135.8	140.9	143.6	146.9	156.3
Electricity Generated [TWh]	131	139	146.8	157.4	164.6	167.8	168.1	174.9	186.3
Yearly Peak Load (YPL) [GW]	19.74	21.33	22.75	23.47	25.71	27.00	26.14	28.02	29.2
Installed capacity [GW]	22.6	23.5	24.7	27.1	29.1	30.8	32.0	35.2	38.9
Population - inside Egypt only – [million]	80.9	82.4	84.1	85.7	87.6	89.5	91.5	93.8	95.7
Average Temperature °C	23.1	23.7	24.9	22.7	23.5	24.1	23.5	23.9	24.3
Average Temperature (Summer only) °C	30.5	30.7	31.5	31.6	31.2	31.5	31.9	31.8	32.3

The Egyptian New and Renewable Energy Authority (ENREA) in 2016 estimated that energy consumption will be doubled by 2022 due to population increases and development (New and Renewable Energy Authority, 2019). Like many other developing countries, the government in Egypt is currently subsidising the energy supply system to make electricity affordable to the mostly poor population (Bahgat, 2013). Such subsidies create an additional burden on the over-stretched Egyptian economy. The budget deficit in 2014/2015 was 10% of its Gross Domestic Product (GDP) accompanied with a high unemployment rate, high poverty rate, and low living standards (Abdou and Zaazou, 2013).

Egypt is currently experiencing serious electricity shortages due to the ever-increasing consumption and the lack of available generation capacity to cope with demand (New and Renewable Energy Authority, 2019). In many instances, power blackouts are experienced many times a day (between 2009 to 2018) (Abdou and Zaazou, 2013). In order to cope with the demand and provide sustainable energy, the Egyptian government embarked on a programme to produce electrical power from onshore wind. However, up until the end of 2017, only a small number of wind farms were in production with a total capacity of around 1 GW, which is insufficient to support the ever-increasing demand (New and Renewable Energy Authority, 2019). In order to alleviate such power shortages offshore wind can play a major part in this respect as the resource is vast and its exploitation will address such power shortages. Investment in offshore wind will also benefit economic development of the country and will reduce pressure on land areas where wind speeds

are high but are of greater commercial importance for recreation and tourism (Mortensen et al., 2006a).

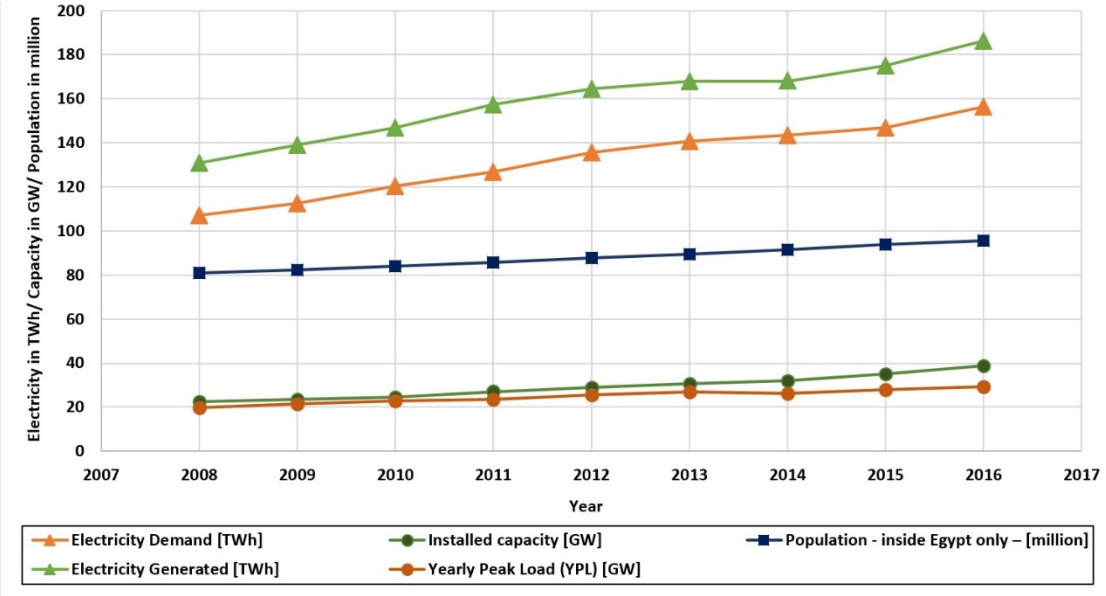

Figure 2-2: Electricity demand, generated, yearly peak and installed capacity increasing curve for the period 2008 to 2016. The population rising curve is plotted in dark blue. The electricity generated [TWh] = installed capacity [GW] * 365 *24 * capacity factor, where capacity factor is the average power generated, divided by the rated peak power.

The average temperature of summer only over Cairo for the last five years increased 0.6 degree compared to the average temperature of summer (29.4°) from 2005 to 2019: see Figure 2-3, which makes another burden on the electricity grid in summer, due to cooling demand. Figure 2-3 represents the data of Cairo's yearly average temperature around the whole year and for summer months only (all day). The number of air conditioning devices doubled from three million to six and a half million devices in a short period of 3 years from 2009 to 2012, which represent around 23% of the consuming electricity through summer (Egypt State Information Service, 2017). The projected increase in energy consumption will undoubtedly lead to more pollution such as CO_2 emissions, as increased capacity will be derived from greater consumption of fossil fuels. CO_2 emissions increased from 182.6 to 198.6 million tonnes between 2011 and 2015 (International Energy Agency, 2017).

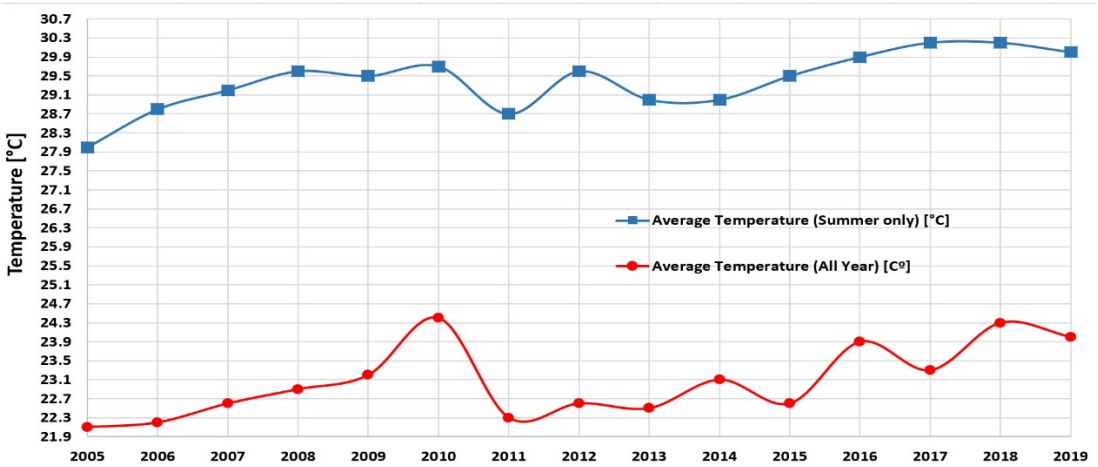

Figure 2-3: Average temperature for the whole year *(all-day)* and for summer months *(from the mid of July to the mid of September, all-day)* for the period 2008 to 2016 over Cairo.

Wind and solar resources are the main types of renewable energy in Egypt. In 2006, and in order to persuade both the public and the public sectors to invest in renewable energy, ENREA conducted a study, which emphasised that Egypt is a suitable place for wind, solar, and biomass energy projects (New and Renewable Energy Authority, 2019). The study urged the government to start building wind farms, and the private sector to develop smaller projects to generate solar and biomass energy (New and Renewable Energy Authority, 2019). Egypt aims to produce 20% of its electricity needs from renewable energy by 2022 with approximately 12% derived from wind energy. Currently, onshore wind supplies only 1.8% of the Egyptian electrical power and nothing from offshore wind energy. Without more and urgent investments in wind energy, it is more than likely that the 2022 target will be pushed back to 2027 (The Ministry of Electricity and Energy of Egypt, 2017).

2.1.2 Egypt Renewable Energy Strategy

The first action taken by the Egyptian government towards generating electricity from wind was the creation of the Egyptian Wind Atlas (Mortensen et al., 2006b). The Atlas was influential in the development of Egypt's first onshore wind farm installation, which has 700 turbines and a total installed capacity of 545 MW. The monthly average wind speed at Zafarana onshore wind farm is in the range of 5 to 9 m/s. The government is now planning to develop three more onshore wind farms in different places in Egypt (The Ministry of Electricity and Energy of Egypt, 2013). As indicated earlier, all wind energy in Egypt is generated onshore, and the emphasis now is to scale

up renewable installed capacity from the 0.89 GW (2016) to 7.5 GW by 2022 (Lashin and Shata, 2012), by going offshore where the wind resource is much higher.

Due to its geographical location, Egypt has one of the highest offshore wind energy potentials in the world (Mortensen et al., 2006a). The Red Sea region of the cost of Egypt has the best wind resource, where, the mean power density is in the range of 300 to 800 W/m^2, at 50 m height, and mean wind speeds between six to more than 10 m/s.

Egypt's offshore wind energy potential in the Mediterranean Sea is estimated to be around 13 GW (Gaudiosi, 1996). For a relatively small land footprint, this resource is tremendous when compared with, for example, the estimated total offshore wind energy resource for much larger countries such as the USA with 54 GW potential (Gaudiosi, 1996). To the author's knowledge, offshore wind energy potentials have not been covered for the Red Sea of Egypt, therefore, this will be one of the questions this thesis will answer.

2.1.3 Wind Studies in Egypt

Egypt has a unique location between two inner seas, a massive need for renewable energy, and wind availability data (Egypt is the only country in the Middle East that has a detailed wind atlas). However, there have been no detailed studies conducted to explore offshore wind energy potential in Egypt. The only available literature consists of a few studies on Egypt's onshore wind potential. Most of these studies are down to the efforts of one primary researcher Dr Ahmed Shata (Shata, 2010, Shata, 2011b, Shata, 2012a, Shata, 2011a, Shata, 2012b, Shata and Hanitsch, 2006a, Shata and Hanitsch, 2008, Lashin and Shata, 2012, Shata and Hanitsch, 2006b).

The economic and environmental impact of wind farms was assessed by (El-Sayed, 2002) using a Cost-Benefits Ratio. It concluded that Zafarana along the Red Sea coast was the most suitable site in Egypt for onshore wind farms. A "roadmap for renewable energy research and development in Egypt" was produced by (Khalil et al., 2010), which emphasised wind energy to be the most suitable renewable energy source for Egypt particularly for technology positioning and market attractiveness. The first survey to assess the wind energy potential in Egypt used 20-year old data from 15 different locations to estimate the wind energy density at 25 m height and the mean wind power density (Mayhoub and Azzam, 1997). It estimated the magnitude of the wind energy density to be in the range of 31–500 kWh/m^2/year and the power density in the range of 30–467 W/m^2. The study

concluded that the Red Sea and the Mediterranean Sea, plus some interior locations (Cairo, Aswan, El-Dabah, and El-Kharga) were the most suitable locations for onshore wind farms (Mayhoub and Azzam, 1997).

Many studies presented a set of analyses that covered the land areas adjacent to the Red Sea and the Mediterranean Sea coasts (Shata, 2011b, Shata, 2012a, Shata and Hanitsch, 2006a, Shata and Hanitsch, 2008, Lashin and Shata, 2012, Shata and Hanitsch, 2006b), as well as some interior locations around Cairo and Upper Egypt. Medium size wind farms (100–200 kW capacity) – in 2001, 100–200 kW was considered medium size wind farms. While, in present time one turbine capacity is at least 2MW – are a suitable solution for the isolated communities in the Red Sea coast and 1 MW capacity farms are appropriate for the northern Red Sea coast area which could be linked to the Egyptian Unified Power Network (Ahmed and Abouzeid, 2001).

The "Wind Atlas of Egypt" was the only institutional effort to explore wind energy potential in Egypt which took nearly eight years to complete through a combined effort of the Egyptian Meteorological Authority (EMA) and Risø National Laboratory (Mortensen et al., 2006b). Figure 2-4 shows one of the main contributions of this Atlas, which is the map for the mean wind speed of Egypt at the height of 50 m.

Table 2-2: Wind power classes, adopted from (Elliott et al., 1987).

Wind Power Class	At a hub height of 10 m		At a hub height of 50 m	
	Wind Power Density [W/m^2]	Wind Speed [m/s]	Wind Power Density [W/m^2]	Wind Speed [m/s]
1	0.0 – 100	0.0 – 4.4	0.0 – 200	0.0 – 5.6
2	100 – 150	4.4 – 5.1	200 – 300	5.6 – 6.4
3	150 – 200	5.1 – 5.6	300 – 400	6.4 – 7.0
4	200 – 250	5.6 – 6.0	400 – 500	7.0 – 7.5
5	250 – 300	6.0 – 6.4	500 – 600	7.5 – 8.0
6	300 – 400	6.4 – 7.0	600 – 800	8.0 – 8.8
7	400 – 1000	7.0 – 9.4	800 – 2000	8.80 – 11.9

The Wind Power Classes (WPC) defined by the United States Department of Energy, categorised wind power density [W/m^2] according to its speeds [m/s] and hub height (10m and 50m). The classification is shown in Table 2-2 and consists of seven wind power classes and two hub heights. The recommended commercial and economical suitable WPC is wind class four (Elliott et al., 1987). The map in Figure 2-4 indicates that the offshore areas of the Red Sea have (WPC >> four),

are centred above both the Gulf of Suez and Gulf of Aqaba, see the black dashed rectangular in Figure (2-4).

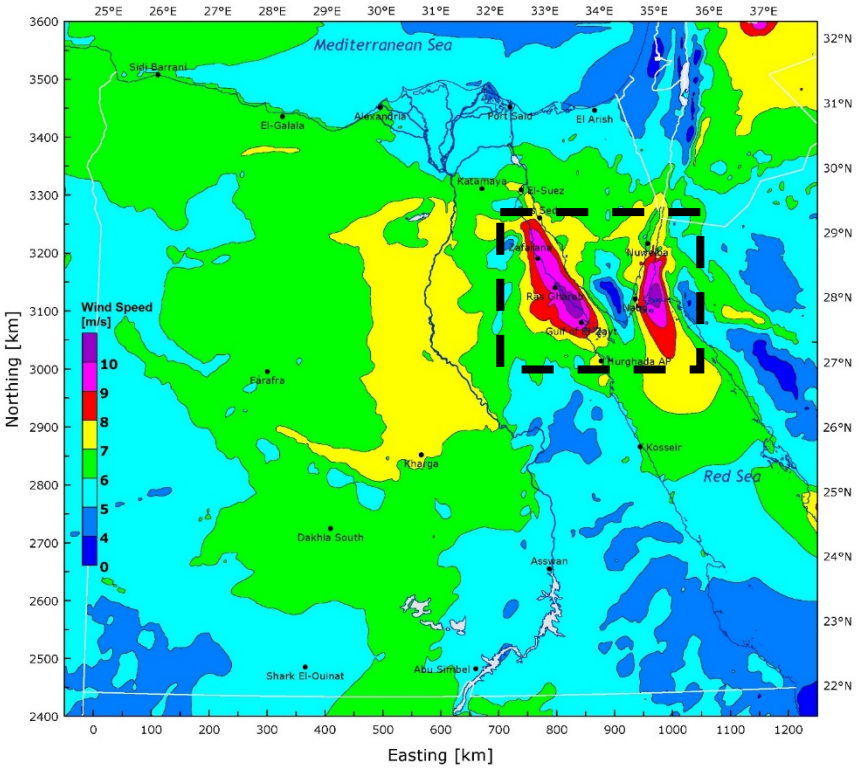

Figure 2-4: "The regional wind climate of Egypt determined by mesoscale modelling. The map shows the mean wind speed in [m/s] at a height of 50 m over a flat, uniform land surface of roughness class 0. Black dots show the locations of the meteorological stations used" (Mortensen et al., 2006b). The black dashed rectangular highlight the areas with (WPC >> four) in Egypt.

2.2 Arabian Peninsula

The Arabian Peninsula bounded between 10°N and 35°N latitude and 35°E and 60°E longitude with a spatial extent, which includes the offshore areas of the Red Sea, the Gulf of Aden, the Arabian Gulf, and the northern part of the Arabian Sea, see Figure 2-5. Figure 2-5 maps the location of the seven countries of Arabian Peninsula, which are Bahrain, Kuwait, Oman, Qatar, Kingdom of Saudi Arabia (KSA), United Arab Emirates (UAE), and Yemen. Most of the countries within the Arabian Peninsula rely on fossil fuel for their electricity supply.

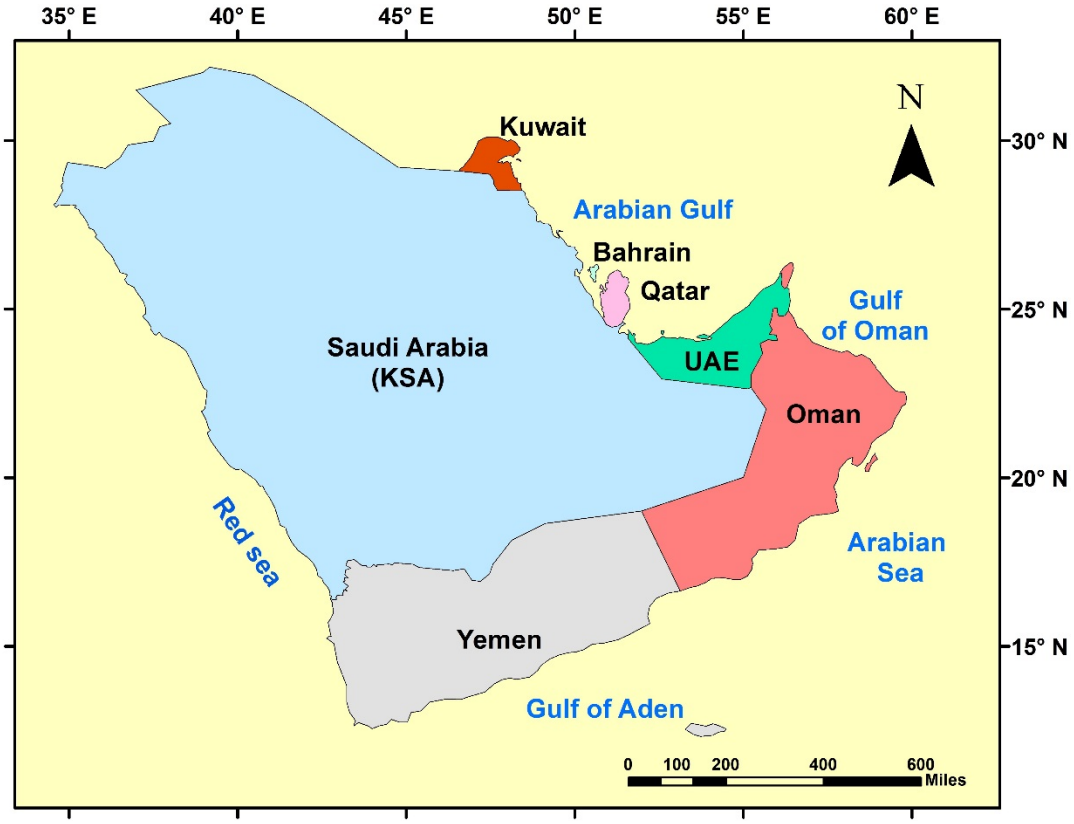

Figure 2-5: Arabian Peninsula countries considered in this study, created using ArcGIS programme.

The Gulf Cooperation Council (GCC) countries, which consist of all Arabian Peninsula countries except Yemen hold more than 500 billion barrels of oil reserves (1/3 of the total known global reserves) and hence most of their electricity is generated using fossil fuels (UNFCCC, 2015). Furthermore, the electricity consumption in the GCC countries is multiplying, and this is due to expansion in the buildings, water, industrial sectors and the over reliance on air conditioning to cope with the high ambient temperatures encountered in these countries.

The GCC countries has an average growth rate of 4.1% between 2008 and 2017 compared to 2.8% for the whole world (World Bank, 2018). While, the population growth rate for same region is 2% per year (Factbook, 2018). High urban growth rates overwhelm the CO_2 emission targets, and hence low carbon solutions are needed to address the increasing power demand in these countries. These countries are also signatories to the Paris Climate Change Agreement and have produced plans to limit their CO_2 emissions according to their Intended Nationally Determined Contributions (INDCs) (Bodansky, 2016). Despite that all GCC countries did not announce clearly their INDCs, they have announced targets for the deployment of renewable energy

technologies that are geared to achieve such targets and to reduce their reliance on fossil fuels (Bahakeem, 2015).

Generally, policies announce by the GCC countries to address the above challenges are: (i) reduce reliance on fossil fuels, (ii) reduce carbon dioxide emissions and (iii) balance its economy. These policies have resulted in the announcement of ambitious plans to replace around 15.8% of their electricity from fossil sources with renewable sources by 2030, see Table 2-3. This target varies between countries with United Arab Emirates (UAE) and Qatar reduction of 20%, Kingdom of Saudi Arabia (KSA), 15% and Bahrain 5%. Table 2-3 depicts various characteristics of the Arabian Peninsula countries including areas, population, installed power capacities, and currently installed and future renewable energy targets. As can be seen from the table the region currently lacks renewable energy capacities.

Table 2-3: Some characteristic of the Arabian Peninsula countries (GCC and Yemen), adopted from Refs. (IRENA, 2016, Factbook, 2018, Alnaser and Alnaser, 2011, Al-Maamary et al., 2017).

Country, (Ref.)	Area (10^6 km^2)	Residents [Million]	Installed Power Capacity [GW]	Current/future Renewable Energy [%]		Coastline [km]
				2017	2030	
Bahrain, (Buflasa et al., 2008)	0.008	1.41	3.93	0.2	5	161
Kuwait, (Munawwar and Ghedira, 2014)	0.017	2.88	16.0	0.00	15	499
Oman, (Kazem, 2011)	0.310	3.42	7.87	0.00	10	2092
Qatar, (Marafia and Ashour, 2003)	0.012	2.31	8.80	0.50	20	563
KSA, (Rehman, 2005)	2.148	28.6	69.1	0.10	15	2640
UAE, (Nematollahi et al., 2016), (Mostafaeipour and Mostafaeipour, 2009)	0.084	6.07	28.9	0.50	20	1318
Yemen, (Mondal et al., 2016)	0.528	28.0	1.50	0.00	-	1906
Total	3.099	72.69	136.1	0.2	15.8	9179

Currently, for most Arabian Peninsula countries these targets are planned to be mainly met through the deployment of solar energy conversion technologies, this is worthwhile as the solar resource is high in these regions. However, it is essential for these countries to plan for a more diverse renewable energy exploitation not only from the point of view of sustainability and growth but also due to the fact that these regions also possess high wind speeds which unlike the solar resource are available over the whole day. Figure 2-5, highlight that these countries are surrounded by water, which increase its suitability for offshore wind energy harnessing. For instance, KSA has two shorelines, one on the Arabian Gulf and the other on the Red Sea, while, Bahrain, Kuwait, Qatar and UAE have shorelines on the Arabian Gulf. Oman has shorelines laying on Gulf of Oman and

the Arabian Sea, while Yemen has shorelines on the Red Sea, Gulf Aden, and the Arabian Sea. Hence, these countries could benefit from identifying the offshore wind energy potentials around their coastlines. Therefore, the exploitation of offshore wind energy resources could contribute significantly to the GCC and Yemen countries 2030 renewable energy targets while addressing the three pillars for change mentioned above.

2.2.1 Wind Studies in the Arabian Peninsula

Despite the vast need to study and invest in renewable energy in the Arabian Peninsula as previously introduced in Section 1.3, to date there is a paucity of relevant wind energy literature for this region, and is mainly related to onshore wind energy. The wind energy potentials for the Arabian Peninsula were evaluated as a part of the Middle East region (Shawon et al., 2013). The paper used three turbine types to convert wind energy into electric power, which are GE energy 2.5-TC3, Enercon E33, and Gaia-Wind 133. They considered Oman, Kuwait, Qatar, and Bahrain as a medium wind speed region, while KSA and UAE were categories as low wind speed regions. Despite the fact that the study used good metrological data for most of the Arabian Peninsula region (except Yemen), the analysis considered very low rated turbines (11 kW), which is very low for 2013. Additionally, they did not evaluate the offshore areas, which have significant wind power densities especially for Oman and KSA.

Baseer et al. (2017) investigated onshore wind potential for the KSA, using GIS-based multi-criteria site selection process. They used wind speed, distance from (roads, electricity grid, and population), terrain slope, and impact on birds as factors to produce a site selection map for the area. Three locations were identified as highly suitable areas for onshore wind farms. The paper has some similarity to the methodology used for the spatial siting part in this thesis.

Rehman (2005) studied the offshore wind energy for the KSA's Arabian Sea area and analysed the available wind data to prove that offshore wind in that area is higher by 1 m/s than onshore. However, he stated that commercial wind farm development becomes feasible at wind speed of 5.4 m/s at a hub height of 60 m. While, (Elliott et al., 1987) consider wind speed of 6.4 m/s at a hub height of 50 m/s to be the minimum requirements for commercial validity.

2.3 Wind Energy

Onshore wind energy is cheaper compared to offshore wind energy; however, it has some disadvantages, for instance, the lost value of the land used, noise, high vibrations, visual impacts, bird paths hazards, and shadow flicker effect. Shadow flicker effect is an infrequent event could happen when the sun's light is at the horizon. Shadow flicker could be responsible for photo-induced seizures or photosensitive epilepsy and other disturbance to humans near the turbines (Knopper and Ollson, 2011). On the other hand, offshore wind energy, on the whole, does not suffer these disadvantages, and has two other advantages: (a) offshore wind speed is on average higher than that onshore, see equation 2-1 and (b) the effect of turbulence is minimal compared to inland projects. The reduced offshore turbulence could extend the life cycle of wind turbines and reduce the materials used to support the wind turbine, as the fatigue stress is minimised (Ismaiel and Yoshida, 2018).

2.3.1 Onshore Wind Spatial Siting

GIS-based MCDA is widely used in the spatial planning of onshore wind farms and siting of turbines. The key relevant literature for these methods is highlighted below and in Table 2-4. Table 2-4 provides a brief comparison between the various onshore approaches discussed in the literature.

In a study of onshore wind farm spatial planning for Kozani, Greece, sufficient factors and constraints were used to produce a high-resolution suitability map with a 150m x 150 m grid cells (Latinopoulos and Kechagia, 2015). The study focussed on three different scenarios:

(a) All factors were given the same weight,

(b) Environmental and social factors had the highest weights, and

(c) Technical and economic factors had greater weight than other factors.

It was found that more than 12% of the study area has a suitability score higher than 0.5, i.e. suitable for wind farms, and all previously installed wind farms were located in areas with a high suitability score, which emphasised and validated their results. Their suitability map was found to be reliable by stakeholders and was used to inform the siting of new wind farms in Greece. However, the first scenario is unrealistic, because factors usually have different relative importance.

Table 2-4: Comparison between the different onshore wind fam spatial siting studies.

Author	Study area	Criteria		Weighting method used	Aggregation Method	Prospective	Year
		Constraints	Factors				
Latinopoulos, and Kechagia (Latinopoulos and Kechagia, 2015)	Kozani, Greece	Buffer exclusion zones (between 0.15 to 3 Km) for: • Protected areas • Historical sites • Airports • Urban areas • Tourism sites • Roads • Farms • wind < 4.5 m/s • Slope >25%	• Slope • Wind speed • land uses • Distance from roads, national parks, tourism facilities, and historical	Pairwise Comparison	WLC	Cost/Benefit prospective	2015
Aydin et al. (Aydin et al., 2010)	Western Turkey	Buffer exclusion zones (between 0.25 to 2.5 Km) for: • Natural Parks • Town centres • Airports • Bird habitats • Noise	• The same criteria as constraints but calculating the distance after the end of the buffer zone. • Wind Speed	other	other	Environmental aspects	2010
Hansen (Hansen, 2005)	Northern Jutland, Denmark	• Protected nature • Bird protection • Protected wetlands	• Wind speed Proximity to: • Coast distance • Forests • Population ares • Water streams • Lakes • Roads • Grid lines • Airports	Not mentioned	WLC	Cost/Benefit, environmental, and Socio-political aspects	2005
Rodmana, and Meentemeyer (Rodman and Meentemeyer, 2006)	Northern California, USA	N/A	• Wind speed • Environment • Human impact	A rank from 1 to 3	Classic aggregation	Socio-political concerns	2005
Baban, and Tim Parry (Baban and Parry, 2001)	Lancashire, UK	• More than 10 km to roads and national grid • wind < 5 m/s • Slope > 10% Buffer exclusion zones (between 0.4 to 2.0 Km) for: • population • Forests • Water streams • National parks	• Land use • Distance to roads • Population zones • Distance to importance sites • Distance to natural parks • Slope • Other	Pairwise Comparison	WLC	Cost/Benefit, environmental, and Socio-political aspects	2001

Aydin et al. (2010) addressed suitable sites for wind farms in Western Turkey. They found the site suitability mapping using 250 m X 250 m grid cells, and considering environmental and social criteria such as noise, bird habitats, preserved areas, airports, and population areas, as well as wind potential criterion. Cells that had satisfaction degree > 0.5 in both environmental objectives and

wind potentials were designated as priority sites for wind farms. The study produced a powerful tool to choose suitable locations for onshore wind farms.

Hansen (2005) completed a spatial planning study to site new wind farms in Northern Jutland, Denmark. This analysis included most common criteria to arrive at a suitability score for grid cell of 50 X 50 m. Although the research is well presented, the method used to weight the factors was not indicated, and the weighting values absent. Hence, it is difficult to ascertain from the final suitability map the methodology used to identify suitable sites.

Rodman and Meentemeyer (2006) developed an approach to find suitable locations for wind farms in Northern California in USA. They considered a 30 x 30 m grid and used a simpler method to evaluate alternatives which only included three factors - wind speed, environmental aspects, and human impact. The factors were scored on a scale from unsuitable = 0 to high suitability = 4, based on their own experience and judgement. They then weighted the three factors by ranking them from 1 to 3, to arrive at final suitability. A suitability map was created by summing the product of each scored factor and its weight and dividing the sum on the weights summation. Although the method was simple, their results could have been greatly improved regarding accuracy and applicability had they used the Analytical Hierarchy Process (AHP) method and considered other important factors such as land slope, grid connection, and land use.

Baban and Parry (2001) elucidated the methodology for choosing a site for new onshore wind farms in the UK, taking the Lancashire region as a case study. In order to identify the problems and the different criteria involved, the authors undertook a public and industrial sector survey (questionnaire) soliciting community/stakeholders' views on wind farms. From the survey results, they constructed a new scoring matrix from 0 to 10 to standardise the different criteria and then used two scenarios to calculate suitability. In scenario, one the same weight was assigned to all criteria, while in scenario two, the criteria were divided into four grades. Pairwise comparisons to weight the grades were used. The study then aggregated the criteria producing two different maps. The results showed that roads and populated areas had the dominant influence on the final decision and the available area for wind farms represented only 8.32% of the total study area. The study is advanced and accurate despite the fact that it was performed in 2001. However, the fact that they scale the “distance to roads factor” from 1 to 0, without applying the same scaling to the other factors will have implications on the accuracy of the final results.

A study of such wind energy potential in the South of the UK (Watson and Hudson, 2015), which was based on the opinion provided by five experts in the wind energy field will be used to estimate the Importance Index. The study used six factors to evaluate the study area, which are wind speed, distance from historically important areas, distance from residential areas, distance from wildlife designations, distance from transport links, and distance from the network connection.

2.3.2 Offshore Spatial Siting

To formally, select suitable offshore wind turbine sites, a number of analytical tools have been combined to form an analytical hierarchy process (AHP). This process provides organised process to generate weighted factors to divide the decision-making procedure into a few simple steps and pairwise comparison methods linked to site spatial assessment in a Geographical Information System (GIS). GIS-based multi-criteria decision analysis (MCDA) is an effective method for spatial siting of wind farms (Jiang and Eastman, 2000). GIS-MCDA is a technique used to inform decisions for spatial problems that have many criteria and data layers. GIS-MCDA is widely used in spatial planning and siting of onshore wind farms. GIS is used to put different geographical data in separate layers to display, analyse and manipulate, to produce new data layers and or provide appropriate land allocation decisions (DeMers, 2008). The MCDA method is used to assess suitability by comparing the developed criteria of the alternatives (Yoon and Hwang, 1995). The alternatives are usually a group of cells that divide the study area into an equally dimensioned grid. The most popular and practical method to deploy MCDA is the Analytical Hierarchy Process (AHP). AHP was defined as an organised process to generate weighted factors to divide the decision making procedure into a few simple steps (Saaty, 2008). Each criterion could be a factor or a constraint. A factor is a criterion that increases or decreases the suitability of the alternatives, while a constraint approves or neglects the alternative as a possible solution. AHP has two main steps: "Pairwise" comparison and Weighted Linear Combination (WLC). Pairwise comparison method is used to weight the different factors that are used to compare the alternatives (Saaty, 2008) while WLC is the final stage in AHP evaluating the alternatives (Eastman et al., 1998). Table 2-5 provides a brief comparison between the various offshore approaches discussed in the literature.

In the UK, for the offshore wind competition "Rounds," a Marine Resource System (MaRS), based on a GIS decision-making tool was used to identify all available offshore wind resources (The Crown Estate, 2012b). After successfully completing Rounds 1, and 2 of the competition, the tool was used to locate 25 GW in nine new zones for Round 3. The MaRS methodology had 3 iterations

(scenarios): (i) it considered many restrictions taking advantages of the datasets from Rounds 1 and 2. The study excluded any unsuitable areas for wind farms, then weighted the factors depending on their expertise from previous rounds, (ii) the same as the first iteration but included stakeholder input, and (iii) aligning Round 3 zones with the territorial sea limits of the UK continental shelf. The Crown Estate, which are responsible for these projects did not publish details of the methodology used, they stated only the criteria and the scenarios/interactions used in the spatial siting process.

Schillings et al. (2012) included capital costs to determine the overall potential of the offshore wind in the North Sea. The work indicated that the use of MCDM in offshore wind feasibility study is rare as it is primarily used in onshore wind studies. Nevertheless, two different maps were created assuming all factors were of the same weight for the first map, and distance to the shore and sea depth factors had the highest weighting in the second map. A Decision Support System (DSS), which is an MCDM programme based on GIS tools was used.

Ntoka (2013) described the constraints were only used in the study of an offshore wind farm (OWF) in Petalioi Gulf, Greece. The work excluded all unsuitable areas in the Gulf using the classical Boolean Mask and then estimated the total capacity as being around 250 MW using the available wind speed data. It was apparent that the Boolean Mask technique was used due to the limited area of the authors' study area (70 km^2), which makes the application of many criteria to locate one OWF difficult.

Waewsak et al. (2015) conducted a study to measure offshore wind power around the Gulf of Thailand, using only four factors with no constraints. The authors used their judgment to weight the factors and then used ArcGIS to select the suitable location for their study area. The work is detailed with appropriate charts. However, using only factors without considering constraints is likely to affect the accuracy of results.

Cavazzi and Dutton (2016) produced a suitability map for offshore wind areas around the UK, but was biased towards cost modelling. The analysis was mainly based on data obtained from the UK Crown Estate using specific Crown Estate restrictions, weights, and scores. The difference between this study and other offshore wind siting studies is that the authors used the overall Levelised Cost of Energy (LCOE) equation to aggregate factors. They produced two maps, one for restrictions (energy available map), and another for factors (cost map/MWh).

Table 2-5: Comparison between the different offshore wind farms siting studies and this study.

Author	Study area	Criteria		Weighting method used	Aggregation Method	Prospective	Year
		Constraints	Factors				
The Crown State (The Crown Estate, 2012b)	North Sea, the UK	• Shipping Routes, Ports • Military zones • Natural Park • Cables and pipe lines • Fishing areas • Oil and gas extraction Areas • Existing or planned farms • Sand Mining • protected wrecks • tunnels, and seascape	• Bathymetry • Soil properties • Wind intensity • Distance to shore • Distance to Grid	Not defined	Not defined	Cost/Benefit, environmental, and Socio-political aspects	2012
Schillings, et al. (Schillings et al., 2012)	The North Sea	• Shipping Routes, Ports • Military zones • Natural Park • Cables and pipe lines • Fishing areas • Oil and gas extraction Areas • Existing or planned farms • Sand Mining • Storm surge • Wave height, and tidal range,	• Cost limit	Not defined	Not defined	Cost/Benefit, environmental, and Socio-political aspects	2012
Ntoka (Ntoka, 2013)	Petalioi Gulf, Greece	• Shipping Routes, Ports • Military zones • Natural Park • Cables and pipe lines • Fishing areas • Oil and gas extraction Areas	• N/A	Boolean Mask	Boolean Mask	Cost/Benefit prospective	2013
Waewsak, et al. (Waewsak et al., 2015)	Gulf of Thailand, Thailand	• Wind speed, water depth, distance from shore, and distance to grid.	• N/A	Not defined	Not defined	Cost/Benefit prospective	2015
Argin, et al. (Argin and Yerci, 2017)	Black Sea, Turkey	• Territorial waters, military areas, civil aviation, shipping routes, pipelines and underground cables	• Wind speed	Not defined	Not defined	Cost/Benefit prospective	2017
Cavazzi, et al. (Cavazzi and Dutton, 2016),	The UK	• Exclusion areas identified by the Crown State	• Bathymetry, wind speed, distance to shore.	Cost modelling	LCOE	Cost/Benefit prospective	2016
This study	Egypt, Arabian Peninsula	• Shipping Routes, Ports • Military zones • Natural Park • Cables and pipe lines • Fishing areas • Oil and gas extraction Areas	• Bathymetry • Wind Intensity • Distance to shore • Distance to Grid • Security and safety	Pairwise Comparison	WLC	Cost/Benefit prospective	2019

As can be seen from the above, offshore wind spatial siting AHP related literature emphasise the importance of identifying the problem correctly, determining the factors affecting the decision making and specifying the factor limitations to suit the case study local conditions and legalisations.

2.3.3 Approaches Utilised in Siting of Wind Farms

Offshore and onshore wind spatial planning may be based on similar techniques, particularly when considering the wind speed factor. However, these techniques differ in terms of the definitions of factors and constraints. For example, the main factors in onshore wind considerations are the distance to roads and the proximity of farms to built-up areas, whereas, for offshore wind, the factors are water depth and wind speed, where the wind speed cube is proportional to power production. In most of the studies reviewed here as well as others not included, the approach taken for determining wind farm spatial planning can be summarised as follows:

1. Identify wind farm spatial characteristics and related criteria using APH or similar techniques.
2. Standardise different factors using the fuzzy membership or some own-derived judgment.
3. Weight the relative importance of the various factors using pairwise comparison or similar methods.
4. Aggregate the different layers of factors and constraints using different GIS tools and WLC aggregation method.

2.3.4 Offshore Wind Energy Resources

Wind speed has a proportional relationship with height (see equation 1-2), due to the reduction effect caused by the drag forces associated with of the surface friction. Therefore, wind speeds increase with height, while surface friction causes a reduction in wind speed at ground level. Therefore, the wind speed is greater away from the ground or water surface (Fjellanger, 2016). Wind velocity U_z in a surface layer can be expressed as a logarithmic relation with height Z approximated (Wallace and Hobbs, 2006):

$$U_z = U_f/k \times \ln (Z/Z_0) \qquad (2\text{-}1)$$

Where: $\mathbf{U_f}$ is the wind friction velocity, $\mathbf{k}$ is the von Karman constant = 0.4, $\mathbf{Z}$ is the wind speed height, where the wind speed is calculated, $\mathbf{Z_0}$ is the aerodynamic roughness length.

Z_0 is equal to 0.0002 for offshore water surfaces, 0.005 for the smooth ground surface, and could extend to higher than 2 for city surfaces (Fjellanger, 2016), while, the friction velocity could be calculated as (Weber, 1999):

$$U_f = (\tau/\rho)^{1/2} \qquad (2\text{-}2)$$

Where: where $\boldsymbol{\tau}$ is the shear stress and $\boldsymbol{\rho}$ the air density.

Figure 2-6 shows the wind speed distribution for different surface types, calculated using equation 2-1 and 2-2, assuming an initial wind speed of 10 m/s at 10m height for open water, smooth open terrain, town, villages, forests, and large cities with high rising building surfaces. As can be seen from the figure, the wind speed and quality is affected significantly by surface type and elevation: the best wind resources are above open water surfaces and altitude above 100m.

According to the previous two equations, wind speed is highly dependent on roughness length and altitude height. As a result, offshore areas have the shortest roughness length (0.0002), and the ability to reach higher altitudes than onshore. Thus, wind resources are significantly higher in offshore areas and even in lower altitudes compared to onshore areas. In addition, wind resources above sea areas has a better quality, as the wind for offshore areas is more predictable than onshore, and the wind is blown from one direction for longer periods, which decrease the need to change the rotor angle over the year (Ismaiel and Yoshida, 2018).

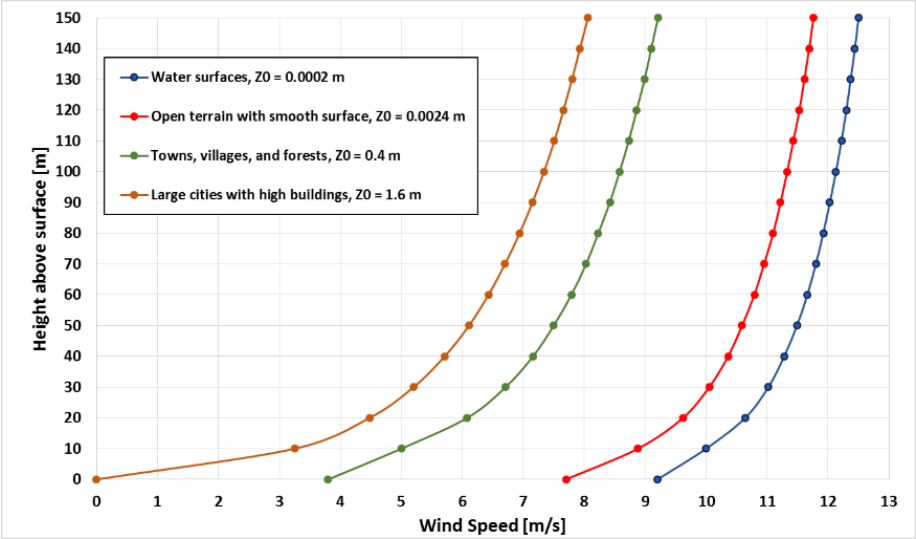

Figure 2-6: Wind speed distribution for different surface types, calculated using equation 2-1 and 2-2, assuming an initial wind speed of 10 m/s at 10m height for a water surface.

2.4 Offshore Wind Turbine (OWT) Foundations

Operating in the sea, offshore wind turbine creates additional challenges designing the turbine foundations. The design has to be robust to transmit withstand turbine loads to the seabed floor as well as the impact of environmental loads conditions. Support systems for the offshore wind turbine is a fundamental factor in the design and installation process as the cost of foundations represents about 25 to 34% of the total cost of offshore wind turbine (Bhattacharya, 2014).

Offshore wind turbines consist of four parts, the rotor-nacelle assembly, tower, sub-structure, and foundation (Figure 2-7). The **Rotor** is a rotating propeller and typically consists of three blades, turns around its horizontal axes, converting the kinetic energy of the wind to mechanical power. The **nacelle** contains the power take-off including the shaft, brakes, generator, and power electronics, which receives the mechanical power from the rotor, transforming it into electricity. The **Tower** is a steel cylinder, which connects the nacelle to the sub-structure. The **Sub-structure** is the part that connects the tower to the foundation, which may be a monopod, which is a cylinder (see A, C in Figure 2-7) or a tripod (see b in Figure 2-7). Finally, **Foundation** is a structure, which transfers vertical and lateral loads to the seabed or the sea floor.

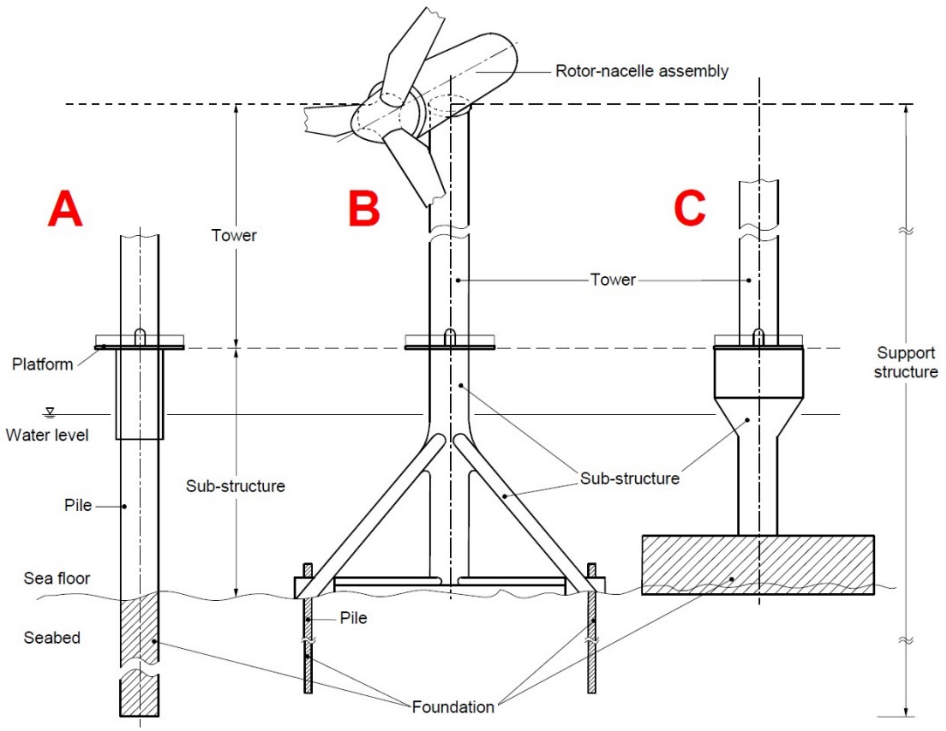

Figure 2-7: The main three concepts of offshore wind turbine foundations and its different parts, adopted from (International Electrotechnical Commission, 2009).

The main three concepts of offshore wind turbine foundations are shown in Figure 2-7 are i) **Monopile** foundation, which is a hollow steel pipe driven into the seabed, (Figure 2-7-A). ii) **Tripod** foundation, which is a tripod (three small hollow steel legs), supported by three short piles, (Figure 2-7-B). iii) **Gravity Base** foundation is the simplest type of offshore wind turbine foundation, comprising of a large pre-cast reinforced concrete block, (Figure 2-7-C). More details and literature review of offshore wind turbine foundation is given below.

Foundation type selection depends mainly on offshore wind turbine installation depth. While monopile foundations are used widely around the world in shallow waters (five to 30m), the Tripod is used for deep water (30 to 60m). For depths greater than 60m, floating foundation may be used. Table 2-5 shows the world's largest OWT foundations built by the end of 2018. The table also gives the number of turbines, turbine electrical capacity, foundation type and diameter, and maximum deployment depth. Reviewing the foundation technologies used or announced for OWT foundations up to the year 2020, the primary foundation type used is monopile, and Tripod is the second place, but most popular significant by less popular than monopile foundations. Approximately, 80% of OWT foundations are monopile, 9.1% are Gravity Base, and Tripods account for 5.3% of the 3,313 OWT deployed in European seas up until the end of 2015 (European Wind Energy Association, 2016).

Table 2-5: Largest OWF around the world until the end of 2018, adopted from (WindEurope, 2019, 4C Offshore Ltd, 2018).

Farm name	OWT numbers	Turbine Rate [MW]	Foundation Type/Diameter	depth [m]	Commissioning Year
London array, UK	175	3.6	Monopile (4.7-5.7 m)	25	2012
Gwynty Môr, UK	160	3.6	Monopile (5 m)	28	2015
Greater Gabbard, UK	140	3.6	Monopile (5 m)	32	2012
Westermost Rough, UK	35	6	Monopile (6.5 m)	25	2015
Northwind, Belgium	72	3	Monopile (5.2 m)	29	2014
Global Tech I, Germany	80	5	Tripile	41	2015
Anholt, Denmark	111	3	Monopile (5.4 m)	19	2013
Borkum Riffgrund II, Germany	56	8	Monopile (7.5 m)	28	2018
Walney Extension, UK	87	8	Monopile (7.4-8.4 m)	29	2017

The majority of commissioned, under construction or consented OWT foundations around the world, are in transition water depths that range from10 to 30 meters, see Figure 2-8. All these projects are using monopile as a foundation support structure (4C offshore, 2017). Only one

consented project to be deployed at 55m water depth, representing the maximum depth for a project up until 2020. The OWT project scheme is Beatrice and will be in Scotland's North Sea, and the support structure is a piled jacket (4C offshore, 2017).

Figure 2-8 shows the average water depth and distance to shore for online, under construction and consented offshore wind farms and confirm that the larger wind farms still in the water rage of 10 to 20 meter until the end of 2025.

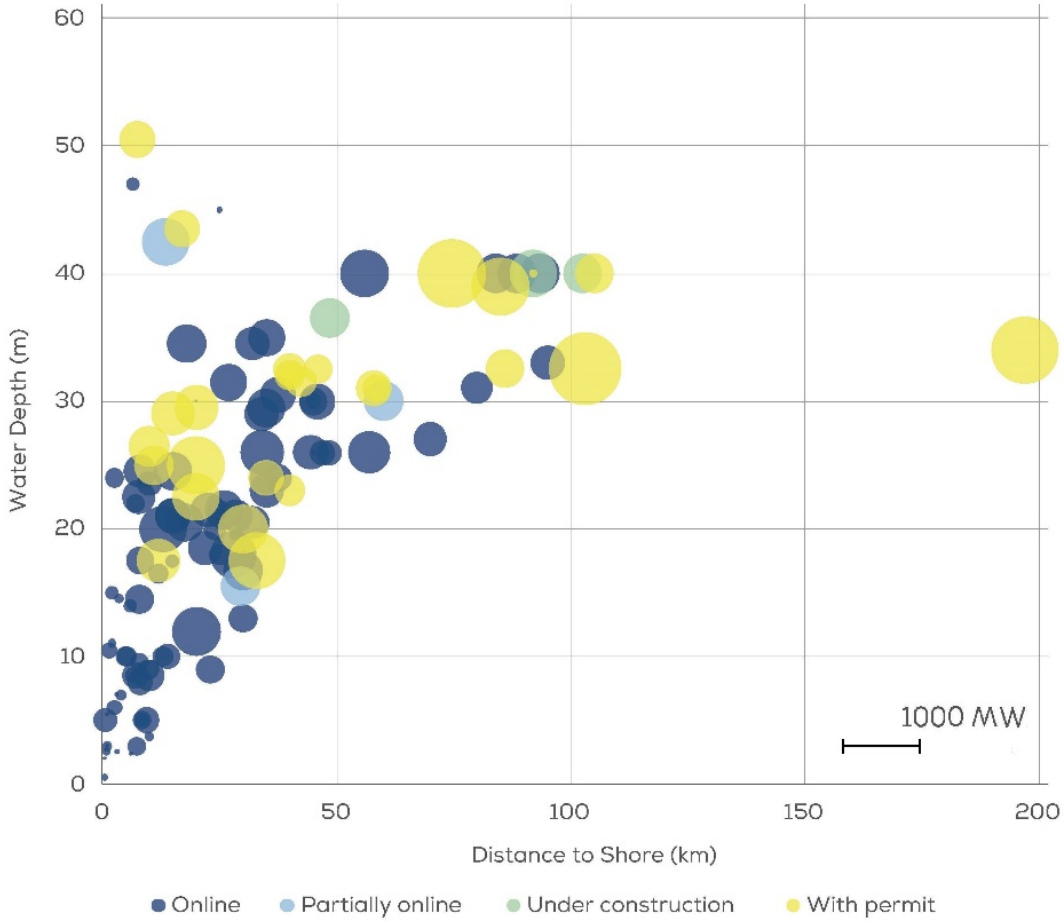

Figure 2-8: The "Average water depth and distance to shore for online, under construction and consented offshore wind farms (bubble size represents the total capacity of the wind farm)", adopted from (WindEurope, 2019).

Most attempts to launch commercial floating OWT foundations are still under development and design, and normally all floating OWT foundations projects consist of one turbine of 2 to 7 MW capacity (Arapogianni et al., 2013). The first commercial offshore wind farm supported by floating foundations is Hywind Scotland Pilot Park, comprising five 6MW turbines, commissioned mid-2018, and supported by a Spar Floater to a water depth of 120m (4C offshore, 2017). Spar floater

is a floating platform, which used originally to support large oil drilling or production operations; spar types and mooring methods are discussed later in section 2.7.6 and shown in Figure 2-11.

2.4.1 Gravity Base Foundations

Gravity base foundations are typically used for OWT in shallow waters less than 15m. The foundation comprises a largely reinforced concrete caisson; see Figure 2-7-C. By the end of 2017, 283 out of 4240 OWT foundations in Europe are Gravity base (Fraile and Mbistrova, 2018), which represents less than 7%, in general, the number of gravity based is decreasing, it was 303 by the end of 2015, where 20 gravity base wind turbines were decommissioned (European Wind Energy Association, 2016). Gravity base foundations resist lateral and rotational displacement due to its mass. The installation process is achieved by pre-casting the foundations as a hollow reinforced concrete case onshore, and then floated to the wind turbine position. Finally, the caisson is backfilled by gravel and or sand. Using a Gravity Base is not an economical solution for water depths more than 20m since the more weight is needed to overcome different lateral forces. Thornton Bank Phase 1 in Germany uses Gravity base foundations despite the deep water depth, which is greater than 20m. This kind of foundations was used because the original monopile design has excessively large due to the weak soil conditions of the site (Peire et al., 2009). The performance of this foundation was enhanced for Thornton Bank Phase 1 by replacing 3.5m of that soil with a ballast layer under the Gravity base foundation.

The available literature for this foundation type is limited compared to monopile, assigns for two reasons: it corresponds to a few challenges in both construction and installation processes, and because offshore wind farms are moving to even deeper water depths. The installation phase of Gravity Base foundations for all project up until 2014 were analysed to identify their common procedures (Esteban et al., 2015). Issues identified included: "seabed preparation, support structure manufacturing, support structure transport, support structure installation, ballasting, and anti-scour protection" during the main installation phases (Esteban et al., 2015). The seabed preparation phase was considered is the most critical disadvantage compared to monopile foundations.

2.4.2 Monopile Foundations

Monopile foundation is a simple structure, which is typically a cylindrical steel pipe that supports a Monopod wind turbine (Figure 2-7-A). The pile depth depends on soil conditions and the depth

of the sand soil layer. It is typically subjected to large lateral displacement, vibration, and torsion due to significant lateral loads and bending moment. The monopile is widely used as a support structure for offshore wind turbines, 81% of OWT foundations installed in Europe are monopile by the end of 2015, while it represents 97% of all installed foundations during year 2015 (European Wind Energy Association, 2016). Nine out of eleven of the largest OWT foundations support structures are monopile in water depths ranging between 19 to 32 m (Table 2-5). A 5 to 7.5 m diameter steel pile is typically needed to support 5MW turbine in shallow waters in the range 15 to 30 m depth. Piles of these size are needed to enhance the bearing capacity to resist high lateral loads from the wind and sea waves (Achmus et al., 2009). A monopile is designed with consideration to two types of stress. First, is the ultimate stresses that the pile can reach due to different load combination (static loads), and the second is the fatigue stress due to cyclic loading (dynamic loads). Despite some difficulties in design and installation, monopile is considered the semi-standard support structure for offshore wind projects around the world.

There is a significant literature for monopile foundations, especially within the last ten years, according to Google Scholar the term ("Monopile" "offshore wind") yields 722 research for the year 2017 alone. Scour protection is a fundamental concern for large number of scholars, for the instance, a computational fluid dynamics (CFD), which is a mathematical numerical method model to analyse the fluid flow behaviour around structures, was used to investigate the seabed stability after installing a monopile (Li et al., 2018). They produce a useful software tool to evaluate the bed shear stress around the monopile and determine the change of the resulted scour due to geometry modification, which could minimize the expected scour, significantly.

2.4.3 Jacket Foundations

Approximately 7% of all OWT are supported by a jacketed structure up to the end of 2017. A jacket structure is a foundation concept developed originally to support offshore oil platforms. This foundation is a steel truss, which is connected to the seabed by short piles (pin piles), see Figure 2-9. Figure 2-9 sketches the main parts of the jacket foundation that supported by four screw piles. The jacket foundations could support offshore wind turbines in water depths up to 60m. The jacket structure may replace the monopile in depths larger than 30 meters; the jacket has high wave load resistance, as the jacket side area facing the waves is significantly small compared to monopile. Jacket structure has also other advantages, which are the wide installation experience gained from oil

platform implementation, and short installation time span compared to other OWT supporting methods.

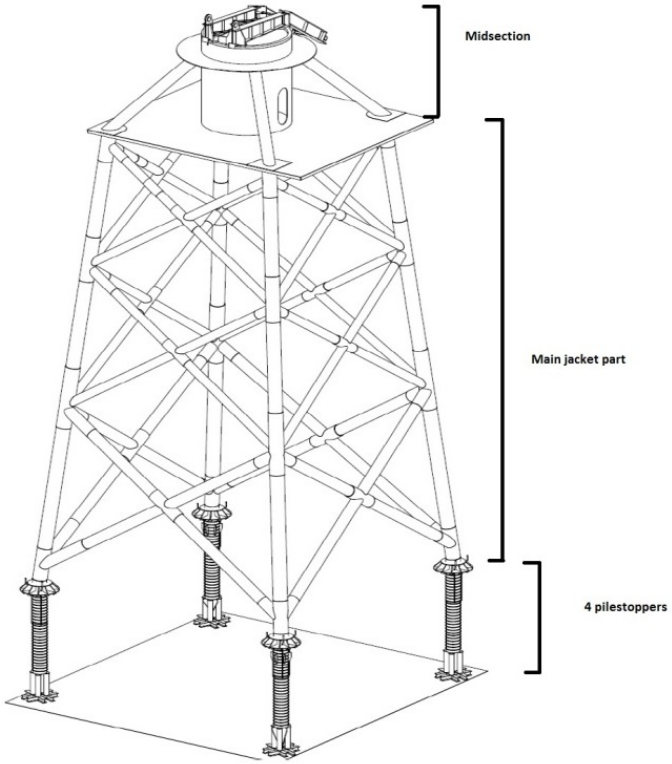

Figure 2-9: Offshore foundation (Jacket type), adopted from (Esteban et al., 2011a).

The main jacket part consists of three or four slender steel pipes connected by a bracing system that works as a stiffener to the jacket legs, as it resists the buckling behaviour of the slender legs (Van Wijngaarden, 2013). The jacket structure is considered economical alternative for deep water depths as it is a lightweight structure that efficiently resists overturning moments (Zhu et al., 2018). Despite this jacket foundations overcome monopile depth limitations, new monopile designs exceeded the 35m water depth threshold, the new projects increased the monopile diameters and reduced the total cost (4C Offshore Ltd, 2018).

2.4.4 Hybrid Monopile Foundation

Offshore hybrid foundation is a foundation that combines two or more different foundation elements. For instance, the hybrid foundation system developed by (Abdelkader, 2015), which is a typical monopile steel foundation attached to a concrete plate to enhance the lateral and rotational

stiffness of the foundation. This type of structure may reduce overall cost, without reducing the performance or the capacity of OWT, according to the author (Abdelkader, 2015). Despite its very low resistance of the water uplifting force, this type of foundation was proven to enhance the rotational stiffness and the moment ultimate loading capacity, which was tested using centrifugal test and ABAQUS simulation programme (Lehane et al., 2014).

The suggested hybrid monopile foundation system can support a 5MW OWT (Abdelkader, 2015). The system consists of a monopod with 6 m diameter attached to a reinforced concrete circular plate with or without ribs. The plate diameter is 12 m or 16 m, then the monopod and the concrete plate connected to a 4 m diameter monopile using cast in place concrete, see Figure 2-10. Figure 2-10 displays the main parts and the installation sequence of the proposed hybrid monopile foundation system. The monopile lengths were 16, 24, and 36 meters long. In order to evaluate the performance of the hybrid system relative to the conventional monopile system, five different foundation systems were analysed.

All suggested dimensions were examined under (ultimate and serviceability static load cases) and calculated the axial and lateral stiffness and capacity of suggested dimensions to compare the effect of his hybrid system with a conventional monopile system. It was found that the axial capacity of the hybrid system is five times greater than the monopile system, while, the lateral capacity is doubled. The Hybrid foundation still needs more studies, especially feasibility study.

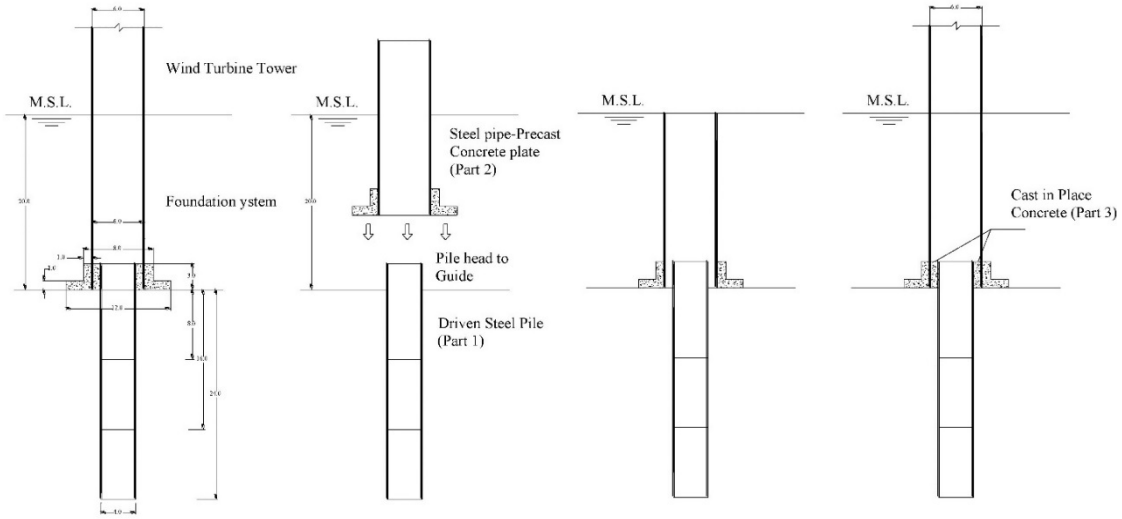

Figure 2-10: The hybrid system installation process, suggested (Abdelkader, 2015).

2.4.5 Tripod Foundations

The Tripod OWT foundation structure is a three-legged-pile (cylindrical steel tubes) to support the Tripod sub-structure, which carries the turbine tower, see Figure 2-7-B. It is used for water depths between 30 and 50m. Although the first Tripod was deployed in 2008, only 175 out of 3,313 of OWT foundations in Europe are Tripod (European Wind Energy Association, 2016). One of the largest OWF around the world uses Tripod, which is "Global Tech I" farm in Germany (European Wind Energy Association, 2016).

2.4.6 Floating Foundations

Floating foundations are used for OWTs in sea depths > 60m; the concept of floating foundation is to fix the OWT on a floating stage and connect the stage to the seabed using flexible steel wires, the wires then fixed to piles, heavy concrete base or anchors, see Figure 2-11. Figure 2-11 demonstrates the three anchoring types of the floating OWT support system structures. The technology of floating OWT is still under research and development.

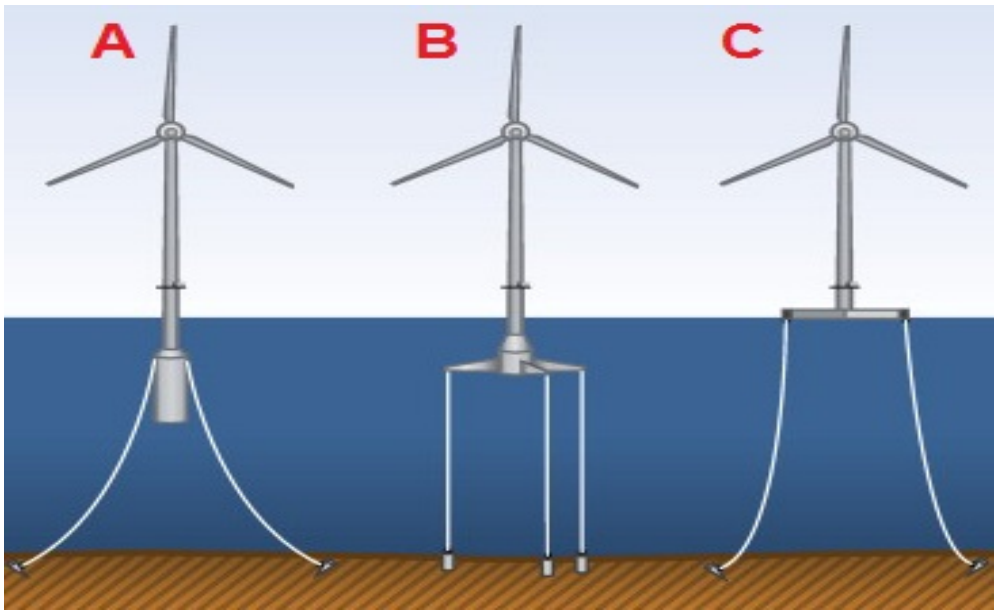

Figure 2-11: Different concepts of floating OWT support structures, adopted from (Hadžić et al., 2014). A) Ballast stabilised "Spar-Buoy" with catenary mooring drag embedded anchors, B) Mooring line stabilised tension leg platform with suction pile anchors. D) Buoyancy stabilised "Barge" with catenary mooring lines.

2.5 Monopile Design

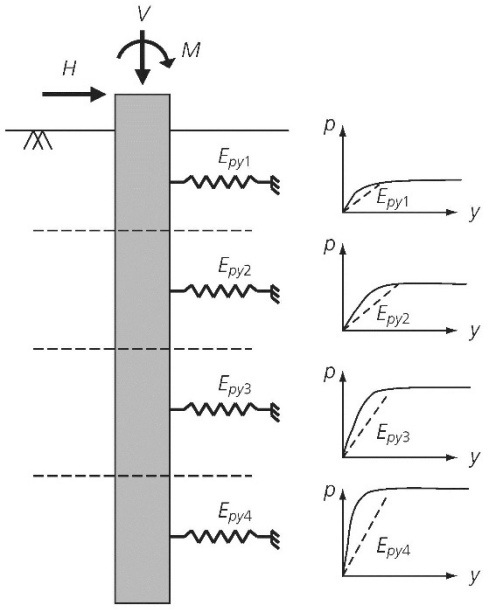

Figure 2-12: The soil behaviour as springs subjected to lateral loads, adopted from (Doherty and Gavin, 2011).

Monopile design is known as the behaviour of a single pile under lateral loads. The very first design standards to design the monopile was adopted from the previous design codes for the oil platforms, for instance, DNV-OS-J101, perhaps the most accessible offshore wind foundation design code, which highly detailed monopile design standards (DNV, 2014). The DNV code employs a Winkler model, which known as *p-y* curves. P-y curves are used to estimate the actual displacement of the monopile (Doherty and Gavin, 2011). This method considers the soil behaviour as a serious of springs that have the stiffness of ($E_s = -p/y$, where p is the lateral load and y is the lateral displacement) (Reese et al., 1974, American Petroleum Institute, 1989), Figure 2-12. Figure 2-12 explains the soil behaviour that subjected to lateral load p. The model was initially built on theoretical assumptions and verified by field full-scale load experiments, the semi-empirical curves shown in Figure 2-12 are divided the penetrated soil into four separate parts, the p-y curve is a piecewise type, which is a horizontal and incline lines connected with a paraplegic one (Matlock and Reese, 1960, Matlock and Reese, 1961).

The main challenge of offshore wind turbine foundation is to safely support all loads (dead, dynamic, and environmental) at the seabed level/Mud Level (ML) without exceeding the allowable

deformation. This challenge can be met if the following three loading states are met (Bhattacharya, 2014):

1. Ultimate Limit State (ULS): This state applies for the ultimate lateral loads from wind and sea waves, especially in extreme events, such as storms or hurricanes, which could be expressed as the combination of the ultimate moment, lateral and axial loads. In this case, the turbine rotor is stopped from moving using brakes to save the turbine from damage.

2. Serviceability Limit State (SLS): The predicted service/environmental loads i.e. wind and wave loads for a whole year are applied on offshore wind turbine (OWT).

3. Fatigue Limit State: The OWT in this state is tested against the fatigue effects. Fatigue effects are expected weakness due to cycle loading. Cycle loading is applying the predicted service wind, waves, and also the expected loads from extreme events for as long as the expected life cycle of the turbine.

The maximum allowable pile head rotation after OWT subjected to ultimate and serviceability static load cases is 0.5 degrees. The maximum cumulative permanent rotation due to cyclic loading over the designed life span of OWT is 0.5 degree (Malhotra, 2011). The maximum allowable pile head lateral and vertical displacements are 6 and 10 cm, respectively (Frank, 2006).

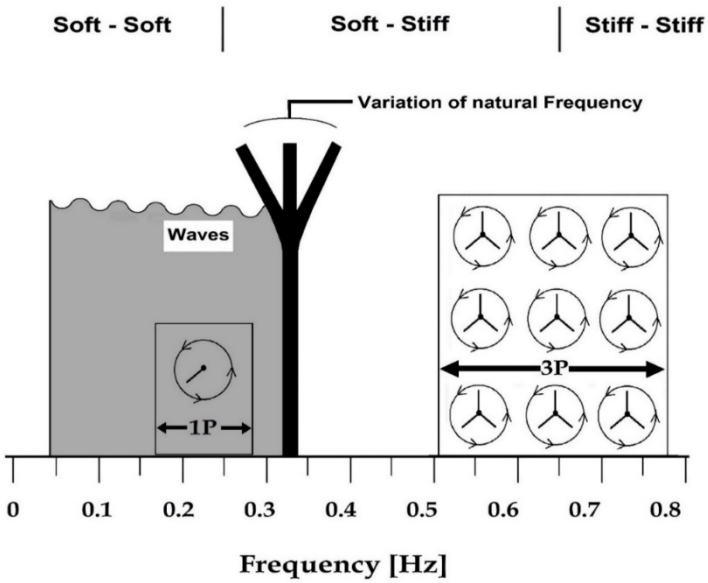

Figure 2-13: Frequency span for foundation, rotors, rotor blades, and waves for a typical offshore wind turbine, adopted from (Malhotra, 2009). P is the blade passing frequency.

Offshore foundations dynamic load capacity is considered in the design process to prevent collapse or damage. The final dynamic frequency of the designed foundation should be in a different frequency than the rotor and the wave frequencies (Malhotra, 2011). The natural frequencies due to sea water wave movement, rotor blade passing and rotor spinning are in a range of (0.04 to 0.34), (0.18 to 0.26 = 1P) and (0.54 to 0.78 = 3P) Hz, respectively (Gaythwaite, 2004), see Figure 2-13. The pervious natural frequencies restrict the foundation designed frequency range to (0.34 to 0.54) Hz, which is relatively stiff. This range will be more expensive to achieve than the flexible foundation (Malhotra, 2011). The semi flexible foundation will need more materials and accuracy to design than the soft flexible one. ABAQUS programme will be used in desgin to secure high accuracy foundations dimensions, as it widely used for these desgin cases.

2.6 Port Feasibility

Comprehensive research to assess the port suitability for the North Sea coast of the United Kingdom to install offshore wind turbines was presented by Akbari et al. (2017). The study used MCDM to rank five Ports, one located in Belgium and four in the UK from the most suitable to the least suitable to install a wind farm in the area of West Gabbard, UK. A detailed questionnaire was accomplished to weigh the criteria suggested by the authors, which was fulfilled by five offshore wind energy experts. The questionnaire includes seventeen criteria to rank the five ports under the investigation.

The paper considered numerous criteria, they analysed all of them as factors, but neglecting that some important factors, such as the quay wall depth, quay load bearing capacity, which are all constraints. These two criteria are constraints because if the port length or bearing capacity is less than the needed requirements, no offshore turbines can be installed from this port, so in that case this port should be excluded from further analysis. In addition, some of the criteria are unrealistic, for instance, the Lo-Lo and Ro-Ro loading techniques are out of date and heavy cranes are mostly used for offshore wind farms at present (DNV-GL, 2016). The authors mentioned that the heavy lifting cranes are used for most of the installation process. The port that finally achieved the highest score was Oostende port in Belgium. However Harwich, UK (ranked 4 in this study) was actually to support the West Gabbard offshore wind farm installation processes (4C offshore, 2017) in 2015. Furthermore, the AHP methodology was used to select the port for maritime transhipment (Chou, 2007), container shipping (Lam and Dai, 2012, Ugboma et al., 2006), commercial shipping lines (Guy and Urli, 2006), deep water shipping (Zavadskas et al., 2015), or port ranking (Asgari et al.,

2015). Reviewing the previous port feasibility confirms that the AHP methodology will be appropriate for port selection for offshore wind installation in Egypt, but considering that port criteria need to be categorise into factors and constraints.

2.7 Offshore Wind Farms Layout Design/Optimisation

Offshore wind farm layout design faces fewer constraints compared to onshore wind farms, but the cost analysis is more complex especially for foundation design and maintenance considerations (B. J. Gribben, 2010). Wind farm layout optimisation aims to gain more energy form a specific onshore or offshore area, which will reduce the final Levelised cost of electricity (LCOE). The second aim is to reduce the impact of the wake effects, which is the turbulence and wind speed reduction due to the impact the proximity of wind turbines on each other. Various methodologies were introduced to optimise wind farm layout design, for instance, a generic model was developed to optimise onshore wind farms (Kusiak and Song, 2010). The model considered that the wake phenomena is expanding linearly to simplify the analysis, the conclusion was that neglecting low presenting wind directions in the wind rose could underestimate the wake loss, which lowers the liability of the layout design in that case. Therefore, all wind directions will be presented in this study layout analysis.

Elkinton et al. (2008) presented an extensive study to compare between five different algorithms of layout optimisation, which are: Gradient search, greedy heuristic, genetic, simulated annealing, and pattern search. The five algorisms have been applied to solve the same problem which is "the design of a small offshore wind farm for the town of Hull, Massachusetts," USA, using real wind data. The comparison concluded that genetic, and simulated annealing are a random, slow, and high quality, while the other algorithms are deterministic, fast, and low quality. Generic and different layout optimisation algorisms are not in the scope of this study, hence a layout software will be used for the layout design.

2.8 Environmental and Social Impact

Kaldellis et al. (2016) compared between offshore and onshore scheme for their environmental and social footprint. The paper considered three impacts of offshore wind farms, which are birds, marine ecosystems, and visual impacts, as the noise from the offshore turbines is remote from population centres and masked by other surrounding noise sources such as sea waves. The study finds that these three expected impacts will be minimised as the offshore farms move further off-

shore and to deeper water depth requiring the turbine hub to be higher. Despite the study being conducted towards the end of 2015, most of its findings were confirmed when the first pilot commercial floating Wind Park was fully commissioned by October 2017 (Afewerki et al., 2018). The park is located 25 km away from the coast, eliminating the visual impact and the floating foundation technology significantly reduce the side effects on marine ecosystems, as the noise, vibration, and water turbulence associated with monopile installation is avoided. In addition, the world's first 12 MW offshore turbine was announced this year 2018 (Hamburg Wind Energy, 2018), the new turbine is 220 m rotor, which requires at least 1.5 km spacing between turbines to allow a safe path for bird migration. Offshore wind farm decommissioning is another environmental impact on the nearby ecosystems and it is still uncertain, as to date, the decommissioning procedure has very limited experience.

Summary

Relevant literature to the research topics is reviewed in this chapter. The leading case study (Egypt) background is introduced, which includes its location, features, current energy status, and previous wind studies. The second wider study case (Arabian Peninsula) is presented as the first case study. In addition, a comparison between onshore and offshore wind energy is briefed, succeed by defining some of the methods used for spatial siting. Recent onshore and offshore wind siting studies are summarised and compared in one table to this study methodology. The literature for spatial wind siting concludes study cases from Europe, Asia, and the USA and varied from the year 2001 to 2017. General approach was conducted for the previous studies and summaries in four procedures. Finally, an appropriate survey is presented to establish a clear understanding of the technologies needed for anchoring offshore wind turbines. Other related literatures for port feasibility, layout design, and environmental impact are presented.

Conclusions

- The rapidly growing electricity demand in Egypt is currently addressed by building more thermal power plants.
- The wind atlas of Egypt indicates the high potentials of wind energy in the Gulf of Aqaba and Gulf of Suez offshore regions.
- As can be seen from the above, there is a gap in addressing the wind renewable energy resource mapping in Egypt, and especially offshore wind. The aim is to address this gap through systematic analysis based on well-understood approaches developed for other global sites. Moreover, reviewing the previous studies in Egypt indicates that offshore wind potentials are exceptional and worth further research.
- The 2030 renewable energy targets for most of the Arabian Peninsula countries are ambitious, but the present renewable energy provisions in these countries is near to zero present, which needs more realistic studies and efforts to support these targets.
- The offshore wind potential is much higher than onshore wind and has fewer restrictions, which will narrow the gap in cost shortly.
- GIS-based MCDA could be able to assist offshore wind spatial siting strategies. A gap in the offshore wind methodologies and their case studies in developed countries is observed.
- Monopile is the dominant foundation system solution around the world, despite some expectation that Jacket structure may dominate by 2020. Monopile designs exceed the 30m water depth in three commissioned projects.
- Moving towards even deeper water depths > 50 meter requires more development for floating foundation solutions to become more commercially viable.
- Floating foundations are still under research and devolvement, and considerable research is currently being undertaken to support their commercialisation.
- Hybrid foundation solution needs a fundamental research to be applicable, and to the author's knowledge, there are no plans to build a 1:1 Hybrid foundation prototype in place.
- AHP is a considered suitable methodology for identifying suitable port sites for supporting offshore wind farms developments.

Chapter 3: Methodology

This chapter addresses the methodology used in the thesis. It covers the analytical hierarchy process (AHP) and the definitions and provides an outline of the processes undertaken to achieve the research aims and objectives.

3.1 The Analytical Hierarchy Process (AHP) Definitions

Analytical hierarchy process (AHP) is a technique used to organise and create weighted criteria to solve complex problems. The first step of the AHP is to define the problem and the branch of science it relates to, and then specify the different criteria involved in the decision-making processes. All the criteria should be specific, measurable, and accepted by stakeholders/researchers or used successfully in similar existing problems. Each criterion could be a factor or a constraint. The next step in the analysis is to find the different relative importance of the factors. The last step is to evaluate all the potential solutions of the problem, and arrive at a solution by selecting the one with highest score. Figure 3-1 illustrates the spatial siting process for offshore wind energy used in this study.

Two efficient ways to solve a multi criteria problem were suggested by Saaty (2008). The first is to study the problem and its characteristics, then arrive at specific conclusions through the different observations undertaken by the study. The second is to compare the study under evaluation with similar problem that has accurately been solved already. In this work, the second approach was selected to define the criteria required using the learning from onshore wind spatial siting provided in the literature to solve the offshore siting problems (see Approaches Utilised in Siting of Wind Farms, part 2.3.4).

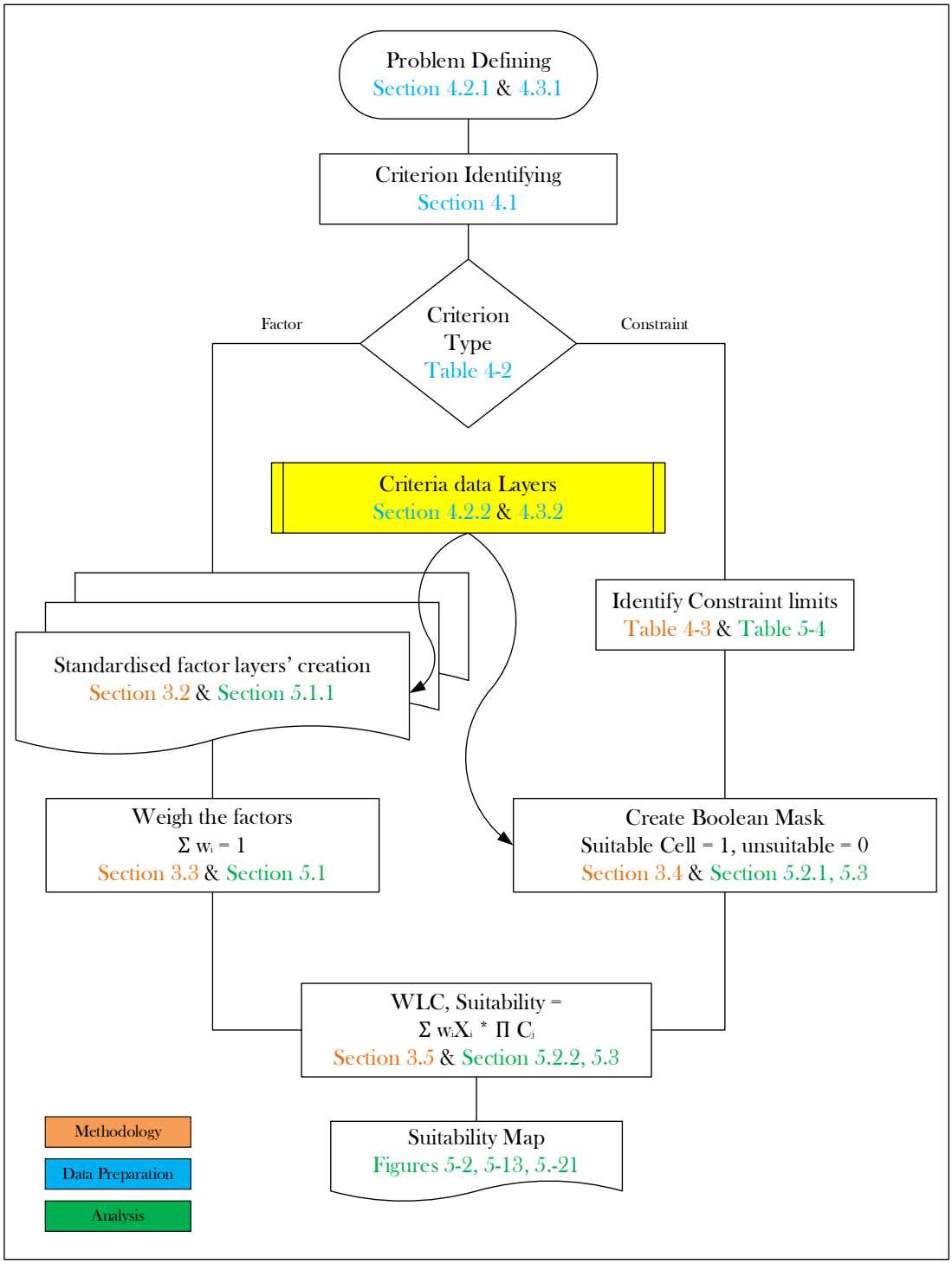

Figure 3-1: Diagrammatic representation of the methodology developed to be used in spatial siting of the offshore wind farms.

Criterion could be a factor or a constraint per the definitions below:

Factors are the criteria that have a cost/benefit relationship with the problem alternatives/suggested solutions. For example, with reference to an offshore wind site, a small distance to shore will be more suitable, as it will reduce the total cost) for deployment of an offshore wind farm, and vice versa. Factors have different categories of measurable units such as (meter, degree, m/s, etc.) or objective measures (very bad – bad – acceptable – good – very good, etc.).

Constraints correspond to the criteria that eliminate the alternatives, it accomplishes the limitations or restrictions of the constraint (gate criteria), creating a true/false relationship. For instance, if the law prevents constructing offshore projects in say, a national marine reserve park, this area will be excluded as a possible solution. Constraints have the same priority, while factors have different weights. Constraints are applied using Boolean logic, "0 or 1". Zero values are when the constraints are true, and vice versa.

3.2 Factor Standardization

Variable methods are utilised to calculate the relative importance/weight of the criteria, such as simple weighting from ranking, ratio weighting, pairwise comparison, simple additive weighting (SAW) method, weighted product method, or median ranking method (Yoon and Hwang, 1995). In this work, due to its dominant applicability in spatial decision-making problems (Akbari et al., 2017), the pairwise comparison method was chosen to find the relative importance. Furthermore, factors have different "measuring" and "objecting" units, so there is a need to unify all factors to the same scale. In order to standardise the processes, a continuous scale (from 0 to 255 (Eastman, 2006)) or (from 0 to 1 (Eastman, 1997)) with 0 for the least suitable measure and 255 or 1 for the most suitable one, is suggested, which is named as the "Non-Boolean Standardisation".

3.3 Pairwise Comparison

In the AHP analysis, the Pairwise Comparison method is used to weigh the different factors, which was developed by (Saaty, 2008, Saaty, 1977). The method depends on comparing factor pairs, as every two different factors considered a pair. In order to address the importance of the factors used and compare them in pairs, the Importance Index is introduced (Saaty, 2008), which is critical in determining the relationship and importance between factor pairs. The pairwise comparison

process is undertaken by linking factor pairs to the Importance Index. Table 3-1 expresses the definitions and the explanations of the intensity of importance scales used to indicate pairwise comparison values between factor pairs. The Importance Index scale starts with a score of one for a pair where both factors are of equal importance and ending with a score of nine, wherein the first factor is of extreme importance compared to the other.

Table 3-1: The Importance Index scale adopted from (Saaty, 2008).

Importance Index	Definition	Explanation
1	Equal Importance	Two activities contribute equally to the objective
2	Weak or slight	
3	Moderate importance	Experience and judgement slightly favour one activity over another
4	Moderate plus	
5	Strong importance	Experience and judgement strongly favour one activity over another
6	Strong plus	
7	Very strong or demonstrated importance	An activity is favoured very strongly over another; its dominance demonstrated in practice
8	Very, very strong	
9	Extreme importance	The evidence favouring one activity over another is of the highest possible order of affirmation

The Importance Index can be chosen using personal judgment, experience, or knowledge (see Equation 3-1). The process is accomplished by building the pairwise comparison matrix P_w (see Equation 3-1), which has equal rows and columns, the number of rows (columns) equal to the number of the factors. If the factor in the left side of the matrix has higher importance compared to the top side factor, the matrix relevant cell will assume the value assigned in the scale of intensity of importance value assigned in Table 3-1. For the opposite case, the cell is equal to the inverse of the scale value, Equation 3-2.

A new normalised matrix N_w can be created by taking the sum of every column and then dividing each matrix cell by its total column value, Equations 3-3 and 3-4. Finally, the weight/priority W_i of each factor is equal to the average of its row in the new matrix; the aggregation of all factor weights equals to one (see Equations 3-5 and 3-6).

$$P_w = \begin{bmatrix} a_{11} & a_{12} & \cdots & a_{1n} \\ a_{21} & a_{22} & \cdots & a_{2n} \\ \vdots & \vdots & \ddots & \vdots \\ a_{n1} & a_{n2} & \cdots & a_{nn} \end{bmatrix} \qquad (3-1)$$

Where: n is the number of factors.

$$a_{ks} = \begin{cases} 1,2,..,9, & if \ [k > s] \\ 1, & if \ [k = s] \\ 1/a_{ks}, & if \ [k < s] \end{cases} \qquad (3-2)$$

Where: (k, s) represent the factor pair.

$$X_i = [x_1 \quad x_2 \quad \cdots \quad x_n] \qquad (3-3)$$

Where: $x_1 = a_{11} + a_{21} + ... + a_{n1}$, and so on.

$$N_w = \begin{bmatrix} A_{11} & A_{12} & \cdots & A_{1n} \\ A_{21} & A_{22} & \cdots & A_{2n} \\ \vdots & \vdots & \ddots & \vdots \\ A_{11} & A_{11} & \cdots & A_{nn} \end{bmatrix} \qquad (3-4)$$

Where: $A_{11} = a_{11}/x_1$, $A_{11} = a_{12}/x_2$, $A_{nn} = a_{nn}/x_n$, and so on.

$$Z_i = [z_1 \quad z_2 \quad \cdots \quad z_n] \qquad (3-5)$$

Where: $Z_1 = A_{11} + A_{12} + ... + A_{1n}$, and so on.

$$W_i = [w_1 \quad w_2 \quad \cdots \quad w_n] \qquad (3-6)$$

Where: $w_1 = z_{11}/n$, $w_2 = z_2/n$, $w_n = z_n/n$ and so on.

Consistency Ratio (CR) was suggested by (Saaty, 1977) to validate the "intensity of importance" assumptions, therefore, if the CR for the final matrix is greater than 0.1, it should be rectified. CR is given by:

$$CR = CI \ / \ RI \qquad (3-7)$$

Where **RI** is the Random Consistency Index and its value depends on the factor number n, (see Table 3-2). CI is the Consistency index given by:

$$CI = (\lambda_{max} - n) / (n - 1) \qquad (3-8)$$

Where λ_{max} is the Principal Eigen value, which equals to sum of the product of final factor weight and the summation of its column in the pairwise matrix (first matrix), (see Equation 3-10).

$$\lambda_{max} = \sum_{i=1}^{n} X_i * W_i \qquad (3-9)$$

Table 3-2: The Random Consistency Index **RI** values adopted from (Saaty, 1977).

n	1, 2	3	4	5	6	7	8	9	10	11
RI	0	0.58	0.9	1.12	1.24	1.32	1.41	1.45	1.49	1.51

3.4 Boolean Mask

To identify a suitable cell, a Boolean Mask is applied before the aggregation process is conducted, so that restricted cells are eliminated. Boolean overlay, in which Boolean relationships such as (And, OR, or Not) are applied to achieve a specific decision with "0 or 1" as a resulting value. The result is a map with only two colours, one is for the restricted areas, and the other represents unrestricted areas. The Boolean overlay is suitable for simple and quick spatial decisions, such as which offshore areas are not restricted and can be developed. In Figure 3-2, the Boolean map shows two colours, the black one is for the unsuitable area and the blue one is for the suitable area. While the WLC displays many different colours, the black one is for the less suitable area, the green for the most suitable area, and the other colours are for suitably scores in between.

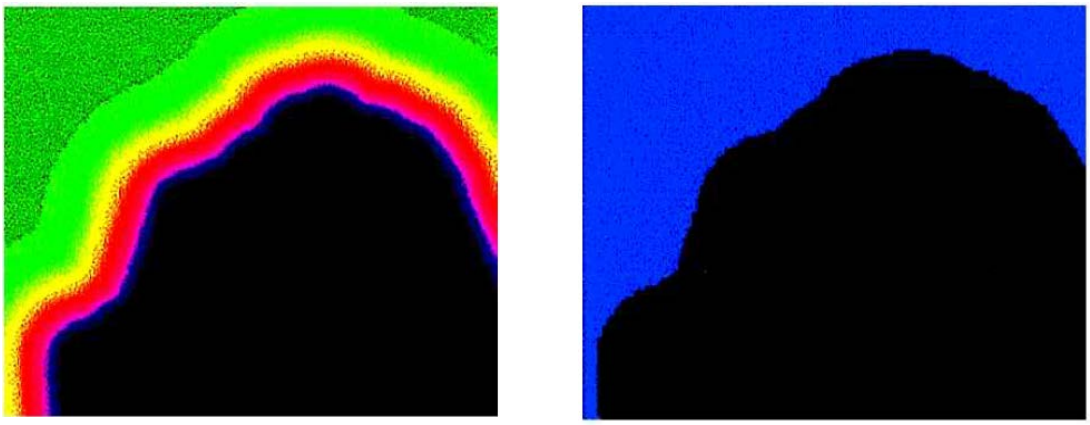

Figure 3-2: The difference between Boolean overlay map (left) and WLC suitability map (right) adapted from (Jiang and Eastman, 2000).

The government regulations have a role to play in the analysis that will be taken into account by converting the regulations into restrictions in the analysis from the start of site consideration (Boolean Mask). The applied Boolean mask fulfils the role of such regulations, providing a generic approach applicable widely in any jurisdiction. The Boolean mask outcomes are unique outputs that differ from location to location, e.g. UK, Egypt, and Arabian Peninsula models considered in this work. On the contrary, factors are not affected by government regulations, for example, water depth, distance to grid, distance to shore, and wind speed factors of the offshore wind energy spatial siting are inherent to the sites and therefore represent the technical aspects of the analysis.

3.5 Weighted Linear Combination (WLC)

Weighted Linear Combination (WLC) is the last step in AHP to find the optimal solution. The WLC method combines the standardised factors after multiplying each factor by its own weight and finally multiplying the result map with a Boolean mask produced by multiplying all the constraints together. The resultant map is called the Suitability Map; see Figure 3-11 for a wider explanation. The WLC equation (Eastman et al., 1998), used to calculate the suitability map is given by:

$$Suitability = \left(\sum_{i=1}^{n} W_i X_i\right) \times \left(\prod_{j=1}^{l} C_j\right) \qquad (3-10)$$

Where: w_i = weight assigned to factor I, X_i = criterion score of factor I, n = number of factors, C_j = constraint j (Boolean Mask j), Π = product of constraints, and ℓ = number of constraints.

3.6 The Representative Cost Ratio (RCR)

The new term *Representative Cost Ratio* (RCR) is introduced to facilitate the determination of the Importance Index and the evaluation of offshore wind energy projects overcoming current methods which are time consuming and less robust. The following steps in the methodology will now provide an approach to estimate these relationships and the values for both the Importance Index and RCR.

The relationship is gained through analysis of data from the literature to assess the onshore wind energy potentials (Latinopoulos and Kechagia, 2015, Baban and Parry, 2001, Watson and

Hudson, 2015), as to the author's knowledge, this work provides the first consideration of offshore wind energy farm siting using AHP and the RCR. Watson and Hudson (2015) considered the opinion of five experts to estimate the relevant Importance Index of six factors to, which are wind speed, distance from historically important areas, distance from residential areas, distance from wildlife designations, distance from transport links, and distance from the network connection. The other two studies (Latinopoulos and Kechagia, 2015, Baban and Parry, 2001) have used their experience and judgment to arrive at an appropriate and relevant Importance Index of each factor pair related to urban studies. These three studies are independent from each other; their work encompassed generic approach for siting of wind farms at different locations (Kozani of Greece, onshore areas of England, and South Central England of the UK) (Latinopoulos and Kechagia, 2015, Baban and Parry, 2001, Watson and Hudson, 2015) . The authors used similar factors (some with more than ten factors) and the same range of the RCR; see Table 3-3 and Figure 3-3. In essence, these three studies, conducted by different scholars, covered different study areas and time conducted. These authors did not rely on each other's work, yet the authors arrived at the same range of RCR for the different locations considered. Hence, factors could be applied at any locale.

Table 3-3 is based on data from the aforementioned studies (Latinopoulos and Kechagia, 2015, Baban and Parry, 2001, Watson and Hudson, 2015) which are used to determine the appropriate RCR range for each Importance Index (1~9). The factor pairs determined from these studies is shown in column A of Table 3-3. RCR is the ratio of factor pairs contribution to the final Levelised Cost of Energy (LCOE) of the project. To estimate RCR for this case, the LCOE given in Table 3-4 is used, by using the ratio between pairs. For example, the Wind Speed Vs Residential Areas Proximity is 52.2:16.2 giving a value of 3.2 in Table 3-3 Column C, and so on. In order to determine the values of the Importance Index in Column B; the pairwise comparison method mentioned above was used. The pairwise matrix and the normalised matrix for onshore wind spatial siting study of Watson and Hudson (2015) are given in Table 3-5 and 3-6 respectively.

Table 3-3: Process of obtaining the RCR range from previous onshore wind studies (Watson and Hudson, 2015) and (Latinopoulos and Kechagia, 2015, Baban and Parry, 2001).

(A) Factor Pair	(B) Importance Index	(C) RCR (Stehly et al., 2016)	(D) Appropriate RCR Range
(Watson and Hudson, 2015)			
Wind Speed vs Residential Areas Proximity	4	52.2/16.2 = 3.2	3~4
Wind Speed vs Wildlife Designations Proximity	5	52.2/12.8 = 4.1	4~7
Wind Speed vs Network Connection Proximity	5	52.2/10.3 = 5.1	4~7
Wind Speed vs Transport Links Proximity	6	52.2/07.3 = 7.2	7~10
Wind Speed vs Historical Areas Proximity	9	52.2/01.2 = 44	> 18
Residential Areas vs Wildlife Designations	2	16.2/12.8 = 1.3	1~2
Residential Areas vs Network Connection	2	16.2/10.3 = 1.6	1~2
Residential Areas vs Transport Links	3	16.2/07.3 = 2.2	2~3
Residential Areas vs Historical Areas	8	16.2/01.2 = 14	13~18
Wildlife Designations vs Network Connection	2	12.8/10.3 = 1.5	1~2
Wildlife Designations vs Transport links	3	12.8/07.3 = 2.1	2~3
Wildlife Designations vs Historical Areas	7	12.8/01.2 = 11	10~13
Network Connection vs Transport Links	2	10.3/07.3 = 1.4	1~2
Network Connection vs Historical Areas	6	10.3/01.2 = 8.5	7~10
Transport links vs Historical Areas	5	07.3/01.2 = 6.1	4~7
Approaches and data from references (Latinopoulos and Kechagia, 2015, Baban and Parry, 2001)			
Land Use vs Road Network Proximity	3	16.2/07.3 = 2.2	2~3
Land use vs Natural Areas Proximity	2	16.2/12.8 = 1.3	1~2
Natural Areas vs Road Network Proximity	3	16.2/07.3 = 2.2	2~3
Urban Areas vs Historic Sites	7	16.2/01.2 = 14	10~13
Roads vs Historic Sites	6	10.3/01.2 = 8.5	7~10

Interpolation is used to arrive at the range for RCR (Figure 3-3) with the results shown in Column D of Table 3-3. For example, the Importance Index for the Wind Speed vs Residential Areas Proximity pair is 4 and from Figure 3-3, this is in the RCR range of 3 ~ 4, and so on. It must be noted that the last five rows of Table 3-3 are from (Latinopoulos and Kechagia, 2015, Baban and Parry, 2001) and are included here to illustrate the process of estimating RCR, based on factor pairs representing land use and urban areas, etc.

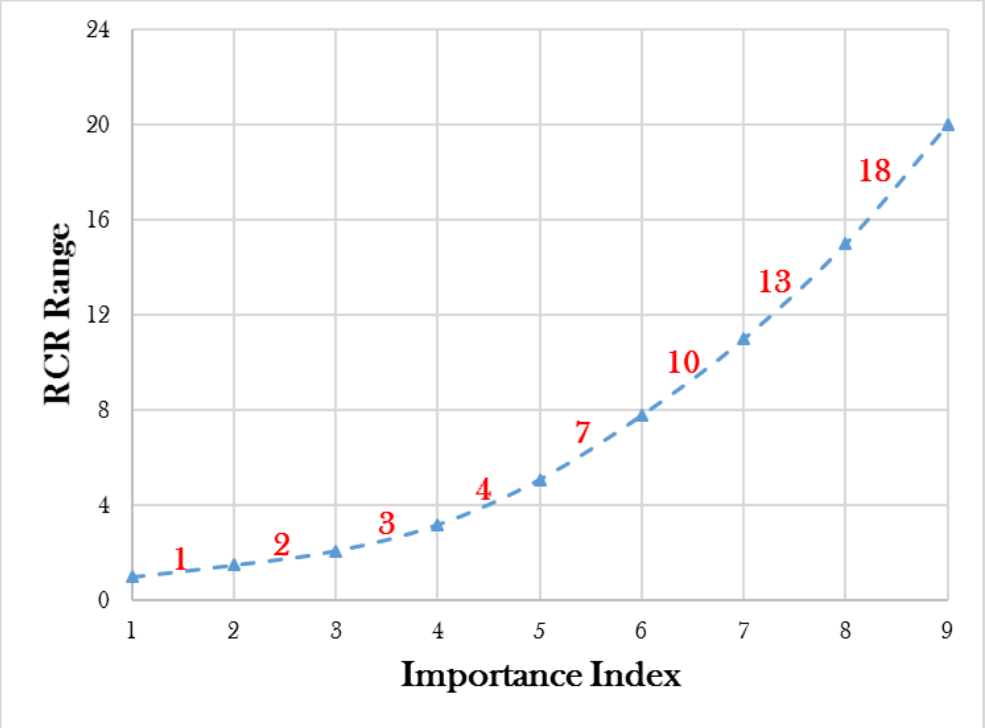

Figure 3-3: The interpolation curve to determine the RCR range (red numbers show RCR range).

Table 3-4: The LCOE contribution to a 2.16 MW Land-Based Turbine, adopted from (Stehly et al., 2016).

	Wind Speed	Residential Area Proximity	Wildlife Proximity	Network Proximity	Transport Links	Historical Sites	Total Cost
LCOE* [$/kWh]	830	258	116	164	203	19	1590
LCOE [%] = (Factor/Total Cost)	52.2	16.2	7.3	10.3	12.8	1.2	

*LCOE [$/kWh] = The Redistribution readjustment number to meet the total capital expenditures.

The Principal Eigenvalue λ_{max} is determined by the product of the factor sum (total) of each column of the pairwise matrix (Table 3-5) and the Factor Weight value (Table 3-6). For example, for the wind speed factor, λ_{max} = 1.93 x 0.512 = 0.99 and so on for the other values.

Table 3-5: The pairwise matrix for onshore wind spatial siting.

	Wind Speed	Residential Area Proximity	Wildlife Proximity	Network Proximity	Transport Links	Historical Sites
Wind Speed	1	4	5	5	6	9
Residential Areas Proximity	1/4	1	2	2	3	8
Wildlife proximity	1/5	1/2	1	2	3	7
Network Proximity	1/5	1/2	1/2	1	2	6
Transport Links	1/6	1/3	1/3	1/2	1	5
Historical Sites	1/9	1/8	1/7	1/6	1/5	1
Sum	1.93	6.46	8.98	10.7	15.20	36.00

In order to ascertain the validity of the assumptions made, the magnitude range of the Consistency Ratio CR (Equation 3-7) should be less than or equal to 0.1. The Consistency Index, *CI*, using Equation 3-8 has a value of 0.0185 since $\Sigma\ \lambda_{max} = 6.09$ from Table 3-6 and n=6. The Random Consistency Index, *RI*, for the six factors has a value of 1.24, (Saaty, 1977). Using these values in Equation 3-7, *CR* has a value of 0.0149, which is < 0.10. Hence, values in Table 3-5 are consistent (Saaty, 2008). The final range of RCR and the corresponding Importance Index are shown in Table 3-7, the table will be used later in Chapter 5 to calculate the factor weights that control the decision making of offshore wind energy spatial siting.

Table 3-6: The normalised matrix for onshore wind spatial siting.

	Wind Speed	Residential Area Proximity	Wildlife Proximity	Network Proximity	Transport Links	Historical Sites	Factor Weight	λ_{max}	Error
Wind Speed	0.52	0.62	0.56	0.47	0.39	0.25	0.512	0.99	0.04
Residential Areas Proximity	0.13	0.15	0.22	0.19	0.20	0.22	0.178	1.15	0.07
Wildlife Proximity	0.10	0.08	0.11	0.19	0.20	0.19	0.135	1.22	0.01
Network Proximity	0.10	0.08	0.06	0.09	0.13	0.17	0.092	0.99	0.05
Transport Links	0.09	0.05	0.04	0.05	0.07	0.14	0.058	0.88	0.01
Historical Sites	0.06	0.02	0.02	0.02	0.01	0.03	0.024	0.88	0.02
Sum	1.00	1.00	1.00	1.00	1.00		1.00	6.09	

Note: Average Error is 0.01

Table 3-7: The Importance Index and the corresponding RCR range.

Importance Index	1	2	3	4	5	6	7	8	9
RCR Range	(0~1):1	(1~2):1	(2~3):1	(3~4):1	(4~7):1	(7~10):1	(10~13):1	(13~18):1	18>:1

3.7 Approach Used in the Spatial Planning for Offshore Wind Energy

The alternatives of spatial siting problem consist of a small unit called "cell or pixel". The study area map is then divided into an equal size grid where each pixel on the grid is a cell/alternative. The process applied to the mapped cells is Boolean Mask, factor aggregation and the final WLC aggregation. Figure 3-4 shows a simple map consisting of nine cells (9 alternatives); the final decision to locate the most suitable cell has five criteria to devise. The decision-making involves evaluating the cells using two factors and three constraints. Factors are X_1, which weights of 0.8 and X_2, which weights of 0.2; constraints are C_1, C_2, and C_3. The first part of equation 3-3 is applied to aggregate the factors considering its weights for each cell, then; the constraints value is multiplied to produce the Boolean mask. Finally, the two parts are multiplied to estimate the final decision. The most suitable cell (alternative) in this example has a score of 0.7 (green colour cell).

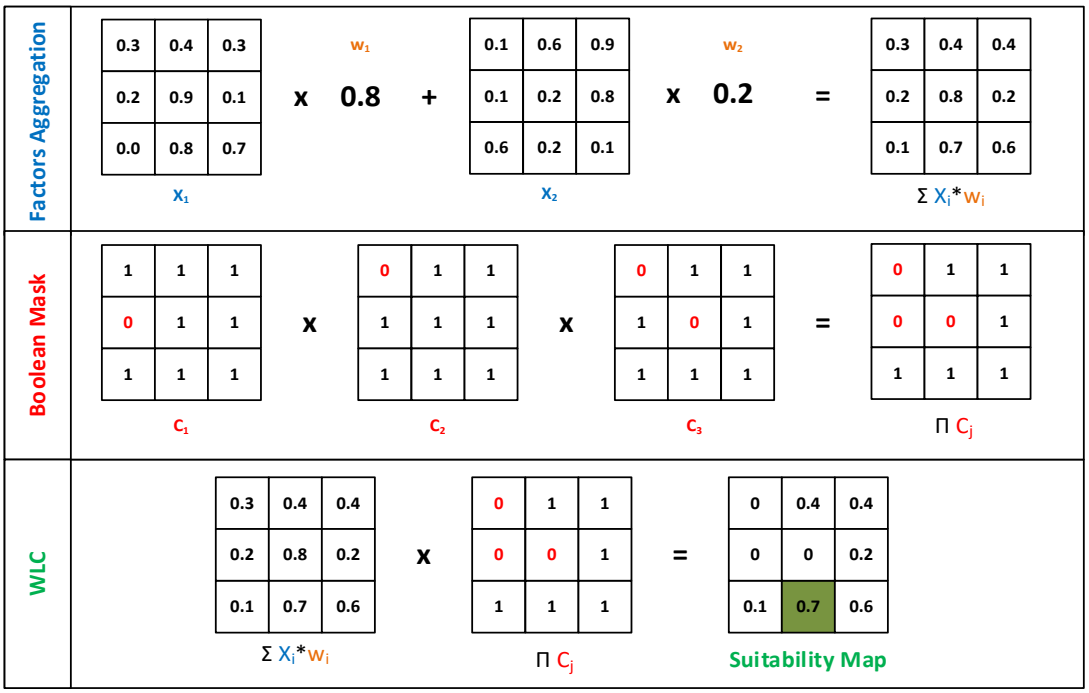

Figure 3-4: Simple illustration sketch to explain the spatial siting process using AHP technique.

In this work, a combination of the approaches discussed above such as (AHP, pairwise comparison, standardised scale, WLC, and Boolean overlay) were used. They provided the basis to develop the models into two software packages - Microsoft® EXCEL, used to complete pairwise process, and ArcGIS, used to configure, design, input, manage, display, manipulate, digitise, and analyse the spatial data. In addition, ArcGIS was used to perform other procedures, such as data processing, factor standardisation, Boolean mask, and WLC aggregation. Additional ArcGIS Tools and commands were also used, such as: Georeferencing toolbar, Euclidean Distance, Feature Toolbar, Feature to Raster Tool, Fuzzy Membership, Fuzzy Overlay Tool, and Weighted Sum Tool, full details can be found in (Esri, 2012).

Below are summaries of the various toolbars utilised in the analysis:

Georeferencing toolbar: was used to georeference the scanned maps, satellite images, or aerial photographs, using controlled point (point on the map ground level) technique, which uses two or more of controlled points to restructures distorted images or scanned maps to be fit into the used geographic projection (Esri, 2012).

Euclidean Distance: calculates the Euclidean distance from the cell to its closest source (Esri, 2012).

Feature Toolbar: creates and modifies wider classes of shapes that could represent a point on map, line, or polygon (Esri, 2012).

Feature to Raster Tool: used to convert any features to a raster data set (Esri, 2012).

Raster Calculator: performs and builds most common basic Algebraic calculations between layers (Esri, 2012).

Fuzzy Membership: converts raster layer information to a standardized scale from 0 to 1 (Esri, 2012).

Fuzzy Overlay Tool: used to combine different fuzzy membership layers together (Esri, 2012).

Weighted Sum Tool: overlays factors layers, multiplying each by their calculated relative weight, and then aggregate them together (Esri, 2012).

3.8 Approach Used in the Monopile Foundation Design for Offshore Wind Turbines

The monopile design is a multistage process that begins with collecting the appropriate soil properties for sites identified by the AHP methodology. Second, is to distinguish the loads that affect the monopile and finally, and then, applying this information to a suitable numerical design analysis programme such as ABAQUS or PLAXIS to check that the settlement resulting from applied loads are less than the allowable settlement.

ABAQUS software is a finite element modelling programme used widely to analyse pile behaviour in different soil types (Jung et al., 2015). Soil is described or represented in the finite element model by different parameters, such as friction angle (φ), submerged unit weight (γ_{sub}), modulus of elasticity (E_s), Poisson's ratio (ν), dilation angle (ψ), and maximum yield stress (f_y).

The cone penetration or cone penetrometer test (CPT) is the common offshore geotechnical investigation method (Seed and De Alba, 1986). The CPT is in-situ test, where a steel rode is pushed through the soil strata until it hits a hard layer. The steel has a cone tip, which contains measuring systems that logs the soil resistance E_s and friction φ.

Despite the high accuracy of CPT test, it is not common in Egypt due to the high cost to perform the test. Therefore, for sandy soils of the chosen sites, E_s and φ parameters are driven from N values of Standard Penetration test (SPT) (Seed and De Alba, 1986). N values is the number of blows need to penetrate the soil service by a standard slide hammer with standard weight and falling distance (Clayton, 1995).

Soil **angle of friction** (ϕ) is derived from the Mohr-Coulomb failure circle; it describes the shear friction resistance between small particles of soil under a normal effective stress. **Poisson's ratio** (ν) is the ratio between horizontal strain to the vertical strain under a stress within the elastic stat of the soil. **Modulus of elasticity** (E_s), called also as Young's modulus, which is the soil stress to its strain, also within the elastic state of the soil. The **dilation angle** (ψ) "controls an amount of plastic volumetric strain developed during plastic shearing and is assumed constant during plastic yielding" (Bartlett, 2010). For sandy soil (non-cohesive sediment), the dilation angle (ψ) relies on the friction

angle (ϕ) of the soil. For sand with $\phi > 30°$ the value of the dilation angle can be estimated as $\psi = \varphi - 30°$, $\psi = 0$ in case of negative values of dilation angle (Bartlett, 2010).

3.9 Approach Used in Layout Optimisation

The WindFarmer software programme was utilised for farm layout optimisation. The software was developed by the DNV-GL (GL-Energy, 2014) to design wind farms (onshore and offshore). The aim is to provide optimised outputs to increase the power produced by wind turbines, and decrease the negative impacts on surrounding environment. The designed the software take advantage of DNV-GL expertise gained from over 25 years in wind energy industry.

The software estimates the energy yield from different offshore wind farm layouts optimised for cost and requires the user to identify geological, environmental, turbine spacing and any locked position for turbines (places where turbines cannot be located), to optimise the most productive layout.

WindFarmer in common with most of wind farms power generation evaluation programmes, such as, WAsP (developed by Risø) (Acker and Chime, 2011), WindPRO (devolved by EMD International) (WindPRO, 2015) and OpenWind (developed by AWS Truepower) (Brower and Robinson, 2012), uses the Park wake model, which expresses the wake profile as a piece-wise linear function (Park and Law, 2015). Further discussion about the Park model is in section 3.4.4.

WindFarmer was chosen to undertake the analysis due to its global utilisation and is the de-facto standard software for this research.

3.9.1 WindFarmer Theory and Assumptions

The WindFarmer software can be used to plan the optimum layout of an offshore wind farm to exploit the maximum available wind energy resource, utilising available wind data and environmental constraints of the chosen sites. The software has three main calculation phases, which are wind flow model, energy calculations, and Park model (GL-Energy, 2014).

3.9.2 Wind Flow Model

The wind flow model assumes that wind speed changes in a linear way to terrain height. The relationship between them is expressed by the following equation:

$$S_{terrain} = 1 + 0.001 \times \Delta_z \qquad (3-12)$$

Where: $\mathbf{S_{terrain}}$ is terrain wind speed-up factor and, $\mathbf{\Delta z}$ is the difference of altitude in meter for terrains with slip less than three degrees.

For the next step, the model will compute the new wind speed at the hub height of the wind turbine using the following wind shear equation:

$$S_h = \frac{\ln\left(\frac{z_h}{z_0}\right)}{\ln\left(\frac{z_m}{z_0}\right)} \qquad (3-13)$$

Where: $\mathbf{S_h}$ is hub wind speed factor, $\mathbf{z_h}$ is the hub height above zero level, $\mathbf{z_m}$ is the mast height, which wind speed was measured, $\mathbf{z_0}$ is the roughness length. Mast station is a tall tower equipped with different meteorological instruments to measure wind speed, wind direction, temperature, pressure, etc.

The final step in the wind flow model is to calibrate the energy yield. This step is achieved by calculating the calibration factor C:

$$C = \sum_t \frac{E_a - E_c}{S_t} \times W_t \qquad (3-14)$$

Where: $\mathbf{E_a}$ is the actual energy yield for a turbine "t", $\mathbf{E_c}$ is the calculated net energy yield for a turbine "t", $\mathbf{S_t}$ is the wind speed sensitivity in the energy yield for a turbine "t", and $\mathbf{W_t}$ is the relative weighting factor for turbine "t".

Calibration factor C represents the difference between the estimated net energy yields of the considered turbine and their energy yield, which is used to modify the wind energy resources that

have been estimated by the flow model previously, the calibration factor, will better match the estimated energy yield to the actual one in the field.

The weighting factor reflects the software user's confidence in the uncertainty level of the production data of the offshore wind turbine. While, wind speed sensitivity $\mathbf{S_t}$ is calculated as follow:

$$S_t = \frac{\text{Difference in net energy [MWh]}}{\text{Difference in wind speed [m/s]}} \qquad (3-15)$$

Where, the wind sensitivity is estimated in a perturbation calculation where wind speed is reduced by 3%.

3.9.3 Energy Estimations

The software programme multiplies the wind speed, which was calculated applying the previous model (the Wind Flow Model), for each offshore wind turbine by the power curve of the turbine, which is supplied by the wind turbine's manufacturer. This process produces the expected energy yield from that turbine. The wind speed distribution from the model may be expressed using Weibull distribution factors, which are wind speed probability (A) and directional probability (K).

3.9.4 Park Model

The Park wake model is used to estimate the wake effects, which is the reduction of the speed and quality of the wind speed due to the influence of the rotating rotors. The wind leaving the turbine after power generating is lower in energy content in terms of wind speed and quality. The Park wake model explains the expansion of wakes as a liner form after it proceeds downstream from the rotor (Park and Law, 2015). Figure 3-5 shows the flow field considered by the Park model to estimate wind speed output behind the wind turbine.

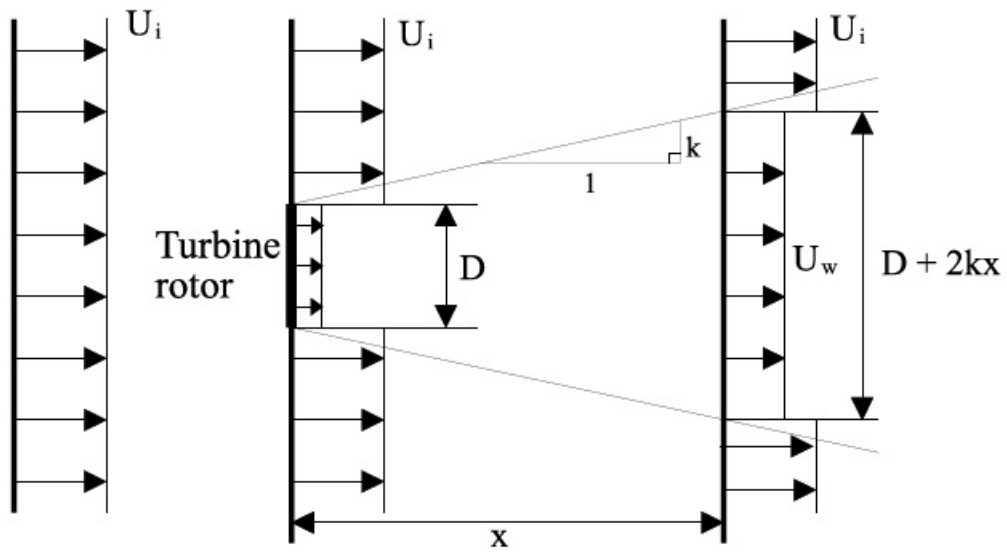

Figure 3-5: Flow field used for the Park model to estimate the wind turbine output, adopted from (GL-Energy, 2014).

The wind speed in the downstream direction $\mathbf{U_w}$ is calculated using the PARK formula shown in the equation below:

$$U_w = U_i\left[1 - \left(1 - \sqrt{1 - C_t}\right)\left(\frac{D}{D+2k*X}\right)^2\right] \qquad (3-15)$$

Where: $\mathbf{U_i}$ is the wind speed just before pathing the rotor, $\mathbf{C_t}$ is the thrust coefficient (obtained from the wind turbine manufacturer), $\mathbf{k}$ is the wake decay constant = $0.5/\ln(z_h/z_0)$, $\mathbf{X}$ is the distance between the two turbines, and $\mathbf{D}$ is the rotor diameter.

Summary

The methods used to accomplish the objectives of the thesis (Section 1.1) were described in this chapter. The key methodology introduced is the AHP methodology, which is used to optimise the offshore wind energy siting problem. The nine procedures of the AHP method to create the required suitability map are explained in detail and summarised in Figure 3-1. Finally, a brief explanation of the software programme WindFarmer and the related theories used to achieve the optimised siting configuration are provided.

Conclusions

- AHP methodology is an appropriate solution to offshore wind energy spatial siting problems, but it needs sufficient data preparation and analysis to represent all the proposed factors and constraints.
- Criteria selection, type, definition, and limitation, are processes built on the experience of the study area and knowledge gained from previous studies.
- Pairwise comparison method is an adequate technique to weigh the factors and to validate the intensity of importance of the assumption.
- WLC process is the last step to create the final product (suitability map), which is an equation to combine effectively between Boolean layers and weighted layers.
- ArcGIS tools and abilities are capable of accomplishing the AHP steps and presenting the data layers and the final suitability map accurately.
- Soil properties are typically assigned through applying the CPT for offshore projects. However, due to the limited information about the area, the data will be obtained from SPT results, which was collected from offshore construction projects in a near distance to the three offshore wind chosen sites.
- WindFarmer software programme predicts the actual energy output of the wind farm, using different models and sufficient wind data near the proposed offshore wind site.

Chapter 4: Data Collection

In order to establish a pathway for exploiting the offshore wind energy for the two case studies, a systematic analysis is needed to understand wind energy resources and any constraints as described in the methodology, Chapter 3. In order to test the proposed AHP methodology outlined in Chapter 3, the analysis will cover the wind energy potential, specify appropriate high resources locations with no imposed restrictions, and generate suitability maps for offshore wind energy exploitation. It will also identify constraints around these locations and other needed additional information required that governs offshore wind farms spatial siting.

4.1 Criteria Selection and Determination (Factors and Constrains)

The comparison between the criteria considered for this case study and similar offshore wind projects are summarised in Table 4-1. The other offshore wind studies are presented in details in Chapter 2. Hence, this work builds on previous analysis by establishing case studies-specific criteria to allow appropriate analysis to be made to determine the scope for offshore wind energy deployment in Egypt and Arabian Peninsula countries.

In accordance with Egyptian conditions, all criteria that affect the cost will be considered, such as, wind power density, water depth, proximity to the electricity grid, soil properties, and, distance to shore. In addition, the expected constraints are accounted and included, for instance, environmental, security, offshore activity, social impact, and shipping traffic restrictions. Most of the criteria of similar projects were considered, but some criteria were neglected because they are not suitable for Egypt circumstances. So bathymetry, soil conditions, wind intensity, shipping routes, distance from national grid, military zones, natural preserved areas, cables and pipe lines, oil and gas extraction areas, distance to shore, fishing areas, and security criteria were applied. The reason for neglecting the other criteria was highlighted in Table 4-1. Table 4-2 indicates definition,

limitations, optimisation, measured unit, and type (factor or constraint) for the criteria used in this study.

Table 4-1: Comparison of criteria used in this study and previous published work on offshore wind energy.

Author	The Crown State (The Crown Estate, 2012b)	Schillings, et al. (Schillings et al., 2012)	Ntoka (Ntoka, 2013)	Egypt	Arabian Peninsula
Criteria	Project location				
	The UK	The North Sea	Petalioi Gulf, Greece	Red and Mediterranean Seas of EGYPT	Arabian Peninsula countries' sounding seas
Bathymetry	Considered	Considered	Not considered	Considered	Considered
Wind power Intensity/Speed	Considered	Considered	Not considered	Considered	Considered
Shipping Routes	Considered	Considered	Considered	Considered	Considered
Storm surge	Not considered	Considered	Not considered	Ineffective, because it's low and separated by a long time intervals (Ismail et al., 2012)	Not considered
Grid	Considered	Considered	Not considered	Considered	Considered
Ports	Considered	Considered	Considered	Considered with Shipping Routes Criteria	Considered
Wave height	Not considered	Considered	Not considered	Not considered	Not considered
Tidal Range	Not considered	Considered	Not considered	Ineffective (T.R in Egypt is less than 30 cm) (The Egyptian Environmental Affairs Agency, 2015)	Not considered
Military zones	Considered	Considered	Considered	Considered	Considered
Natural Park	Considered	Considered	Considered	Considered	Considered
Cables and pipe lines	Considered	Considered	Considered	Considered	Considered
Fishing areas	Considered	Considered	Considered	Considered	Not considered
Oil and gas extraction Areas	Considered	Considered	Considered	Considered	Considered
Existing or planed farms	Considered	Considered	No existing or planed	No existing or planed offshore wind farms are in the study area	Not considered
Distance to shore	Not considered	Considered	Not considered	Considered	Considered
Sand Mining	Considered	Considered	Not considered	Not considered	Not considered
Security and safety	Not considered	Not considered	Not considered	Considered	Not considered

Table 4-2: Criteria definitions, which used to locate offshore wind farm, where F is factor, and C is constraint.

Criterion	Description	Unit	Optimisation	Type
Wind Power Density	Energy in the wind, proportional to the cube of wind speed (Lashin and Shata, 2012).	W/m^2	Choose areas with high and continuous wind blowing.	F
Wind Speed	It is the atmospheric rate value of the moving air measured at 50m above MSL.	m/s	Choose areas with high wind speed above 3 m/s.	F
Bathymetry	Water depth in the selected area of the sea.	m	Choose areas with seabed depth varied between 5 to 60 meters (The Crown Estate, 2012b)	F
Cables and tunnels	Submerged cable paths.	location	Avoid	C
Oil & Gas Wells Pipelines Gas and Oil Storage Areas	The ares where gas and oil are or will be extracted	location	Avoid	C
Marine Nature Reserves	Protected places in the sea area by the power of law to reserve the endangered marine ecosystem species.	Location	Avoid	C
Shipping Routes, ports, approach channels	The ship vessels movement around the study area.	Location, path	Avoid	C
Distance from National Grid Connections	The distance required to connect the offshore wind farm to the national unified power network.	m	Choose places closer to them	F
Military Practice and Exercise Areas	Identified by the military authorities.	location	Avoid	C
Soil Properties	Determined by the borehole test, which used to draw a vertical log showing soil strata type and depth.	m	Choose sites with sandy sediment layer closer to the seabed (less than 20m), to reduce foundation construction cost	F
Distance to shore	The distance between the shoreline and the wind farm in the sea.	m	Choose sites far for 1.5 to 200 km from shoreline, to reduce submerged cable extension (Schillings et al., 2012)	F
Security and safety	Terrorism (unsafe areas) determine by military authorities	location	Avoid	C
Fishing areas	The areas determine by the authorities for different kinds of fishing.	location	Avoid	C

4.2 Egypt (Case Study 1)

Getting detailed information about Egypt is difficult, and researchers in Egypt normally suffered from data shortage especially data availability from governmental authorities. For example: Zalla and Fawzy (2000) studied the agricultural land use in Egypt and they found that the data given by the authorities was poor in quality and incomplete. Awad (2002) referred to the difficulty to present the results due to insufficient data he obtained from Egypt Cairo Metro authority. Also, Lavanchy (2011) highlights that his inaccurate result about the C virus in Egypt was due to the poor quality of data supplied by the Egyptians' health authorities. There is a lack of detailed information on renewable energy in Egypt. In order to overcome this, this work has in some instances, utilised information and data from different sources written in Arabic, such as, offshore gas and oil projects technical reports covering the study areas, geotechnical reports near study area, and Egypt's Government official web sites.

4.2.1 Problem Definition

Problem definition is the first part of the AHP, and it is need to be done before collecting data. Egypt could benefit from offshore wind, where the high wind speeds areas in the sea are recognised to be greater than those onshore In addition exploiting such areas also save the high valued coastal land areas. Figure 4-1 shows the high wind speed above the Gulf of Suez, Egypt and its surrounding onshore lands. Table 4-3 shows the area percentages of land and sea areas, for high wind potential above the Suez Gulf area (The area values were estimated using ArcGIS feature tools). For instance, the sea area represents 51% of the total area with high-speed wind > 10 m/s, while the rest 49% is coastal land areas, which are used or planned for recreational activity. Therefore, using the sea areas to deploy offshore wind farms is an optimal solution to limit impact on coastal land areas and to increase the installed capacity of renewable energy in Egypt.

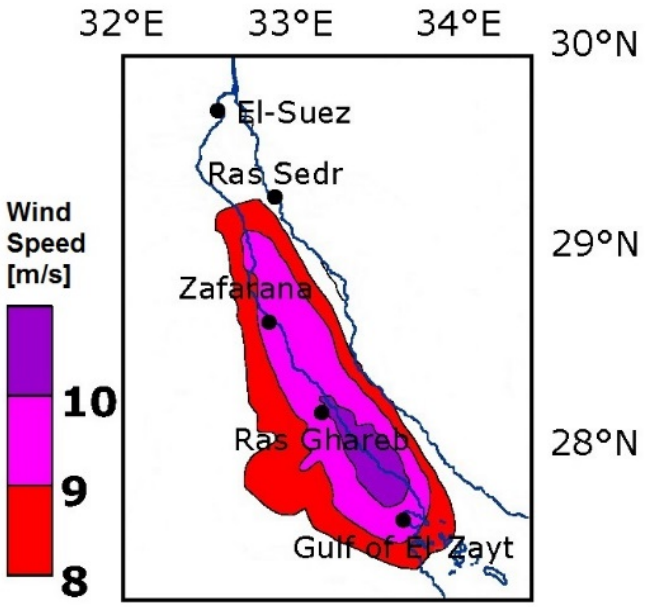

Figure 4-1: High wind speeds map at 50m altitude of the Gulf of Suez, Egypt, modified using the ArcGIS and adopted from (Mortensen et al., 2006a).

Thus, the suggestion is to produce electricity from offshore wind in Egypt due to its advantages and the expected installation improvements, and cost reduction, in the near future. Therefore, the problem description is to identify the proper location for offshore wind farms in Egypt. The spatial siting of offshore wind energy has many criteria to locate the most suitable areas, therefore, a detailed description of these criteria is needed, and in addition, sufficient data to fully represent each criteria for each case study is required.

Table 4-3: The area distribution between land and sea in respect to different wind speeds, at the Gulf of Suez area[1].

Wind Speed at 50m altitude	Land (%)	Sea (%)
8-9 m/s	64	36
9-10	43	57
> 10	49	51

[1] The map in (Figure 4-1) and ArcGIS tools were used to estimate the area values in this table.

4.2.2 Data Preparation

A map layer in ArcGIS was created for each criterion, using the available and relevant spatial data. These data and sources for each criterion are shown in Table 4-4. Original maps, their digitalised

layers, and figure numbers are located in the table. In addition, steps to convert each source layer to the digital form are displayed below.

Table 4-4: Egypt's Case study data sources

Criteria	Data Source	Original data	Digitalized data
Wind Power	New and Renewable Energy Authority, Egyptian Meteorological Authority (Mortensen et al., 2006b)	Figure (4-4)	Figure (4-5)
Bathymetry	British Oceanographic Data Centre (BODC), 2014	-	Figure (4-3)
Cables and tunnels	TeleGeography company, 2015, and National Authority for Tunnels (NAT), 2015	Figure (4-6)	Figure (4-7)
Oil & Gas Wells Pipelines Gas and Oil Storage Areas	The Egyptian Natural Gas Holding Company (EGAS), 2015	Figure (4-6)	Figure (4-7)
Marine Reserves	The Egyptian Environmental Affairs Agency, 2015.	Figure (4-8)	Figure (4-9)
Shipping Routes, ports	Marine Traffic, 2015	Figure (4-10)	Figure (4-11)
Distance to National Grid	The Ministry of Electricity and Energy of Egypt, 2016	Figure (4-12)	Figure (4-13)
Military Areas	Ministry of Defence and Military Production, 2015	Table (4-5)	Figure (4-14)
Distance to shore	Null	-	Figure (4-15)
Soil Properties	Different sources	-	-
Fishing areas	Ministry of Agriculture and Land Reclamation of Egypt, 2016	-	-
Security and safety	Ministry of Defence and Military Production, 2016	-	Figure (4-16)

A shape file of the land cover of Egypt was created using data from (Food and Agriculture Organization of the United Nations, 2015) and was used as a base map (Figure 4-2), the shape file is converted to raster file to exclude all land cells from the spatial siting process, see Section 6.1.

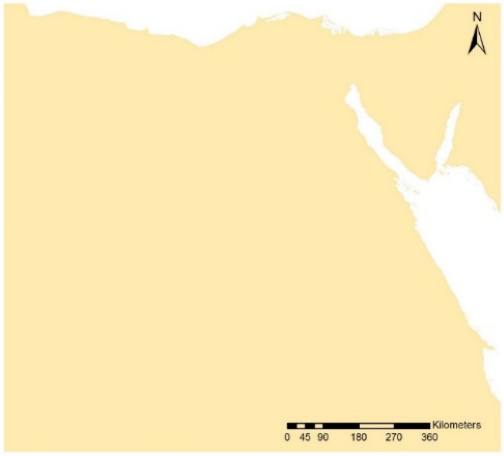

Figure 4-2: Study area basic map generated from (Food and Agriculture Organization of the United Nations, 2015).

The bathymetry data for both Red and Mediterranean Seas was adopted from the British Oceanographic Data Centre (The British Oceanographic Data Centre, 2014), the file was already in raster form. Figure 4-3 shows the topography of Egypt raster map in meter; later a Boolean mask will be applied to eliminate levels above - 5 meters and below - 60 meters. The cell size for this layer is (x, y) = (0.8, 0.8) km, and the Geographic Coordinate System used is "GCS_WGS_1984". These two considerations cell size and coordinate system are used for all new layers to be compatible with the bathometry raster layer source data.

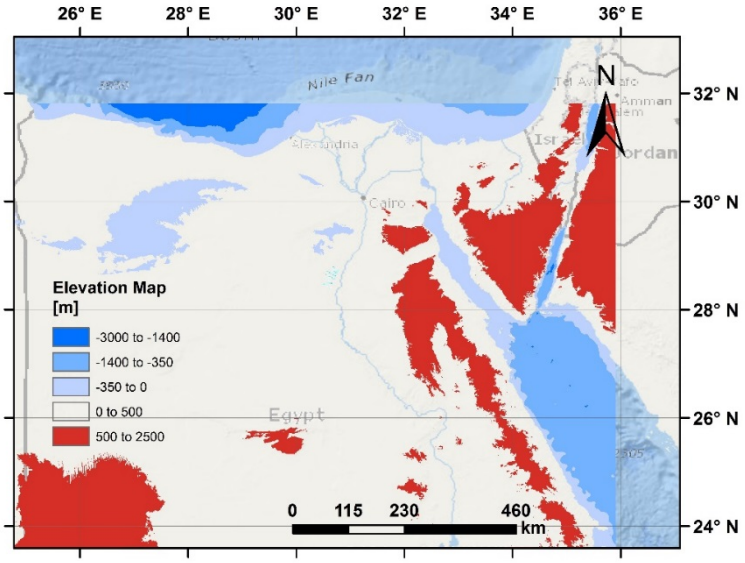

Figure 4-3: Topography map of Egypt generated from (The British Oceanographic Data Centre, 2014).

Wind power density data was derived from the "Wind Atlas for Egypt" (Mortensen et al., 2006b). Figure 4-4 shows "the regional wind climate of Egypt, the map shows mean power density in [W/m^2] at a height of 50 m over a flat, uniform land surface". To represent the wind power density as a layer in the ArcGIS, the Georeferencing Tool was used to produce a map image, where, four geographical control points were considered in this procedure and following similar layers. The power density contour map was then entered as a shape features. Finally, the shape feature was converted to a raster file with, see Figure 4-5.

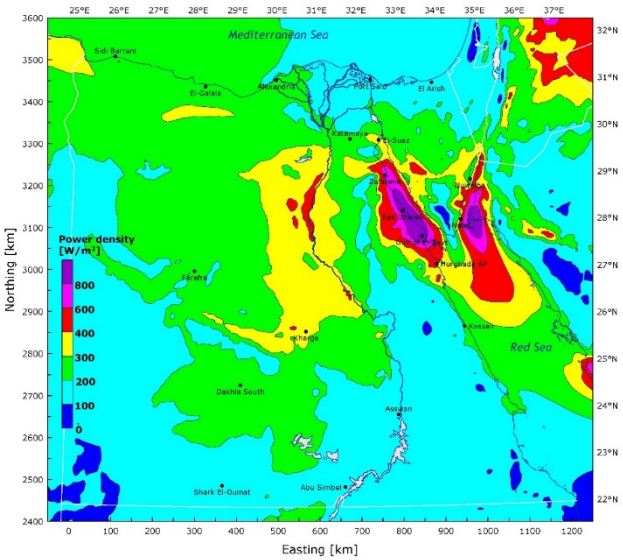

Figure 4-4: Mean power density [W/m^2] of Egypt at 50m altitude.

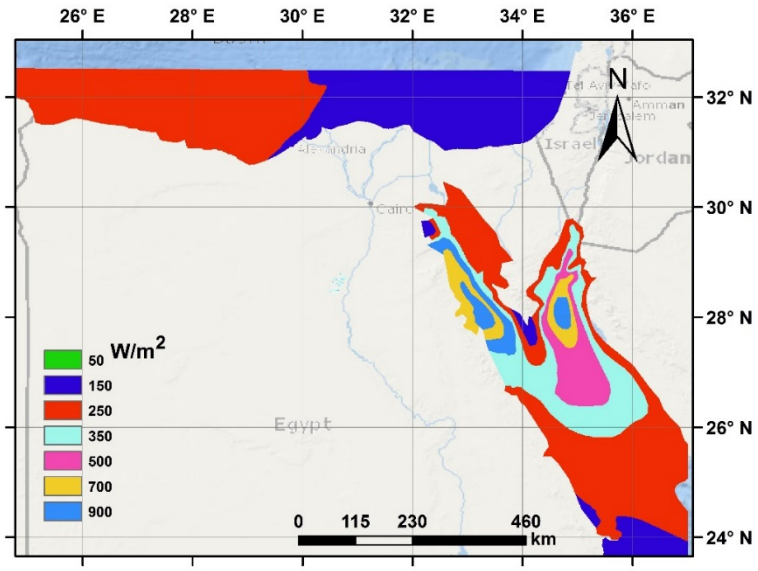

Figure 4-5: Mean wind power density [W/m^2] of Egypt at 50m altitude.

Tunnels in Egypt exist only in Cairo, and underneath the Suez Canal according to the National Authority for Tunnels (NAT) (2015), so, there is no need to consider tunnel data as a constraint. Undersea cables locations were extracted from the Submarine Cable Map web (TeleGeography Company, 2015). Egyptian Law No. 20 of 1976 allows offshore structures in areas that are preserved for future excavation or mining to be constructed (Ministry of Petroleum and Mineral Resources, 2015), but for safety, a restricted buffer zone of 1000 meters was created around present and future offshore oil and gas wells. The data was captured from a map for gas and petroleum oil around

Egypt created by The Egyptian Natural Gas Holding Company (EGAS) (2015), see Figure 4-6, and Figure 4-7.

Figure 4-6: Oil and Gas wells map in Egypt.

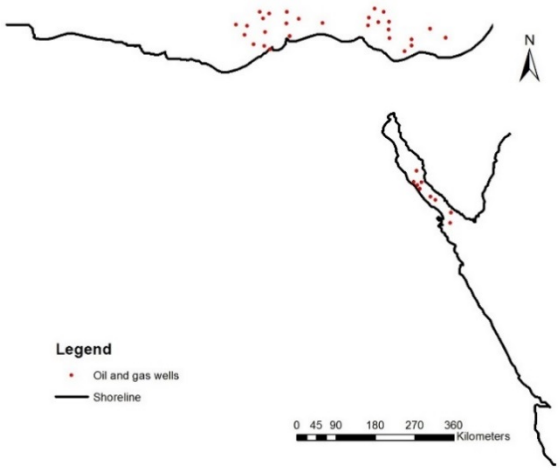

Figure 4-7: Oil and Gas wells ArcGIS layer.

Under Egyptian Law No. 102 (1983), 30% of the Egyptian footprint, encompassing 30 regions, was declared as Nature Reserves. Nine of them are Sea Marine Nature Reserves, where seven of them are in the Red Sea: Ras Mohamed, Nabq, Abu Galum, Hamata/Wadi El-Gemal, Elba, Taba, and Red Sea Northern Islands. The other two are located in the Mediterranean Sea: El-Salum, and El-Omayed. The locations and dimensions of the Marine Nature Reserves were established from the official web site of The Egyptian Environmental Affairs Agency (2015). The data processing was done using the Georeferencing, Shape Features, and Feature to Raster ArcGIS tools, in the same way as the wind power density layer (Figures 4-8, and 4-9).

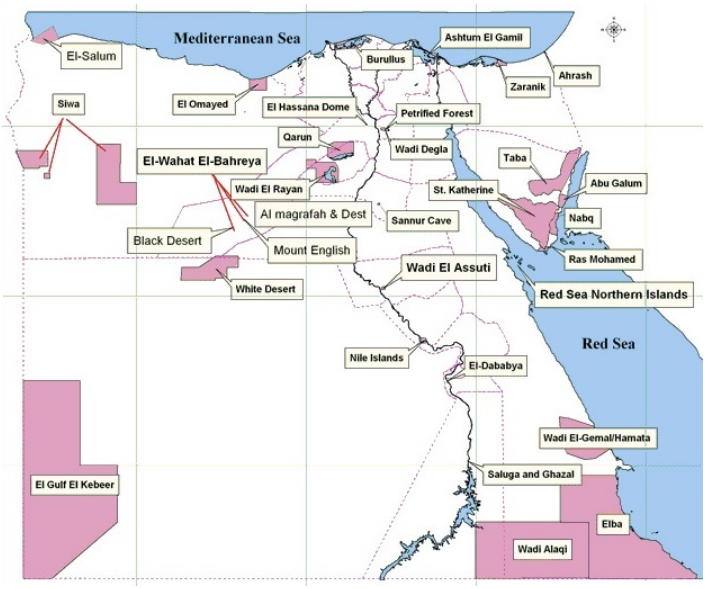

Figure 4-8: Map of the Nature Reserves areas in Egypt.

Shipping Routes around Egypt were drawn from the ship density maps of Marine Traffic for two years 2013, and 2014 (The MarineTraffic, 2015). The high-density areas (red and orange paths) were restricted. Ports and approach channels areas were identified from (Maritime Transport Sector, 2015), see Figures 4-10, and 4-11.

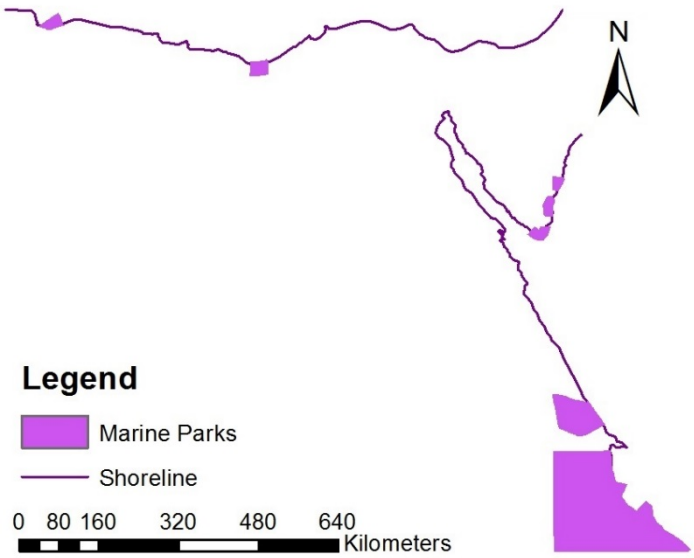

Figure 4-9: Raster map for the Nature Reserves areas.

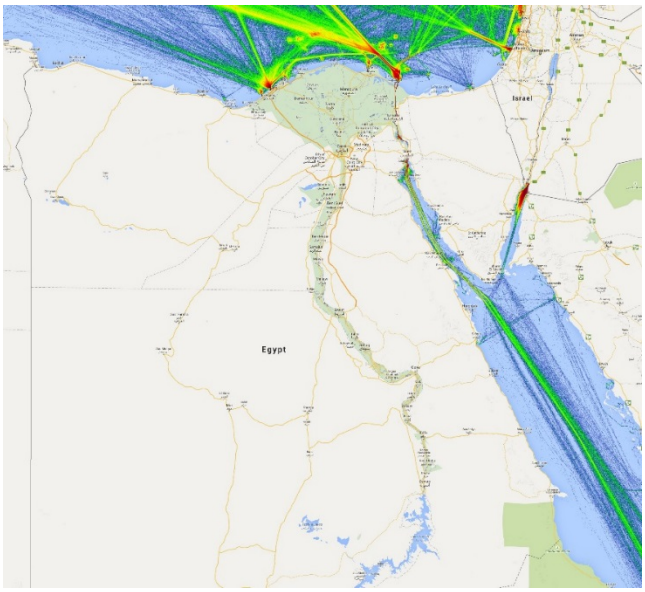

Figure 4-10: Shipping routes around Egypt

Figure 4.12 shows the map of the Egyptian unified power network map (The Ministry of Electricity and Energy of Egypt, 2016), which was used to locate the electricity grid connection. The Euclidean Distance Tool was deployed to calculate the distance from each electricity line, see Figure 4-13.

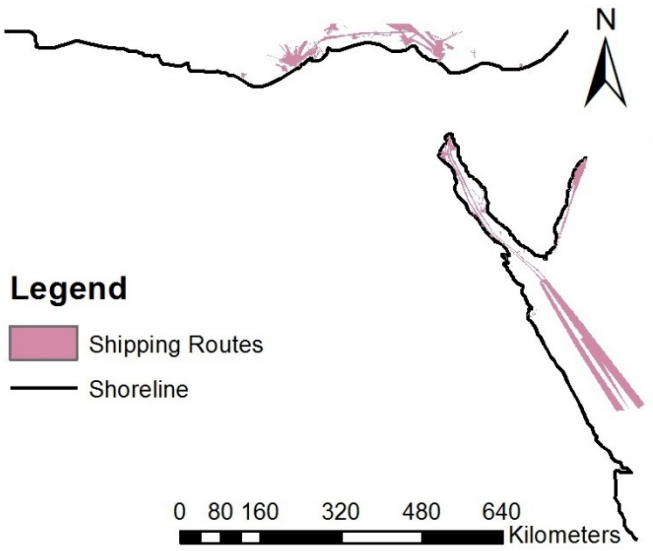

Figure 4-11: Shipping routes raster layer.

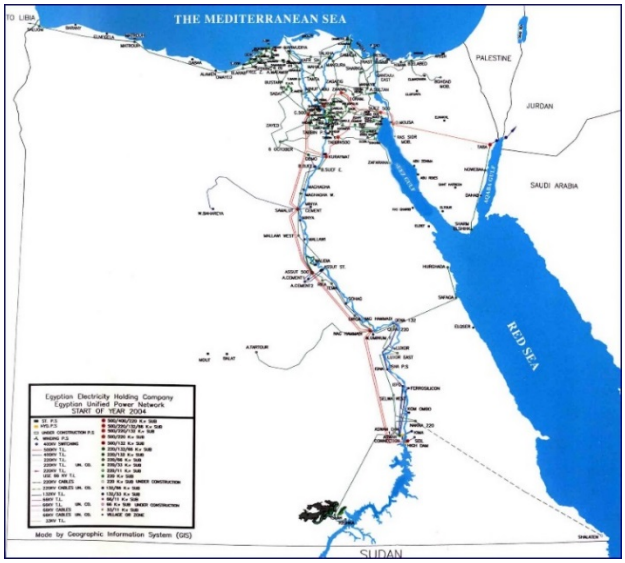

Figure 4-12: The Egyptian unified power network map.

Military practice and exercise areas were assessed from the official website of the Ministry of Defence and Military Production (Ministry of Defence and Military Production, 2015). There are seven different marine manoeuvres held in the Egyptian seas. Table 4-5 details the manoeuvres and its locations. The Military law of Egypt has some flexibility to change its exercise locations for the public benefit (Ministry of Defence and Military Production, 2015), but for safety these areas were excluded, see Figure 4-14.

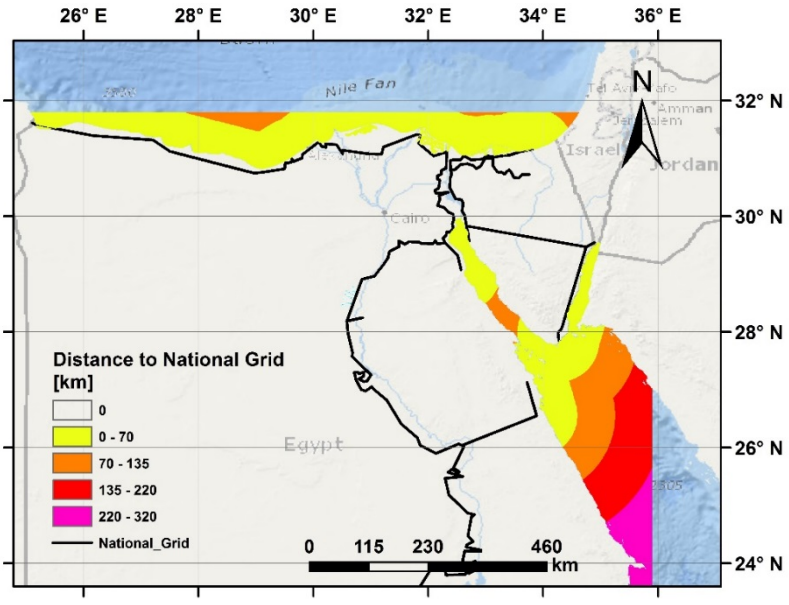

Figure 4-13: Raster map for distance form national grid lines.

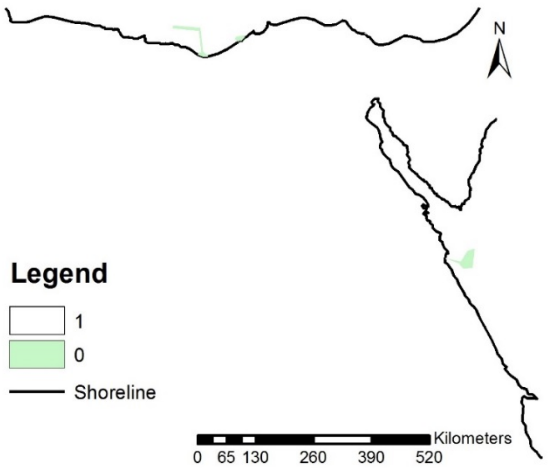

Figure 4-14: The military exercise areas in Egypt.

In terms of ground conditions, most of the seabed adjacent to the Egyptian coast comprises a medium to coarse sandy soil (El Diasty et al., 2014, Ghaly et al., 2013, MAS Consultant Office, 2005). Therefore, the soil factor will be neglected. According to Egyptian's law No. 124 for the year 1983, the allowed depth for large fishing vessels is more than 70 meters (General Authority for Fish Resources Development, 2009). In addition, fishing using simple techniques must not interfere with offshore-submerged cables (The Egyptian Environmental Affairs Agency, 2015). Hence fishing activities around Egypt will have no effect on offshore wind farm locations, as these will operate at a maximum depth of 60 meters.

Table 4-5: Marine military manoeuvre exercise areas around Egypt, adopted from (Ministry of Defence and Military Production, 2015).

Name	The Egyptian Navy in partnership with	Purpose	Frequency	Place
Alexandroupoli	Greece Navy	Defence	Once per year	The Mediterranean Sea
Sea Victory	Egyptian Air Force	Secure the Egyptian coast line	Twice per year	The Mediterranean and The Red Sea
Sea of Friendship	Turkish Navy	Defence	Stopped in 2013	The Mediterranean Sea
Morgan	Saudi Arabia Navy	Raise the combat readiness	Once per year	The Red Sea
Cleopatra	Italian, German, and French Navy	Defence and attack	Once every 2 years	The Mediterranean Sea
Eagle Salute	USA, and UAE Navy	Ship rescue	Once per year	The Mediterranean Sea
Friendship Bridge	Russian Navy	Defence and attack	Once per year	The Mediterranean Sea

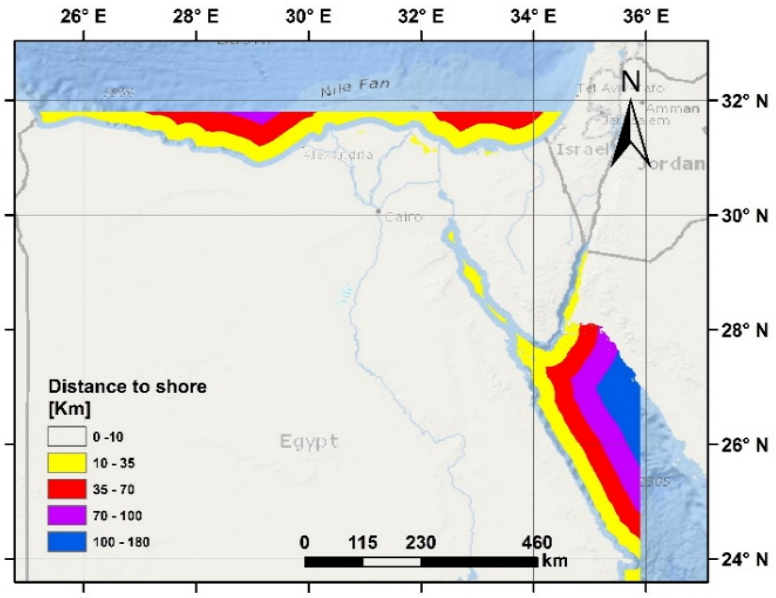

Figure 4-15: Distance to the shore.

The coastlines of Egypt were drawn to calculate the distance from the sea to the shoreline, applying the Euclidean Distance Tool, see Figure 4-15. Egypt is considered to a secure and safe country for tourists according to study of hotel service attributes in Africa done and conducted in the end of 2017 (Ukpabi et al., 2018). In contrast, a recent study (2018), concluded that Egypt still suffers from the risk of terrorist attack especially in the north east part of Sinai Peninsula (Tomazos, 2017).

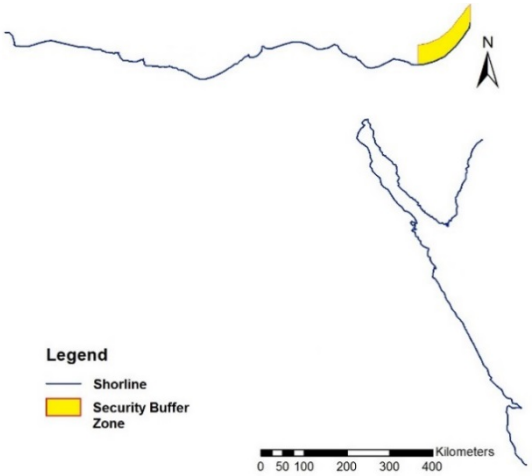

Figure 4-16: Safety restriction buffer zone.

Therefore, a security and safety restriction zone will be deployed to eliminate the offshore areas around the Northern East part of Sinai shoreline, see Figure 4-16.

4.3 Arabian Peninsula (Case Study 2)

4.3.1 Problem Definition

To the author's knowledge, offshore wind energy potential in the AP region has not been fully investigated. In addition to testing the methodology for a regional scale, the research will also provide the quantification of the potential of offshore renewable wind energy for these countries contributing to both knowledge and understanding. The outcomes of the research based on the optimised methodology applied at scale could also assist in the speedy achievement of the regional renewable energy targets.

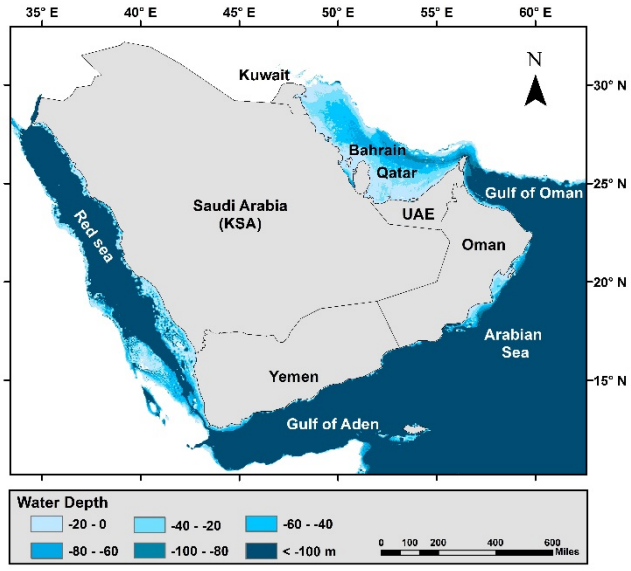

Figure 4-17: Bathometry (water depth) map around Arabian Peninsula.

The following section outlines the steps undertaken to produce an overall outcome for offshore wind farm spatial siting in the AP region. Due to the wide area footprint of the region and the different conditions presented by the considered countries, the analysis was conducted using nine criteria. Four of these criteria are factors covering: (i) wind speed (m/s), (ii) water depth in (m), (iii) distance from alternative cells to the shoreline in (km), and (iv) distance to the grid lines in (km). While the constraints used, which were selected due to their appropriateness for the region, are (a) maritime boundaries, (b) oil and gas extraction areas, (c) reserved maritime natural parks, (d) shipping routes paths, and (e) underwater (sea) cables paths.

4.3.2 Data Preparation

In order to carry out the analysis, an ArcGIS (Esri, 2012) map layer for each criterion was created utilising available and relevant published spatial data. The bathymetry (water depth) data for the offshore areas around GCC countries and Yemen were adopted from (The British Oceanographic Data Centre, 2014). The source file of the bathymetry data was created in raster format, with a cell size of 800 x 800 m, and its Geographic Coordinate System was "GCS_WGS_1984". The results for the water depth for the considered countries are shown in Figure 4-17. It must be noted that all other criteria layers were also confined to the same cell size and coordination system type as that of the bathymetry source file.

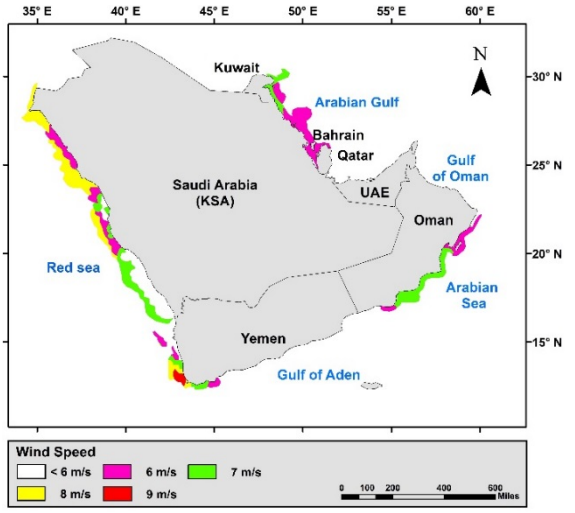

Figure 4-18: Wind Speed [m/s] map around offshore areas of the Arabian Peninsula.

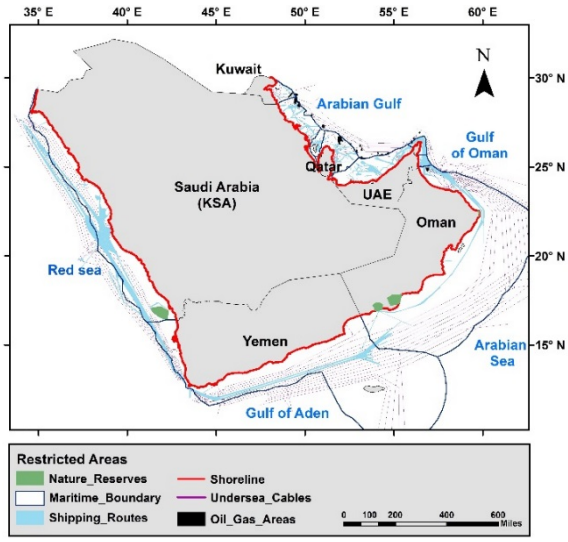

Figure 4-19: Restricted areas raster layer around the offshore areas of the Arabian Peninsula.

Table 4-6: Maritime reserved parks for Arabian Peninsula countries.

Country	Park name	Source
Oman	Daymaniyat Islands Nature Reserve, Jabal Samhan Nature Reserve, Ras Al Jinz Turtle Reserve, The Khawrs of the Salalah Coast Reserve	(Ecotravelworldwide, 2017a)
Yemen, Qatar, UAE, Bahrain, Kuwait	N/A	(Ecotravelworldwide, 2017c, Ecotravelworldwide, 2017b)
KSA	Umm al-Qamari Islands Farasan Islands	(SWA, 2017)

Wind speed data was adopted from the "Wind Atlas for Egypt" (Mortensen et al., 2006b) and from the Global Atlas for Renewable Energy (Kieffer and Couture, 2015). The determined values were

then verified using data available from (Yip et al., 2017, Yip et al., 2016). The map layer in Figure 4-18 shows the results of the average wind speed in [m/s] at a height of 50m over a flat and uniform sea.

All layers for area restrictions were adopted from different sources. Locations, shapes, dimensions of maritime reserved parks were taken from the official websites of different Wildlife Authorities of these countries, as documented in Table 4-6. All oil extraction areas are located on the Arabian Gulf, according to data from Saudi Aramco (Aramco, 2017). Shipping Routes within the study area were identified using the data available from ship density maps of the Marine Traffic website (The MarineTraffic, 2015). Undersea submerged cable locations and paths were extracted from the submarine cable map given in (TeleGeography Company, 2015). Figure 4-19 maps the overall results of restrictions for the region covering: natural reserves, oil and gas areas, shipping routes, and undersea cables.

Figure 4-20 shows the results map layer of the National Electricity Transmission Grid of the GCC and Yemen. The data were adopted from the Global Energy Network Institute (GENI, 2017) and the GCC Interconnection Authority (Al-Mohaisen and Sud, 2006). The Euclidean Distance Tool in ArcGIS (Esri, 2012) was deployed to calculate the distance between the nearest electricity line to each cell, and the results are depicted in Figure 20. Figure 4-21 illustrates the results of the distance from each cell considered in the analysis to the coastline utilising data from (Esri, 2012).

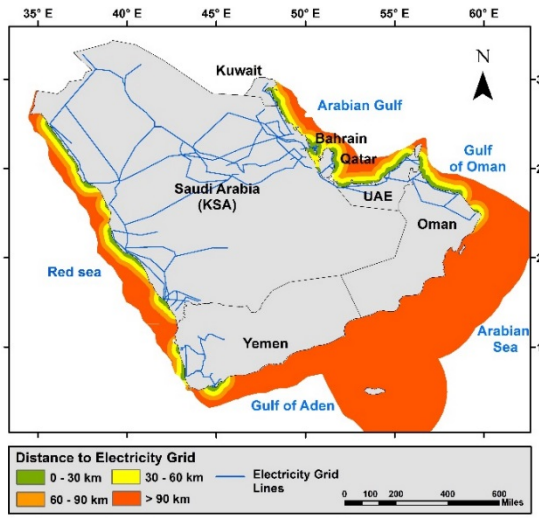

Figure 4-20: Distance between representative cells of the offshore wind resources and electricity grid lines.

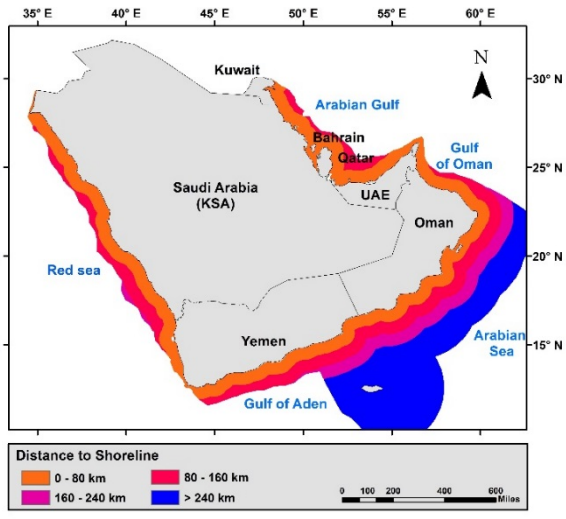

Figure 4-21: Layer map of the distance between representative cells of the offshore wind resources and shoreline.

4.4 Loads States Affecting the Offshore Wind Turbine

The main challenge of OWT foundation is to safely support all loads (dead, dynamic, and environmental) at the seabed level/Mud Level (ML) without exceeding the allowable deformation. This challenge can be met if the following three loading states are met (Bhattacharya, 2014):

1. Ultimate Limit State (ULS): This state applies for the ultimate lateral loads from wind and sea waves, especially in extreme events, such as storms or hurricanes, which could be expressed as the combination of the ultimate moment, lateral and axial loads. In this case the turbine rotor is stopped from moving using brakes to save the turbine from damage.

2. Serviceability Limit State (SLS): The predicted service/environmental loads i.e. wind and wave loads for a whole year are applied on OWT.

3. Fatigue Limit State: The OWT in this state is tested against the fatigue effects. Fatigue effects are expected weakness due to cycle loading. Cycle loading is applying the predicted service wind, waves, and the expected loads from extreme events for as long as the expected life cycle of the turbine.

4.4.1 Serviceability Steady State Loads (SLS)

The chosen offshore wind turbine is that specified by NREL (National Renewable Energy Laboratory) of capacity 5MW. Table 4-7 displays the 5MW NREL wind turbine characteristics, including the tower hub Height, nacelle mass, rotor diameter and blade angles. Figure 4-22 displays the loads combinations used for both the ultimate and serviceability limit stats. Six load components were calculated in each limit state, which are F_x (Perpendicular load in x direction), F_y (Perpendicular load in y direction), F_z (vertical load/own weight), M_x, M_y, and M_z (moments rotate around x, y, and z axis respectively). Three-load combination were suggested, which are 6C, 3C, and 2C, see Figure 4-22 and Table 4-8.

Table 4-7: 5MW NREL wind turbine characteristic adopted from (Jonkman et al., 2009).

Parameter	Value
Rating	5 MW
Rotor Orientation, Configuration	Upwind, 3 Blades
Control	Variable Speed, Collective Pitch
Drive train	High Speed, Multiple-Stage Gearbox
Rotor, Hub Diameter	126 m, 3 m
Hub Height	90 m
Cut-In, Rated, Cut-Out Wind Speed	3 m/s, 11.4 m/s, 25 m/s
Cut-In, Rated Rotor Speed	6.9 rpm, 12.1 rpm
Rated Tip Speed	80 m/s
Overhang, Shaft Tilt, Pre-cone angles	5 m, 5º, 2.5º
Rotor Mass	110,000 kg
Nacelle Mass	240,000 kg
Tower Mass	347,460 kg

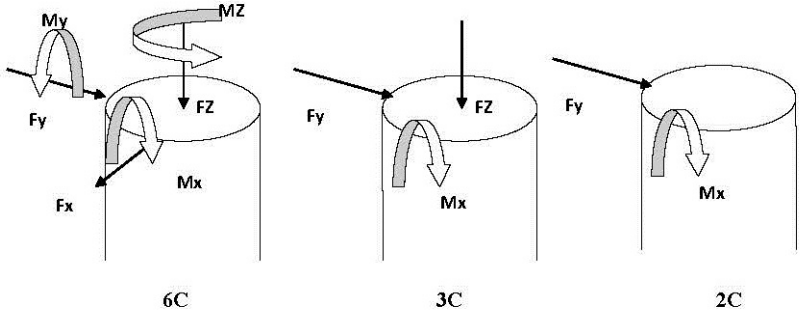

Figure 4-22: Different load combinations applied at MSL (mean sea level), adopted from (Abdelkader, 2015).

Table 4-8: Load combination description.

Load Combination	Loads applied
6C	All components
3C	F_y, F_z, and M_x
2C	F_y, and M_x

The serviceability steady state is the state where offshore wind turbine is exposed to the natural surrounding environmental events, which requires the design to ensure that the settlement due to such loads will not exceed the allowable threshold (Carswell et al., 2016). The loads considered for the serviceability steady state are the wind, wave and the turbine own weight forces (Arany et al., 2017).

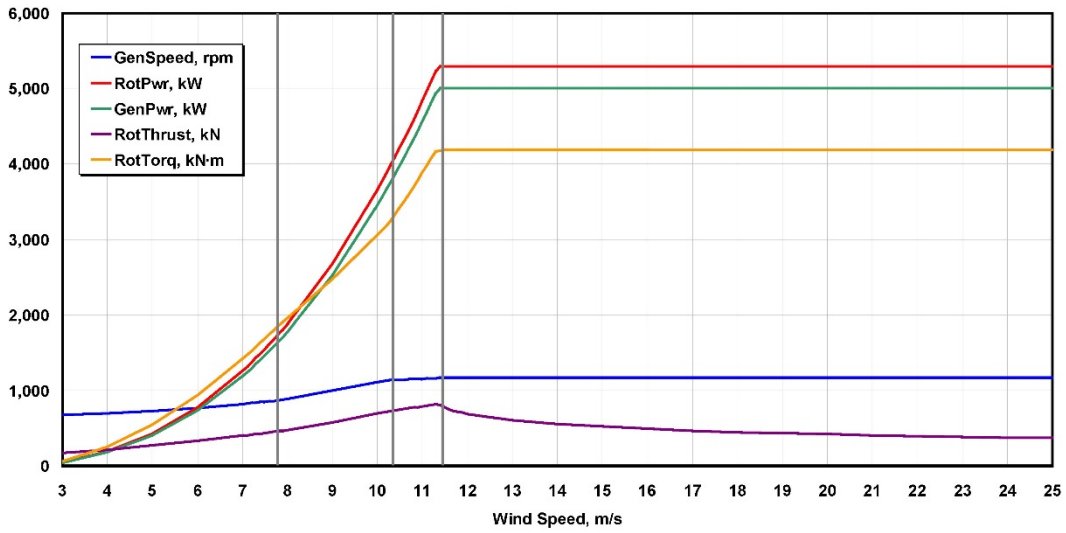

Figure 4-23: Service load due to wind effect, adopted from (Jonkman et al., 2009), response of the turbine due to wind effect in terms of the rotor thrust (purple plot line) and rotor torque (yellow curve).

Wind loads in the Serviceability Steady State loads, were adopted from NREL's report (Jonkman et al., 2009), which was done utilising FAST (Fatigue, Aerodynamics, Structures, and Turbulence) simulation programme, they neglect the aerodynamic loads affecting the wind turbine tower before calculating the loads (Jonkman et al., 2009). Neglecting these loads on the tower was because such loads are very small relative to those of the rotor thrust loads. Using Jonkman et al. (2009) s' charts (Figure 4-23) and wind speed data from Mortensen et al. (2006b), the rotor thrust is estimated to be 750 kN and acting as F_y a the rotor torque is 4100 kN.m acting as M_x.

The wave properties used to calculate the corresponding loads that affect the wind turbine tower adopted from (Fery et al., 2012) are:

- Max Significate Wave Height (H_s) = 4 m
- Mean Wave Time Period (T) = 7 s
- Average Water Depth (d) = 20m

The equations adopted from (Manual, 1984) are used to calculate the wave force acting on the proposed monopile system:

$$L = \frac{g\,T^2}{2\pi} * \tanh\frac{2\pi d}{L} \qquad (4-1)$$

$$P = \rho g * \frac{H_s}{2} * \cos\theta * \frac{\cosh\frac{2\pi\,(z+d)}{L}}{\cosh\frac{2\pi d}{L}} \qquad (4-2)$$

Where: L is the wave length [length], g is the gravitational acceleration [L/s^2], P is the pressure at any distance below the fluid surface [F/L^2], ρ is the mass density of salt water = 1,025 [kg/m^3], θ is the principal (central) direction for the spectrum measured counter clockwise from the principal wave direction [degree], and z is the water depth below the MSL [L] (see Figure 4-24).

These equations are used to investigate the wave forces affecting solid surfaces in an offshore environment. Equation 4-1 calculates the wave length of the wave due to the measured wave period and water depth, to figure the wave length a try and error method is used to solve equation 4-1. While, Equation 4-2 computes the pressure of the wave, then pressure will be multiplied by the monopile side surface area to derive the wave force.

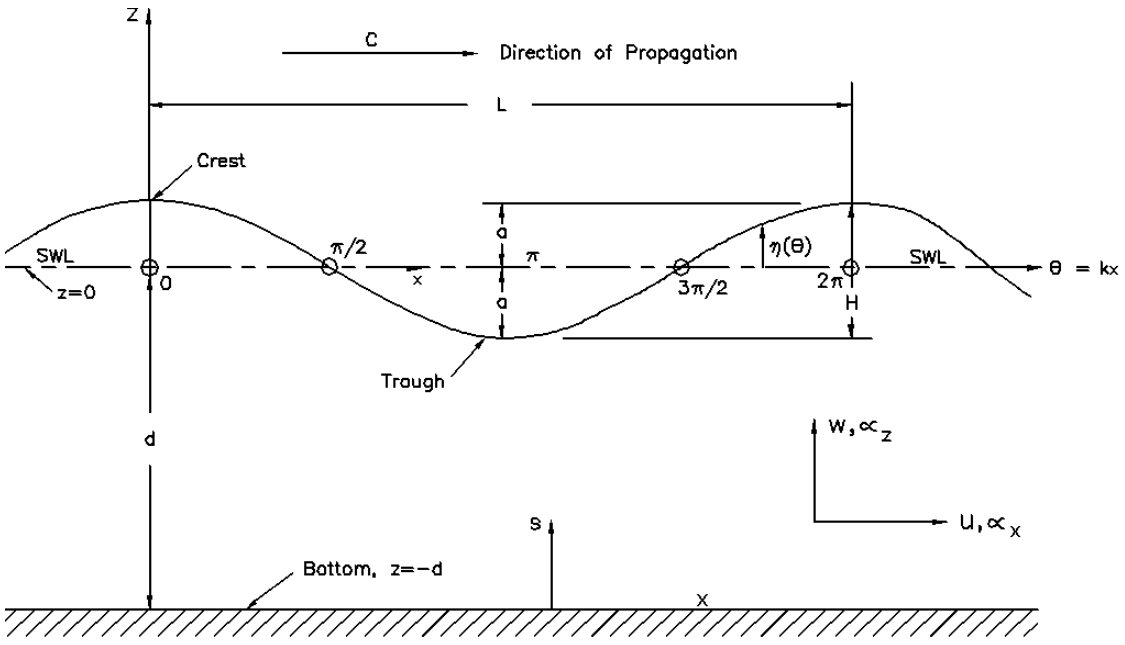

Figure 4-24: Simple, periodic progressive wave, propagating over a flat sea, adopted from (Manual, 1984).

Using site wave conditions, which is listed above, and using equations 4-1 and 4-2, the estimated wave load is equal to 850 kN and acting in the y direction. The final OWT weight force was calculated using data from Table 4-7 to be 6800KN, which is the summation of rotor, nacelle, and tower masses. The final forces affecting the wind tower due to serviceability steady state limit is summarised in Table 4-9. These components will be applied at MSL (mean sea level).

Table 4-9: Loads values for the serviceability steady state limit.

Load	F_x	F_y	F_z	M_x	M_y	M_z
Value	-	1600 kN	6800 kN	4100 kN.m	-	-

4.4.2 Ultimate State Loads

The ultimate limit state loads (ULS) is the load expected to affect the turbine due to extreme events such as a storm (Morató et al., 2017). Six load component (three forces and three moments) were obtained from Ref. (Abdelkader, 2015), see Table 4-9. Table 4-9 values were concluded using scale model test (1:150), see Figure 4-25. The force and moment loads were calculated at the base of the scaled turbine model, which was robust (no-displacements were allowed at the base of the prototype) and light-weight (Abdelkader, 2015). He applied the extreme wind and wave values, which were extracted from (Jonkman and Musial, 2010). All results were measured in a parked rotor position (the wind turbines rotors are normally parked during the extreme events), the results were conducted using different "blade configuration scenarios with the wind coming from all possible directions" (Abdelkader, 2015), see Figure 4-25, **B, and C**. T. The experiment was carried out to ensure accuracy and precision of the measuring and acquisition system. Two arrangements of testing were used:

(i) First case, where the rotor was locked and one of the blades was located vertically in its extreme upper position (see Figure 4-25 B) and
(ii) Second case, where the rotor was locked and one of the blades was located vertically in its extreme bottom position (see Figure 4-25 C).

Then, the results was compared with FAST (Fatigue, Aerodynamics, Structures, and Turbulence) programme simulations, which were done by (Jonkman et al., 2009). Finally, he found that his lab results are more creditable than FAST numerical results to be used in offshore wind foundation. To the author's knowledge, this is the only publicly accessible scale test to calculate the ultimate

state loads for an operational wind turbine, therefore, the values in Table 4-10, will be considered for the offshore wind design in this study.

Table 4-10: Ultimate loads combinations secured from the wind tunnel tests done by (Abdelkader, 2015).

Load	F_x	F_y	F_z	M_x	M_y	M_z
Value	1750 kN	1500 kN	8000 kN	15E4 kN.m	15E4 kN.m	15E3 kN.m

Figure 4-25: Wind Tunnel test configurations: (A) 5 MW wind turbine prototype with 1:150 scale, (B) rotor angle = (0°-120°-240°) and (C) rotor angle = (60°-180°-300°), adopted from (Abdelkader, 2015).

4.5 Turbine Data Required for Layout Optimisation

The wind turbine used for the layout optimisation analysis is the "NREL offshore 5-MW baseline wind turbine" (Jonkman et al., 2009), which is a conventional three-bladed upwind variable-speed variable blade-pitch-to-feather-controlled turbine. This turbine was developed for research purposes by the National Renewable Energy Laboratory.

The information needed to identify the wind turbine in Wind Turbine Studio of the WindFarmer software is the turbine main characteristics, power output, rotor speed, and thrust coefficient curves. The main turbine configurations are shown in Table 4-11. The Wind turbine power curve is a graph indicates the electricity output from the turbine, related to the wind speed; see Figure 4-26.

Table 4-11: 5MW NREL wind turbine characteristics adopted from (Jonkman et al., 2009).

Parameter	Value	Description
Nominal Power	5000 kW	Maximum power the turbine can generate
Control	Variable Speed, Collective Pitch	Gearbox type and blades angle adjustments.
Rotor Diameter	126 m	The diameter of the rotor blades.
Hub Height	90 m	Distance from surface (MSL) to the centre of the rotor.
Cut-In Wind Speed	3 m/s	The wind speed that turbines starts to run
Rated Wind Speed	11.4 m/s	The turbine is able to generate maximum energy at this speed, and the output energy is at its rated limit.
Cut-Out Wind Speed	25 m/s	The turbine is shut down at this speed.
Cut-In Rotor Speed	6.9 rpm	Rotor speed equivalent at cut-in wind speed.
Rated Rotor Speed	12.1 rpm	Rotor speed equivalent at rated wind speed.

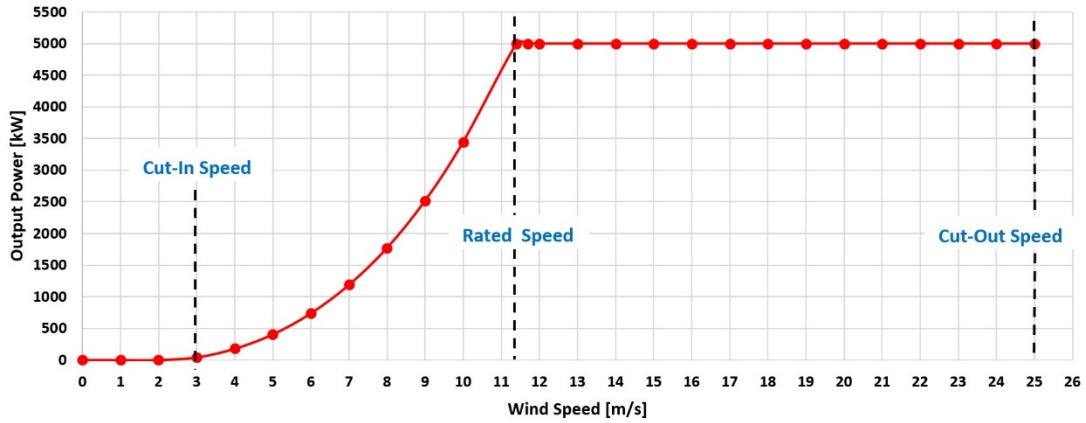

Figure 4-26: Wind turbine power curve for the 5MW NREL offshore wind turbine.

The thrust coefficient C_t is thrust force divided by the dynamic force of the wind and it used mainly to calculate the wind speed in the downstream of the turbine, it shows how much the energy affected (reduced) by the extraction device (blades) and how this affects the fluid flow (the new wind speed). Figure 4-27 shows the thrust coefficient curve related to wind turbine speed for the wind turbine under study, while Figure 4-28 shows the rotor speed curve according to the wind speed.

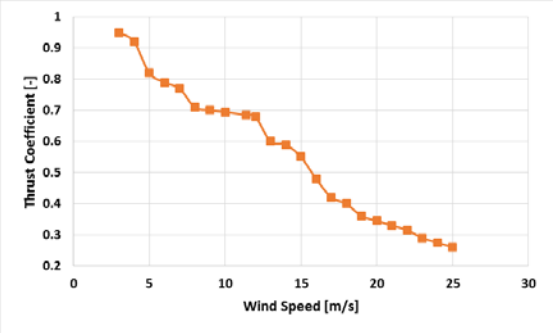

Figure 4-27: Thrust Coefficient curve.

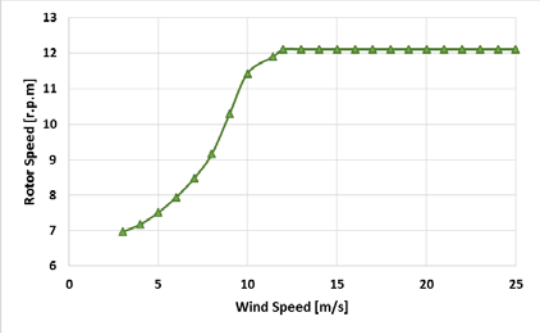

Figure 4-28: Rotor Speed curve.

Summary

The chapter starts with the first study area problem, explaining why offshore energy is an appropriate remarkable energy technology. Then the criteria that affect offshore wind energy spatial siting were chosen and described. Finally, all additional needed data for a more comprehensive site analysis is described:

1- Map data that represent criteria layers.
2- Loads combinations that affect the foundations.
3- Turbine data for the layout optimisation part.

Conclusions

- Accessible data in Egypt has some limitations, but this problem was overcome.
- In the high wind potential areas in Egypt, the offshore wind projects will avoid the land loss of the alternative onshore options.
- Wind data for the chosen sites verify that the siting process is valid and accurate where the wind potentials are high in these locations
- The expected capacity factor for an offshore wind farm in the chosen areas in Egypt will be higher than similar farms in Europe.

Chapter 5: Analytics, Results, and Discussion

The chapter introduces the weights of the factor governing the process using the RCR range introduced in Chapter 3 and data collected in Chapter 4. Then, the factor weights were validated using UK deployed projects. Finally, the chapter covers the spatial siting for the two case studies Egypt and Arabian Peninsula to locate the most suitable locations for offshore wind energy.

5.1 Criteria (Factors) Ranking / Pairwise Comparison

As indicated earlier, using the Representative Cost Ratio (RCR) as the new approach to calculate factor weighs will reduce time and effort to rank the criteria for offshore wind spatial siting. The Importance Index, of each possible factor pair, using the RCR range given in Table 3-7. The selected values for the Importance Index are chosen based on the contribution to the final Levelised Cost of Energy (LCOE) as shown in Table 5-1 (Cavazzi and Dutton, 2016). The contribution to the LCOE for wind speed is 50%, water depth is 20% and distance to shoreline is 5% and distance to grid is 2% (Cavazzi and Dutton, 2016) (Table 5-1). To arrive at the RCR value the contribution of these pairs in relation to each other will need to be established.

That is, the Wind Speed (WS) will need to be paired with other factors (Water Depth (WD), Distance to Shore (DS) and Distance to the Grid (DG)) and so on. Hence, the Importance Index score will be dependent on these combined contributions and the range of RCR given in Table 3-7, also shown in Table 5-1 for the specific RCR. For example, the Importance Index for Wind Speed compared to Water Depth is determined by their contribution to the LCOE as follows: WS:WD=50%:20%=2.5 this falls in the RCR range to 2~3:1 (Table 3-7) and hence was given a value of 3 (Table 5-1). Similarly, WS:DG=50%:2%=25, this falls in the RCR range 18>:1 (Table 3-7) and hence the Importance Index given is 9 (Table 5-1) and so on.

Table 5-1: Importance Index of each possible factor pair, using definition given in Table 3-7.

Contribution to LCOE, %	*Representative Cost Ratio* (RCR) = (Contribution to LCOE/other pair contribution)		Importance Index										Contribution to LCOE, %
			Equal	Weak or slight	Moderate	Moderate plus	Strong	Strong plus	Very strong	Very, very strong	Extreme		
			1	2	3	4	5	6	7	8	9		
50	2.5	WS[1]			x							**WD**	20
	10								x			**DS**	5
	25										x	**DG**	2
20	4	**WD**					x					**DS**	5
	10							x				**DG**	2
5	2.5	**DS**			x								2

[1] Where: **WS** is the Wind Speed factor, **WD** is the Water Depth factor, **DS** is the distanced to shoreline factor, and **DG** is the distance to grid factor.

The values in Table 5-1 were then used to establish the pairwise comparison matrix P_w (Table 5-2), using the two rules discussed earlier. The normalised matrix N_w (Table 5-3) is determined by dividing each matrix element of Table 5-2 by its column sum (described above). For instance, the wind speed value in the normalised matrix is determined by 1÷1.59 = 0.63 and so on for the other values. The Factor Weight values in Table 5-3 are the average of all values determined in the row for each factor.

Table 5-2: Pairwise comparison matrix P_w, Equations 3-1 and 3-2.

A \ B	Wind Speed	Water Depth	Distance to Shoreline	Distance to Grid
Wind Speed/Wind Power Intensity	1	3	7	9
Water Depth	1/3	1	5	6
Distance to Shoreline	1/7	1/5	1	3
Distance to Grid	1/9	1/6	1/3	1
Total (Σ)	1.59	4.37	13.33	19

The Principal Eigenvalue λ_{max} (Equation 3-9) is determined by the product of the factor sum (total) of each column of the pairwise matrix (Table 5-2) and the Factor Weight value (Table 5-3). For example, for the wind speed factor, λ_{max} = 1.59 x 0.58 = 0.93 and so on for all other values.

In order to ascertain the validity of the assumptions made, the magnitude range of the Consistency Ratio CR (Equation 3-7) should be less than or equal to 0.1. The Consistency Index, *CI*, using (Equation 3-8) has a value of 0.077 since $\Sigma \lambda_{max} = 4.23$ from Table 5-3 and n=4. The Random Consistency Index, *RI*, for the four factors has a value of 0.9, (Saaty, 1977). Using these values in (Equation 3-7), *CR* has a value of 0.085, which is < 0.10. Hence, the values in Table 5-1 are consistent (Saaty, 2008).

Table 5-3: Normalized matrix and final factors weight value.

	Wind	Water Depth	Shoreline	Grid	Factor Weight	λ_{max}
Wind	0.63	0.69	0.53	0.47	0.58	0.93
Water Depth	0.21	0.23	0.38	0.32	0.28	1.23
Shoreline	0.09	0.05	0.08	0.16	0.09	1.23
Grid	0.07	0.04	0.03	0.05	0.05	0.84
Σ	1.00	1.00	1.00	1.00	1.00	4.23

5.1.1 Factor Standardisation (Fuzzy Membership Function)

Fuzzy function describes the relationship between the increases in a factor's magnitude as compared to overall cost appreciation or reduction. Such an assessment also depends on the experience and the knowledge about the factors. Figure 5-1 shows the relationship between the scale factors for cost increase and water depth, and distance to shore – adopted from data provided in (Green and Vasilakos, 2011, EEA, 2009) tables. Scale factor is the cost rise due to water depth or shore distance increasing. Figure 5-1 indicates that the relationship is almost linear. This means that the fuzzy membership function for the increases in water depth, and distance to shore are decreasing linearly. Therefore, linear fuzzy membership using ArcGIS tools will be used to standardise the factors.

The cost change with depth in particular will show a step change with a certain water pressure, which is not present in Figure 5-1. The data was adopted from (EEA, 2009) where the data was normalised for 'year of installation' to account for the learning rate effect on wind turbine cost. The average water depths for the study areas here is around 25m and the distance to cost is 50 km; these figures are located in the first part of the curves in Figure 5-1, see the red dashed rectangular. The first part of the curve is acceptable where the rest of it needs more investigation.

In order to apply the above analysis to the two case studies, a consideration of the membership limitations for the factors to be used in each study area is needed. These limitations were adopted from Table 4-3, Section 4.2. These limitations are depicted in Table 5-4. A Fuzzy Membership tool will be applied to produce a new linear standardised layer for each factor. Such a process will be accomplished for each case study separately.

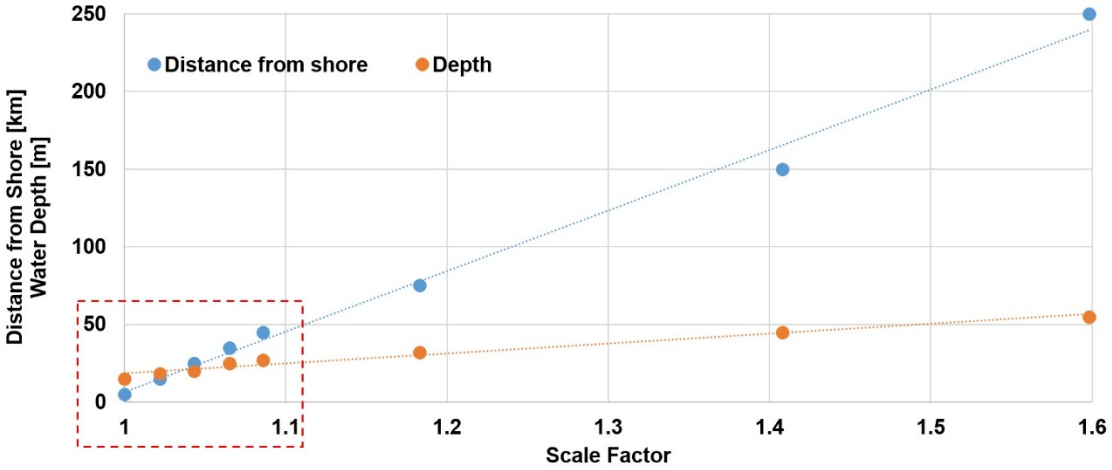

Figure 5-1: Relationship between increase of cost (the scale factor), in relation to increasing water depth, and distance to shore, adopted from (Green and Vasilakos, 2011, EEA, 2009).

Table 5-4: Fuzzy membership limitations and related values.

Factor	Fuzzy Type	Max	Min	Condition	Value	Condition	Value
Mean power density	Linear	850 W/m²	45 W/m²	> Max	1.0	< Min	0.0
Wind Speed	Linear	7 m/s	3 m/s	> Max	1.0	< Min	0.0
Water Depth (Below MSL)	Linear	- 60.0 m	- 5.0 m	< Max	0.0	> Min	0.0
Distance to Shoreline	Linear	140 km	5.0 km	> Max	1.0	< Min	0.0
Distance to the Grid	Linear	180 km	10.0 km	> Max	0.0	< Min	1.0

5.1.2 UK (RCR Validation Model)

The UK has ambitious programme for offshore wind. This is normally managed through the Crown Estate, which is an independent authority, with leasing responsibility of the seabed of the UK including the promotion and the exploitation of the resources around and within the UK's shores. For offshore wind energy, such exploitation was undertaken through a process called "leasing rounds" or "Rounds" for short. The Crown Estate utilised a Marine Resource System (MaRS) tools

based on a GIS database to identify potential offshore wind areas under various government investments stages to support each Round. There are three Rounds - 1 to 3 - where offshore wind farm projects are tendered for deployment at various locations around the UK (The Crown Estate, 2012b). Rounds and 1 and 2 have already been deployed whilst Round 3 is in partial deployment.

The UK's Round 3, announced in mid-2008 covered an approximate area of 27,000 km^2 and aimed to exploit more than 32 GW of offshore wind energy(The Crown Estate, 2012b). However, by the end of 2018 only 30% of this area has been exploited. Nevertheless, this represents 49% of Europe's gross offshore wind installed capacity in 2018, with the UK representing the highest installed capacity in the world (WindEurope, 2018).

For the development of these projects, the Crown Estate has only published the location maps for the three Rounds, and has not disclosed details of the methodology used for the spatial siting of the wind farms in the selected locations (The Crown Estate, 2012b, The Crown Estate, 2012a, The Crown Estate, 2014, The Crown Estate, 2017, The Crown Estate, 2019). However, their reports state the criteria and the scenarios/iterations considered when approving projects (The Crown Estate, 2012b, The Crown Estate, 2012a, The Crown Estate, 2014, The Crown Estate, 2017, The Crown Estate, 2019). Such considerations are useful to allow us to undertake analysis to compare the methodology with that of the results achieved through the Crown Estate considerations.

The Factor Weight values in Table 5-3, which were calculated using the introduced *Representative Cost Ratio* approach, were used to create a suitability map for the UK's offshore regions. The UK has the rights to exploit their shores out to 200 miles of the seabed or 50% spatial distance with neighbouring countries for renewable energy power generation. This section provides the analysis undertaken which is geared to check the appropriateness and validity of this study proposed methodology and its assumption. This is accomplished by applying it to assess the suitability of the locations of the UK offshore wind farms' ongoing deployments.

Four suitability factor maps were produced using the available information from the Crown Estate Maps and their GIS Data website, which was updated in 2019 (The Crown Estate, 2019). The source shape files of the water depth, grid connection, wind speed, and shoreline were converted to a raster format, with a cell size of 200 x 200 m, and its Geographic Coordinate System was "WGS 1984 UTM Zone 31N". The data for different factors were established in different dimensions (wind speed, water depth, distance to shore, and distance to grid – referred to as layer) and scales

of values. Therefore, to arrive at the Weighted Linear Combination (WLC) step (last step in Figure 3-1, linear fuzzy limits were applied to unify their scales and dimensions to a scale from (1 to 0) (see methodology). These new layers called factor suitability maps represent: (a) Water depth factor, (b) Distance to electricity grid line, (c) Distance to UK shorelines, and (d) Wind speed factor. The four maps are processed using the Fuzzy-membership Tool in ArcGIS programme with the resulting suitability maps for these four factors shown in Figure 5-2.

The Boolean mask was not used in this analysis as the Crown Estate had already eliminated the constraints criteria from the mapping of the three Rounds. The four suitability maps shown in Figure 5-2 were integrated using ArcGIS Raster Calculator Tool, applying Equation (3), (Weighted Linear Combination (WLC) method). The final UK suitability score for each map cell equals [0.28 x water depth suitability + 0.05 x distance to grid suitability + 0.09 x distance to shorelines suitability + 0.58 x wind speed suitability], where the factors weight values are those given in Table 5-3.

These considerations resulted in the offshore wind suitability map for the UK shown in Figure 5-3. The suitability score shown in Figure 5-3 ranged from 0 (least suitability) to 1 (highest suitability). The results indicate that around 26% of the UK's offshore areas have high suitability (Figure 5-3 legend range - 0.6 to 1.0) for offshore wind and that these areas are concentrated in the East of England and most of Scottish waters.

To validate the new approach, the suitability of the operational and planned UK's offshore wind farms under Rounds 1, 2 and 3, were identified using their original locations and boundaries derived from Crown Estate maps, which were superimposed onto the newly generated UK offshore wind suitability map. The appropriate validation is to ascertain whether all the cells identified by the Crown Estate to develop the offshore wind energy Rounds through the last two decades, coincide within the high and moderate suitability areas generated through this work methodology, shown in Figure 5-3.

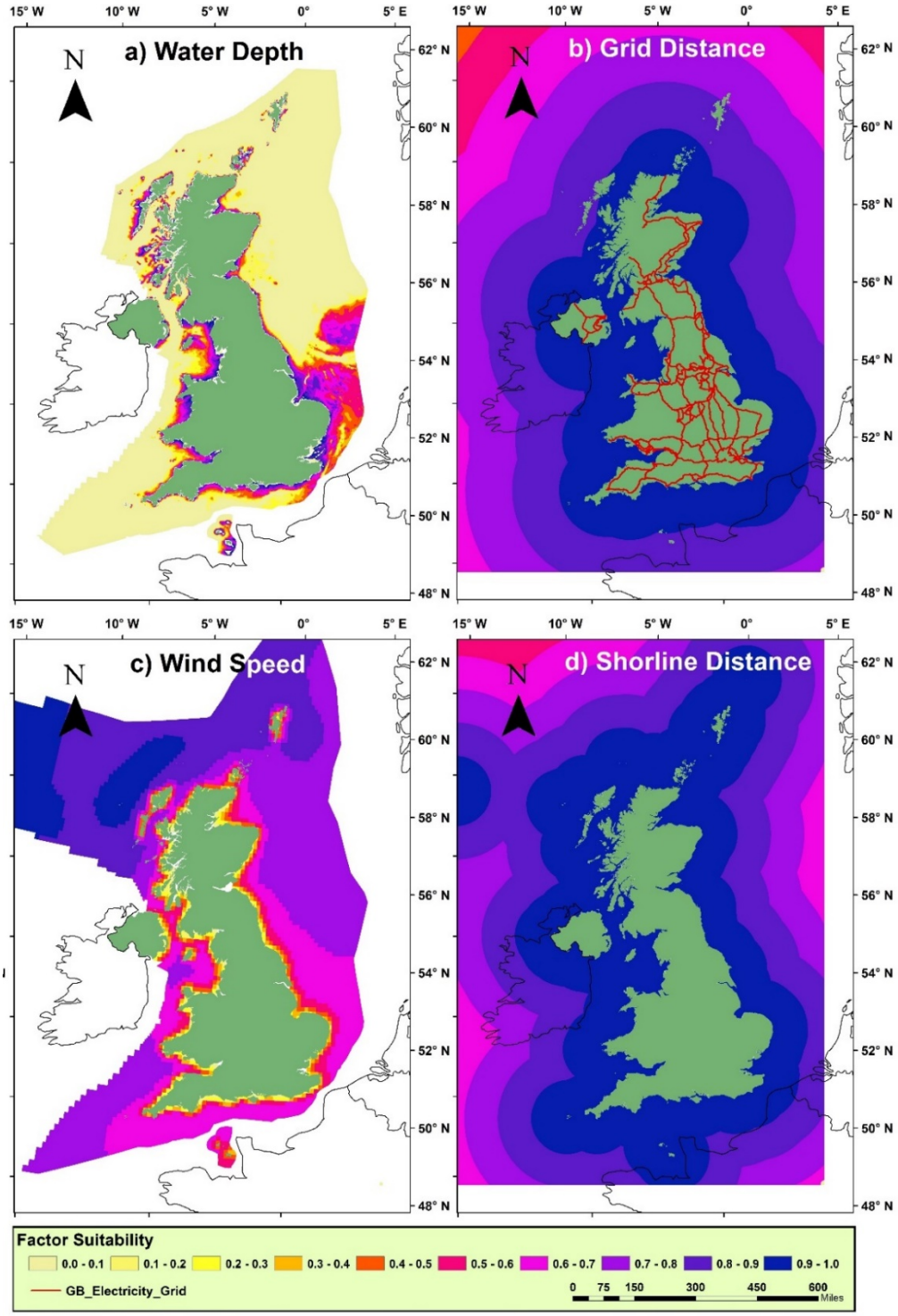

Figure 5-2: The suitability maps for the four considered factors: (a) Water depth factor, (b) Distance to electricity grid line, (c) Distance to UK shorelines, and (d) Wind speed factor.

The Boolean mask was not used in this analysis as the Crown Estate had already eliminated the constraints criteria from the mapping of the three Rounds. The four suitability maps shown in

Figure 5-2 were integrated using ArcGIS Raster Calculator Tool, applying Equation (3), (Weighted Linear Combination (WLC) method). The final UK suitability score for each map cell equals [0.28 x water depth suitability + 0.05 x distance to grid suitability + 0.09 x distance to shorelines suitability + 0.58 x wind speed suitability], where the factors weight values are those given in Table 5-3.

These considerations resulted in the offshore wind suitability map for the UK shown in Figure 5-3. The suitability score shown in Figure 5-3 ranged from 0 (least suitability) to 1 (highest suitability). The results indicate that around 26% of the UK's offshore areas have high suitability (Figure 5-3 legend range - 0.6 to 1.0) for offshore wind and that these areas are concentrated in the East of England and most of Scottish waters.

To validate the new approach, the suitability of the operational and planned UK's offshore wind farms under Rounds 1, 2 and 3, were identified using their original locations and boundaries derived from Crown Estate maps, which were superimposed onto the newly generated UK offshore wind suitability map. The appropriate validation is to ascertain whether all the cells identified by the Crown Estate to develop the offshore wind energy Rounds through the last two decades, coincide within the high and moderate suitability areas generated through this work methodology, shown in Figure 5-3.

Figure 5-4 shows the locations of three Rounds of the UK's offshore wind energy farms superimposed on this work resultant analysis of Figure 5-3. Figure 5-4 is the same as Figure 5-3, but enlarged to show more details. The Clipping Tool in ArcGIS was used to clip the suitability map of the UK resulting in the outlines shown in the figure covering three sets: (i) Round 1 and 2 operating wind farms (shown in grey), and (ii) Round 3 operational wind farms areas outlined in red and (iii) Round 3 under construction or planned shown dotted. The suitability score in Figures 5-3 and 5-4 is ranged from 0 (least suitability) to 1 (highest suitability). The results in the Figure 5-3 is also duplicated in Figure 5-4 opposite where it is enlarged to allow more details to be shown including superimposing the 3 Rounds of the current and future offshore wind farms. It is clear from the results in Figure 5-4 that the UK offshore wind rounds are within the high and medium suitability areas generated by this work analysis.

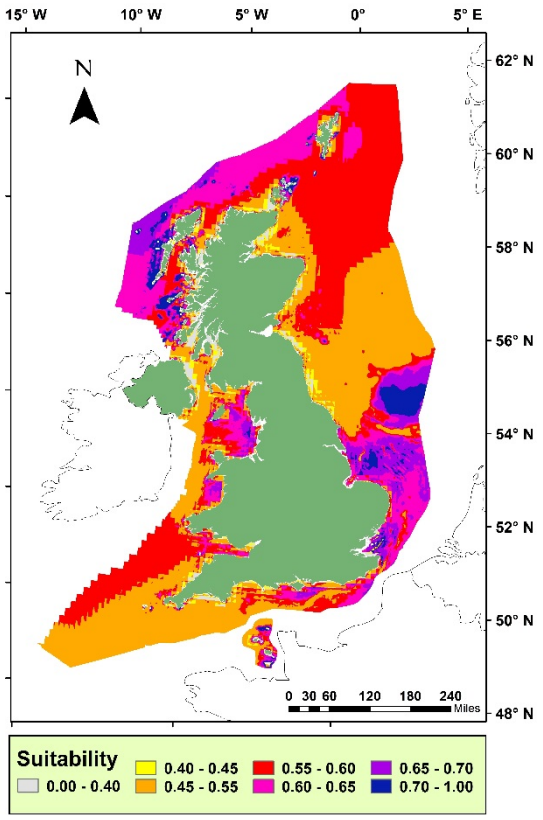

Figure 5-3: UK's offshore wind suitability map produced by the methodology presented here.

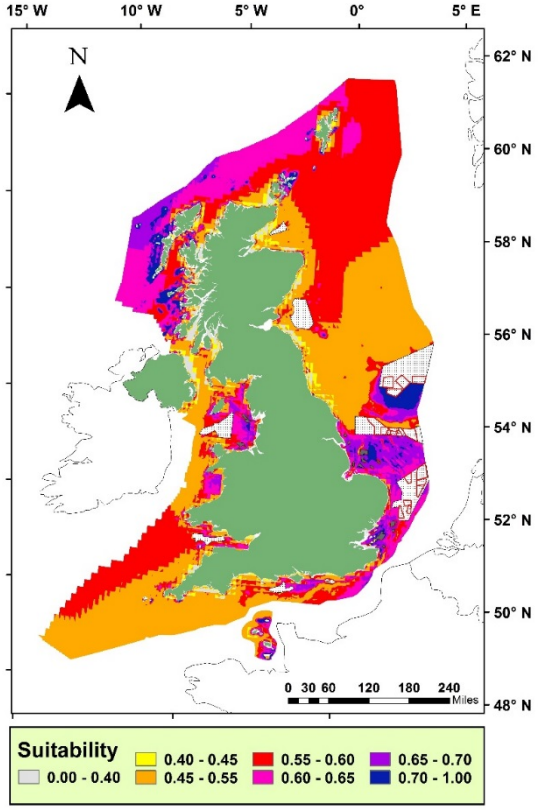

Figure 5-4: Same suitability distribution map as Figure 5-3. The UK Rounds 1 and 2 are shown in grey and Round 3 dotted areas with current wind farms outlines are in red.

In order to estimate the suitability percentage distribution for the three sets, (i), (ii) and (iii) mentioned above, the Attribute Table which identifies the geographic feature of an ArcGIS Layer for each set was used to arrive at the number of cells for every suitability score range (0 to 1). The Attribute Table and the scores for these sets are given in appendix C. Table 5-5, depicts the suitability percentages for all the three Rounds of the UK offshore wind projects. The table shows the estimated areas for each Round as well as the predicted suitability determined by the methodology presented here. The cell suitability distribution in Table 5-5 is divided into three ranges - unsuitable cells (0.0 to 0.39 score), moderately suitable cells (0.4 to 0.59), and highly suitable (0.6 to 1.0). As can be seen from the results in Table 5-5, all the UK's operational or planned offshore wind locations are in moderate and high suitability ranking. For Rounds 1 and 2, 92.4% of the farms were found to be in the high suitability areas with an estimated area of 1,342 km^2. While for operational farms in Round 3, 85.8% were in high suitability areas, with an estimated area of 8,565 km^2. For under construction or planned farms in Round 3 only 64.2% are within highly suitable areas, while the remaining (35.8%) areas are in moderately suitable areas, covering an estimated area of 27,039.9 km^2. The reason for this split is the high water depth average that exceeds

39.4 meters, which will reduce the percentage of high suitability cells for the wind farms planned in Round 3.

Table 5-5: Percentages of suitability distribution for the UK offshore wind projects.

Round / [Location Source]	Estimated Area (km^2)	Installed Capacity (GW)	Predicted Suitability Distribution [%]*		
			Unsuitable	Moderate	High
Round 1 and 2 / (Lambkin et al., 2009)	1342.4	7.5	0	7.6	92.4
Round 3 operating wind farms until the end of 2018 / (The Crown Estate, 2019)	8565.8	10.1	0	14.2	85.8
Round 3 under construction /planned / (Flood, 2012)	27039.9	32	0	35.8	64.2

* Cell scores: Unsuitable < 0.39; Moderate 0.4 to 0.6; High > 0.6 (suitability maps Figures 5-3 and 5-4).

The spatial sitting verification was performed using the pre-planned UK offshore wind energy projects announced under Rounds 1 to 3. As can be seen from the results, the verification proved that the new *Representative Cost Ratio* (RCR) approach is very accurate as all of the cells of these farms are located in either moderate or high suitability categories (Table 5-5). Furthermore, this verification is significant, as the data used by the UK have been simulated, the country with highest installed capacity of offshore wind farms coupled with unmatched experience in planning, financing, and constructing such farms globally.

Considering that, the UK's offshore wind developers are spending around £90k per MW for the cost of the offshore wind spatial planning process alone (Cavazzi and Dutton, 2016), this means that their commissioned maps are highly precise and accurate. The proposed new approach will save on such expenditure and reduce the time and effort needed to achieve the optimal spatial siting plan decision. It is therefore concluded, that the results given in Figure 5-3, Figure 5-4, and Table 5-5 confirm the quality of the different assumptions and calculation of the new RCR approach to accurately estimate the suitability of offshore wind energy farms. This approach will now be tested further by applying it to the analysis of the potential for offshore wind energy at local and regional scale, in un-investigated areas around the shores of Egypt and the Arabian Peninsula.

5.2 Egypt (Case Study 1) Offshore Wind Farms Spatial Siting

5.2.1 Constraint Layers and the Boolean Mask

A Boolean mask was created to exclude the restricted cells by giving them value 0 or 1, see Table 5-6. Table 5-6 shows the 0 and 1 conditions, which were adopted from the constraints shown in Table 4-3. Figures from 5-5 to 5-12 show each constraint Boolean mask layer. Finally, all these constrains were gathered in one layer. The Raster Calculator tool in ArcGIS was used to aggregate all restriction layers in one layer (over all Boolean Mask), see Figure 5-13. The 5-1 equation was used to calculate the new Boolean Mask layer:

Boolean_Mask = Depth_Const * Shore_Dis_Const * Fising_Const * Military_Const * Shiping_Const * Oil_Gas_Const * Cables_Const * Natural_Res_Const (5-1)

Table 5-6: Constrains 0, and 1 definition and related figures numbers.

Constrain	0	1	Representing Figure
Depth	Depths less than 5.0 m or more than 60.0 m	Else	(5-5)
Distance from shore	Distance less than 1.5 km or more than 200.0 km	Else	(5-6)
Fishing areas	Depths more than 70.0 m	Else	-
Military Practice and Exercise Areas	Military areas as shown in Figure (4-14)	Else	(5-8)
Shipping Routes, ports, approach channels	Areas as shown in Figure (4-10)	Else	(5-7)
Oil & Gas Wells Pipelines Gas and Oil Storage Areas	Areas as shown in Figure (4-6)	Else	(5-10)
Cables and tunnels	Lines as shown in Figure (5-9)	Else	(5-9)
Nature Reserves	Marine parks as shown in Figure (4-8)	Else	(5-11)
Terrorism activity areas	Rafah and El-Arish coast lines	Else	(5-12)

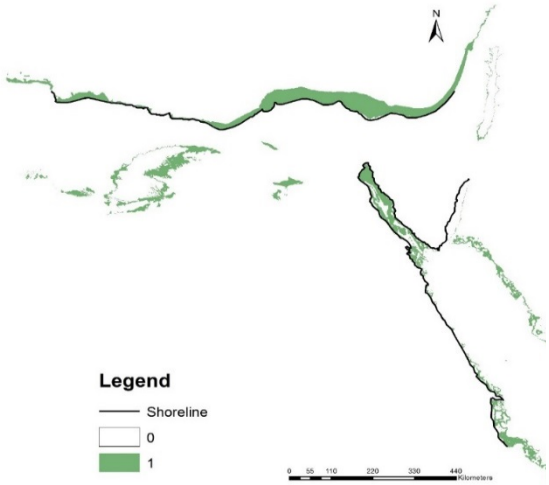

Figure 5-5: Boolean layer for water depths.

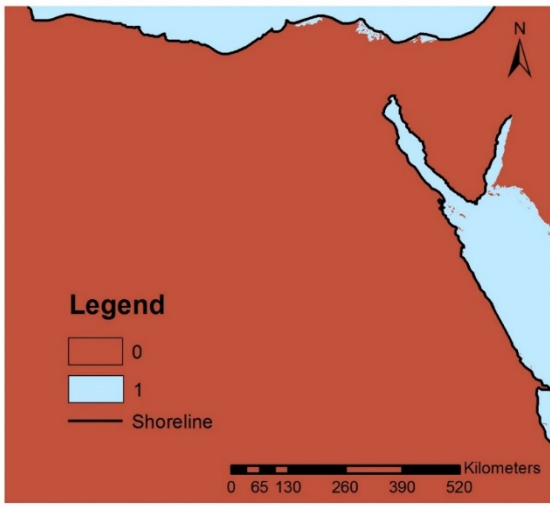

Figure 5-6: Boolean layer for distance from shore

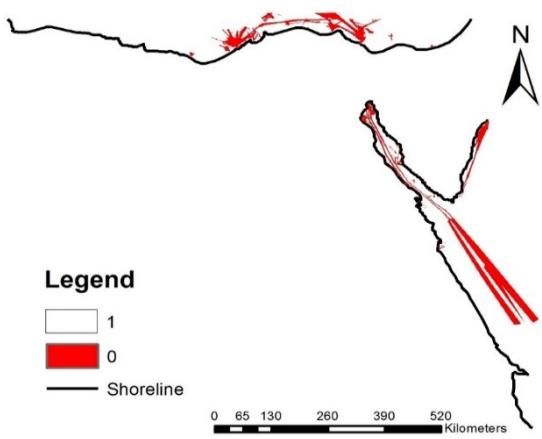

Figure 5-7: Boolean layer for the shipping routes and ports

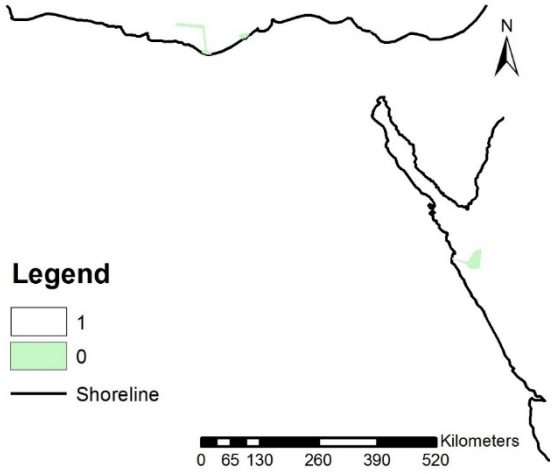

Figure 5-8: Boolean layer for restricted marine military areas

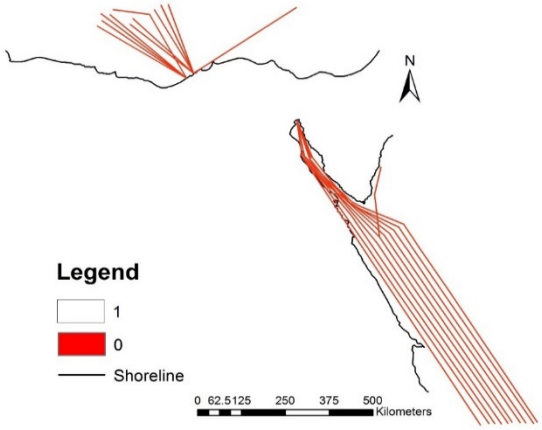

Figure 5-9: Boolean layer for the submerged cables lines

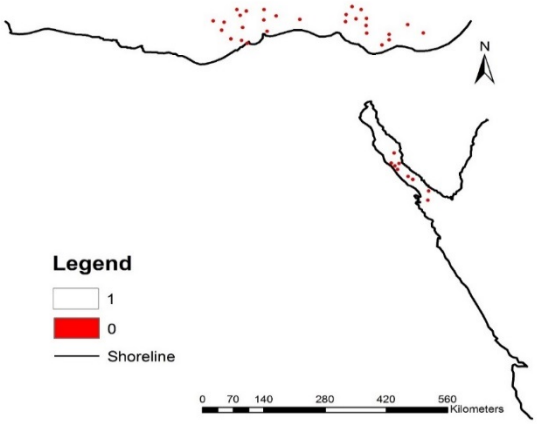

Figure 5-10: Boolean layer for oil and gas wells areas.

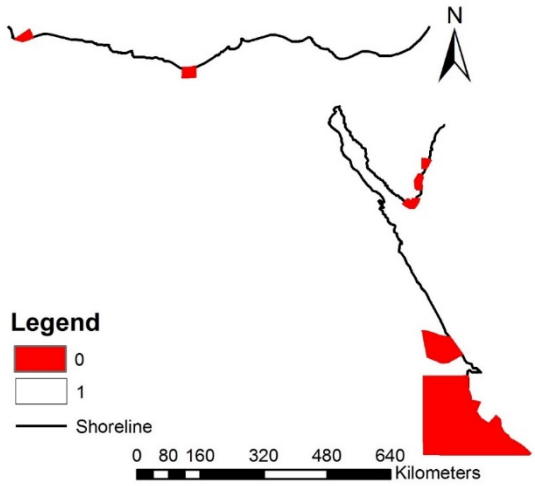

Figure 5-11: Boolean layer for the protected marine national parks in Egypt.

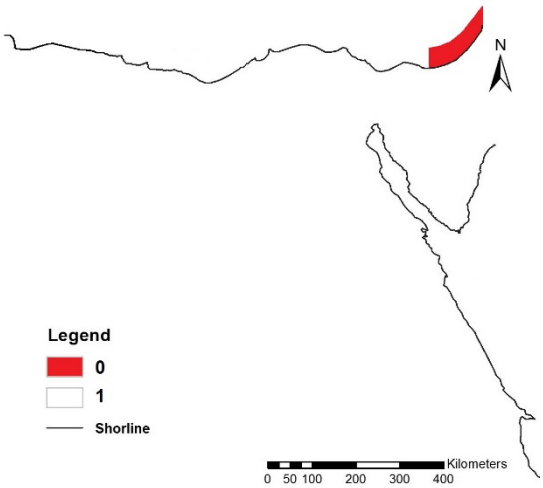

Figure 5-12: Boolean layer Safety and Security areas.

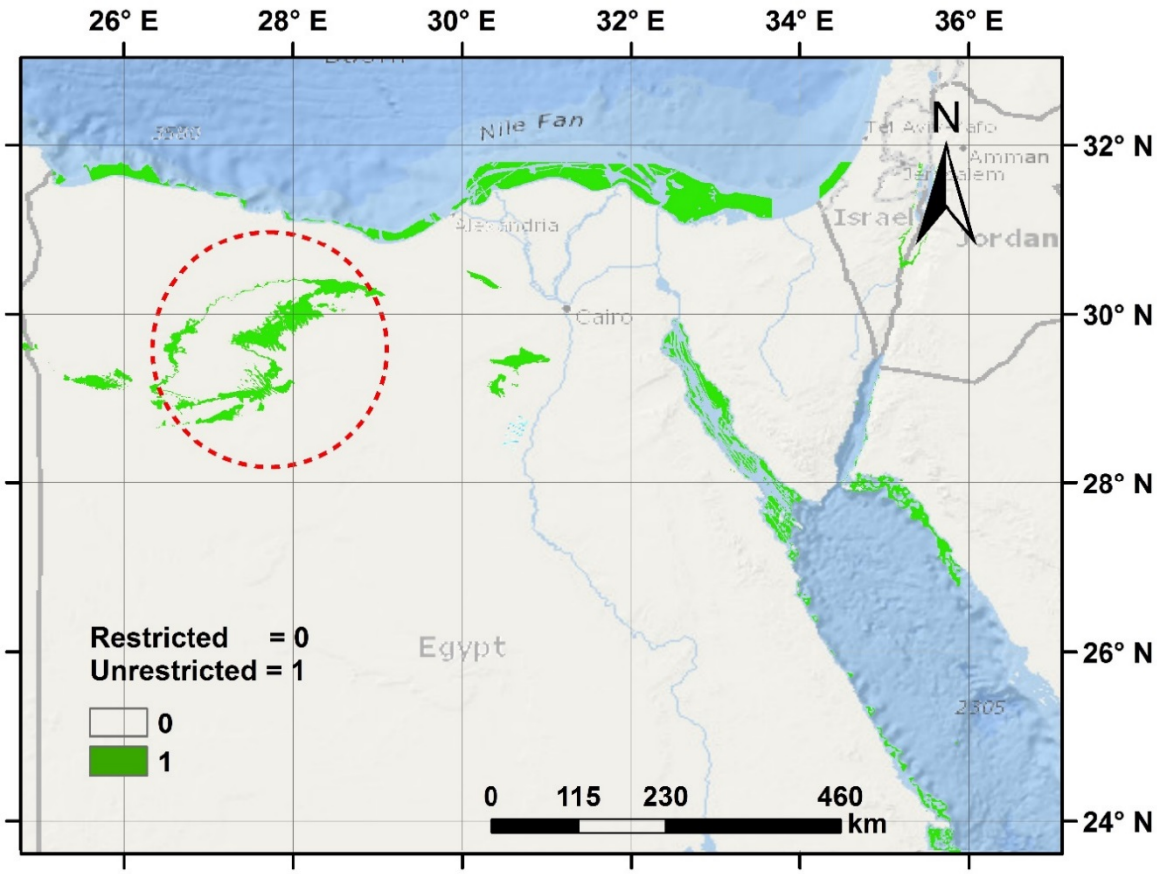

Figure 5-13: The final Boolean mask layer after multiplying all constraints together, where green cells are valid alternatives and other that is not considered as alternatives. The red circle showing the Qattara Depression (see Section 5.2.4 for more explanations).

5.2.2 Criteria Aggregation

All criteria were aggregated to create a suitability map of offshore wind farms in Egypt. The Weighted Linear Combination (WLC) equation was used to conduct the aggregation. The standardised layers were first multiplied by its weights, then summed together, using the Weighted Sum tool in ArcGIS. Finally, the Weighted Sum layer was multiplied by the Boolean Mask layer, using the Raster Calculator tool. The final Suitability Map layer is shown in Figure 5-14.

5.2.3 Results Validation (Sensitivity Analysis)

Sensitivity analysis can be thought of as a set of tests to validate the solutions derived from the work. The tests were done by increasing or decreasing the factor weight values by a small parentage (0 to 20%). Then a check is made to see if such a changes have a major influence on the suitability results or otherwise. Each factor was changed in a separate process, and its impact on the results was evaluated. In essence, the tests provide more confidence in the results and the reliability of the model (Jankowski et al., 1997).

In order to achieve confidence in the results of this spatial siting work, two sensitivity considerations were introduced (Chen et al., 2009, Chen et al., 2010):

(a) Emphasise that the error is less than 10% for the all small changes ≤ 4%

(b) Check that no cells moved from unsuitable to high suitability or vice versa for all changes (see Appendix B for more details).

Hence to follow the above requirements, the factors weights in Table 5-3 were adjusted (decreased or increased) by 4%, 8%, 12%, 16%, and 20 %. The decreased or increased by 4% was conducted to test the model robustness under minor changes, while the other decreases / increases were applied to observe the cells suitability behaviour under major changes. The redistribution method was utilised to readjust the other weights by adding or reducing the remaining weights according to its percentage to the sum of the weights, in a way to keep the total weights equal one. For example, if wind speed factor weight is reduced by 20% = 0.58 x 0.8 = 0.46, then the water depth factor weight will be 0.28 + 0.28 x (0.58-0.46) = 0.31.

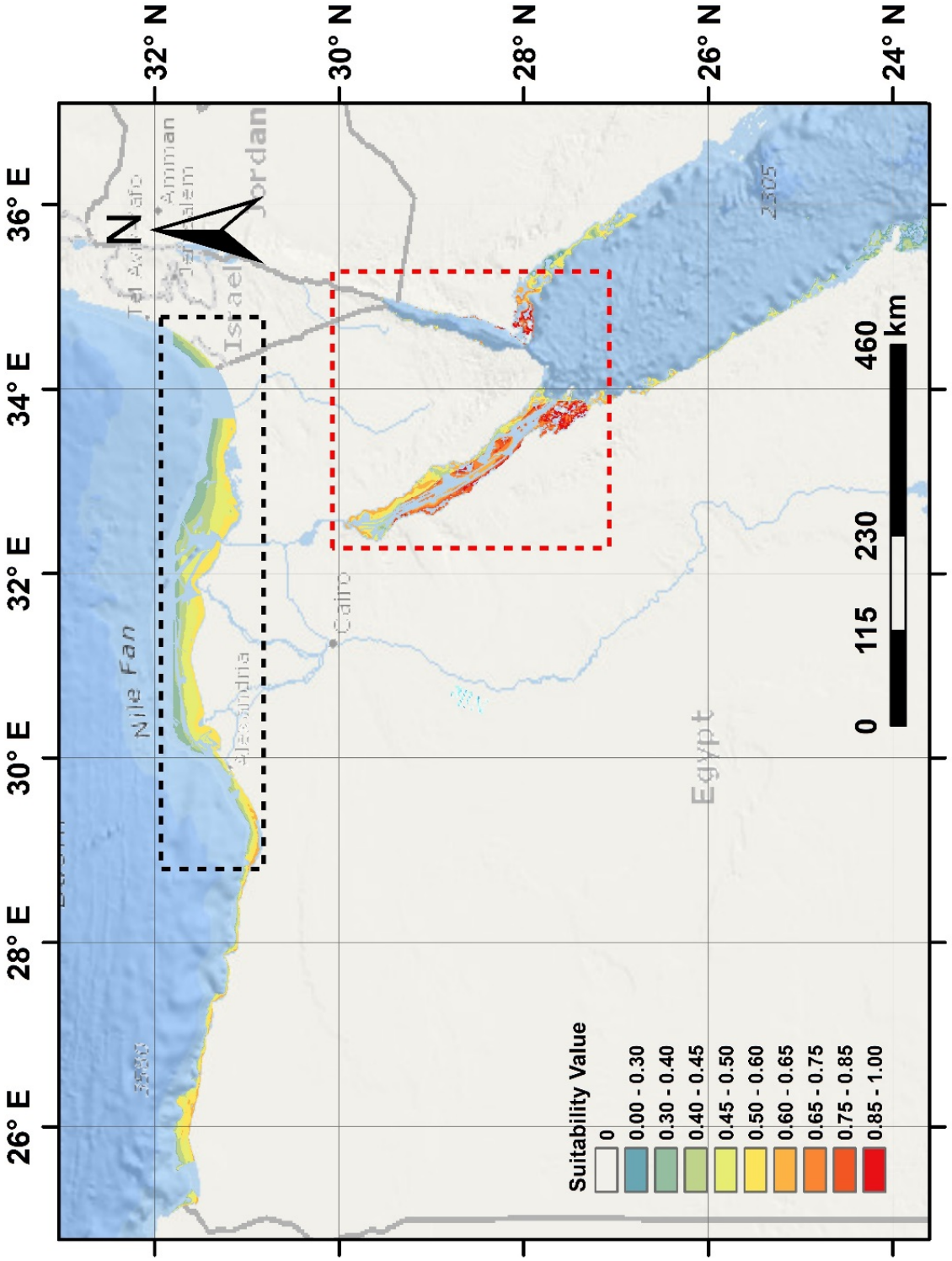

Figure 5-14: Final Suitability Map for offshore wind in Egypt, where the legend indicates the weights of suitability where 0 = least suitable and 0.99 = most suitable. Black and red rectangles represent areas of moderate and high suitability, respectively.

The cells were categorised into three groups according to its suitability: (a) unsuitable for ranks less than 39%, (b) moderate for ranks between 40 to 59%, and (c) high suitability for ranks greater than 60%. Figures 5-15 to 5-18 show the change of the factors weights and the corresponding alteration on the cells numbers.

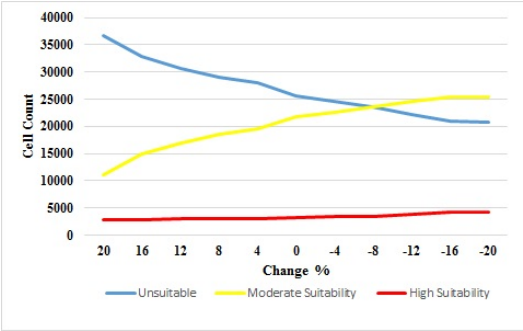

Figure 5-15: Wind Power Factor sensitivity test

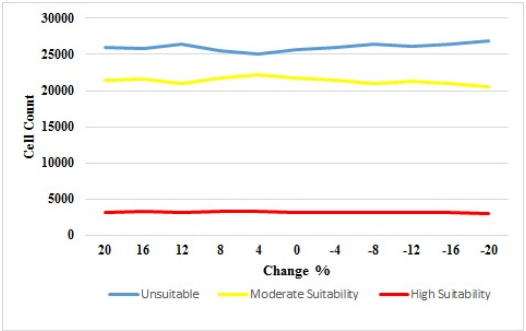

Figure 5-16: Water Depth Factor sensitivity test.

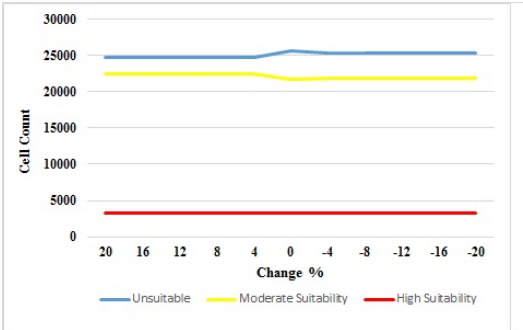

Figure 5-17: Distance to Grid Factor sensitivity test

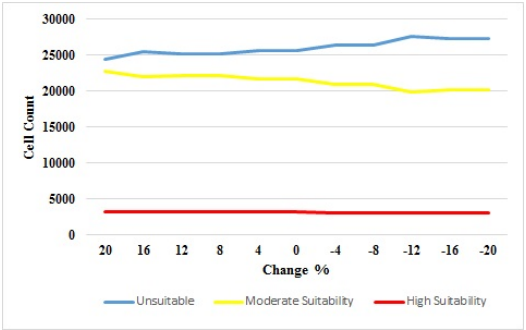

Figure 5-18: Distance to Shore Factor sensitivity test

In the sensitivity analysis, it was observed that no cells moved from high suitability to unsuitable categories or vice versa for all factors and percentage changes. The error percentage is less than 10% for all the factors for the changes less than 4%; see Tables B-1 to B-4 (Appendix B). The wind power factor (Figure 5-15) has the highest sensitivity and the distance to the national grid factor (Figure 5-17) has the lowest sensitivity between all the factors. For example, when the wind factor weight (Figure 5-15) was increased by 20%, the high suitability cells decrease by 11% and the unsuitable increase by 43% (see Table B.1 Appendix B). Conversely, when wind factor is reduced by 20%, the high suitability cells increase by 35% and the unsuitable decrease by 19%. On the other hand, all errors percentages for grid factor (Figure 5-17) changes are less than 3.5% (see Table B.3 Appendix B). As there are no major changes in the results due to the small adjustments made in

the factors' values, these sensitivity test emphasised that the pairwise assumptions are valid and the data collected is sufficient and robust.

5.2.4 Discussion

The study area presented here is based on Geographical Information System (GIS) encompassing multi-criteria decision analysis (MCDA) methodology through which a model was developed to create the suitability map for offshore wind energy for local and large regional scales. The developed spatial siting model handled different criteria that govern the spatial planning for offshore wind farms. The spatial analysis was undertaken at a medium resolution (800 m by 800 m), confined to the cell size of the bathymetry map source.

In the spatial analysis, was applied across all Egypt here, an onshore area with a value of one was found in the Boolean mask layer, circled in red (Figure 5-13). The reason for this confliction is that the onshore area considered has an altitude less than -5 m below mean sea level and corresponds to the Qattara Depression, located in the north-west of Egypt. Qattara Depression is "the largest and deepest of the undrained natural depressions in the Sahara Desert," with the lowest point of -134 m below mean sea level (Albritton et al., 1990). Identifying such areas gives further confidence in the robustness of the spatial siting modelling and analysis. These areas were excluded from the final suitability map (Figure 5-14).

From the final suitability map, Figure 5-14, it is clear that most of the high suitability cells are concentrated in areas that have wind power density > 600 W/m^2, which reflects the strong influence of wind power criterion on final score/rank of each cell. This result is reasonable because the wind power has a relative importance of more than 50%. The second factor is water depth which it has 28% share of the total weight, which explains the extended, wide area with moderate suitability, which appeared adjacent to the northern coast of Egypt. These moderate suitability areas are shown in yellow within the black rectangle in Figure 5-14. Here, the average mean power density is less than 200 W/m^2 along the coastal areas, where the slope is mild (shallow) approximately less than 1:800 for more than 50 km away from the sea (The British Oceanographic Data Centre, 2014). Therefore, the area has an advantage of shallow depths for a long distance in the sea, which allow for a significant number of cells to have a score in the range of 0.5 to 0.6. These moderate areas were not considered for further analysis; however, these areas could be exploited for future research for lower rate wind energy exploitation.

Final suitability cells were categorised into three groups according to its their suitability: (a) unsuitable for ranks less than 39%, (b) moderate for ranks between 40 to 59%, and (c) high suitability for ranks greater than 60%. The analysis conducted was for cell dimensions of 800m by 800 m, which represent an area of 0.64 km^2. The total number of high suitability areas for offshore wind farms is approximately 7356 cells, which represent about 4708 km^2, while the moderate suitability area is about 18727 cells which equal to 11985 km^2. These figures are promising when compared with, for example, the 122 km^2 of London Array, one of the world's largest offshore wind farms, which has a capacity of 630 MW (The Crown Estate, 2012b).

Unsuitable areas for offshore wind farms are equal to 14600 km^2. These areas are not suitable for any further studies or development, because the return on investments from offshore wind energy for these areas will be low.

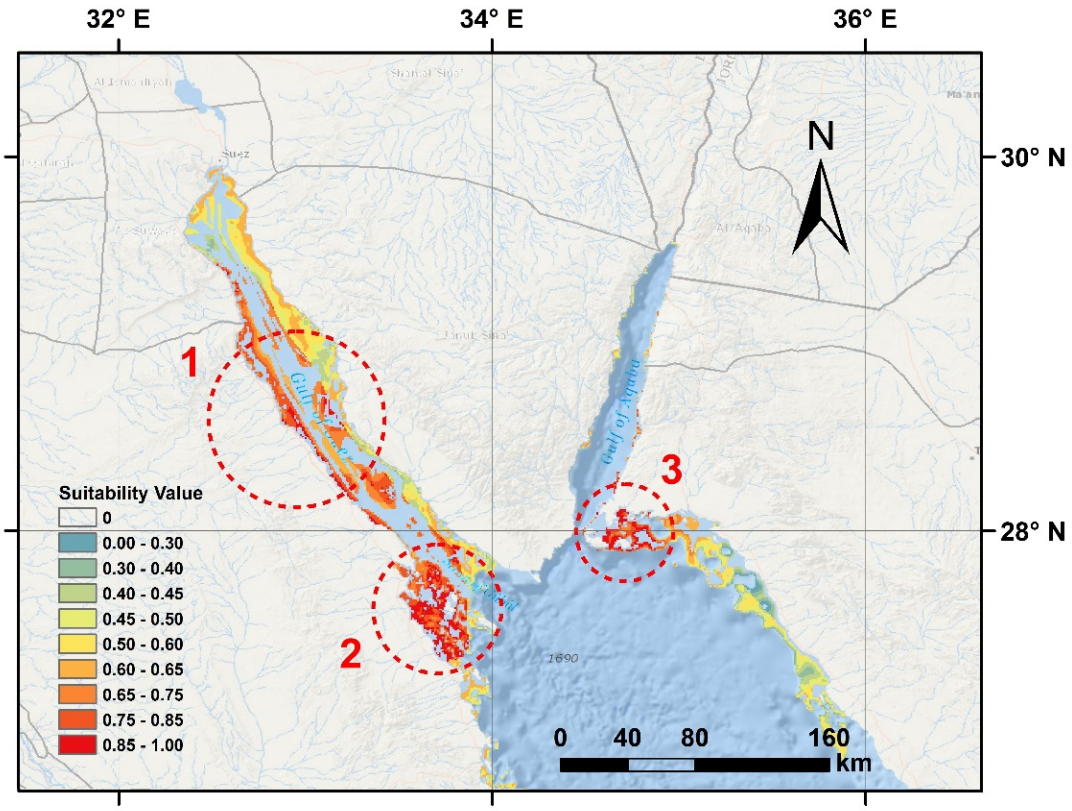

Figure 5-19: The Suitability Map for offshore wind farms around the southern coast of Sinai Peninsula, Red Sea, Egypt. The encircled area areas show high wind energy potentials.

The final locations of these are provided in the suitability map (Figure 5-19) with most suitable locations for offshore wind farms in Egypt, are shown circled. Location 1(Zafarana), 2 (El-Gouna), and 3 (Nabq Bay) contain 1647.9, 2124.4, 390.7 km^2 of highly suitable areas for offshore wind farms, respectively. Locations 1 and 2 are in the Egyptian territorial waters, while location 3 is situated between Egypt and Saudi Arabia. Most of location 3 was in Egyptian territories until 17 June 2017, "when Saudi Arabia and Egypt reached a delimitation agreement, granting Saudi Arabia the sovereignty over Tiran and Sanafir islands," which make most of location 3 in Saudi Arabia (Alfadhli, 2018, Embabi, 2018). That is the reason location 3 was included in the analysis in the first place. The areas that have high suitability were counted for additional analysis and investigation; see Chapter 6.

In order to estimate the potential wind energy capacity of these areas, the equation provided by (E.ON, 2012, Sheridan et al., 2012) is used. They estimated the effective footprint per turbine (array spacing area) using this expression:

$$S = (R_d)^2 \times L^d \times L^c \qquad (5\text{-}2)$$

Where: $\mathbf{S}$ is the array spacing area giving the footprint for each offshore wind turbine, $\mathbf{R_d}$ is the rotor diameter, $\mathbf{L_d}$ is the downwind spacing, and $\mathbf{L_c}$ is the cross wind spacing.

A turbine spacing of 5 to 8 times rotor diameter is used in order to reduce turbulence between turbines for average wind speeds around 10 m/s (E.ON, 2012). Therefore, for a 5 MW turbine (126 m rotor diameter), one square kilometre of the chosen area would yield ~ 7.87 MW of installed capacity. Following these considerations, for the three locations considered above, the total wind power capacity is estimated to be around 33 GW (Table 6-1).

Table 5-7: Estimate wind power potential per considered area.

Location (Figure 5-19)	Area (km^2)	Estimated power capacity (GW)
Location 1 (Zafarana)	1647.9	12.97
Location 2 (El-Gouna)	2124.4	16.72
Location 3 (Nabq Bay)	390.7	3.1
Total (GW)		32.8

These three sites are chosen for further investigations and designs (Chapter 6). Prior to these advanced analyses, there is a need to check if the wind energy power production meets the high electricity demand in summer of Egypt. Figure 5-20 shows the mean monthly wind speed for the

three chosen locations. As can be seen from the figure, the monthly summer speeds ranged between 7 to 12 [m/s], which supports the view that offshore wind energy yield will secure the high electricity demand in these particular periods of the year. For example, if three 500 MW offshore wind farms were deployed in the chosen sites, this can generate in July electricity of 284.6, 325.5, and 178.6 GWh, considering a capacity factor of 0.45, 0.5, and 0.4, respectively. These wind farm will secure 5.6% of the 14.2 TWh expected electricity demand in Egypt, July 2022, (The Ministry of Electricity and Energy of Egypt, 2017).

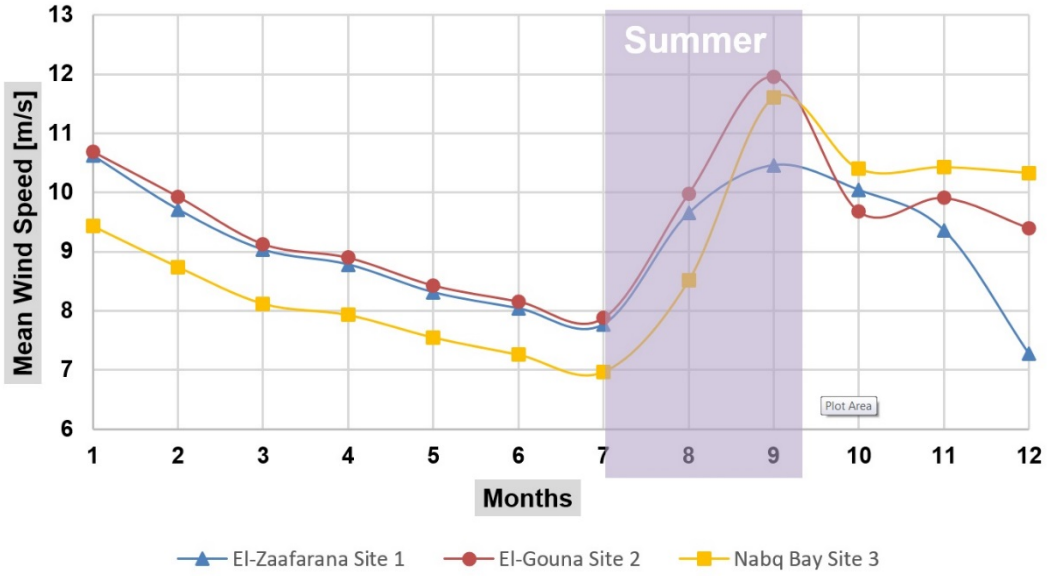

Figure 5-20: Monthly mean wind speed in [m/s] at a height of 50 m for the 3 chosen cites, adopted from (Essa et al., 2007, Shata and Hanitsch, 2006b, Mortensen et al., 2006b).

The overall results of this case study were verified by applying sensitivity tests. The tests were performed on the 40 different suitability maps produced, 10 for every single factor. The results indicated in Section 5.2.3 imply that the factor weights are reasonable as no anomalous results were found in the 40 sensitivity runs undertaken. For the small changes 4%, the error for any factor was less than 10%, which emphasis that the spatial siting model for Egypt including the data collected are not sensitive to small errors or assumptions.

5.3 Arabian Peninsula (Case Study 1) Offshore Wind Farms Spatial Siting

A Boolean mask was created to eliminate restricted cells for this case study, so that constraint cells have a value of zero, and unrestricted cells have a value of one. The Raster Calculator tool in ArcGIS was used to produce the final Boolean Mask given by Equation (5-3).

Boolean Mask = (Oil and Gas Areas) x (Shipping Routes) x (Cables Paths) x (Natural Parks) x (Maritime Boundaries) (5-3)

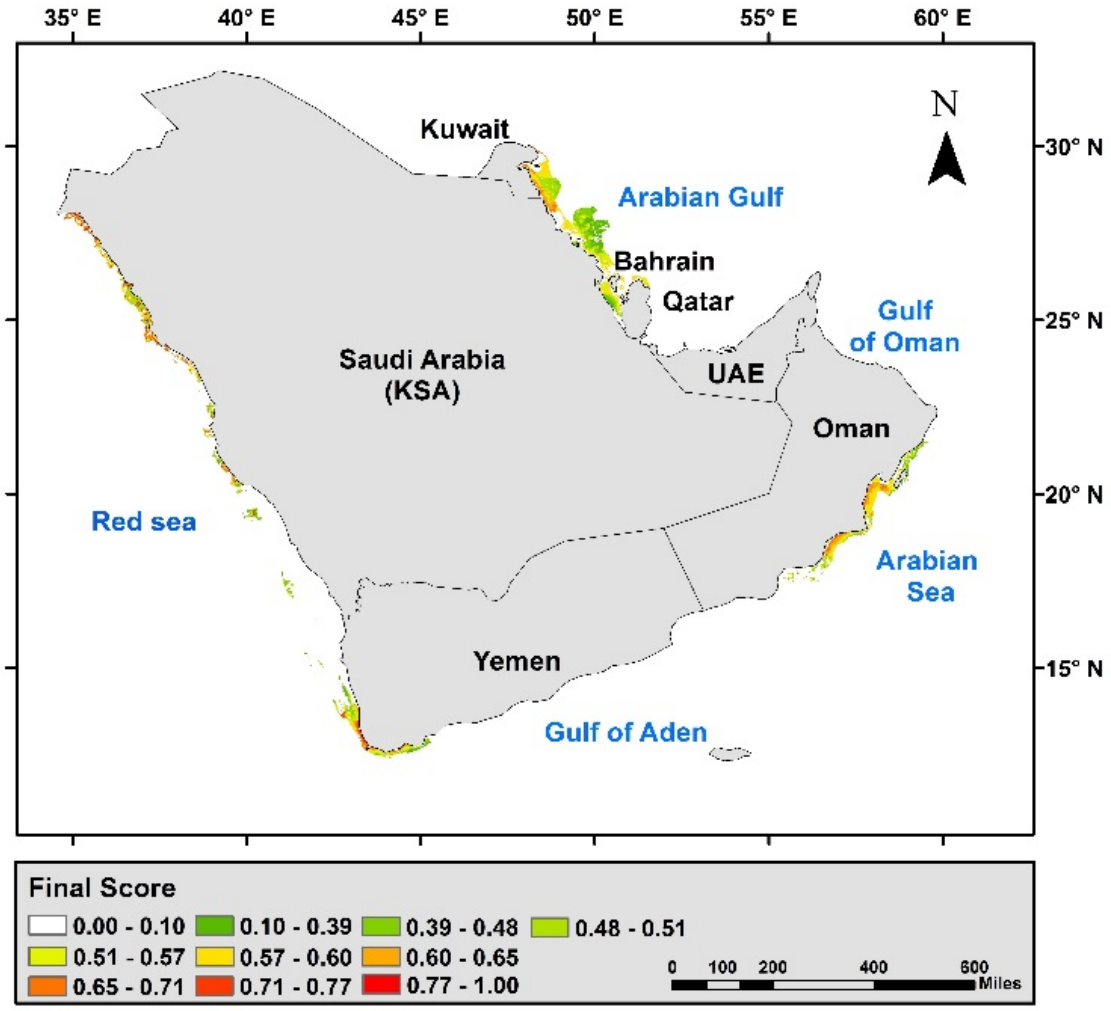

Figure 5-21: Offshore wind energy Suitability Map around the Arabian Peninsula. Where 0.0 score is not suitable area, while a score of 1.00 represents areas of the highest possible suitability. Grid availability, blue line.

All considered criteria were aggregated using Weighted Linear Combination (WLC) given by Equation 3-10, to create the final suitability map for offshore wind for the AP case study. Four standardised layers were first multiplied by their Factor Weight from Table 5-3, then summed together, using the Raster Calculator tool in ArcGIS by applying Equation 3-10. Finally, restricted cells were removed from the WLC layer using the Boolean Mask layer.

As indicated earlier, the modelling was undertaken using an 800x800 m cell size confined to the source file of the bathymetry map. Four factors and five constrained criteria were chosen to evaluate the alternatives/cells around the countries of the Arabian Peninsula. The model solved the spatial siting for offshore wind farms dealing with the chosen conflicted factors and constraints in an efficient manner.

The suitability map for the studied area (Figure 5-21) represents the cells around the shores of the AP where the cells final scores and their corresponding areas are graded as follows:

(i) 0.0 < Cell Score < 0.39 - not suitable. This represents 20,935 km^2 of the studied regions (the 0 score assigned by the Boolean Mask is not accounted in this area).
(ii) 0.4 < Cell Score < 0.59 - moderately suitable. This represents 23,080 km^2 of the studied regions.
(iii) Cell Score > 0.6 – highly suitable. This represents around 3,251 km^2 of the studied regions.

The results for the overall suitability map of the Arabian Peninsula is shown in Figure 5-21 with high resolution details of the regional sites given in Figure 5-22. It must be noted that in the final suitability map, the UAE has no suitable cells (due to low wind speeds and dense shipping routes as indicated by Figure 4-18 and Figure 4-19, respectively), while Qatar and Bahrain have moderate suitability cells and no high suitable cells. In addition, the suitable areas for Yemen and Oman are centred on one area of their shoreline due to the lack of wider electricity grids provisions, (see Figure 5-21). Yemen, Kuwait, Oman, and KSA have the most suitable sites for offshore wind, with KSA having the highest suitable areas in the region (due to high wind speeds in the Red Sea).

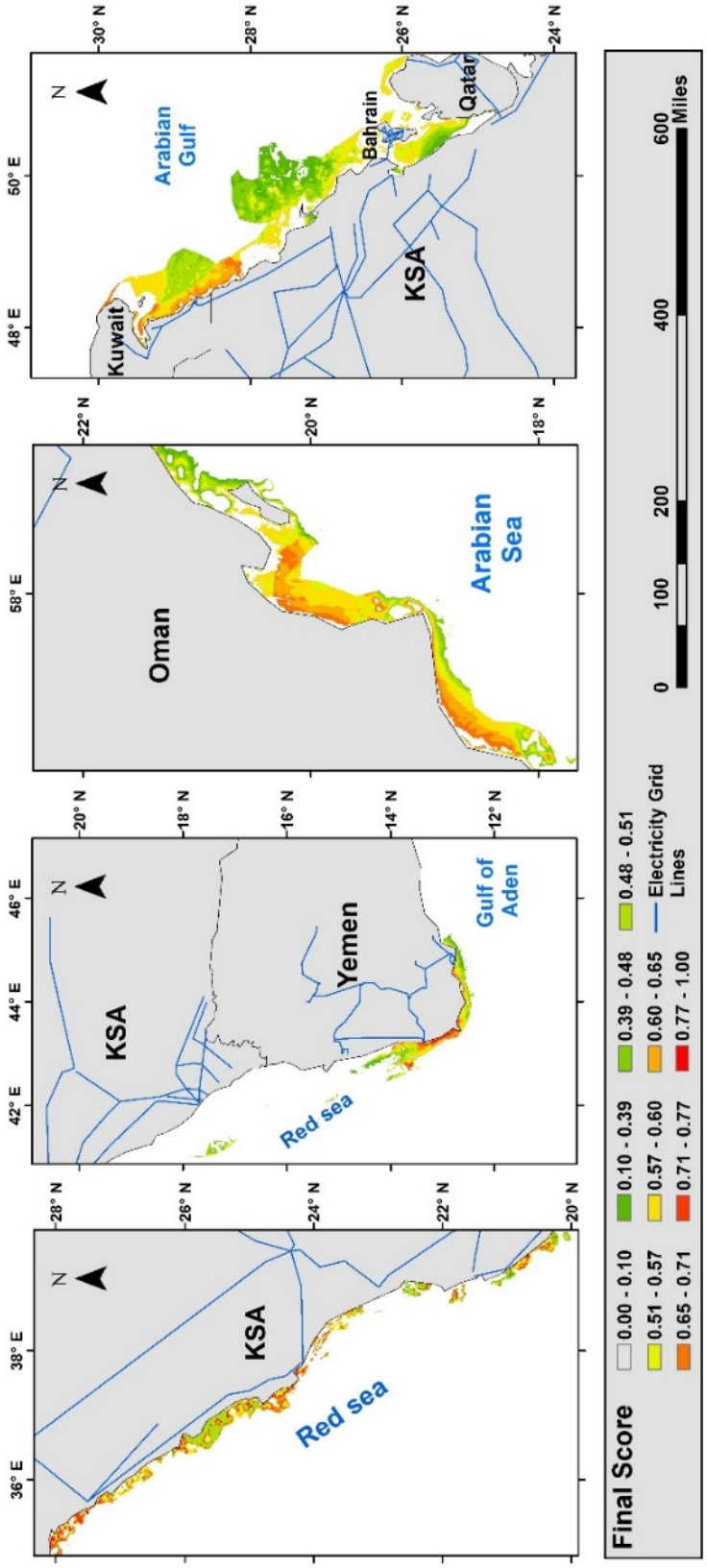

Figure 5-22: High-resolution offshore wind energy Suitability Map for the countries with highest offshore wind energy potential - KSA, Yemen, Oman, Qatar, Bahrain, and Kuwait - around the AP. Where a 0.0 score indicates areas which are not suitable, while a score of 1.00 represents areas of the highest possible suitability.

5.3.1 Discussion

The methodology and its resilience were tested through application to regional scale case study. The second case study provided outcomes at regional scale of the Arabian Peninsula (AP) covering an area ~3.1 million km^2 and coastline of 9180 km with Figure 5-21 showing the results map for offshore wind energy potential in the region. The outcomes in that figure are used to estimate the suitability distribution for the seven countries in the AP as shown in Table 5-8. As can be seen from Table 5-8, the KSA has more than 25,000 km^2 of unrestricted areas, which represents 54% of the total available area for offshore wind energy potential in the Arabian Peninsula region. Despite, the high wind potentials in KSA around the Red Sea region (Figure 4-18), less than 3.5% of the total available area of the region is considered to be of high suitability. This is due to fact that most of the Red Sea region of the KSA has a water depth of 60m or more (Figure 4-17) which beyond current turbine foundations technologies. Therefore, to extend suitability it is feasible for the KSA to consider investigating floating offshore wind turbines, which are more suitable for deeper water.

Oman's share of the total available area of the region is around 18%, and only 8.7% of that is highly suitable for offshore wind, which is surprising at it has a shoreline of 2,092 km, which is not too dissimilar to that of the KSA (Tables 2-3 and 5-8). Despite this, Oman has a significant average wind speed on the Arabian Sea, but unfortunately, this is remote, located over 90 km from the nearest electricity grid in the area, see Figure 4-20. Nevertheless, Oman does however have a well-established national power grid near the Gulf of Oman (Figure 4-20), but the wind speed in this location is less than desirable. Kuwait has around 14% of the total available unrestricted area, with a similar percentage of the highly suitable area within the region. These numbers are relatively high when compared to its short shoreline (around 5% of the total coastlines of the region considered). Kuwait has high offshore wind potentials compared to its footprint, since it has minimum restriction on the Arabian Gulf (Figure 4-19), average wind speed of 6.2 m/s (Figure 4-18), and a shallow water depth range of 35m (Figure 4-17).

Table 5-8: Suitability distribution for the Arabian Peninsula countries offshore wind sites.

	Unsuitable Suitable Area (km^2)	Moderate Suitable Area (km^2)	High Suitable Area (km^2)	Total Available Area
KSA	14732	9204	1586	25522
Oman	493	7410	769	8672
Kuwait	2800	3319	455	6574
Yemen	2742	2843	441	6026
Qatar	162	220	0	382
Bahrain	6	84	0	90
UAE	0	0	0	0
Total	20935	23080	3251	47266

Yemen's offshore wind potential and grid proximity are concentrated in the same area (Figures 4-18 and 4-20), which justifies its 441 km^2 of high suitability areas, despite its current poor infrastructure when compared to others in the Gulf States. Qatar and Bahrain have no high suitable offshore wind energy areas. UAE has more than 23 seaports; seven of them are mega container ports, resulting in a high volume shipping route density (Figure 4-19) and hence zero availability for offshore wind energy.

To estimate the offshore wind power potential for the investigated sites, one needs to provide a spatial siting of the turbines and their inter turbine spacing in an array or farm. To estimate the array spacing between offshore wind turbines, Equation (5-2) developed in (Sheridan et al., 2012) was used. To reduce turbulence interaction between turbines, the ideal turbine spacing is in the range of 5 to 8 times the turbine rotor diameter (E.ON, 2012). In this work analysis, L_c was given the value 5 and L_d the value 8. Hence a wind turbine footprint $S = 5x8x164^2$ for an 8 MW turbine (rotor diameter 164 m, (Desmond et al., 2016)). The estimated number of wind turbines for 8 MW configuration given in Table 5-9, is derived by dividing the Suitable Area (km^2) by S for the turbine size used.

Table 5-9: National installed electrical power capacities in Arabian Peninsula countries compared with estimated power capacity achieved from offshore wind energy high suitability sites from an 8 MW capacity turbine in these countries.

Country	National installed capacity (GW) (Factbook, 2018)	High Suitable Area (km^2)	Estimated offshore wind Capacity (GW)	No. of turbines	Potential offshore wind contribution to capacity (%)	Potential generated electricity (TWh)
KSA	69.1	1586	17.06	2125	24.7	59.8
Oman	7.87	769	8.28	1031	105.2	29.0
Kuwait	16.0	455	4.90	610	30.6	17.2
Yemen	1.5	441	4.75	591	316.5	16.6
Qatar	8.8	0	-	-	-	-
Bahrain	3.93	0	-	-	-	-
UAE	28.9	0	-	-	-	-
Total	136.1	3555	35	4765	25.7	122.6

The estimated offshore wind power capacities for each country using the 8 MW turbine specifications in combination with Equation (5-2) are shown in Table 5-9. The table also provides details of the Arabian Peninsula countries currently installed power capacity and the percentage contribution from the estimated offshore wind energy capacities established here.

As can be seen from Table 5-9, the estimated overall total cumulative capacity of offshore wind power contribution (from the high suitability areas only) to these countries is approximately 35 GW for an 8 MW turbine capacity. The results indicate that for the 8 MW turbine case around 25.7% of the overall Arabian Peninsula countries power capacity can be achieved from offshore wind. In terms of country, specific capacity potential of offshore wind energy determined in this study, Saudi Arabia has 17 GW, Oman 8 GW, Kuwait 4.9 GW, and Yemen 4.8 GW. Bahrain and Qatar have moderate offshore wind energy capacities of 2.37 GW and 0.9 GW respectively. The United Arab Emirates (UAE) has small forefront to the sea and has many restrictions especially around shipping lanes (Dubai being a world commercial centre). When combined with the limited wind resources around its shores the analysis indicates that UAE has very limited suitable areas and hence negligible wind power potential. This latter outcome provides more rigorous analysis providing stronger evidence than (Saleous et al., 2016), where only two factors were used to select a suitable site for offshore wind energy around Abu Dhabi, only in the UAE.

It must be noted that the markets, especially in Europe, are now leaning towards the 8 MW capacity turbine with some developers now upgrading these turbines to 9.5 -10 MW and are thinking about 12 MW turbines in the next two years with research now being directed towards 13 – 15 MW turbines (Jimichi et al., 2018). In the case of the countries studied here, it is imperative that any development of the sites highlighted should bear these developments in mind. In the author's view, the 8MW option seems to be the most sensible option to go for at this stage.

Chapter 6: Results and Discussion on Logistic and Infrastructure in Egypt

The following chapter considers the foundation, port feasibility, farm layout, and environmental considerations for the Egypt Case study only. These details are not considered for the Arabian Peninsula case study.

6.1 Foundation Selection, Cost and Design

6.1.1 Soil Properties for the Chosen Sites in Egypt

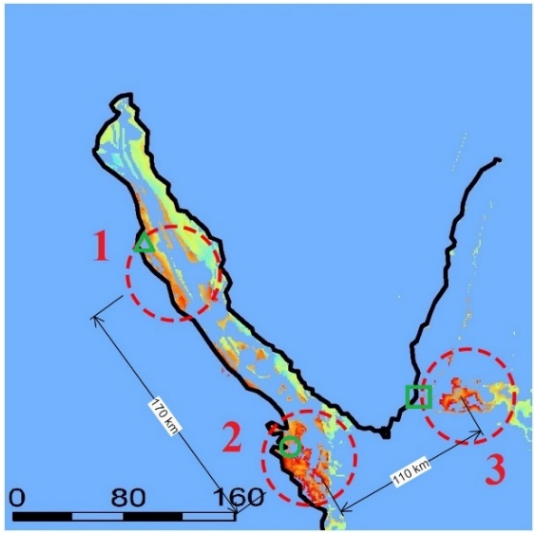

Figure 6-1: Proposed Offshore wind farms location around the southern coast of Sinai Peninsula, Egypt. The green triangle is pointing the locations for borehole 1 and 2, the green circle is locating borehole 3 and 4, and the green rectangular is the location of borehole 5.

Three sites were identified using the AHP methodology, see Section 5.2. The locations are reasonably close to each other (Figure 6-1) and have an average water depth of 20m. The monopile foundations will be installed in a sandy soil, the different soil characteristics for each location is described below. The soil properties considered are in terms of friction angle (φ) in degrees, submerged unit weight (γ_{sub}) in kN/m^3, Young's modulus / modulus of elasticity (E_s) in MPa, Poisson's ratio (ν), dilation angle (ψ) in degrees, and maximum yield stress (f_y) in kPa.

Soil **angle of friction** (ϕ) is derived from the Mohr-Coulomb failure circle, it describes the shear friction resistance between small particles of soil under a normal effective stress. **Poisson's ratio** (ν) is the ratio between horizontal strain to the vertical strain under a stress within the elastic stat of the soil. **Modulus of elasticity** (E_s)/ Young's modulus, which is the soil stress to its strain, also within the elastic stat of the soil. The **dilation angle** (ψ) "controls an amount of plastic volumetric strain developed during plastic shearing and is assumed constant during plastic yielding" (Bartlett, 2010). For sandy soil as a non-cohesive soil, the dilation angle (ψ) relies on the friction angle (ϕ) of the soil. For sand with $\phi > 30°$ the value of the dilation angle can be estimated as $\psi = \varphi - 30°$, $\psi = 0$ in case of negative values of dilation angle (Bartlett, 2010).

Five boreholes were allocated near the proposed sites (ORASCOM Construction Limited, 2012, HIDELECCO Construction company, 2010, Redcon Construction, 2007). The location of these boreholes are shown in Figure 6-1, the five boreholes were extracted from shallow waters depths ranged from 3.00m to 10.00, and were conducted originally for coastal protection for recreational projects near the centre of the chosen wind farms sites, see Figures A-1 to A-5. The five borings were conducted by using a mechanical rotary drilling rig mounted on a boat. Boreholes were advanced by power rotation of drilling bit and removal of cuttings by circulating a bentonite fluid. The data collected from these boreholes will provide a basic information that can be used to identify the soil conditions for the three locations, the boreholes are in very close proximity to these locations.

Standard penetration tests (S.P.T) were conducted on non-cohesive deposits, the test results also are presented through figures A-1 to A-5. Laboratory tests on granular soils include direct shear using shear box on samples prepared on different densities and grain size analysis. All tests were performed in accordance with (American Society for Testing and Materials) ASTM specifications. The result of direct shear box is the angle of friction and the soil unit weight. Then an unconfined compressive strength of cemented sand soil was performed. Finally, a grain size analysis tests fulfilled on the sand samples, the results showed that the percentage of the fine particles passed sieve No. 200 is around 2% for all samples, while the effective diameter D_{10} is 0.24 mm, which indicate the very low presence of the fine particles in the soil samples.

The boreholes attached in Appendix A describe the soil layers near the centre of the three chosen sites. The soil deposits in the different sites consist of medium dense to coarse-dense sand stratums. Starting from the seabed and extended to the end of the borehole. A layer of cemented sands exists

at depths from 15.00m to 26.00m below seawater at boring 1 to 4. The cemented sand has a high modulus of elasticity > 400 MPa, and the average unconfined compressive strength is 3.97 MPa. A small pocket of silty medium dense sand found in borehole 2; see Figure A-2, Appendix A. The silty pocket can be neglected from the analysis, as it is expected to disappear in the 20m water depth of the offshore wind farm. The expected soil type for the three locations is summarised in Table 6-1, where the first layer of sand soil and the trace of the crushed shells is expected to disappear at such depths. The cemented layer of sand will be at depth more than 90m and 110m blew sea levels for sites 1 and 2 respectively. The data of Table 6-1 will be used to simulate the soil layers for the ABAQUS Model for the different load combinations. The sandy soil with this range of Modulus of elasticity (32 to 63) MPa is very suitable for offshore foundation deployment (DNV, 2014).

Table 6-1: Soil properties for the three chosen sites in Egypt

Variable	Unit	Site 1 (Zafarana)	Site 2 (El-Gouna)	Site 3 (Nabq Bay)
		Medium Sand	Medium Sand	Dense Sand
ϕ	Degree °	30	34	39
γ_{sub}	kN/m^3	9	9.5	11
E_s	MPa	32	44	63
ν	-	0.3	0.3	0.3
ψ	Degree °	0	0	0
f_y	kPa	0.001	0.001	0.001
Source		(HIDELECCO Construction company, 2010)	(ORASCOM Construction Limited, 2012)	(Redcon Construction, 2007)

6.1.2 Foundation Selection (Egypt Case Study)

The foundation selection for the Egyptian sites depends on two parameters (water depth and overall cost). The average water depth of the three chosen sites (Figure 6-1) is < 20 m. The maximum depth for deploying Gravity base is 15 m, while the minimum depths for tripod, jacket, and floating are 30, 30, and 60 m, respectively. Therefore, the gravity base, tripod, jacket, and floating foundations are not considered. The optimal monopile and hybrid foundation depths are in range of (15 to 35m). Hence, the cost comparison will be between monopile and hybrid monopile foundations.

According to The Crown Estate (2012a), the foundation cost is sensitive to steel price, and it represents about 40 to 50% of the total cost of the foundation. Table 6-2 compares between the monopile and its equivalent Hybrid monopile foundation. The monopile and Hybrid monopile systems are both capable to support 5 MW offshore wind turbine (Abdelkader, 2015). One part of a 40m long, 6m diameter pile comprises the monopile foundation. While, the equivalent Hybrid

monopile system as previously explained in Section 2.4.4, consist of two parts one is 16m long, 4m diameter pile and the other one is a 20m long, 6m diameter pile. The scour protection cost for the hybrid system was not considered as the reinforced concrete connection part is acting as a scour protection measure.

Table 6-2: Monopile and Hybrid monopile cost comparison

Cost[3]	Monopile ([20m long, 6m diameter] + [20m long, 6m diameter], 0.08m thickness)	Hybrid monopile (Abdelkader, 2015) ([16m long, 4m diameter] + [20m long, 6m diameter], 0.08m thickness)
Steel volume [m^3]	111.6	71.64
Steel weight [ton]	870.5	558.8
Concrete volume [m^3]	-	166.9 (see Figure 2-10)
Scour protection Volume [m^3]	2804.8	-
Steel cost [£][1]	1,681,000	1,117,600
Concrete cost [£][2]	-	584,150
Pile Driving cost [£]	2,521,500	2,607,700
Scour Protection cost [£]	420,720	420,720
Pile overall cost [£]	4,623,220	4,309,450

[1] Steel price is £2000 per ton (Gielen, 2012), scour protection is £150 per one cube meter (Petersen et al., 2015), and Steel density is 7800 kg/m^3.

[2] Concrete price is £3500 per one cube meter (Hamada et al., 2017).

[3] The final cost reduced for the new hybrid concept is -£106950, which is around a %2.3 increase.

The comparison in Table 6-2 showed that reduction of cost for using the hybrid system could reduce 6.7% of the foundation cost, not considering the uncertainty for more cost for constructing a new foundation concept. Therefore, monopile foundation system is chosen to complete the project foundations due to extended experience of using monopile for offshore wind turbine foundation and the small reduction margin of using the new foundation. Later in Section 6.2.4, the scour protection was not considered, as the soil and climate conditions of the chosen sites will not form any scour holes, which will reduce the monopile foundation cost and then be cheaper than the hybrid monopile by 2.5%. On the other hand, if the concrete cap of the hybrid system failed to protect the pile from scour, the monopile system will be cheaper by 11.1%, which will make the hybrid system not acceptable technically or economically.

6.1.3 Monopile Foundation Cost

Foundation cost is estimated by considering two elements: manufacturing cost and the cost of transport and installation. Manufacturing cost are determined according to water depth, actual loads (wind and waves), and soil conditions. The simplest way, is to design the offshore foundation for

ease of serviceability and environmental loads, then to calculate the actual cost of the proposed design. However, for comparison purposes, empirical equations are used to estimate the foundation cost. These empirical equations were derived from back analysed costs.

Table 6-3: Largest offshore wind turbine foundations around the world until the mid of 2017 (Oh et al., 2018, European Wind Energy Association, 2016, 4C Offshore Ltd, 2018).

	Park	Region	Year	OWT no	OWT rate [MW]	Capacity [MW]	Max depth [m]	Foundation type	Cost/one Foundation [M£]
1	London array	UK	2013	175	3.6	630	25	Monopile	4.2
2	Gemini	Netherland	2017	150	4	600	34	Monopile	5.4
3	Gwynt y Môr	UK	2015	160	3.6	576	28	Monopile	4.2
4	Greater Gabbard	UK	2011	140	3.6	504	32	Monopile	4.7
5	BARD offshore 1	Germany	2013	80	5	400	40	Tripile	10.6
6	Global Tech I	Germany	2015	80	5	400	41	Tripile	6.1
7	Anholt	Denmark	2013	111	3.6	399.6	19	Monopile	3.7
8	Duddon Sands	UK	2014	108	3.6	388.8	23	Monopile	4.1
9	Sheringham Shoal	UK	2013	88	3.6	316.8	22	Monopile	4.4
10	Borkum Riffgrund 1	Germany	2015	78	4	312	29	Monopile	4.7
11	Thanet	UK	2010	100	3	300	25	Monopile	3.2
12	Nordsee Ost	Germany	2015	48	6.15	295.2	25	Jacket	7.6
13	Amrumbank West	Germany	2015	80	3.6	288	25	Monopile	3.3
14	Butendiek	Germany	2015	80	3.6	288	22	Monopile	4.4
15	DanTysk	Germany	2015	80	3.6	288	21	Monopile	4.3
16	EnBW Baltic2	Germany	2015	80	3.6	288	20	Monopile	4.2
17	Sandbank	Germany	2017	72	4	288	31	Monopile	4.9
18	Meerwind Sud/Ost	Germany	2014	80	3.6	288	22	Monopile	4.4
19	Lincs	UK	2013	75	3.6	270	15	Monopile	4.7
20	Burbo Bank Ext	UK	2017	32	8	256	17	Monopile	8.8
21	Humber Gateway	UK	2015	73	3	219	16	Monopile	3.5
22	Northwind	Belgium	2014	72	3	216	23	Monopile	3.4
23	Westermost Rough	UK	2015	35	6	210	25	Monopile	8.7
24	Horns Rev 2	Denmark	2010	91	2.3	209.3	13	Monopile	1.5
25	Rødsand 2	Denmark	2010	90	2.3	207	9	Gravity	1.5
26	Trianel Bokum I	Germany	2015	40	5	200	33	Tripile	6.3

The next three empirical equations to estimate the monopile foundation cost were adopted from (Nielsen, 2003, Dicorato et al., 2011):

$$C_f = 269.2P_{WT}\,(1+0.02\,(D-8))\,*\,(1 + 0.08\,*\,10^{-6}\,(h\,(d/2)^2 - 10^5)) \quad [k£/turbine] \qquad (6\text{-}1)$$

$$C_f = 4.53\,(D-5) + 258.1 \quad [k£/MW] \qquad (6\text{-}2)$$

$$C_f = 6.871D + 327.5 \quad [k£/MW] \quad (6\text{-}3)$$

Where: C_f [k€/MW] is the estimated foundation cost, D [m] represents sea depth, P_{wr} [MW] is the rated power of a single offshore wind turbine, h [m] is hub height, d [m] is rotor diameter.

These equations were derived using a regression analysis considering the available data in that time 2013 and 2011, where the authors considered the water depth only in two equations as a parameter in estimating the monopile cost, while in one they considered irrelevant parameters like hub height and rotor diameter.

Applying equations (6-1 to 6-3), using the available data form Table 6-3 to calculate the error between the estimated foundation cost and actual cost. The error was more than 50% for all recently installed mega projects. Therefore, a new regression analysis was conducted to produce a revised foundation cost equation, containing more up to date factors. This is now given as Equation (6-4), which was derived using STATA software programme (StataCorp, 2007) and the collected data shown in Table 5-8.

$$C_f = 0.0397P_{WT} * D + 0.939 \quad [M£/turbine] \quad (6\text{-}4)$$

The final estimated foundation cost is £4.9 million; the value was calculated using equation (5-5) C_f = 0.0397x5x20 + 0.939 = 4.9 [M£/turbine]. The value is near the value estimated before in Section 6.1.2, which was £4.6 million per turbine. In addition, Cavazzi and Dutton (2016) approximate the average cost of foundation to be 0.74 £m/MW, which is also close to the value estimated by equation 6-4. The 6-4 equation is limited to predict the foundation cost only for large wind farms with capacity of 250 to 600 MW.

6.2 Monopile Foundation Design

The proposed system for a 5MW offshore wind turbine in the three chosen sites of Egypt is the monopile system as discussed in Section 6.1.2. The system contains of two parts:

- First part is steel pile wall 8 cm thickness, 6 m diameter, and 40 m length. The first 20 meter of the pile will be driven into the sandy soil of the chosen sites (Section 6.1.1), and the other 20 m elevates the turbine tower above the mean sea water level MSL.
- The second part is the transition piece, which is subjected to the tidal range and sea waves. The transition piece is used to connect the pile to the OWT tower, and they are connected

using a grouted, bolted flange, or welding beads connections, but the bolted flange connection is widely used. The vertical level of the pile after driven into the soil bed by the hummer is normally less or more than 180 degree°, therefore, the transition piece is adjusted to provide the required vertical level to connect the turbine tower correctly.

6.2.1 3-D Numerical Model and Meshing

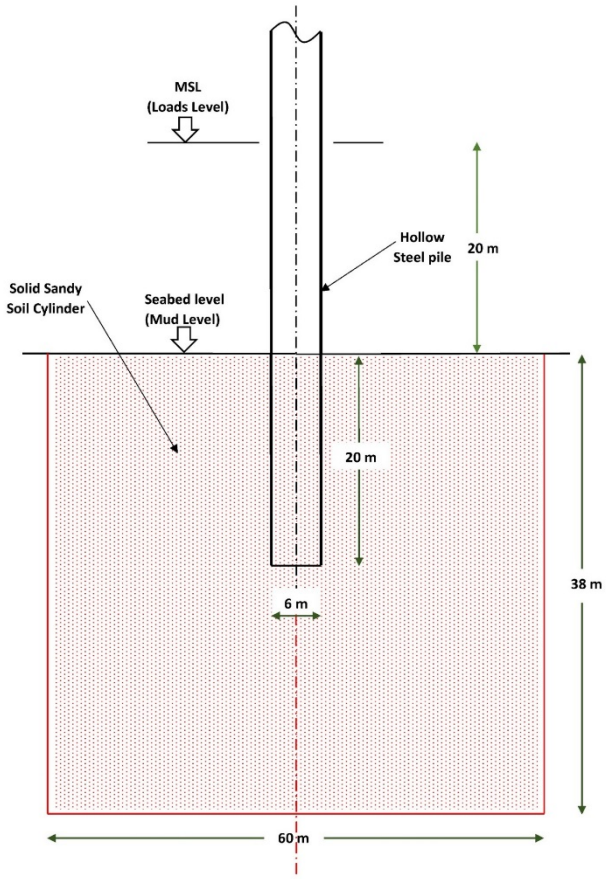

Figure 6-2: Proposed monopile foundation and the boundaries for the soil 3-D model.

The numerical analysis to examine the proposed system for the different soil conditions of the three chosen sites was done using the finite element method programme. The ABAQUS (Hibbett et al., 2010) programme was applied to model the foundation system and soil as a 3-dimensional nonlinear finite element model, see Figure 5-23. Two different materials to be represented in the model, which are the soil surrounding the pile and the hollow steel pile its self, these two elements need to be identified by dimension, properties and deformation behaviour. The soil and the

monopile **steel pile** system were modelled using 3-D deformable solid elements with different material models.

The different sandy **soils** for the three sites were simulated with an elastic-perfectly plastic constitutive model and the Mohr-Coulomb failure criterion. Soil properties were specified using data discussed in Section 6.1.1, Table 6-1. Soil boundary distance in the model depends on pile diameter (d):

- Vertical direction extent was estimated to be three times the pile diameter 3d (3×6m = 18m), measured from the pile toe.
- In the horizontal direction extent, soil circle boundary was estimated to be ten times the pile diameter 10d (10×6m = 60m), measured from the centre of the pile.
- Therefore, soil will be represented as a cylindrical shape with (18+20 = 38m) height and 120m diameter, see Figure 6-2.
- The mesh was developed using the automatic sweep meshing technique and the medial axis algorithm, which is available in the ABAQUS (Hibbett et al., 2010).
- The steel shaft and soil circumfluence faces were divided into 16 sectors. In addition, the vertical and horizontal mesh cell dimensions were set to be 1-meter step, see Figure 6-3.
- Boundary conditions for the 3-D soil model are:
    1. Nodes of the soil model cylindrical **bottom base** were fixed from translations in X, Y and Z directions.
    2. Vertical boundaries nodes of the soil model cylindrical **curved surface** were fixed translations in X, and Y directions, so nodes can move only in Z direction.

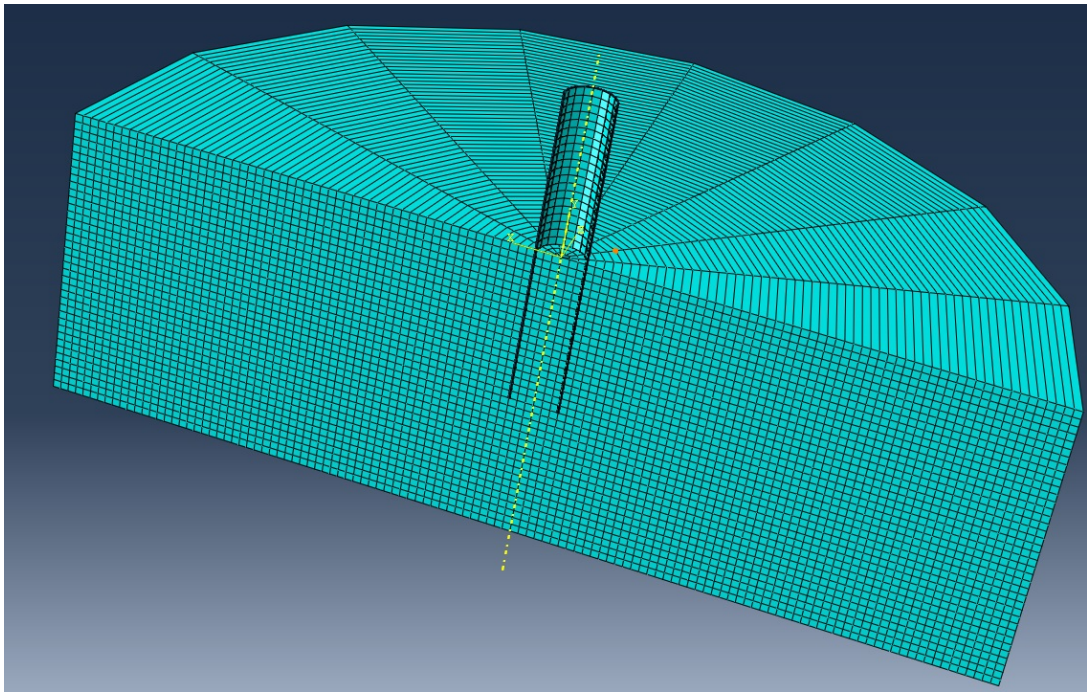

Figure 6-3: The 3-D model for the Soil and the monopile foundation, where every square segment is 1m side dimension.

The **steel pile** was represented using elastic-perfectly plastic model and the Mohr-Coulomb failure criterion with the steel properties, see Table 6-4. All steel pile nodes are free to move in X, Y, and Z directions.

Interaction properties were applied soil and steel materials to simulate the actual behaviour as:

1. Tangential behaviour with friction coefficient equal to 0.5.
2. Fraction of characteristic surface dimension equal to 0.005.
3. Normal behaviour using the constraint enforcement method and pressure-overclosure as hard contact with allowing separation after contact.
4. Interaction surfaces were applied at the interfaces between soil and steel pile that allow steel pile slippage and separation, which will imitate tangential and normal behaviours.

Table 6-4: Materials properties for the 3-d model.

	Unit	Site 1	Site 2	Site 3	Pile steel	Soil Test
ϕ	Degree °	30	34	39	-	30
γ_{sub}	kN/m^3	9	9.5	11	66.5	9
E_s	MPa	32	44	63	200000	30
ν	-	0.3	0.3	0.3	0.3	0.3
ψ	°	0	0	0	-	1
f_y	kPa	0.001	0.001	0.001	240000	0.001

Different load combinations were applied, for the serviceability limit, only the 3C, and the 2C combinations were applied, and for the ultimate limit the 6C, 3C, and 2C load combinations were used, see Figure 4-22.

Table 6-5: Results comparison for the Serviceability limit state.

Displacement	Previous Model	Verification Model
Lateral displacement at MSL [cm]	19.20	20.10
Lateral displacement at ML [cm]	01.20	01.21
Pile rotation at ML [degree]	0.0020	0.0019
Vertical displacement [cm]	-	-4.9

The model was verified using data and results from (Abdelkader, 2015). A 16 m long steel pile with a 6 m diameter and an 8 cm steel wall thickness, was analysed under ultimate and serviceability load combinations. The model was re-established and analysed using the load data from (Abdelkader, 2015). The steel pile and soil was represented by properties showed in Table 6-4. The calculated lateral displacements at the MSL in for the new model was in the same range reported by Abdelkader (2015). The comparison showed that the new model is behaving in a similar way of the pervious verified models. For example lateral displacement at mud level reported by Abdelkader (2015) in range of (6 to 12cm), while the calculated settlement range under the same circumstances was from 6.1 to 11.8cm. The rest of comparison is shown in Table 6-5 and 6-6.

Table 6-6: Results comparison for the Ultimate limit state.

	Previous Model			Verification Model		
Displacement	**6C**	**3C**	**2C**	**6C**	**3C**	**2C**
Lateral displacement at MSL [cm]	40	39	23	39	39	24
Lateral displacement at ML [cm]	12	10.5	6	11.8	10.7	6.1
Pile rotation at ML [degree]	0.014	0.014	0.009	0.014	0.014	0.009
Vertical displacement [cm]	-5.4	-5.1	-2.2	-5.4	-5.1	-2.3

6.2.2 Displacement Results

The three proposed sites were tested using their soil characteristics, see Table 5-9. The monopile foundation system with 8 cm thickness, 6 m diameter, and 20 m depth under the sea bed to support 5 MW OWT, was used for the different locations. First, the system was modelled under serviceability working loads and subjected to 3C (one horizontal load, one vertical load and one rotating moment) and 2C (one horizontal force and one rotating moment). The values of displacements for the three sites subjected to serviceability limit loads are stated in the first part of Tables 6-7 to 6-9. The displacements measured using ABAQUS 3-D modelling; the displacements are lateral displacement at MSL (Mean Sea Level) in [cm], lateral displacement at ML (Sea bed level) in [cm], Pile rotation at ML [degree], and vertical displacement of the pile in [cm].

Thereafter, the system was modelled under ultimate limit forces, and subjected following load combinations are used:

- 6C (two horizontal forces, one vertical force and three rotating moments),
- 3C (one horizontal load, one vertical load and one rotating moment) and
- 2C (one horizontal force and one rotating moment).

The values displacements for the three sites subjected to ultimate limit loads are shown in the second part of Tables 6-7 to 6-9. Where, A is the allowable settlement or deformation.

Table 6-7: Results for location Site 1 (Zafarana). 6C, 3C, and 2C explanations are in Figure 4-22.

	Serviceability limit state			Ultimate limit state			A
Displacement	**6C**	**3C**	**2C**	**6C**	**3C**	**2C**	
Lateral displacement at MSL [cm]	-	18.70	13.30	31	30	20	-
Lateral displacement at ML [cm]	-	01.01	00.82	7	6	5	< 6
Pile rotation at ML [degree]	-	0.002	0.001	0.013	0.013	0.009	< 0.5
Vertical displacement [cm]	-	-4.1	-2.0	-4.3	-4.1	-2.0	> -10

Table 6-8: Results for location Site 2 (El-Gouna).

	Serviceability limit state			Ultimate limit state			A
Displacement	**6C**	**3C**	**2C**	**6C**	**3C**	**2C**	
Lateral displacement at MSL [cm]	-	10.32	09.21	17	19.8	14.9	-
Lateral displacement at ML [cm]	-	00.83	00.54	5	4.9	4.1	< 6
Pile rotation at ML [degree]	-	0.001	0.001	0.007	0.007	0.005	< 0.5
Vertical displacement [cm]	-	-3.9	-1.7	-2.5	-2.7	-1.3	> -10

Table 6-9: Results for location Site 3 (Nabq Bay).

	Serviceability limit state			Ultimate limit state			A
Displacement	**6C**	**3C**	**2C**	**6C**	**3C**	**2C**	
Lateral displacement at MSL [cm]	-	09.85	07.99	12	17.2	11.8	-
Lateral displacement at ML [cm]	-	00.69	00.49	4.3	4.7	4	< 6
Pile rotation at ML [degree]	-	0.001	0.001	0.005	0.005	0.005	< 0.5
Vertical displacement [cm]	-	-3.3	-1.3	-2	-2.1	-1.1	> -10

6.2.3 Scour Protection

Installing a monopile, which is a vertical hollow pile, in the seabed soil creates significant turbulence to the seawater stream and wave action in the shallow waters. This change could results in moving the soil sediments resulting a "scour hole" around the pile. Scour is an environmental side effect, which is an erosion of soil particles from the seabed due to the mechanism of waves and currents loads. Monopile driven to sandy or silty soils may suffer from erosion around its cylinder pile, which leads to scour holes, see Figure 6-4. Scour depth and shape around the monopile, S, is mainly dependent on local weather conditions (currents and waves). In wave-dominated weather, scour depth is relatively small, and rely on (Keulegan–Carpenter number) and pile diameter. While, current-dominated weather produces relatively deep scour feature. The other factors affecting scour depth are Shield's parameter, Froude's number, the water depth, the bed shape and the sediment dimensions (Sørensen and Ibsen, 2013). Scour depth S is the equilibrium scour depth, where the amount of eroded sediment deposits equals the accretion (backfilling). The scour phenomenon could case a structure failure to offshore pile, therefore, the scour depth is calculated to reduce the effective length of the pile, or a scour protection is needed.

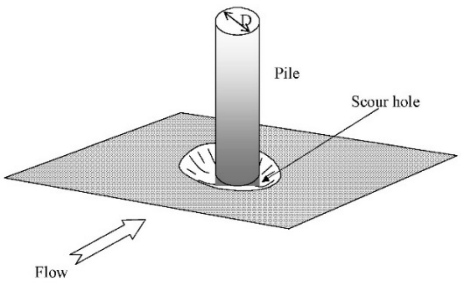

Figure 6-4: Monopile scour formation phenomenon.

Scour protection is a fundamental concern for large number of scholars, for the instance, a computational fluid dynamics (CFD), which is a mathematical numerical method model to analyse the fluid flow behaviour around structures, was used to investigate the seabed stability after installing a monopile (Li et al., 2018). They produce a useful software tool to evaluate the bed shear stress

around the monopile and determine the change of the resulted scour due to geometry modification, which could minimize the expected scour, significantly.

Typical scour protection for the offshore wind turbines in the European seas were designed as rock dumps (Petersen, 2014). Edge scour is the erosion of sediment particles formed after the edge of the rubble mount protection, or after cylindrical piles of offshore wind turbines (Monopile) if the monopile was driven without a scour protection. The edge scour reached more than 2.7 m in depth in some of large offshore wind farms (Petersen et al., 2015), which represent a considerable challenge designing the monopile, because it could reduce the effective driven depth of the pile. Scour could be considered as an environmental load, which has a negative impact on the bearing capacity of the pile, and could change the calculations of ultimate and fatigue load values (DNV, 2014). Therefore, scour protection measures should be counted to mitigate these passive effects (Veritas, 2010, DNV, 2014).

DNV-GL in their Offshore Wind energy Standard manual, suggested three different procedures to reduce scour load (DNV, 2014):

1. Rubble mound protection to be placed to surround the pile after installing process.
2. Calculating the expected scour depth, and then adding this depth to the designed pile depth.
3. Monitoring soil movement around the pile, and applying the first mitigation method if the scour depth reaches a critical stage.

As the weather in the chosen three sites is a wave dominate one as previously proved by (Fery et al., 2012), the Keulegan–Carpenter number (KC) is calculated to estimate the scour depth:

$$KC = \frac{u_{max}.T}{D} \qquad 6-5$$

$$u_{max} = \frac{\pi.H_s}{T\sinh(k.h)} \qquad 6-6$$

$$\left(\frac{2\pi}{T}\right)^2 = g.k\ \tanh(k.h) \qquad 6-7$$

$$\frac{S}{D} = 1.3\ (1-\exp(-0.03(KC-6)) \qquad KC\ \geq 6 \qquad 6-8$$

Where: T is the wave period, D is the cylinder diameter of the monopile and u_{max} is the maximum value of the orbital velocity. Hs is the significant wave height, h is the water depth, k is the wave number and g denotes the acceleration of gravity, which equals to 9.81 m/s^2 (DNV, 2014). S is the scour depth and scour zone is the external region of the soil, which is located around the monopile and is exposed to scour.

Using the following wave data [Significant Wave Height (Hs) = 4 m, Mean Wave Time Period (T) = 7 s, Average Water Depth (h) = 25m and pile diameter (D) = 6m] and applying Equations 6-5 to 6-7, the final for the three chosen sites KC equals 0.501. As Equation 6-8 is used for KC ≥ 6, scour for the designed monopiles will not be formed through the expected piles life cycle (DNV, 2014).

6.2.4 Comparing Foundation Results with Implemented Projects

As a verification step for the monopile design, previous projects that used such a design will be used to compare their results with the archived foundation design in Section 6.2.1. If the designs in similar soil conditions are similar to those achieved here, this will confirm that the methodology and the achieved design are acceptable to evaluate piles and compliant (DNV, 2014). Table 6-10 shows typical offshore wind farms monopile foundation specifications up to the end of 2017, as well as, the monopile design achieved here (Section 6.2.1).

Table 6-11 describes the soil conditions and categorises them according to 3 types A, B, and C. As seen from Tables 6-11 and 6-12, soil (A) properties description is similar to the research sites under consideration D, E, and F. Soil (A) has soil conditions in the mid-range between soil of site 1 and 2. The average diameter, water depth, and penetration depth of the monopile of soil type (A) is similar to the diameter, water depth, and penetration depth of site 1 and 2. This similarity confirm that the methodology and the achieved design are acceptable to evaluate piles and compliant (DNV, 2014).

Table 6-10: Soil classification and monopile dimensions for the largest OWT and the chosen sites (Oh et al., 2018, European Wind Energy Association, 2016, 4C Offshore Ltd, 2018, Bond et al., 1997).

	Park	Region	Year	Water depth [m]	Pile depth	Soil Type	Pile Diameter	OWT Capacity [MW]
1	London array	UK	2013	25	31	A	5.2	3.6
2	Gemini	Netherland	2017	34	27	A	6	4
3	Gwynt y Môr	UK	2015	28	27	B	5	3.6
4	Greater Gabbard	UK	2011	32	26	A	5	3.6
5	Anholt	Denmark	2013	19	21	C	5.4	3.6
6	Duddon Sands	UK	2014	23	28	C	5.8	3.6
7	Sheringham Shoal	UK	2013	22	38	B	5.2	3.6
8	Borkum Riffgrund 1	Germany	2015	29	25	A	5.8	4
9	Amrumbank West	Germany	2015	25	45	C	6	3.6
10	Butendiek	Germany	2015	22	45	B	6.5	3.6
11	DanTysk	Germany	2015	31	34	B	6	3.6
12	EnBW Baltic2	Germany	2015	35	37	C	5.5	3.6
13	Sandbank	Germany	2017	34	33	C	6.8	4
14	Meerwind Sud/Ost	Germany	2014	26	30	A	5.9	3.6
15	Lincs	UK	2013	15	31	C	4.9	3.6
16	Westermost Rough	UK	2015	25	35	C	5.6	6
17	Site 1: El-Zafarana	Egypt	-	20	24	D	6	5
18	Site 2: El-Gouna	Egypt	-	20	20	E	6	5
19	Site 3: Nabq Bay	Egypt	-	20	20	F	6	5

Table 6-11: Soil types description and properties, and monopile average diameter, water depth, and penetration depth.

	Soil Description	(ϕ)	(E_s)	AV. OWT rate	Av. Pile Diameter	Av. Water Depth	Av. Pile depth
		°	MPa	MW	m	m	m
A	Fine to coarse sand with Scattered seams and beds of soft to stiff silty clays and clays.	38	40	3.8	5.5	29.2	27.6
B	Stiff to very stiff over-consolidated stiff clay and clays interbedded with dense fine sand.	-	200	3.6	5.6	25.8	36
C	Stiff to very stiff over-consolidated silty clays and clays	-	200	4	5.7	25.1	32
D	Medium Sand	30	32	5	6	20	24
E	Medium Sand	34	44	5	6	20	20
F	Dense/Coarse Sand	39	63	5	6	20	20

6.2.5 Foundation Results Discussion

The three sites identified in Section 5.2.4 were subjected to a further study. Firstly, a foundation design analysis was done for the three sites. The analysis was accomplished using the ABAQUS finite element analysis programme and the soil data for the three sites. The three monopile foundation models were subjected to all possible load combinations for both steady and ultimate limit states conditions to calculate the produced settlements, see Tables 5-12 to 5-14.

The maximum allowable displacements for the monopile are:

- Lateral displacement at Mud level/ seabed level (ML) must be **< 6 cm**.
- Pile head rotation at ML must be **< 0.5º**.
- Vertical displacement of the pile must be **< 10 cm**.

The displacement results stated in Tables 6-7 to 6-9 due to the Serviceability limit state are less than the allowable limits for the three sites, which confirms the foundation system resistance under serviceability limit loads/environmental loads. Furthermore, the displacement results under ULS conditions are less than the allowable limits, except for the Zafarana site, where lateral displacements at ML are 7 and 6 cm for 6C and 3C loading combination, which are higher than or equal to the 6 cm lateral displacement allowable limit.

To avoid failure under ultimate state loading at the Zafarana site, a-24-meters pile is suggested instead of the 20-meter pile. The 3-D model was modified for the new pile, and the analysis was reapplied only under 6C and 3C ultimate limit state load combination. The new results were stated in Table 6-12. The new results are below the displacements allowable limits, confirming that the 24-meter pile length for site number 1 is acceptable. A is the allowable settlement or deformation (Table 6-12).

Table 6-12: Results for location Site 1 (Zafarana) after applying a 24 m depth pile.

	Serviceability limit state			Ultimate limit state			A
Displacement	**6C**	**3C**	**2C**	**6C**	**3C**	**2C**	
Lateral displacement at MSL [cm]	-	-	-	31	30	-	-
Lateral displacement at ML [cm]	-	-	-	5	4	-	< 6
Pile rotation at ML [degree]	-	-	-	0.011	0.012	-	< 0.5
Vertical displacement [cm]	-	-	-	-4.1	-4.0	-	> -10

A is the allowable settlement or deformation

6.3 Port Feasibility for Egypt Case Study

Ports are an essential infrastructure facility in offshore wind farm industry, as it is used for unloading, storing, pre-assembling, shipping wind farm parts to offshore sites. Ports should be carefully identified so that it saves money and time during the offshore wind farm installation. Five types of ports were defined by DNV-GL in their report (DNV-GL, 2016), are used in the offshore wind installation phases, which are wind turbine manufacturing port, foundation manufacturing port, offshore substation manufacturing port, operations and maintenance port, and marshalling (or staging) port. Staging port is used as an intermediate port between offshore wind turbine manufacturing components and turbine site. The port is ideally located near the project sites of the offshore wind farms to receive, unload, store and pre-assemble wind farm parts and then load them again on the installation vessels.

For the first offshore wind farm in Egypt, it is assumed that all wind turbine components will be imported from Europe. Therefore, the installation port will be considered only for the port feasibility study in Egypt. To ensure that installation/staging port is working functionally, a few required criteria should be satisfied. For offshore wind energy installation ports the criteria used to evaluate their feasibility are identified according to the local characteristic of Egypt's project.

Egypt's ports Authorities' own 55 ports vary in size, loading capacities, storage area spaces, equipment capabilities, and activity type (commercial, fishing, mining, dry cargo, container cargo, bulk cargo, liquid cargo, military, and passengers). Only 12 of the Egyptian ports (Figure 5-25) are suitable for future offshore wind energy installation, as the rest of them are a fishing ports or petrol oil terminals.

A feasibility study was conducted assuming a 500 MW offshore wind farm (which is the average offshore wind farm capacity until the end of 2017), will be installed in the middle of the proposed three locations around Egypt, Figure 6-5. Port feasibility study was conducted for the installation of 100-5MW turbines supported by a 40 m length monopile foundation (20m driven length pile).

The 12 suitable ports for the evaluation process are: El-Arish, Ain Sokhna, Port Said, East Port Said, Damietta, Alexandria, Suez, Adabiya, Dekheila, Nuweiba, Safaga, and Sharm Sheikh Ports, position of these ports are plotted in Figure 6-5. Five of them are located on Mediterranean Sea, six on Red Sea, while the Port Said Port is located inside the Suez Canal itself.

Figure 6-5: Arial map of Egypt, showing the 12 ports under study, and location of the proposed offshore wind farms, adopted and modified using Google Earth programme (Brown, 2006).

The methodology used to evaluate the suitability of ports is the same one used for spatial siting of offshore wind energy, which is the AHP method and pairwise comparison, which were discussed in Section 3.1. The methodology steps are summarised in Figure 6-6. Eight criteria were chosen to evaluate the feasibility of the Egyptian ports to support the installation of a 500MW offshore wind farm. The criteria are described in Table 6-13 where criteria (C1-C3) being constraints, and acts as filter one. If the port does not fulfil the constraint condition, it will be excluded from the evaluation process. The five remaining criteria are factors (F1-F5), which control the second filter.

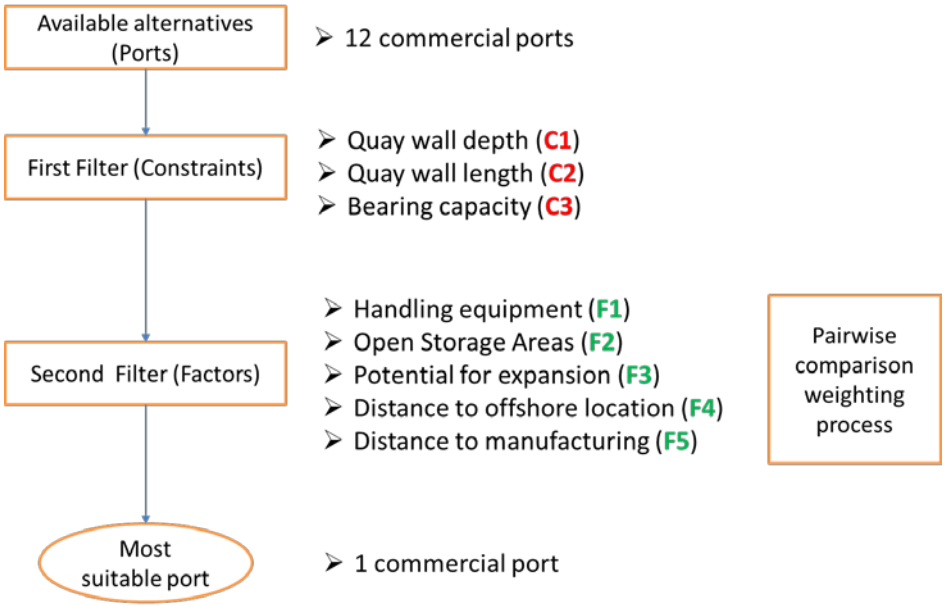

Figure 6-6: Flow chart for AHP process used to assess the port feasibility for the proposed offshore wind energy projects in Egypt.

Table 6-13: Criteria used for the port feasibility in Egypt and its definitions, where C is constraint and F is a factor.

Criteria	Type	Definition and limitations (DNV-GL, 2016, Akbari et al., 2017)	Unit
Quay wall depth (C1)	C	Equal to the maximum installing ship draft plus 2 meter of clear water for safety and sediment deposition = 10m	[m]
Quay wall length (C2)	C	Equal to the maximum installing ship length = 200	[m]
Bearing capacity (C3)	C	Port storage and handling area must bear the pressure of these components weights, minimum bearing capacity is 32	ton/m^2
Handling equipment (F1)	F	The port ability to handle the heavy component of the wind turbines	[no.]
Open Storage Areas (F2)	F	The area need to store, assemble, load, and unloaded different components of the turbine and its substructure.	[m^2]
Potential for expansion (F3)	F	The port with this kind of availability has a higher score compared with other ports, (0.5 for storage extension (0.5 for unlimited, 0.2 for limited, and 0.0 for no extension) + (0.5 for berth length extension (0.5 for unlimited, 0.2 for limited, and 0.0 for no extension).	[m^2]
Approximate to offshore wind farm location (F4)	F	The measured distance between the proposed offshore wind farm location and the ports under evaluation, it has a high impact on the overall time and cost	[km]
Approximate to manufacturing locations (F5)	F	The distance from turbine and turbine substructure to the installing port under evaluation.	[km]

The second filter will be applied on the remaining ports from the first elimination process. Finally, ports that passed the first filter will have a score ranged from 1 to 0. The port with highest score will be the most suitable port for installing the 500 MW offshore wind farm. As the factors have different weights, the pairwise comparison is used to scale their influence.

6.3.1 First Filter

The Egyptian ports were examined using the first filter conditions, any port with one or more constraint not accomplishing its condition was eliminated from the analysis to go through the second filter (factors). Table 6-14 shows first filter process, where the red values are less than the lower limit of the constraint. Seven out of twelve were eliminated because they failed to meet one or more constraint limits.

Table 6-14: First filter step, value in red does not satisfy the constraint limit.

no.	Port Name	Ref.	Berth depth C_1 [m]	Berth length C_2 [m]	Bearing capacity C_3 [t/m^2]
			Constraint Rejection Condition		
			< 10 [m]	< 200 [m]	<32
P1	El-Arish	(MTS, 2018, Galal, 2017)	7	240	<32
P2	Ain Sokhna	(MTS, 2018, Abdallah, 2014, Eed, 2012, Nasr and Smith, 2006)	17	740	>32
P3	Port Said	(MTS, 2018, Badran and El-Haggar, 2006)	13	1000	>32
P4	East Port Said	(MTS, 2018, Kaiser, 2009)	16.5	2400	>32
P5	Damietta	(MTS, 2018, Abdel-Aziz et al., 2007, Shereet, 2009)	14.5	1050	>32
P6	Alexandria*	(MTS, 2018, El-Geziry et al., 2007)	12.8	550	>32
		(MTS, 2018)	11	370	<32
P7	Suez	(MTS, 2018)	7.5	1320	<32
P8	Adabiya	(MTS, 2018)	11	150	<32
P9	Dekheila	(MTS, 2018)	9.4	1200	>32
P10	Nuweiba	(MTS, 2018)	8	180	>32
P11	Safaga	(MTS, 2018)	10	250	<32
P12	Sharm Sheikh	(MTS, 2018)	8	540	<32

* Alexandria Harbour has two separated docks with different berth dimensions and loading capacities.

The remaining five ports are Ain Sokhna, Port Said, East Port Said, Damietta, and Alexandria ports. The data shown in Table 6-15 were gathered or estimated to evaluate the remaining five ports through the five factors explained before. The manufacturing location distance was calculated

assuming that all offshore wind turbines parts could be imported from Europe; therefore, according to this assumption an imaginary point in the middle of the Mediterranean Sea was used to calculate the distance to the alternative port.

Table 6-15: Factors data required for the second filter.

	Port Name, [Ref]	Handling equipment F1	Storage area F2 [m2]	Potential for expansion F3 *		Distance to wind farm F4 [km]			Manufacturing locations F5 [km]
				S	B	1	2	3	
P2	Ain Sokhna (MTS, 2018, Abdallah, 2014, Eed, 2012, Nasr and Smith, 2006)	4	423000	UL	L	137	282	409	+ 913
P3	Port Said (MTS, 2018, Badran and El-Haggar, 2006)	8	475000	N/A	N/A	313	458	583	+ 714
P4	East Port Said (MTS, 2018, Kaiser, 2009)	12	900000	UL	UL	308	453	578	+ 718
P5	Damietta (MTS, 2018, Abdel-Aziz et al., 2007, Shereet, 2009)	6	550000	L	L	394	539	664	+ 650
P6	Alexandria (MTS, 2018, El-Geziry et al., 2007)	0	95000	N/A	N/A	605	750	875	+ 495

* Where, S = Potential for storage expansion, B = Potential for berth length extension, UL = unlimited, L = limited, and N/A = no potential.

6.3.2 Second Two (Factor Weighting)

Pairwise comparison method was used to weight the five factors (F1 - F5) to evaluate the remaining ports after applying the first filter. The Relative importance value for the compared pairs, which are demonstrated in Table 6-16 was adopted from (Akbari et al., 2017). The Relative importance values listed in Table 6-16 are the average values derived from survey analysis conducted by Akbari et al. (2017). Five experts in the study field fulfilled the questionnaire. The final weight values (Table 6-17) applied to the factors were calculated by constructing the Comparing Matrix P_w and the Normalised Matrix N_w as described in Section 3.3.

Table 6-16: Factor comparing pairs, the scale and its definition is adopted from (Saaty, 2008)

	Equal I	Weak	Moderate	Moderate plus	Strong	Strong plus	Very strong	Very, very strong	Extreme	
	1	2	3	4	5	6	7	8	9	
Distance to wind farm						x				Handling equipment
							x			Storage area
					x					Potential for expansion
				x						Manufacturing locations
Potential for expansion		x								Handling equipment
				x						Storage area
	x									Manufacturing locations
Manufacturing locations					x					Storage area
							x			Handling equipment
Storage area			x							Handling equipment

Table 5-17: Pairwise matrix, normalised matrix, and the final factor weights.

	F1	F2	F3	F4	F5	
F1	1	1/3	1/2	1/6	1/7	
F2	3	1	1/4	1/7	1/5	
F3	2	4	1	1/5	1	
F4	6	7	5	1	4	
F5	7	5	1	1/4	1	
						Weight
F1	0.05	0.02	0.06	0.09	0.02	**0.05**
F2	0.16	0.06	0.03	0.08	0.03	**0.07**
F3	0.11	0.23	0.13	0.12	0.14	**0.14**
F4	0.32	0.40	0.65	0.58	0.54	**0.50**
F5	0.37	0.29	0.13	0.15	0.14	**0.21**

6.3.3 Applying Second Filter

The second filter is processed by multiplying every port factor value by the factor weight and the product used to obtain the final score for that particular port, (Table 6-18). The final score ranged from 0 to one, where 0 is not suitable and 1 is the maximum suitable, the port scored the height value is the most suitable port for offshore wind farms in Egypt.

Table 6-8: Second filter; factors score and the accumulative score for each port.

	Port Name	F1	F2	F3	F4			F5	Final Score		
					Site1	2	3		Site1	2	3
P2	Ain Sokhna	0.33	0.41	0.40	1.00	1.00	1.00	0.00	0.65	0.65	0.65
P3	Port Said	0.67	0.47	0.00	0.62	0.62	0.62	0.48	0.48	0.48	0.48
P4	East Port Said	1.00	1.00	1.00	0.63	0.63	0.63	0.47	0.68	0.68	0.68
P5	Damietta	0.50	0.57	0.40	0.45	0.45	0.45	0.63	0.48	0.48	0.48
P6	Alexandria	0.00	0.00	0.00	0.00	0.00	0.00	1.00	0.21	0.21	0.21

Figure 6-7: Arial view for the Port Said East port for years (2015 and 2017), adopted from (Google Earth, 2018).

Twelve ports were evaluated using a group of criteria: quay length, water depth, loading capacity, cranes structure, distance to offshore wind farm location, layout suitability, and distance to manufacture. The most suitable port final decision was rated using Multi-Criteria Decision Making (MCDM) methodology. "Distance between port and wind farm location" factor has the highest weight between factors. (East Port Said port) is highly recommended to install the first 500MW offshore farm in Egypt for three different locations. The nearest three ports to the location failed to pass the first filter, which emphasise the need to evaluate all the possible criteria before making such

decision. (Port Ain Sokhna) comes in the second place after (East Port Said Port) with very low difference, which could be changed in the future with proper investment in the infrastructure of the port, because of its proximity to the offshore locations.

6.4 Wind Farm Layout Optimisation of Egypt

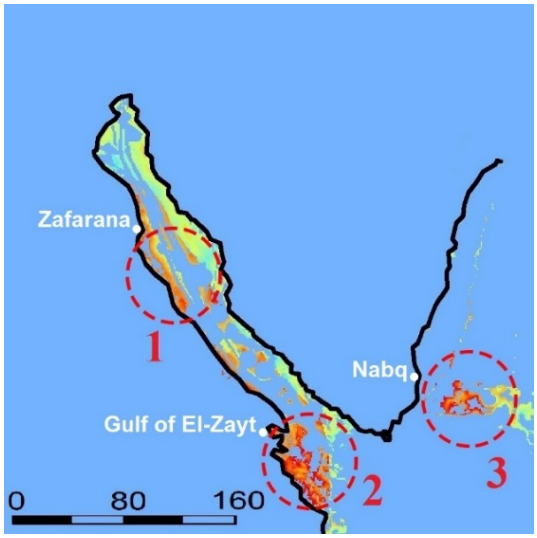

Figure 6-8: Proposed Offshore wind farms location around the southern coast of Sinai Peninsula, Egypt. The map indicates the location of the mast station that recorded the wind data used for the layout optimisation analysis.

Kinetic energy is reduced, when wind flows through wind turbine blades, which mean the wind speed downstream of the turbine is less than upstream. Therefore, the first turbine will face the initial wind speed, while, the second turbine in a row will encounter a reduction of the initial wind speed, and the third turbine in row will face a further wind reduction, and so on. The modified PARK model (Park and Law, 2015) is used in this work to calculate the wind speed reduction, which was explained previously in Section 3.9.4.

The layout design/optimisation is done assuming a 500 MW offshore wind farm (which is the average offshore wind farm capacity until the end of 2017), will be installed in the middle of the proposed three locations around Egypt, Figure 6-8. There are three types of annual net energy yield:

- The ultimate annual net energy yield, assuming that the rated wind speed (the wind speed that will make the turbine work at its generation maximum power), will be available at site all year time and the wake effects are neglected.

- The ideal annual net energy yield, in which the actual wind data in site is considered to calculate the net energy yield but neglecting the wake effects.
- The actual estimated annual net energy yield, which is estimated by using the actual wind data in site and considering the wake effects due to the offshore wind farm layout alignment design.

The first phase of the analysis is to estimate the ultimate annual net wind energy power production The ultimate annual net wind energy yield will equal the nominal power multiplied by the number of hours per year = 5000kW × 365 × 24 x (100 turbine) = 4380 GWh/year. This value is not realistic because the wind speed is fluctuating all the year from calm wind speed to windy speeds. Hence, the ideal annual net wind energy power production will be calculated. One year of wind speed distribution for one year is needed to estimate the ideal annual energy yield for each site.

6.4.1 Required Wind Records

The specific site data needed for the layout optimisation is the wind speed distribution, site map, turbine characteristics, and site topographic features. The topographic data for the three sites shown in Figure 6-8 is a flat surface as the three sites are offshore areas and the Aerodynamic roughness length for open sea is 0.0002 [m]. A clear map for the chosen files is needed to locate the wind farm turbines and mast station correctly. The map data was downloaded from the WindFarmer software programme online map data, the one was used in this analysis is the Open Street Map Worldwide Street Maps (GL-Energy, 2014). Wind and turbine data are explained in detail below.

Table 6-19: Wind mast stations information, adopted from (Mortensen et al., 2006b).

Station	Site	Location		Distance to the coastline	Mast Elev.[1]	P.W.D[2], Mean wind Speed	Weibull factors	
		N	E				A [m/s]	K
Zafarana	site 1	29° 06' 48.7"	32° 36' 38.9"	5000	49.5	N, 9.0	10.2	3.19
Gulf of El-Zayt	site 2	27° 47' 23.9"	33° 28' 23.3"	1300	38.5	NNW, 10.1	11.5	3.29
Nabq	site 3	28° 07' 45.2"	34° 25' 46.3"	1000	39.5	N, 6.8	7.7	2.04

[1] The elevation is in meter and measured from MSL (Mean Sea Level).

[2] P.W.D is the prevailing wind direction which is the direction that has the heist percentage of wind blowing per year regardless the wind speeds. Mean wind speed [m/s] is calculated for the whole 12 direction per year.

The data was extracted from the wind Atlas of Egypt (Mortensen et al., 2006b). This Wind Atlas is rarely found in the Middle East, where most of the similar wind information for the region is not complete and lacks accuracy. Wind Atlas of Egypt used wind data observations from 30 different mast stations, distributed to cover Egypt's extent, to produce the feasibility report for implementing onshore wind in Egypt. Luckily, each of the three offshore wind farms sites has at least one or two coastal mast stations in close proximity. The three met stations are shown in Figure 6-8, namely: Zafarana mast station (site 1), Gulf of El-Zayt mast station for (site 2), and Nabq for (site 3). Table 6-19 shows the characteristics of these stations.

The data adopted from the wind Atlas of Egypt for the three masts shows that the chosen sites has a high wind potential that blows from one direction for at least third of the year (Zafarana 57% from the North, Gulf of El-Zayt 51.3% from the Northwest, and Nabq 37% from the North). These high percentages indicate that the layout design should consider the direction of the prevailing wind to minimise the wake effect. To do so, the spacing between turbines is perpendicular to the prevailing wind direction (crosswind spacing) will be higher than the spacing in the parallel direction (downwind spacing, see Figure 6-9. In addition, the mean wind speed for the sites is high as 10.1 m/s for site number two.

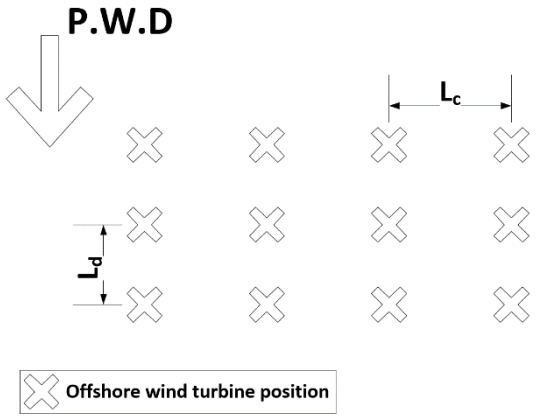

Figure 6-9: Illustration for the layout alignment example of an offshore wind farm, where $L_c > L_d$.

The Weibull factors are used to describe the wind variation, which is required to optimise and calculate the wind energy yield per year from wind turbines. The Weibull **k** value (Weibull shape factor) is a value that describes the shape of wind speed distribution curve. **K** values ranged from low as 1 to high as 4, low values explain that wind speed variations are similar (wide distribution), while the high values express that wind blows constantly most of the time (narrow distribution). The

Weibull **A** parameter (Weibull scale factor) is related to the mean value of the wind speed. The calculated **A** and **K** for the three sites suggest that the wind speed distributions are narrow and around a high wind speed (7.7, 10.5, and 11.2 m/s), which is promising for wind energy yield for the chosen sites and the capacity factors for the proposed sites are expected to be higher than 0.5. Table 6-20 shows the wind speed distribution for site 1 (Zafarana), the table is one-year average distribution, which was generated from the survey done between 1991 and 2005; the data was measured using mast/met station near the Zafarana site. Figure 6-10 illustrates the wind rose and the wind speed distribution for the previous site.

Table 6-20: Distribution of wind measurements for Zafarana mast station, adopted from (Mortensen et al., 2006b).

Sector	0	30	60	90	120	150	180	210	240	270	300	330
Direction	**N**			**E**			**S**			**W**		
Freq. %	57	15	1.7	0.7	1.1	2	0.7	0.4	3.2	8.5	5.6	4.2
Speed												
1	1	2	17	31	25	10	20	37	9	4	4	5
2	1	10	81	147	86	50	99	167	39	23	37	43
3	5	17	136	234	155	73	134	186	59	50	96	101
4	9	31	206	307	184	88	136	147	56	75	149	157
5	16	47	192	164	167	97	121	108	59	111	202	185
6	29	68	162	68	106	94	86	108	75	146	205	168
7	52	94	117	30	82	87	78	89	100	161	157	127
8	86	118	59	12	51	84	60	63	111	126	88	85
9	114	129	19	3	31	73	51	34	117	86	36	47
11	276	248	10	3	45	146	104	46	203	108	18	49
13	240	160	1	0	35	104	64	6	119	65	5	22
15	125	60	0	0	25	57	27	4	34	28	2	9
17	39	13	0	0	6	25	10	2	14	12	1	2
18	7	3	0	1	2	12	10	3	5	5	0	0

Values of wind speed distribution are normalised to 1000 per each direction, i.e. the sum of each column is equal to 1000. The P.W.D column is shaded in green.

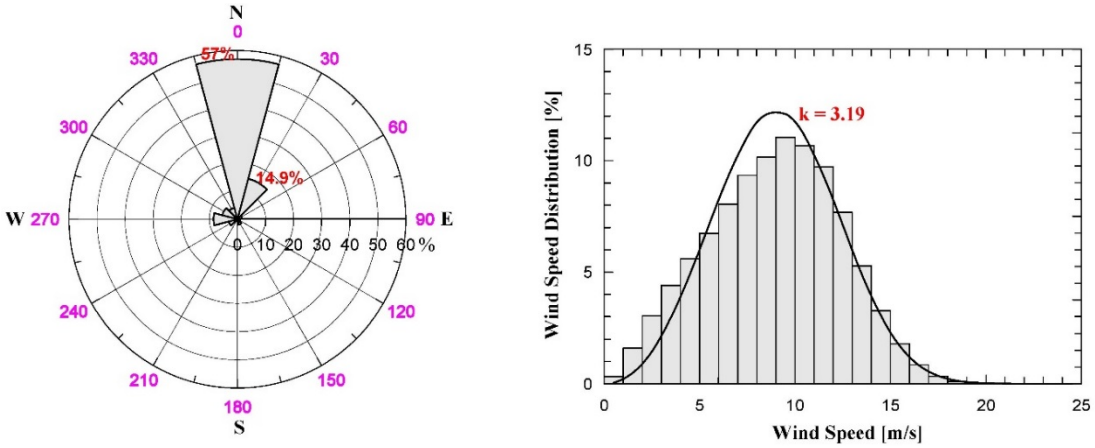

Figure 6-10: Wind Rose and wind speed distribution for Zafarana mast station.

Table 6-21: Distribution of wind measurements for Gulf of El-Zayt mast station, adopted from (Mortensen et al., 2006b).

Sector	0	30	60	90	120	150	180	210	240	270	300	330
Direction	**N**			**E**			**S**			**W**		
Freq. %	7.5	0.7	0.6	1.8	2.6	1.6	1.1	0.3	0.4	1.8	30	51
Speed												
1	6	45	43	21	12	31	50	64	52	29	2	1
2	26	172	171	61	57	84	159	176	148	84	9	7
3	43	261	233	113	93	116	183	231	135	74	13	14
4	48	254	249	184	120	153	198	248	135	62	18	22
5	47	138	126	233	145	181	183	148	105	67	28	35
6	56	69	88	193	151	158	127	74	112	108	41	40
7	62	34	59	126	136	126	59	18	96	159	55	46
8	76	16	26	52	107	72	24	23	75	194	73	54
9	93	6	3	13	99	43	6	11	65	107	90	64
11	198	5	1	4	70	31	6	2	64	82	220	169
13	191	0	1	0	9	5	4	0	8	25	199	213
15	126	0	0	0	1	0	1	0	5	8	166	200
17	25	0	0	0	0	0	0	4	0	1	70	100
18	3	0	0	0	0	0	0	1	0	0	16	35

Values of wind speed distribution are normalised to 1000 per each direction, i.e. the sum of each column is equal to 1000. The P.W.D column is shaded in green.

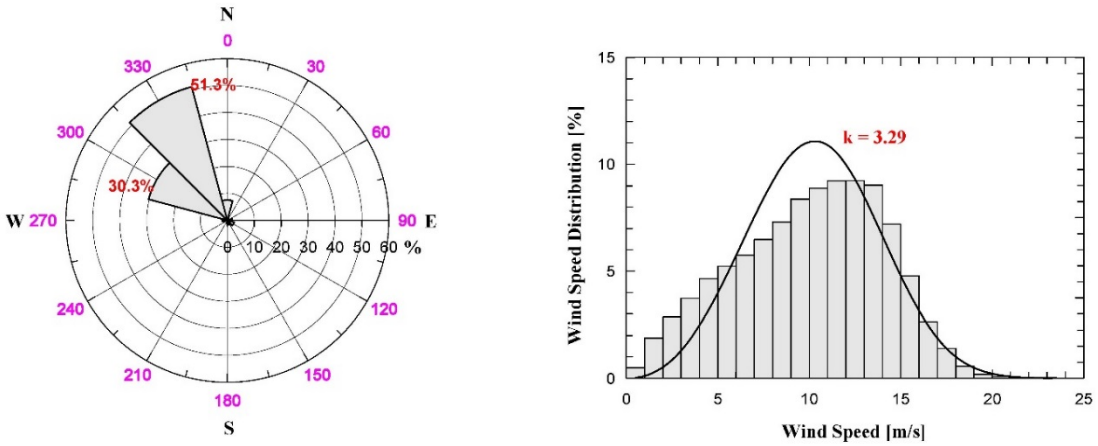

Figure 6-11: Wind Rose and wind speed distribution for Gulf of El-Zayt mast station.

Table 6-22: Distribution of wind measurements for Nabq mast station, adopted from (Mortensen et al., 2006b).

Sector	0	30	60	90	120	150	180	210	240	270	300	330
Direction	**N**			**E**			**S**			**W**		
Freq. %	37	28	3.4	1.1	1.2	2	1.6	0.8	1.3	1.4	4.6	18
Speed												
1	2	6	65	42	58	43	54	58	66	68	32	8
2	14	16	168	190	112	111	137	287	172	295	141	42
3	39	23	195	325	217	108	167	223	176	257	177	121
4	54	34	282	365	309	150	202	120	200	126	302	249
5	74	51	196	70	148	165	181	85	114	62	244	319
6	97	58	69	4	95	163	141	79	71	45	83	177
7	120	60	13	1	39	104	58	82	86	47	17	56
8	127	68	6	3	12	75	33	25	61	39	3	19
9	125	76	4	0	10	32	8	28	27	22	0	6
11	206	230	2	0	0	37	10	13	19	30	1	3
13	97	263	0	0	0	12	9	0	3	3	0	0
15	38	97	0	0	0	0	0	0	5	6	0	0
17	7	17	0	0	0	0	0	0	0	0	0	0
18	0	1	0	0	0	0	0	0	0	0	0	0

Values of wind speed distribution are normalised to 1000 per each direction, i.e. the sum of each column is equal to 1000. The P.W.D column is shaded in green.

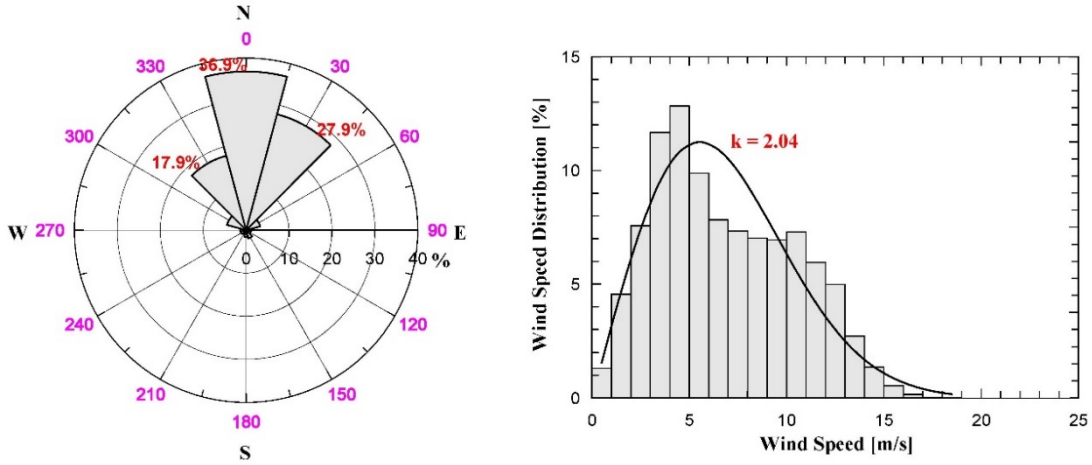

Figure 6-12: Wind Rose and wind speed distribution for Nabq mast station.

Table 6-21 identifies the wind speed distribution for site 2 (Gulf of El-Zayt), the table is oneyear average distribution, which was generated from the survey done in these periods (1995–97, 2000-02, and 2004-05); the data was measured using mast/met station near the previous site. Figure 6-11 shows the wind rose and the wind speed distribution for the Gulf of El-Zayt site.

Table 6-22 records the wind speed distribution for site 3 (Nabq Bay), the table is oneyear average distribution, which was generated from the survey done in the year between 2004 and 2005; the data was measured using mast/met station near the Nabq Bay site. Figure 6-12 illustrates the wind rose and the wind speed distribution for the previous site.

6.4.2 Ideal Energy Power Production

The ideal annual net wind energy power production is estimated assuming the wake effect is neglected. The value is identified by the number of hours per year for every recorded wind speed regardless the blow direction multiplied by output power of this speed for the turbine used. The wind speed distributions for the three sites are shown in Tables 6-23 to 6-25, and 4-14. Tables 6-23 to 6-25 estimate the ideal energy yield per year for the three sites, the calculation done for one 5 MW turbine and then multiplied by 100 to get the ultimate energy yield per year per farm. The final values of the ultimate energy yield for the three farms are 2669.1, 3013.1, and 1742.0 GWh/year respectively. The capacity factor, which equals the ideal energy yield divided by the ultimate one, is calculated below for the three sites:

- C.F$_1$ = 2669.1/4380 = 60.9%
- C.F$_2$ = 3013.1/4380 = 68.8%
- C.F$_3$ = 1742.0/4380 = 39.8%

The previous capacity factors are very high comparing to the highest capacity factor of similar offshore wind farms around world, but as discussed in Section 6.4, these values did not considered the wake effects, which will reduce the capacity factor accordingly; the following section is estimating the capacity factors considering the wake effects.

Table 6-23: Ideal net energy yield estimations for site 1.

Wind Speed	Sectors												5 MW Turbine		
	0	30	60	90	120	150	180	210	240	270	300	330	No. of hours/ speed	Output Power [kw][2]	Net Yield [GWh]
1	5.0[1]	2.6	2.5	1.9	2.4	1.8	1.2	1.3	2.5	3.0	2.0	1.8	28.0	0	0.0
2	5.0	13.1	12.1	9.0	8.3	8.8	6.1	5.9	10.9	17.1	18.2	15.8	130.1	0	0.0
3	25.0	22.2	20.3	14.3	14.9	12.8	8.2	6.5	16.5	37.2	47.1	37.2	262.2	40.5	0.01
4	44.9	40.5	30.7	18.8	17.7	15.4	8.3	5.2	15.7	55.8	73.1	57.8	383.9	177.7	0.06
5	79.9	61.3	28.6	10.1	16.1	17.0	7.4	3.8	16.5	82.7	99.1	68.1	490.5	403.9	0.20
6	144.8	88.8	24.1	4.2	10.2	16.5	5.3	3.8	21.0	108.7	100.6	61.8	589.7	737.6	0.44
7	259.6	122.7	17.4	1.8	7.9	15.2	4.8	3.1	28.0	119.9	77.0	46.7	704.3	1187.2	0.84
8	429.4	154.0	8.8	0.7	4.9	14.7	3.7	2.2	31.1	93.8	43.2	31.3	817.9	1771.1	1.45
9	569.2	168.4	2.8	0.2	3.0	12.8	3.1	1.2	32.8	64.0	17.7	17.3	892.5	2518.6	2.25
11	1378.1	323.7	1.5	0.2	4.3	25.6	6.4	1.6	56.9	80.4	8.8	18.0	1905.6	4550	8.67
13	1198.4	208.8	0.1	0.0	3.4	18.2	3.9	0.2	33.4	48.4	2.5	8.1	1525.4	5000	7.63
15	624.2	78.3	0.0	0.0	2.4	10.0	1.7	0.1	9.5	20.8	1.0	3.3	751.3	5000	3.76
17	194.7	17.0	0.0	0.0	0.6	4.4	0.6	0.1	3.9	8.9	0.5	0.7	231.4	5000	1.16
18	35.0	3.9	0.0	0.1	0.2	2.1	0.6	0.1	1.4	3.7	0.0	0.0	47.1	5000	0.24
												Net Yield [GWh/yr/turbine]			26.7
												Net Yield/farm [GWh/yr]			2669.1

[1] This value is calculated by multiplying the similar value from Table 4-12 by the frequency of value direction multiplied by no. of hours per year divided by 1E3 = 1 * 0.57 / 1E3 * 8760 = **5.0 hours.**

[2] **The output power values are interpolated from the graph in Figure 4-26.**

Table 6-24: Ideal net energy yield estimations for site 2.

Wind Speed	Sectors												5 MW Turbine		
	0	30	60	90	120	150	180	210	240	270	300	330	No. of hours/ speed	Output Power [kw][2]	Net Yield [GWh]
1	3.9[1]	2.8	2.3	3.3	2.7	4.3	4.8	1.7	1.8	4.6	5.3	4.5	42.0	0	0.0
2	17.1	10.5	9.0	9.6	13.0	11.8	15.3	4.6	5.2	13.2	23.9	31.5	164.7	0	0.0
3	28.3	16.0	12.2	17.8	21.2	16.3	17.6	6.1	4.7	11.7	34.5	62.9	249.3	40.5	0.01
4	31.5	15.6	13.1	29.0	27.3	21.4	19.1	6.5	4.7	9.8	47.8	98.9	324.7	177.7	0.06
5	30.9	8.5	6.6	36.7	33.0	25.4	17.6	3.9	3.7	10.6	74.3	157.3	408.5	403.9	0.17
6	36.8	4.2	4.6	30.4	34.4	22.1	12.2	1.9	3.9	17.0	108.8	179.8	456.3	737.6	0.34
7	40.7	2.1	3.1	19.9	31.0	17.7	5.7	0.5	3.4	25.1	146.0	206.7	501.7	1187.2	0.60
8	49.9	1.0	1.4	8.2	24.4	10.1	2.3	0.6	2.6	30.6	193.8	242.7	567.5	1771.1	1.01
9	61.1	0.4	0.2	2.0	22.5	6.0	0.6	0.3	2.3	16.9	238.9	287.6	638.8	2518.6	1.61
11	130.1	0.3	0.1	0.6	15.9	4.3	0.6	0.1	2.2	12.9	583.9	759.5	1510.6	4550	6.87
13	125.5	0.0	0.1	0.0	2.0	0.7	0.4	0.0	0.3	3.9	528.2	957.2	1618.3	5000	8.09
15	82.8	0.0	0.0	0.0	0.2	0.0	0.1	0.0	0.2	1.3	440.6	898.8	1423.9	5000	7.12
17	16.4	0.0	0.0	0.0	0.0	0.0	0.0	0.1	0.0	0.2	185.8	449.4	651.9	5000	3.26
18	2.0	0.0	0.0	0.0	0.0	0.0	0.0	0.0	0.0	0.0	42.5	157.3	201.8	5000	1.01
													Net Yield [GWh/yr/turbine]		30.1
													Net Yield/Farm [GWh/yr]		3013.1

[1] This value is calculated by multiplying the similar value from Table 4-13 by the frequency of value direction multiplied by no. of hours per year divided by 1E3 = 6 * 0.075 / 1E3 * 8760 = **3.9 hours.**

[2] **The output power values are interpolated from the graph in Figure 4-26.**

Table 6-25: Ideal net energy yield estimations for site 3.

Wind Speed	Sectors												5 MW Turbine		
	0	30	60	90	120	150	180	210	240	270	300	330	No. of hours/ speed	Output Power [kw][2]	Net Yield [GWh]
1	6.5[1]	14.7	19.4	4.0	6.1	7.5	7.6	4.1	7.5	8.3	12.9	12.5	111.0	0	0.0
2	45.3	39.1	50.0	18.3	11.8	19.4	19.2	20.1	19.6	36.2	56.8	65.5	401.3	0	0.0
3	126.1	56.2	58.1	31.3	22.8	18.9	23.4	15.6	20.0	31.5	71.3	188.7	664.0	40.5	0.03
4	174.6	83.1	84.0	35.2	32.5	26.3	28.3	8.4	22.8	15.5	121.7	388.3	1020.5	177.7	0.18
5	239.2	124.6	58.4	6.7	15.6	28.9	25.4	6.0	13.0	7.6	98.3	497.4	1121.1	403.9	0.45
6	313.5	141.8	20.6	0.4	10.0	28.6	19.8	5.5	8.1	5.5	33.4	276.0	863.1	737.6	0.64
7	387.9	146.6	3.9	0.1	4.1	18.2	8.1	5.7	9.8	5.8	6.9	87.3	684.4	1187.2	0.81
8	410.5	166.2	1.8	0.3	1.3	13.1	4.6	1.8	6.9	4.8	1.2	29.6	642.1	1771.1	1.14
9	404.1	185.7	1.2	0.0	1.1	5.6	1.1	2.0	3.1	2.7	0.0	9.4	615.9	2518.6	1.55
11	665.9	562.1	0.6	0.0	0.0	6.5	1.4	0.9	2.2	3.7	0.4	4.7	1248.3	4550	5.68
13	313.5	642.8	0.0	0.0	0.0	2.1	1.3	0.0	0.3	0.4	0.0	0.0	960.4	5000	4.8
15	122.8	237.1	0.0	0.0	0.0	0.0	0.0	0.0	0.6	0.7	0.0	0.0	361.2	5000	1.81
17	22.6	41.5	0.0	0.0	0.0	0.0	0.0	0.0	0.0	0.0	0.0	0.0	64.2	5000	0.32
18	0.0	2.4	0.0	0.0	0.0	0.0	0.0	0.0	0.0	0.0	0.0	0.0	2.4	5000	0.01
											Net Yield [GWh/yr/turbine]				17.4
											Net Yield [GWh/yr]				1742.0

[1] This value is calculated by multiplying the similar value from Table 4-14 by the frequency of value direction multiplied by no. of hours per year divided by 1E3 = 2 * 0.37 / 1E3 * 8760 = **6.5 hours.**

[2] The output power values are interpolated from the graph in Figure 4-26.

6.4.3 Estimated Energy Yield (Layout Optimisation)

The specific site data needed for the layout optimisation is the wind speed distribution, site map, turbine characteristics, and site topographic features. The topographic data for the three sites shown in Figure 6-8 is a flat surface as the three sites are offshore areas and the Aerodynamic roughness length for open sea is 0.0002 [m]. A clear map for the chosen files is needed to locate the wind farm turbines and mast station correctly. The map data was downloaded from the WindFarmer software programme online map data, the one was used in this analysis is the Open Street Map Worldwide Street Maps (GL-Energy, 2014). Wind speed distributions are introduced in Section 6.4.1.

The estimated electricity production per year for a wind farm is the one considers the wake effects. As indicated in Section 3.9 WindFarmer software programme was used to consider the wake effects. The data in Section 4.5 and 6.4.1 is used to run the energy calculation module in the programme. Only the spacing between wind turbine, turbine boundaries, and turbine coordinates need to be proposed and then identified into the software. An approximate turbine spacing of 5 to 8 times rotor diameter is suggested to reduce turbulence between turbines for average wind speed around 10 m/s (Mortensen et al., 2006b, Sheridan et al., 2012, E.ON, 2012). Therefore, ten layouts (L_1 –L_{10}) are suggested to calculate the net energy yield per year, which are listed in Table 6-26. Figures 6-13 to 6-18 are presenting the proposed layouts alignment.

Table 6-26: Proposed offshore wind farm layouts spacing and angle.

Layout name	Spacing in x direction	Spacing in Y direction	Alignment angle	Farm Area [km²]
L_1	8d = 1008m	8d = 1008m	0	101.6
L_2	7d = 882m	7d = 882m	0	77.8
L_3	6d = 756m	6d = 756m	0	57.2
L_4	5d = 630m	5d = 630m	0	39.7
L_5	8d = 1008m	5d = 630m	0	63.5
L_6	5d = 630m	8d = 1008m	0	63.5
L_7	8d = 1008m	8d = 1008m	45	101.6
L_8	5d = 630m	5d = 630m	45	39.7
L_9 (Optimisation)	8d = 1008m	8d = 1008m	0	101.6
L_{10} (Optimisation)	5d = 630m	5d = 630m	0	39.7

d is rotor diameter, which is 126m for the 5MW turbine.

Table 6-27 shows the net energy yield per year for each location considering the proposed layouts in Table 6-26. Where: L_0 is for the values calculated in Tables 6-23 to 6-25. L_5 is a layout, where the spacing in x direction spacing equals 8d, while in y direction equals 5d. L_6 is a layout, where the spacing in x direction spacing equals 5d, while in y direction equals 8d. L_9 is a layout, where the spacing in both direction is 8d, but the internal optimiser of the WindFarmer programme defines the final layout. L_{10} is a layout, where the spacing in both direction is 5d, but the internal optimiser of the WindFarmer programme defines the final layout.

Table 6-27: Net yield energy and capacity factor for the three offshore 500MW wind farm.

Layout name		Site 1			Site 2			Site3		
		C.F [%]	Net Yield [GWh/yr]	Net Yield per 1 km	C.F [%]	Net Yield [GWh/yr]	Net Yield per 1 km	C.F [%]	Net Yield [GWh/yr]	Net Yield per 1 km
L_0		60.9	2669	-	68.8	3013	-	39.8	1742	-
L_1	8d	50.6	2216	21.8	61.2	2680	26.4	34.8	1522	15
L_2	7d	49.2	2155	27.7	60.1	2633	33.8	33.9	1483	19.1
L_3	6d	47.7	2091	36.6	58.6	2565	44.8	32.8	1435	25.1
L_4	5d	46.0	2013	50.7	56.8	2486	62.6	31.4	1376	34.7
L_5	8d-5d	49.3	2158	34	59.6	2610	41.1	33.8	1479	23.3
L_6	5d-8d	48.2	2110	33.2	59.0	2585	40.7	32.9	1441	22.7
L_7	8d-45°	51.3	2247	22.1	61.1	2677	26.3	35.1	1537	15.1
L_8	5d-45°	46.0	2015	50.8	56.2	2463	62	31.7	1387	34.9
L_9	8d	50.6	2216	21.8	61.1	2680	26.4	34.8	1522	15
L_{10}	5d	46.0	2015	50.8	56.8	2486	62.6	31.9	1397	35.1

The ideal annual net wind energy power production for the three sites (excluding the turbulence and wake effects) were estimated, and the capacity factors are 60.9, 68.8, and 39.8%, respectively. The wake effect is an inevitable phenomenon; therefore, ten layouts were suggested to reduce the expected losses due to the wake effect.

The suggested layouts used a spacing that ranged from five to eight time the rotor diameter of the 5MW turbine (126m). The ten layouts were subjected to the actual wind speed distribution for the three sites, and the actual net yield energy was estimated using the WindFarmer programme. The net energy yield was also estimated for a 1 km x 1 km area to compare different layouts, Table 6-27. The results showed that for (site one and three) the optimum layout was the 5d x 5d spacing with 45-degree alignment angle, while for site two the optimum layout was the 5d x 5d spacing with 0-degree alignment angle, see Table 6-28. The final capacity factors for the three sites are 46.0, 56.8, and 31.7%, respectively.

Table 6-28: Optimum layouts for the 500MW offshore wind farm for the chosen sites.

Site	Optimum layout	Net Yield per 1 km	C.F [%]	Net Yield [GWh/yr]
Site 1	L_8 5d x 5d 45°	50.8	46.0	2015
Site 2	L_4 5d x 5d - 0°	62.6	56.8	2486
Site 3	L_8 5d x5d - 45°	34.9	31.7	1387

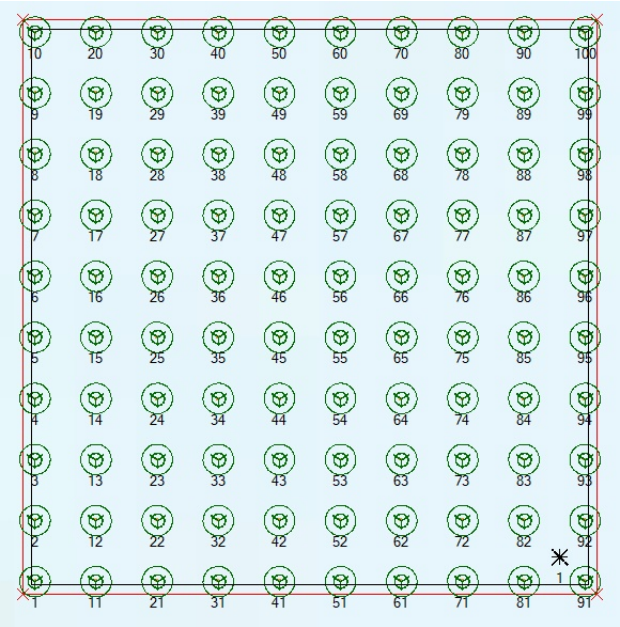

Figure 6-13: Layout alignment number 1 for 8d x 8d spacing.

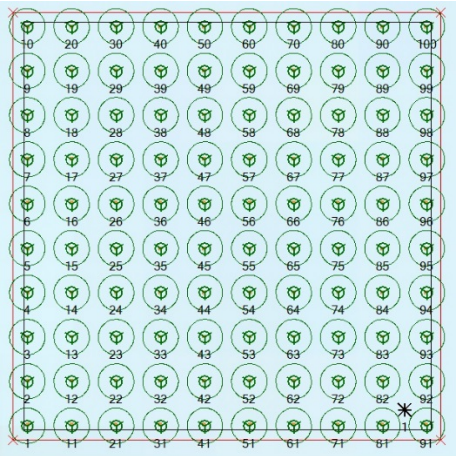

Figure 6-14: Layout alignment number 5 for 5d x 5d spacing.

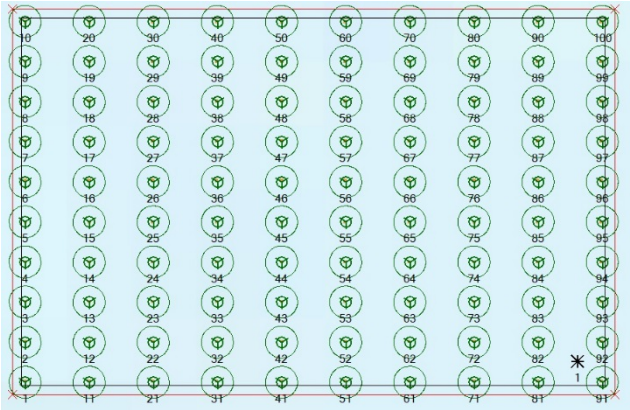

Figure 6-15: Layout alignment number 6 for 8d x 5d spacing.

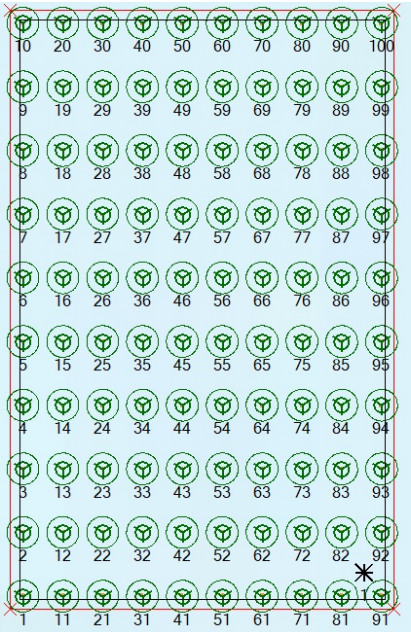

Figure 6-16: Layout alignment number 4 for 5d x 8d spacing.

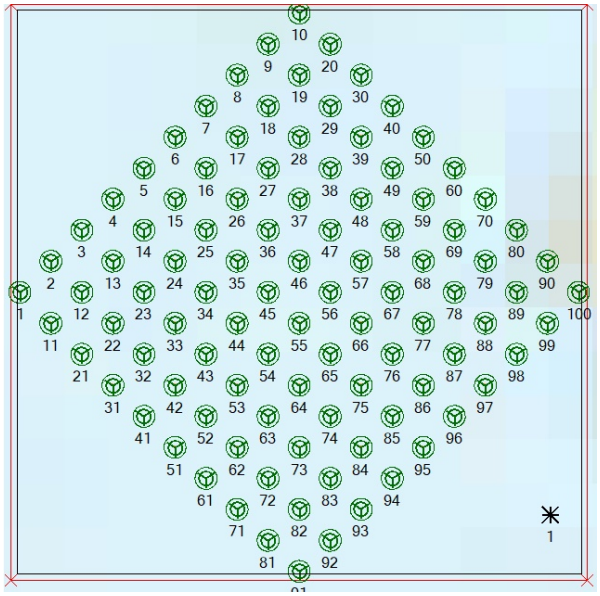

Figure 6-17: Layout alignment number 7 for 8d x 8d spacing with 45° alignment angle.

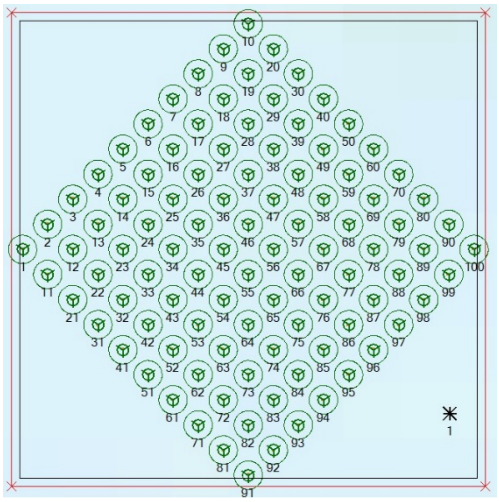

Figure 6-18: Layout alignment number 8 for 5d x 5d spacing with 45° alignment angle.

The internal optimiser simulator available within the WindFarmer software is slightly improving the energy net yield per year. The optimised layout 5d x 5d for site 1 is higher than the original 5d x 5d layout by 2 GWh/yr while it is the same for site 2. The optimised layouts were not considered as for small or no improvement it disturbs the final layout alignment, where it will be a very hard task to design the cables network for the final layout, see Figure 6-19.

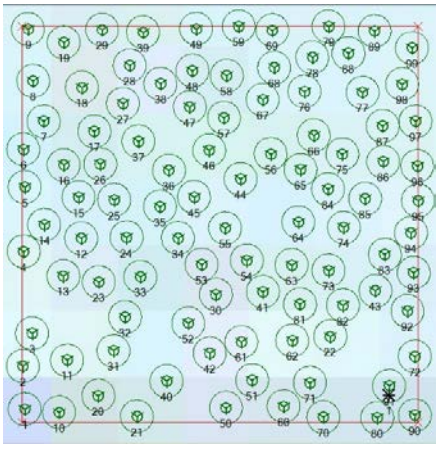

Figure 6-19: The optimised layout for a 5d x 5d for site 1, the turbine locations assigned by the WindFarmer internal optimiser.

Curtailments are the reduction of the capacity factor due to these operational problems. Final curtailment will be the magnitude of wind sector management and grid curtailment. Wind sector management is reduction of the turbine loading due to the wake effects from nearby wind turbines. Close spacing layouts will force the wind farm control to shut some of the turbines down at high wind speeds, which will reduce the final net energy yield of the wind farm. Grid curtailment is connection agreements or protocols where the wind farm will reduce its output as the gird cannot handle that much electricity or the electricity demand is failing down in certain time of the day or the year.

The final capacity factors for the three sites are 46.0, 56.8, and 31.7%, respectively. The first and the second sites capacity factors are higher than expected and greater than similar wind farms in the UK, which require more investigation to consider the curtailment effect that will occur due to high gust wind speeds effect. Westermost Rough offshore wind farm data is used to estimate the wind speed management curtailment and apply it to the first and second sites of this study. The lifetime capacity factor of the Westermost Rough offshore wind farm in North Sea of the UK is 46.1% and its average wind speed is 9.06 m/s, which is the highest capacity factor for offshore wind farm globally (EnergyNumbers, 2019). The wind speed data for the Westermost Rough offshore wind farm (ABPmer, 2018) and its performance/monthly capacity factor data (EnergyNumbers, 2019) are used to estimate the curtailment associated with high wind speed.

Table 6-29 and Figure 6-20 shows the expected change due to wind speed management for the Westermost Rough offshore wind farm, as the curtailment due to grid connection management for this offshore wind farm is zero (Joos and Staffell, 2018). The estimated figures showed that the reduction in capacity factor is neglected for average wind speed less than 8.67 m/s and the reduction in the capacity factor is more than 40%for average wind speeds beyond 10.5 m/s. The produced curve shown in Figure 6-20 is used to re-estimate the capacity factor for site 1 and 2 of this study. Tables 6-30 and 6-31 are presenting the new capacity factor estimations for site 1 and 2 considering the curtailment due to wind speed management. The new capacity factors are 44.5 and 53% compared to 46 and 56.8%, which is still higher than the UK's offshore wind farms. These higher capacity factors are due to the high quality of the wind in these sites (high wind speed with one direction blowing for most of the year) compared to wind quality in the UK. In addition, the near onshore wind farm recorded 41.6% capacity factor for 2004-2005 year where the hub heights for the turbines were between 40 and 46m (El-Shimy, 2010).

Table 6-29: Westermost Rough Change in capacity factor estimations.

Month	Sep-2017	Oct-2017	Nov-2017	Dec-2017	Jan-2018	Feb-2018	Mar-2018	Apr-2018
Max power [GWh]	4.32	4.464	4.32	4.464	4.464	4.032	4.46	4.32
Wind Speed [m/s]	8.94	10.79	11.51	10.47	10.45	10.7	11.2	8.64
Power KW	3241.8	5582.4	5817.6	5051	5040.2	5436	5676	2960
Estimated power [GWh]	2.33	4.15	4.19	3.76	3.75	3.65	4.22	2.13
Ideal C_f	0.54	0.93	0.96	0.84	0.84	0.91	0.95	0.49
Actual C_f	0.49	0.52	0.532	0.51	0.51	0.51	0.52	0.5
Change in C_f	-0.09	-0.44	-0.45	-0.39	-0.39	-0.43	-0.45	0.01

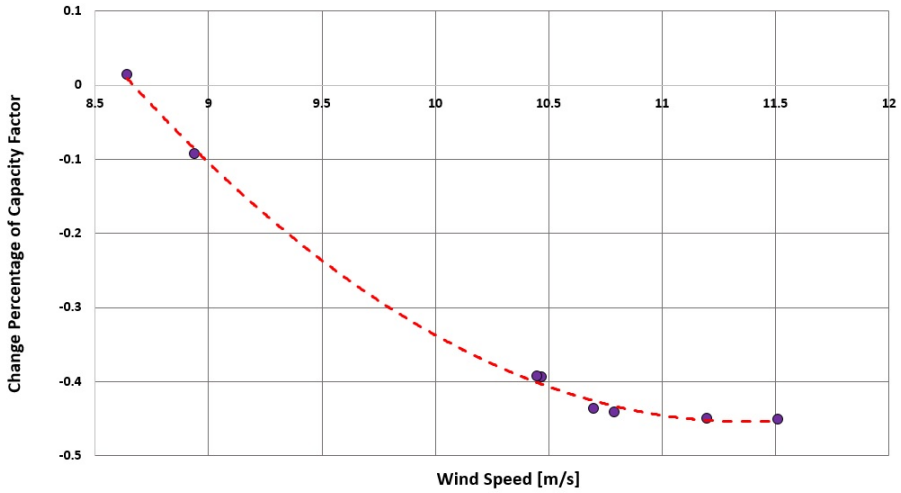

Figure 6-20: The expected C_f change due to wind speed management of the Westermost Rough offshore wind farm.

Table 6-30: New estimation for the site 1 C_f considering wind speed management curtailments.

Month	Max power [GWh]	Wind Speed [m/s]	Power [KW]	Ideal power [GWh]	Ideal C_f	Change in C_f	Estimated C_f	Estimated Power [GWh]
Jan	3.72	6.79	1116.80	0.83	0.22	0.00	0.22	0.83
Feb	3.36	7.12	1365.10	0.92	0.27	0.00	0.27	0.92
Mar	3.72	10.39	3824.10	2.85	0.76	-0.40	0.46	1.71
Apr	3.60	10.28	3780.30	2.72	0.76	-0.38	0.47	1.68
May	3.72	10.17	3655.80	2.72	0.73	-0.37	0.46	1.72
Jun	3.60	12.03	4799.14	3.46	0.96	-0.43	0.54	1.96
Jul	3.72	11.92	4748.20	3.53	0.95	-0.44	0.53	1.97
Aug	3.72	11.48	4745.35	3.53	0.95	-0.46	0.51	1.91
Sep	3.60	12.80	4850.00	3.49	0.97	-0.33	0.65	2.33
Oct	3.72	11.16	4471.39	3.33	0.89	-0.46	0.49	1.81
Nov	3.60	7.88	1663.80	1.20	0.33	0.00	0.33	1.20
Dec	3.72	8.21	1957.90	1.46	0.39	0.00	0.39	1.46
Total	43.80							19.48

The final capacity factor considering wind speed management curtailment = 19.48/43.80 = 44.5 %

Table 6-31: New estimation for the site 2 C_f considering wind speed management curtailments.

Month	Max power [GWh]	Wind Speed [m/s]	Power [KW]	Ideal power [GWh]	Ideal C_f	Change in C_f	Estimated C_f	Estimated Power [GWh]
Jan	3.72	8.83	2392.10	1.78	0.48	-0.06	0.45	1.68
Feb	3.36	9.21	2842.90	1.91	0.57	-0.17	0.47	1.59
Mar	3.72	11.62	4789.40	3.56	0.96	-0.46	0.52	1.94
Apr	3.60	11.10	4468.90	3.22	0.89	-0.45	0.49	1.75
May	3.72	11.30	4685.20	3.49	0.94	-0.46	0.51	1.89
Jun	3.60	12.30	5000.00	3.60	1.00	-0.41	0.59	2.14
Jul	3.72	12.86	4859.10	3.62	0.97	-0.32	0.66	2.45
Aug	3.72	12.53	4813.20	3.58	0.96	-0.38	0.60	2.23
Sep	3.60	12.25	4801.60	3.46	0.96	-0.41	0.56	2.03
Oct	3.72	12.71	4831.90	3.59	0.97	-0.35	0.63	2.34
Nov	3.60	8.32	1957.80	1.41	0.39	0.00	0.39	1.41
Dec	3.72	9.20	2839.80	2.11	0.57	-0.16	0.47	1.77
Total	43.80							23.21

The final capacity factor considering wind speed management curtailment = 23.21/43.80 = 53 %

6.5 Environmental Impacts Evaluation

Environmental Impact Assessment (EIA), which is a term used is to describe the evaluating procedures of the expected environmental impacts of a project under investigation. The assessment considers both environmental and social impacts, discussing the advantages and disadvantages of the project. EIA is a tool presented to the stockholder prior to the project consent, where they can accept or reject the plan. The following Table 6-32 summarise the potential hazards accompanied by offshore wind monopile 5MW turbine installation/operation processes.

Table 6-32: Potential environmental hazards associated with offshore wind farms installing and operation, adopted from (Kaldellis et al., 2016).

	Hazards	Source	Mitigations
Sea life	Underwater noise/vibration	Monopile driving hammer	- Hydro sound damper and double big bubble curtain. - Seasonal Mitigation.
	Electromagnetic fields	Undersea cables	-
	Water sediment turbulence	Monopile driving into soil seabed	-
Aves	Noise and collision	Rotor noise and rotating blades	-
Social impact	No fishing activity	Fishery is banded within the farm area.	-
	Stress and sleep disturbances	Noise and shadow flicker effect	-

Offshore wind farms social impacts are minimum for the three locations identified in this study, as they are at least 10 km away from urban areas. Stress and sleep disturbances related to noise operation from the wind farm are minimised in offshore wind energy case as the shoreline criteria limited the distance to shoreline to more than 5 km from the coast, which guarantees at least 5 km buffer zone between any residents and the offshore wind farm. In addition, any possible wind farm noise will be discarded by sea wave noise (Kaldellis et al., 2016).

For the fishery activity as clear before in Section 5.2.1, according to the Egyptian law 124 (1983), the allowed depth for large fishing vessels is more than 70 meters (General Authority for Fish Resources Development, 2009). Hence, the offshore wind energy industry will not interfere with large fishing activity as the water depth criteria in the spatial siting process confined the water depth of the offshore farms at 60-meters maximum. In addition, the total areas of the three sites represent less than two percent of the total areas of the Red Sea belong to Egypt, which will not reduce the available fishing area significantly.

6.5.1 Artificial Reefs and Ecosystems

The area occupied by offshore wind farm turbines in the smallest proposed offshore wind farm (L_4 in Section 6.4.3) is less than 0.008% of the total seabed area of the farm (Kaldellis et al., 2016). This percentage is a very small area, which will leave the fauna and flora with no interventions. In addition, the spatial siting of the offshore wind farms excludes all maritime natural reserves, which avoid any potential damage to the artificial reefs of the Red Sea areas.

A long term behaviour monitoring study confirms that tuna fishes and other fish species that exposed to low frequency noise from offshore wind turbines, adapt significantly to avoid the noise by increase its speed (Pérez-Arjonaa et al., 2014). The marine ecosystem could benefit from the scour protection measurements (if any) and the side surface of the monopile, which will provide a suitable region for some of the sea species and coral reefs to colonise.

The main concern related to offshore wind farm construction is foundation installation, which accompanied by noise, and water turbidity that could affect the sea life near installation area. Hydro sound damper and double big bubble curtain technology could reduce these effects through the foundation construction phase. Bubble curtain/pneumatic barrier is a ring tube surrounding the bottom of the pile mud level that has numerous small holes, and the small pipe is air pressured to

release a curtain of bubbles around the pile driving path to reduce the sound and water turbulence effects (Nehls et al., 2007).

Hydro Sound Dampers (HSD) is a new field mitigation measure used while driving monopile by hydraulic hammer to reduce the noise induced by this installation method. HSD implemented by deploying a buoyancy ring around the monopile before using the hammer, and the ring filled by gas to float, the upper ring is attached to a ballast box at the bottom of the sea by a fishing net, the fishing net is covered by a PE-foam element to reduce sound and water turbulence (Elmer and Savery, 2014). Figure 6-21 shows a typical HSD system with was first used and successfully tested in London Array monopile installation, 2012 (zur Minderung, 2016).

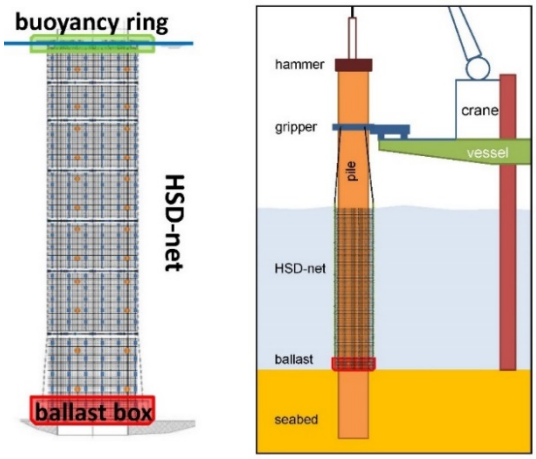

Figure 6-21: HSD-net system used in the London Array project, adopted (Bruns et al., 2014).

Seasonal restrictions on piling activity may also mitigate the piling and hammering effects on the near sea life, especially during fish breeding and pupping season. On the other hand, the restricted ship movement inside the offshore wind farm border will create a safe area for sea life and fish to flourish.

6.5.2 Impact on Birds

The major potential impacts on birds from the offshore wind farm installation are the barrier effect to the mitigation routs and the potential collision due to rotating blades. Other minor impacts could be disturbance of the breeding and staging areas (the area where birds stop to field through the migration path) of birds due to noise pollution. Figures 6-22 and 6-23 show the soaring birds

supporting areas (breading/staging areas) and its migration routes (flight paths). As can be seen from the figures, the three chosen sites are remote from the supporting areas, since bird reservation areas were excluded from the spatial siting analysis. On the other hand, satellite images indicate that some of the avian migration tracks are directly above the three chosen sites. Therefore, further impact assessment is required for this hazard.

Figure 6-22: Soaring birds supporting areas [in pink colour], around the study area, adopted from (BirdLife International, 2018).

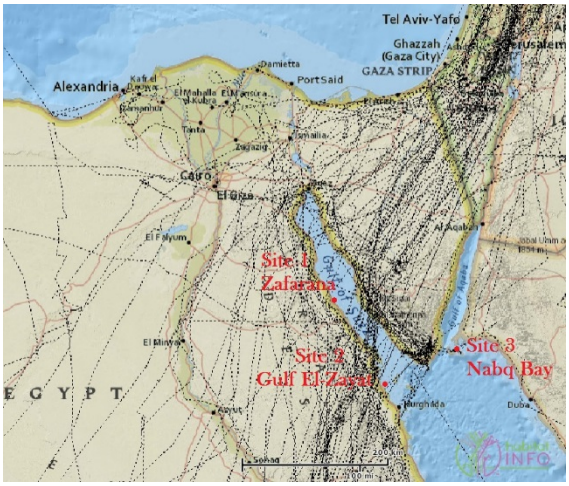

Figure 6-23: Soaring birds satellite track, adopted from (BirdLife International, 2018).

As the offshore wind energy industry in Europe is expanding rapidly, many studies were performed to assess the environmental impacts on avian animals, which all emphasise that offshore wind energy development has a very limited effect on bird habitat, migration paths, or breeding rates. A study on the bird mortality emphasised that less than 0.01% of the 830 million bird deaths in the USA, in 2005 due to human activity is due to wind turbines (Erickson et al., 2005), which declares the intangible effect of offshore wind on the bird mortality.

A recent study on the 108 MW offshore wind farm on Egmond aan Zee (Netherlands) estimated that 581 out of two million birds fluxes flown over the offshore wind farm per year are mortal (Fijn et al., 2012), which is less than 0.03% that confirms the same finding by the previous study. In addition, another radar monitoring study of birds and Waterfowl at Horns Rev Offshore Wind Farm observed that less collision risk of bird to an offshore turbine is less than 0.0002% (Sovacool et al., 2008). Figure 6-24, shows that Eiders birds tend to avoid pathing through the offshore wind farm during its autumn migration movement.

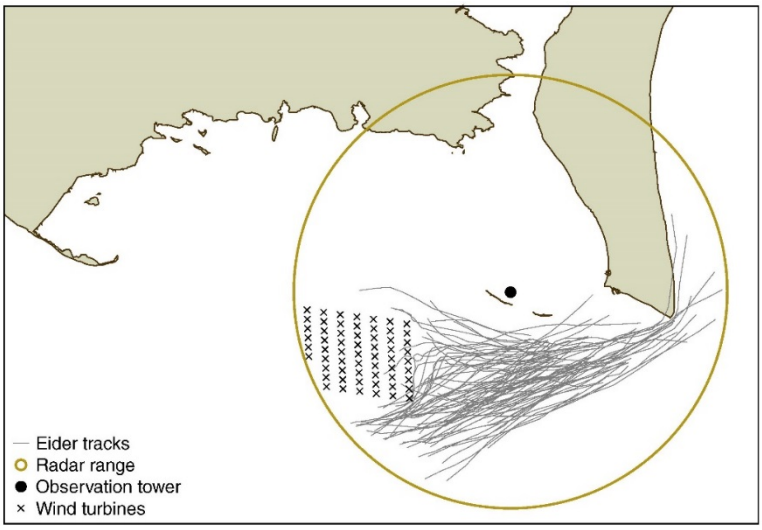

Figure 6-24: "Radar registrations of 84 flocks of migrating Eiders determined visually at Rødsand during autumn 2003", adopted from (Kahlert et al., 2004).

Chapter 7: Conclusions and Future Work

The main aim of the thesis is to carry out a framework to evaluate the possible potentials of deploying offshore wind farms in Egypt, and the Arabian Peninsula. The other aim is to investigate the infrastructure feasibility and requirements for the first case study for offshore wind farms installation in Egypt. The objectives to support such aims were divided into six objectives, which are:

A. Identify, address, and quantify the criteria that govern offshore wind farm siting.
B. Produce suitability maps of the offshore wind energy in Egypt, and the Arabian Peninsula, then, identify the appropriate sites and their potential for both case studies.
C. Develop a clear understanding of the technologies needed for anchoring such turbines, by assessing typical soil conditions at appropriate sites, then design the appropriate foundation for the chosen sites as a function of the Egyptian soil and weather condition.
D. Find the optimized design of the wind farm layout for the chosen sites in Egypt.
E. Create a feasibility study to identify the Egyptian ports availability and associated infrastructure to support the installation presses of offshore wind turbines.
F. Provide an initial environmental assessment study for deploying offshore wind farms in Egypt.

7.1 Spatial Siting

Offshore wind energy, similar to most of the other renewable sources, has a low power density, for instance, it could occupy 50 times more space than a comparative gas fuelled electrical power plants, which makes the spatial siting for offshore wind farms a critical process not only in addressing the appropriate data needs but also for optimised decision-making.

Multiple-criteria decision-making (**MCDM**) analysis coupled with AHP are widely used to solve complex renewable energy spatial planning problems. Here a new approach is proposed to use the *Representative Cost Ratio* (RCR) to assist in the rapid and accurate determination of offshore wind energy potential areas. This approach was quantified through a robust methodology and was used in two case studies (Egypt and the Arabian Peninsula) to support its applicability and usefulness. The spatial results obtained for the UK offshore wind energy programme matched well with the "costly mapping" determined by the Crown Estate for their projects (£90k/MW) for the three Rounds (Cavazzi and Dutton, 2016). This gives confidence that the RCR approach is accurate as all of the cells for these projects are located in either moderate or high suitability categories determined by this study.

The methodology to model and identify suitable areas for offshore wind energy sites is introduced to address the gap in knowledge in the offshore wind energy field. The methodology can be easily utilised in other regions by applying the four steps summarised in Section 2.3.4 and the process depicted in Figure 3.1. There are some assumptions, requirements, and limitations related to the proposed methodology. The methodology is limited to national or regional scales requiring a wide knowledge and data (wind speed and bathometry) at these scales. The model was built on the assumption that cost related criteria are higher in weight than those assigned to the environmental aspect of the site to be exploited.

The approach presented here provided a suitability map for offshore wind energy in Egypt and the Arabian Peninsula. The methodology is capable of dealing with the conflicting criteria that govern the spatial planning for offshore wind farms. To the author knowledge's, no detailed studies have been conducted either onshore or offshore, that have considered such a footprint, provided spatial planning examination of appropriate sites and performed sensitivity analysis.

The final results indicate that Egypt could potentially benefit from around 32.8 GW, which is double the total installed electricity capacity of Egypt until the end of 2014. The 32.8 GW is achieved only by considering installations at the identified high suitability offshore wind energy sites. This significant amount of green renewable energy could provide a solution to the electricity shortage in Egypt; furthermore, the offshore wind energy solution has no effect on important tourist recreational areas around the chosen sites. This outcome confirms the huge offshore wind energy potential in Egypt. In addition, as the fuel from wind electrical power production is free, exploitation of offshore wind energy could positively contribute to the country's Gross domestic product (GDP) and budget balances, reducing dependence on imported fuels whilst providing a cleaner and more sustainable approach to electricity production in Egypt. Nevertheless, a coherent policy coupled with capacity building would be needed to allow such exploitation to occur.

Egypt case study provides the evidence needed to establish an appropriate programme to exploit the offshore wind energy resources. This will contribute to the energy mix so that it can cope with its ever-increasing energy demand. In essence, the work presented here not only plugs a knowledge gap but also provides realistic evaluation of the Egyptian offshore wind energy potential which can form the basis of a blueprint for developing the appropriate policies for its exploitation. The existence of vast commercial experience in offshore wind energy projects is more than likely to consider such a resource and can be marshalled to support it exploitation in Egypt.

In the second case study, the regional area of the Arabian Peninsula is considered to test the methodology across the whole process (Figure 3-1) and to provide detailed indication of the offshore wind energy potential in this region. The analysis and modelling covered seven countries, for which final suitability maps were generated using appropriate factors and weights of relevance to the region's countries. The identified sites were analysed in terms of potential power capacities based on an 8 MW wind turbine which now seems to be the standard capacity being deployed in Europe and elsewhere. The results shown in Table 5-8 indicate a cumulative regional capacity of up to 35 GW for the turbine capacity selected. This Middle East region has not seen any significant or meaningful development to exploit its offshore wind energy potential and this work and its outcomes has also addressed this gap in knowledge. To the author's knowledge the outcomes represent the first detailed assessment of the offshore wind energy potential for the Arabian Peninsula countries. This work will contribute to the stimulation of interest in the region of the importance of offshore wind energy as part of a regional energy mix.

It must be noted that this work does not compare the various attributes of the available renewable energy resources in the region, but provides seminal work for understanding the offshore wind energy potential. The outcomes also show the effective aspect of the presented methodology and its utilisation at such a large regional scale.

In summary, the proposed new approach has been verified by the UK offshore wind energy programme projects and has predicted the sites and capacities of the Arabian Peninsula offshore wind energy potential at a large scale. The use of the *Representative Cost Ratio* to assist in the rapid and accurate determination of offshore wind energy potential regions will save money and reduce the time and effort taken to achieve the optimal spatial siting decisions for offshore wind energy farms.

Lastly, the scope and methodology of this part addressed a knowledge gap in the development of renewable energy systems, particularly, which of offshore wind energy. The methodology used here provides a robust offshore spatial siting analysis that may have applications in different locations around the world.

7.2 Infrastructure Feasibility Structure of Egypt

Monopile foundations are the dominant foundation system around Europe and the world, despite some expectation that offshore wind turbine Jacket structures will become dominant by 2020. Monopile exceed the 30m water depth limit and have only been excessed it in three offshore wind farm projects. Gravity base offshore foundations are less often used as the offshore wind farms move to ever deeper waters for higher wind resources, however, this foundation type is more suitable for weak soil conditions. Moving toward deeper water depths > 50mr requires more time for the floating foundation solution to become commercially viable. Floating foundations are still under devolvement, and considerable research is currently being undertaken to develop the infrastructure to support their commercialisation. Hybrid foundations are also still under fundamental research, and to the author's knowledge, there are no plans to build a 1:1 Hybrid foundation prototype in place.

The structural analysis using ABAQUS programme provided a preliminary design to allow computation with the more conventional monopile system at the identified sites. The analysis has shown that a 24-meter pile is needed to deploy offshore wind turbine at site 1, a 20- meter pile is

suitable for site number 2, and a 16-meter pile could be suitable for use at site 3 (subject to further investigation). The prior scour assessment indicates that the seabed of the three sites are stable and no scour issues are expected to occur.

AHP methodology is suitable to identify the most appropriate port for an offshore wind farm development. The methodology was accomplished to find the most suitable port for installing a 500MW offshore wind farm in Egypt. The results indicate that East Port-Said port is a most suitable harbour to facilitate the installation at the three sites.

Layout optimisation analysis showed that the layout for the three sites is a square layout with five times the rotor diameter spacing between the turbine array, and the angle between the x-axis and prevailing wind direction is 45 degrees. The final capacity factors for the three sites are 46.0, 56.8, and 31.7%, respectively. The first and the third capacity factors are close to capacity factors in Europe, which indicates the suitability and cost feasibility of these sites. The second capacity factor is 7.5% higher than the highest lifetime capacity of offshore wind farm globally, which is Dudgeon offshore wind farm on the UK, this could be to the high quality of the wind in this site compared to wind quality in the UK. In addition, the capacity factors of site 1 and 2 still higher than the UK offshore wind farms even when considering the wind management curtailment, which confirm the higher offshore wind quality of these sites.

The expected environmental impacts for deploying offshore wind farms in the three chosen sites are shown to be limited. The social impacts are minimal as the sites are remote; while the impacts on the sea life could be mitigated, using tested and approved techniques. The main conclusion of chapter 6 is that offshore wind energy is applicable, economical, and has minimum environmental hazards in Egypt.

7.3 Future Work

Spatial siting models are sensitive by the data quality and availability for the analysis. In this case, factor layers needed to be available at 500 to 1000 m resolution (cell size). Hence, future spatial siting investigations accuracy to other study areas will depend on the data availability and quality. The analysis has considered cost-related criteria as factors, while other criteria, such as environmental and social impacts were considered as restrictions. Therefore, future work will

expand the analysis to include environmental and social impacts as factors and compare the results with this study outputs.

Logistic and infrastructure research to check these feasibilities to deploy future offshore wind farm on the suitable locations identified here for the Arabian Peninsula's countries. Foundations analysis did not apply the loads of fatigue limit state, thus, further fatigue effects analysis needed to test the cycle loading effects (from applying the predicted service wind, and waves) on the stability of the monopile foundations designed for the chosen sites in Egypt. In addition, the expected loads from extreme events for as long as the expected life cycle of the turbine will be studied.

Appendix A (Boreholes Logs)

Strata		Description	S.P.T	
Depth [m]	Legend		Depth [m]	N values
	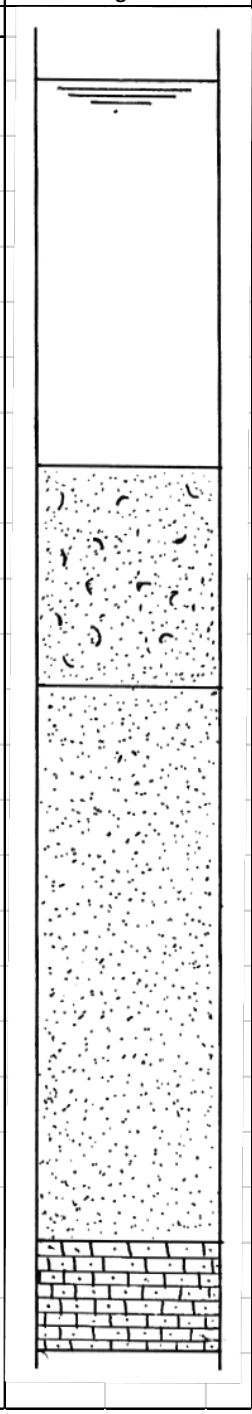			
0.00		Sea Water		
7.00		Grey medium dense sand, trace very fine crushed shells		
11.00		Yellow medium dense sand	11	12
			12	11
			13	13
			14	15
21.00		Very Dense Cemented sand	21	50
23.00		End of Boring 23.00 m		

Figure A-1: Boring log number 1 near site 1.

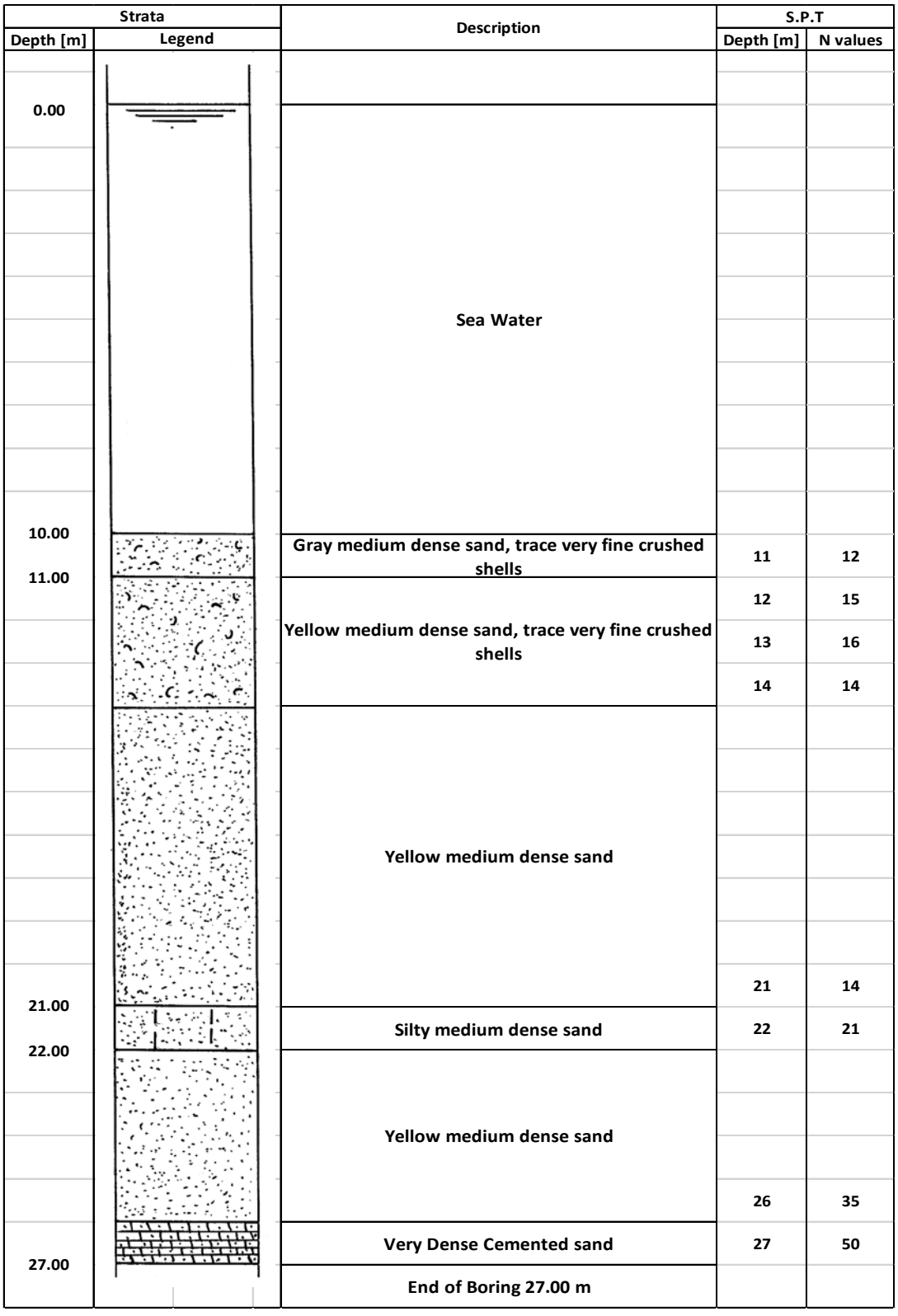

Figure A-2: Boring log number 2 near site 1.

Strata		Description	S.P.T	
Depth [m]	Legend		Depth [m]	N values
0.00	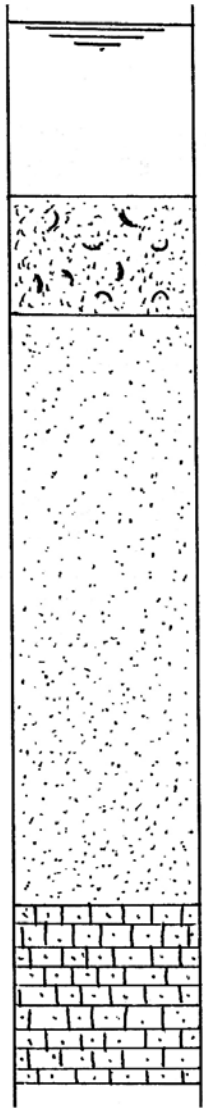			
		Sea Water		
3.00				
		Brown medium dense sand, trace very fine crushed shells	3	16
5.00			5	18
		Yellow medium dense sand	6	21
			7	21
			14	31
15.00			15	> 50
		Very Dense Cemented sand		
18.00			18	> 50
		End of Boring 18.00 m		

Figure A-3: Boring log number 3 near site 2.

Strata		Description	S.P.T	
Depth [m]	Legend		Depth [m]	N values
0.00	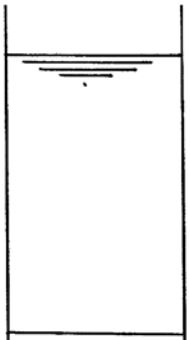	Sea Water		
5.00		Brown medium dense sand, trace very fine crushed shells	6	14
7.00	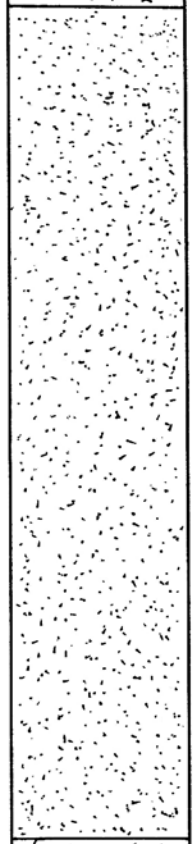	Yellow medium dense sand	7	15
			8	13
			9	15
			10	18
			11	22
			21	29
			22	35
22.00	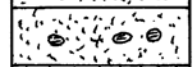	Yellow medium dense sand, pebbles of cemented sand	23	> 50
23.00	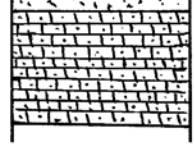	Very Dense Cemented sand		
25.00		End of Boring 25.00 m		

Figure A-4: Boring log number 4 near site 2.

Strata		Description	S.P.T	
Depth [m]	Legend		Depth [m]	N values
0.00	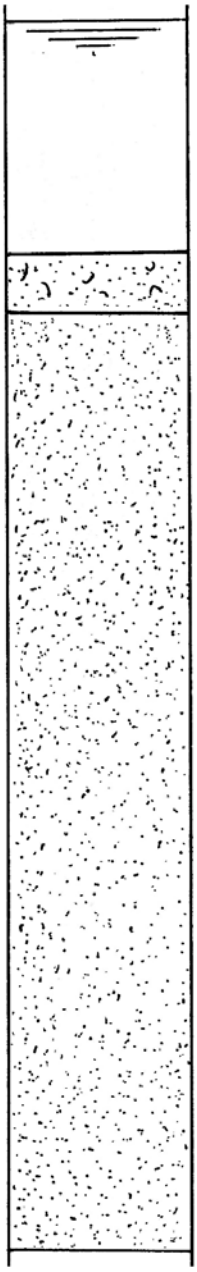			
		Sea Water		
4.00		White/Yellow coarse sand, trace very fine crushed shells	5	29
5.00		Yellow dense sand	6	31
			7	31
			8	35
			9	38
			10	39
			11	40
			12	41
			13	41
			22	47
			21	47
21.00		End of Boring 21.00 m		

Figure A-5: Boring log number 5 near site 3.

Appendix B (Sensitivity Analysis Tables)

Table B-1: Sensitivity test for the wind power factor

	Change %	-20%	-16%	-12%	-8%	-4%	0%	4%	8%	12%	16%	20%
Weight values of the factors	Wind	0.44	0.46	0.48	0.50	0.52	0.54	0.57	0.59	0.61	0.63	0.65
	Depth	0.29	0.28	0.27	0.26	0.25	0.24	0.23	0.21	0.20	0.19	0.18
	Soil	0.08	0.08	0.08	0.07	0.07	0.07	0.06	0.06	0.06	0.05	0.05
	Grid	0.05	0.05	0.05	0.05	0.05	0.04	0.04	0.04	0.04	0.04	0.03
	Shore	0.13	0.13	0.12	0.12	0.11	0.11	0.10	0.10	0.09	0.09	0.08
Number of cells	Unsuitable	20811	20989	22075	23484	24582	25630	27956	28957	30580	32811	36643
	Moderate	25391	25366	24632	23527	22605	21685	19512	18574	17014	14853	11033
	High suitablity	4315	4162	3810	3506	3330	3202	3049	2986	2923	2853	2841
Error %	Unsuitable	-18.8	-18.1	-13.9	-8.4	-4.1	0.00	9.1	13.0	19.3	28.0	43.0
	Moderate	17.1	17.0	13.6	8.5	4.2	0.00	-10.0	-14.3	-21.5	-31.5	-49.1
	High suitablity	34.8	30.0	19.0	9.5	4.0	0.00	-4.8	-6.7	-8.7	-10.9	-11.3

Table B-2: Sensitivity test for the water depth factor.

	Change %	-20%	-16%	-12%	-8%	-4%	0%	4%	8%	12%	16%	20%
Weight values of the factors	Wind	0.58	0.57	0.56	0.56	0.55	0.54	0.54	0.53	0.52	0.52	0.51
	Depth	0.19	0.20	0.21	0.22	0.23	0.24	0.25	0.26	0.27	0.28	0.28
	Soil	0.07	0.07	0.07	0.07	0.07	0.07	0.07	0.07	0.06	0.06	0.06
	Grid	0.05	0.05	0.05	0.04	0.04	0.04	0.04	0.04	0.04	0.04	0.04
	Shore	0.11	0.11	0.11	0.11	0.11	0.11	0.11	0.10	0.10	0.10	0.10
Number of cells	Unsuitable	26867	26474	26058	26370	25975	25630	25041	25588	26413	25752	25958
	Moderate	20605	20961	21349	21036	21385	21685	22169	21678	21003	21541	21420
	High suitablity	3045	3082	3110	3111	3157	3202	3307	3251	3101	3224	3139
Error %	Unsuitable	4.8	3.3	1.7	2.9	1.3	0.00	-2.3	-0.2	3.1	0.5	1.3
	Moderate	-5.0	-3.3	-1.5	-3.0	-1.4	0.00	2.2	0.0	-3.1	-0.7	-1.2
	High suitablity	-4.9	-3.7	-2.9	-2.8	-1.4	0.00	3.3	1.5	-3.2	0.7	-2.0

Table B-3: Sensitivity test for the distance to national grid factor.

	Change %	-20%	-16%	-12%	-8%	-4%	0%	4%	8%	12%	16%	20%
Weight values of the factors	Wind	0.55	0.55	0.55	0.55	0.55	0.54	0.54	0.54	0.54	0.54	0.54
	Depth	0.24	0.24	0.24	0.24	0.24	0.24	0.24	0.24	0.24	0.24	0.24
	Soil	0.07	0.07	0.07	0.07	0.07	0.07	0.07	0.07	0.07	0.07	0.07
	Grid	0.04	0.04	0.04	0.04	0.04	0.04	0.05	0.05	0.05	0.05	0.05
	Shore	0.11	0.11	0.11	0.11	0.11	0.11	0.11	0.11	0.11	0.11	0.11
Number of cells	Unsuitable	25369	25369	25369	25369	25369	25630	24738	24738	24738	24738	24738
	Moderate	21903	21903	21903	21903	21903	21685	22463	22463	22463	22463	22463
	High suitablity	3245	3245	3245	3245	3245	3202	3316	3316	3316	3316	3316
Error %	Unsuitable	-1.0	-1.0	-1.0	-1.0	-1.0	0.00	-3.5	-3.5	-3.5	-3.5	-3.5
	Moderate	1.0	1.0	1.0	1.0	1.0	0.00	3.6	3.6	3.6	3.6	3.6
	High suitablity	1.3	1.3	1.3	1.3	1.3	0.00	3.6	3.6	3.6	3.6	3.6

Table B-4: Sensitivity test for the distance to shoreline factor.

	Change %	-20%	-16%	-12%	-8%	-4%	0%	4%	8%	12%	16%	20%
Weight values of the factors	Wind	0.56	0.56	0.55	0.55	0.55	0.54	0.54	0.54	0.54	0.53	0.53
	Depth	0.24	0.24	0.24	0.24	0.24	0.24	0.24	0.23	0.23	0.23	0.23
	Soil	0.07	0.07	0.07	0.07	0.07	0.07	0.07	0.07	0.07	0.07	0.07
	Grid	0.04	0.04	0.04	0.04	0.04	0.04	0.04	0.04	0.04	0.04	0.04
	Shore	0.09	0.09	0.09	0.10	0.10	0.11	0.11	0.12	0.12	0.12	0.13
Number of cells	Unsuitable	27268	27268	27528	26409	26409	25630	25630	25193	25193	25443	24443
	Moderate	20133	20133	19916	20954	20954	21685	21685	22118	22118	22013	22803
	High suitablity	3116	3116	3073	3154	3154	3202	3202	3206	3206	3161	3271
Error %	Unsuitable	6.4	6.4	7.4	3.0	3.0	0.00	0.0	-1.7	-1.7	-0.7	-4.6
	Moderate	-7.2	-7.2	-8.2	-3.4	-3.4	0.00	0.0	2.0	2.0	1.5	5.2
	High suitablity	-2.7	-2.7	-4.0	-1.5	-1.5	0.00	0.0	0.1	0.1	-1.3	2.2

Appendix C (UK's Attribute Tables)

Table C1: Attribute tables for the three sets of the UK's offshore wind areas.

Set a. Round 1 and 2			Set b. Round 3 all operating			Set c. Round 3		
ID	Suitability Value [x 100]	Cells Count	ID	Suitability Value [x 100]	Cells Count	ID	Suitability Value [x 100]	Cells Count
1	41	140	1	40	215	1	42	163
2	42	129	2	41	429	2	43	236
3	44	49	3	42	314	3	44	417
4	45	110	4	43	297	4	45	471
5	46	882	5	44	438	5	46	675
6	47	61	6	45	240	6	47	423
7	48	354	7	46	1081	7	48	113
8	49	65	8	47	240	8	49	380
9	50	81	9	48	267	9	50	1244
10	51	23	10	49	104	10	51	2981
11	52	44	11	50	396	11	52	5343
12	53	4	12	51	664	12	53	7656
13	54	109	13	52	887	13	54	23030
14	56	106	14	53	727	14	55	38889
15	57	7	15	54	2190	15	56	37240
16	59	389	16	55	5117	16	57	43640
17	60	617	17	56	4553	17	58	42704
18	61	1120	18	57	3542	18	59	36686
19	62	1264	19	58	4324	19	60	32195
20	63	1020	20	59	4672	20	61	42883
21	64	1002	21	60	4692	21	62	43159
22	65	2052	22	61	6844	22	63	44510
23	66	2854	23	62	8619	23	64	62563
24	67	3736	24	63	13518	24	65	54082
25	68	3165	25	64	26100	25	66	32675
26	69	5418	26	65	35765	26	67	46389
27	70	3887	27	66	11893	27	68	13139
28	71	1798	28	67	12573	28	69	10860
29	72	1117	29	68	8702	29	70	13526
30	73	781	30	69	10447	30	71	19247
31	74	529	31	70	12728	31	72	17132
32	75	652	32	71	16562	32	73	1347
			33	72	13023			
			34	73	1703			
	Moderate Suitability		35	74	185			
	High Suitability		36	75	95			

Appendix D (Published Papers)

1- Multi Criteria Decision Analysis for Offshore Wind Energy Potential in Egypt
Paper type: Journal Paper
Status: Published
Date of publishing: April 2018
Place of publishing: Renewable Energy Journal

2- ASSESSMENT OF THE OFFSHORE WIND ENERGY POTENTIAL AROUND THE RED SEA, KSA
Paper type: Conference Paper
Status: Published and will be present on SWC2017 conference in Abu Dhabi, United Arab Emirates (UAE).
Date of publishing: 29 OCT 2017
Place of publishing: Solar World Congress 2017 conference

3- Selection and Design of Offshore Wind Turbine Foundations for the Red Sea Area – Egypt
Paper type: Conference Paper
Status: Published and was present on SET2017 conference in, Bologna, Italy
Date of publishing: 20 JULY 2017
Place of publishing: SET 2017 conference

4- New approach to determine the Importance Index for developing offshore wind energy potential sites: Supported by UK and Arabian Peninsula case studies
Paper type: Journal Paper
Status: Published
Date of publishing: June 2020
Place of publishing: Renewable Energy Journal

Renewable Energy 118 (2018) 278–289

Contents lists available at ScienceDirect

Renewable Energy

journal homepage: www.elsevier.com/locate/renene

Multi criteria decision analysis for offshore wind energy potential in Egypt

Mostafa Mahdy*, AbuBakr S. Bahaj

Sustainable Energy Research Group, Energy & Climate Change Division, Faculty of Engineering and the Environment, University of Southampton, SO17 1BJ, United Kingdom[1]

ARTICLE INFO

Article history:
Received 19 April 2017
Received in revised form
7 November 2017
Accepted 10 November 2017
Available online 10 November 2017

Keywords:
Offshore wind
Suitability maps
GIS
MCDA
Red Sea
Egypt

ABSTRACT

Offshore wind energy is highlighted as one of the most important resource to exploit due to greater wind intensity and minimal visual impacts compared with onshore wind. Currently there is a lack of accurate assessment of offshore wind energy potential at global sites. A new methodology is proposed addressing this gap which has global applicability for offshore wind energy exploitation. It is based on Analytical Hierarchy Process and pairwise comparison methods linked to site spatial assessment in a geographical information system. The method is applied to Egypt, which currently plan to scale renewable energy capacity from 1 GW to 7.5 GW by 2020, likely to be through offshore wind. We introduce the applicability of the spatial analysis, based on multi-criteria decision analysis providing accurate estimates of the offshore wind from suitable locations in Egypt. Three high wind suitable areas around the Red Sea were identified with minimum restrictions that can produce around 33 GW of wind power. Suitability maps are also included in the paper providing a blueprint for the development of wind farms in these sites. The developed methodology is generalised and is applicable globally to produce offshore wind suitability map for appropriate offshore wind locations.

1. Introduction

Most of onshore wind farms are located in the best resource areas. The exploitation of further land-based onshore areas in many countries is currently impeded due to visual impacts, threats to birdlife, public acceptance, noise and land use conflicts [1]. All these conflicts are likely to hinder future development of onshore wind farm deployment [2–4]. Hence, most major developments world-wide have now shifted towards offshore wind where the resource is high, and less likely to be affected by the drawbacks of land-based wind farms mentioned earlier. The advantage of offshore wind is that despite being 150% more costly to install than onshore wind, the quality of the resources is greater as is the availability of large areas to build offshore wind farms (OWFs). Furthermore, scaling up is likely to result in cost reductions propelling offshore wind on a trajectory that will be on par with onshore wind in the future [5].

However, to our knowledge, there is no general approach to accurately assess wind resources. This work provides a new methodology to address this lack of knowledge which has global applicability for offshore wind energy exploitation. It is based on Analytical Hierarchy Process (AHP) defined as an organised process to generate weighted factors to divide the decision making procedure into a few simple steps and pairwise comparison methods linked to site spatial assessment in a Geographical Information System (GIS). GIS based multi-criteria decision analysis (MCDA) is the most effective method for spatial siting of wind farms [6]. GIS-MCDA is a technique used to inform decisions for spatial problems that have many criteria and data layers and is widely used in spatial planning and siting of onshore wind farms. GIS is used to put different geographical data in separate layers to display, analyse and manipulate, to produce a new data layers and/or provide appropriate land allocation decisions [7]. The MCDA method is used to assess suitability by comparing the developed criteria of the alternatives [8]. The alternatives are usually a number of cells that divide the study area into an equally dimensioned grid. The most popular and practical method to deploy MCDA is the *Analytical Hierarchy Process* (AHP). AHP was defined as an organised process to generate weighted factors to divide the decision making procedure into a few simple steps [9]. Each criterion could be a factor or a constraint. A *factor* is a criterion that increases or decreases the

* Corresponding author.
E-mail address: m.mahdy@soton.ac.uk (M. Mahdy).
[1] www.energy.soton.ac.uk

https://doi.org/10.1016/j.renene.2017.11.021

suitability of the alternatives, while a *constraint* approves or neglects the alternative as a possible solution. AHP has two main steps: "Pairwise" comparison and *Weighted Linear Combination* (WLC). Pairwise comparison method is used to weight the different factors that are used to compare the alternatives [9] while WLC is the final stage in AHP evaluating the alternatives [10].

In order to establish a pathway for exploiting offshore wind resources, a systematic analysis for such exploitation is needed and this is at the core of this work. Our aim is to address the paucity of generalised modelling to support the exploitation of offshore wind energy. In order to do this, this work will utilise a countrywide case study where the developed methodology will be used to investigate the wind energy potential, specify appropriate locations of high resources with no imposed restrictions and generate suitability maps for offshore wind energy exploitation. The development methodology will appropriately identify the essential criteria that govern the spatial siting of offshore wind farms.

The work is structured as follows: in the first section we develop the literature review further, followed by the detailed methodology considerations, description of Egyptian offshore wind, analysis and criteria followed by detailed results and discussion and then conclusions.

2. Relevant literature

GIS based MCDA is widely used in the spatial planning of onshore wind farms and siting of turbines. Below are highlights of some of the literature for these methods and Table 1 provides a brief comparison between the relevant approaches discussed in the literature.

In a study of onshore wind farm spatial planning for Kozani, Greece, sufficient factors and constraints were used to produce a high-resolution suitability map with grid cell (150 by 150 m) [11]. The study focussed on three different scenarios: (a) scenario 1 were all factors are of equal weight, (b) scenario 2, environmental and social factors have the highest weights, and (c) scenario 3, technical and economic factors have more weights than other factors. It was found that more than 12% of the study area has a suitability score greater than 0.5 i.e. suitable for wind farms, and all previously installed wind farms were located in areas with a high suitability score, which emphasised and validated their results. Their suitability map was found to be reliable by stakeholders and was used to inform the siting of new wind farms in Greece. However, in our opinion, scenario 1 is unrealistic, because normally factors normally have different relative importance.

A further study elucidated the methodology for choosing a site for new onshore wind farms in the UK, taking the Lancashire region as a case study [15]. In order to identify the problems and the different criteria involved, the authors undertook a public and industrial sector survey (questionnaire) soliciting community/stakeholders' views on wind farms. From the survey results, they constructed their own scoring matrix from 0 to 10 to standardise the different criteria and then used two scenarios to calculate suitability. In scenario 1 the same weight was assigned to all criteria, while in scenario 2 the criteria were divided into 4 grades. Pairwise comparisons to weight the grades were used. The study then aggregated the criteria producing two different maps. The results showed that roads and population areas had the dominant influence on the final decision and the available area for wind farms represented only 8.32% of the total study area. The study is advanced and accurate despite the fact that it was performed in 2001. However, the fact that they scale the "distance to roads factor" from 1 to 0, without applying the same scaling to the other factors will have implications on the accuracy the final results.

Another research group [12] addressed suitable sites for wind farms in Western Turkey. They found the satisfaction degree for a 250 m by 250 m grid cells, using environmental and social criteria such as noise, bird habitats, preserved areas, airports, and population areas, as well as wind potential criterion. Cells that had satisfaction degree >0.5 in both environmental objectives and wind potentials were designated as a priority sites for wind farms. The study produced a powerful tool to choose new locations for wind farms.

A completed spatial planning [13] study was performed to site new wind farms in Northern Jutland in Denmark. This included most criteria to arrive at a suitability score for grid cell of 50 by 50 m. Although the research is well presented, the method used to weight the factors was not indicated and the weight values were absent. Hence, it is difficult to ascertain from the final suitability map the methodology used to reach the conclusion.

Rodman and Meentemeyer [14], developed an approach to find suitable locations for wind farms in Northern California in the USA. They considered a 30 by 30 m grid and used a simpler method to evaluate alternatives which only included 3 factors - wind speed, environmental aspects, and human impact. The factors were scored on a scale from unsuitable = 0 to high suitability = 4, based on their own experience to judge the factors. They then weighted the three factors by ranking them from 1 to 3, to arrive at final suitability. The suitability map was created by summing the product of each scored factor and its weight, and dividing the sum on the weights summation. Although the method was simple, their results could have been greatly improved in terms of accuracy and applicability had they used the AHP method and considered other important factors such as land slope, grid connection, and land use.

In the UK, for the offshore wind competition "Rounds", a Marine Resource System (MaRS), based on a GIS decision-making tool was used to identify all available offshore wind resources [16]. After successfully completing Rounds 1, and 2 of the competition, the tool was used to locate 25 GW in nine new zones for Round 3. The MaRS methodology had 3 iterations (scenarios): (i) it considered many restrictions taking advantages of the datasets from Rounds 1 and 2. The study excluded any unsuitable areas for wind farms, then weighted the factors depending on their expertise from previous rounds, (ii) the same as the first iteration but included stakeholder input, and (iii) alligning Round 3 zones with the territorial sea limits of the UK continental shelf. The Crown Estate responsible for these projects did not publish details of the methodology used stating only the criteria and the scenarios used in the spatial sitting process. Capital cost was taken into account in the above studies of offshore wind [17]. The work indicated that the use of MCDM in offshore wind is rare as it is primarily used in onshore wind studies. Nevertheless, two different maps were created assuming all factors were of the same weight. A Decision Support System, which is an MCDM programme based on GIS tools was used [17].

Constraints were only used in the study of an offshore wind farms (OWF) in Petalioi Gulf in Greece [18]. The work excluded all unsuitable areas in the Gulf using the classical simple Boolean Mask, and then estimated the total capacity as being around 250 MW using the available wind speed data. It was apparent that the old Boolean Mask technique was used due to the limited area of the authors' study area (70 km^2), which makes the application of many criteria to locate one OWF difficult. Another study was conducted to measure offshore wind power around the Gulf of Thailand, using only four factors with no constraints [19]. The authors used their own judgment to weight the factors, and then used ArcGIS to select the suitable location for their study area. The work is detailed with appropriate charts. However, using only factors without considering constraints is likely to affect the accuracy of results. Further research to produce a suitability map for offshore wind areas around the UK was also undertaken but was biased

Table 1
Comparison between the different onshore and offshore wind siting studies and this study.

Location, year	Constraints	Factors	Method	Aggregate Method
Greece [11], 2015	• Buffer exclusion zones (between 0.15 and 3 km) for: Protected areas, historical sites, airports, urban areas, tourism sites, roads, farms, other sites • wind < 4.5 m/s and Slope >25%	• Slope • Wind speed • land uses • Distance from roads, national parks, tourism facilities, and historical	Pairwise Comparison	WLC
Western Turkey [12], 2010	• Buffer exclusion zones (between 0.25 and 2.5 km) for: Natural Parks, town centres, airports, bird habitats, and noise	• The same criteria as constraints but calculating the distance after the end of the buffer zone, and Wind Speed	RIM	OWA
Northern Jutland, Denmark [13], 2005	• Protected nature • Bird protection • Protected wetlands	• Wind speed • Proximity to: Coast, forests, population areas, water streams, lakes, roads, grid lines, and airports	fuzzy membership	WLC
Northern California, USA [14], 2006	N/A	• Wind speed, Environment, Human impact	Abundance rank	Classic aggregation
Lancashire, UK [15], 2001	• More than 10 km to roads and national grid • Wind < 5 m/s - Slope > 10% • Buffer exclusion zones (between 0.4 and 2.0 km) for: population, Forests, Water streams, and national parks	• Land use • Distance to roads • Population zones • Distance to importance sites • Distance to natural parks • Slope	Pairwise Comparison	WLC
The UK [16], 2012	Shipping Routes, Ports, Military zones, Natural Parks, Cables and pipe lines, Fishing areas, Oil and gas extraction Areas, Existing or planned farms, Sand Mining, protected wrecks, tunnels, and seascape	• Bathymetry, soil properties, wind intensity, distance to shore, and distance to Grid	Not defined	Not defined
The North Sea [17], 2012	Shipping Routes, Ports, Military zones, Natural Park, Cables and pipe lines, Fishing areas, Oil and gas extraction Areas, Existing or planned farms, Sand Mining, Storm surge, Wave height, and tidal range,	• Bathymetry, soil properties, wind intensity, distance to shore, distance to grid, and cost limit	Not defined	Not defined
Petalioi Gulf [18], 2013	Shipping Routes, Ports, Military zones, Natural Park, Cables and pipe lines, Fishing areas, Oil and gas extraction Areas	N/A	Boolean Mask	Boolean Mask
Gulf of Thailand [19], 2015	Wind speed, water depth, distance from shore, and distance to grid.	N/A	Not defined	Not defined
Black Sea, Turkey [20], 2017	• Wind speed	• territorial waters, military areas, civil aviation, shipping routes, pipelines and underground cables	–	–
The UK [21], 2016	• Bathymetry, wind speed, distance to shore.	• Exclusion areas identified by the Crown State	Cost modelling	LCOE
Egypt [This paper]	• Shipping Routes, Ports, Military zones, Natural Park, Cables and pipe lines, Fishing areas, and Oil and gas extraction Areas	• Bathymetry, soil properties, wind Intensity, Distance to shore, and distance to Grid	Pairwise Comparison	WLC

towards cost modelling [21]. The analysis was mainly based on data obtained from the UK Crown Estate using specific Crown Estate restrictions, weights and scores. The difference between this study and other offshore wind sitting studies is that authors used the overall Levelised Cost of Energy (LCOE) equation to aggregate factors. They produce two maps, one for restrictions (energy available map) and another for factors (cost map/MWh).

3. Approach utilised in siting of wind farms

Offshore and onshore wind spatial planning can be based on similar techniques, particularly when considering the wind speed factor. However, these techniques differ in terms of definitions of factors and constraints. For example, the main factors in onshore wind considerations are distance to roads and the proximity of farms to built-up areas, whereas for offshore wind, the factors are water depth and wind speed where the wind speed cube is proportional to power production. In most of the studies reviewed here as well as others not included, the approach taken for determining wind farm spatial planning can be summarised as follows:

1. Identify wind farm spatial characteristics and related criteria using APH or similar techniques.
2. Standardise different factors using fuzzy membership or some own-derived judgment.
3. Weight the relative importance of the various factors using pairwise comparison or similar methods.
4. Aggregate the different layers of factors and constraints using different GIS tools and WLC aggregation method.

As mentioned earlier, AHP is a technique used to organise and create weighted criteria to solve complex problems. The first step of AHP is to define the problem and the branch of science it relates to, and then specify the different criteria involved. All the criteria should be specific, measurable, and accepted by stakeholder/researcher or previously used successfully in the solution of similar problems. The next step in the analysis is to find the different relative importance of the factors. The final step is to evaluate all the potential solutions for the problem, and arrive at a solution by selecting the one with highest score. In Fig. 1, we illustrate the whole AHP process used in this study.

Two efficient ways to solve a multi criteria problem were suggested by Ref. [9]. The first is to study the problem and its characteristics, then arrive at specific conclusions through the different observations undertaken by the study. The second is to compare a specific problem with similar ones that have been solved

previously. In this work, we have selected the second approach to define the criteria required and this could be a factor or a constraint.

Due to its dominant applicability in spatial decision-making problems, the pairwise comparison method was chosen to find the relative importance. Furthermore, factors have different "measuring" and "objecting" units, so there is a need to unify all factors to the same scale. In order to standardise the processes, a continuous scale suggested by Ref. [22] from 0 to 1 with 0 for the least suitable measure and 1 for the most suitable factor, which is named as the "Non-Boolean Standardisation". The scale should be used with different fuzzy functions because not all the factors act linearly.

In our AHP analysis, we used the Pairwise Comparison method to weight the different factors developed in Refs. [9,23]. The intensity of importance definitions and scales used to indicate pairwise comparisons between factors are the same as those used in Ref. [9]. That is starting with a score of 1 for a pair where both factors are of equal importance and ending with 9 to score a pair wherein the first factor is of extreme importance compared to the other. The intensity of importance can be chosen using personal judgment, experience, or knowledge. The process is accomplished by building the pairwise comparison matrix (see e.g. Table 5), which has equal rows and columns, the number of rows (columns) equal to the number of the factors. If the factor in the left side of the matrix has higher importance compared to the top side factor, the matrix relevant cell will assume the value assigned in the scale of intensity of importance. In the opposite case, the cell will equal the inverse of the scale value. A new normalised matrix can be created by taking the sum of every column and then dividing each matrix cell by its total column value. Finally, the weight of each factor is equal to the average of its row in the new matrix. The aggregation of all factor weights equals to one (see Tables 5 and 6 below).

Consistency Ratio (CR) was suggested by Ref. [23] to validate the pairwise comparison assumptions: any matrix with CR greater than 0.1 should be rectified. CR is given by: CR = CI/RI; where RI is the Random Consistency Index, and its value depends on the factor number n, RI values adopted from Ref. [23]. CI is the Consistency Index given by: CI = (λ_{max} - n)/(n - 1); where λ_{max} is the Principal Eigen value, equals to the product of factor weight and the summation of its column in the pairwise matrix.

WLC is the last step in AHP to find the optimal solution. The WLC method combines the standardised factors after multiplying each factor by its weight and finally multiplying the result map with a Boolean mask produced by multiplying all the constraints together. The resultant map is called the Suitability Map. The WLC equation [10], used to calculate the suitability map is given by:

$$Suitability = \left(\sum_{i=1}^{n} W_i X_i\right) \times \left(\prod_{j=1}^{l} C_j\right) \quad (1)$$

where W_i = weight assigned to factor i, X_i = criterion score of factor i, n = number of factors, C_j = constraint j (Boolean Mask j), Π = product of constraints, and ℓ = no. of constraints.

WLC used in parallel with Boolean overlay, in which Boolean relationships such as ("And", "OR", or "Not") are applied to achieve a specific decision with "0 or 1" as a result value. In this work, a combination of the approaches discussed above such as (AHP, pairwise comparison, standardised scale, WLC, and Boolean overlay) were used. These provided the basis to develop the models into two software packages - Microsoft® EXCEL, (used to complete pairwise process), and ArcGIS, (used to configure, design, input, manage, display, manipulate, digitise, and for analysis of the spatial data).

After reviewing the information in the literature contained in Refs. [11–20], the identified and appropriate constraints for our methodology are as follows: Shipping Routes, Ports, Military Zones, Natural Park, Cables and Pipe Lines, Fishing Areas, and Oil and Gas Extraction Areas. The factors are: Bathymetry, Soil Properties, Wind Intensity, Distance to Shore, and Distance to Grid. These are listed in Table 2 where more detailed definitions and limitations of the different factors and constraints used in this methodology are given. The analytical methods are Pairwise Comparison and WLC.

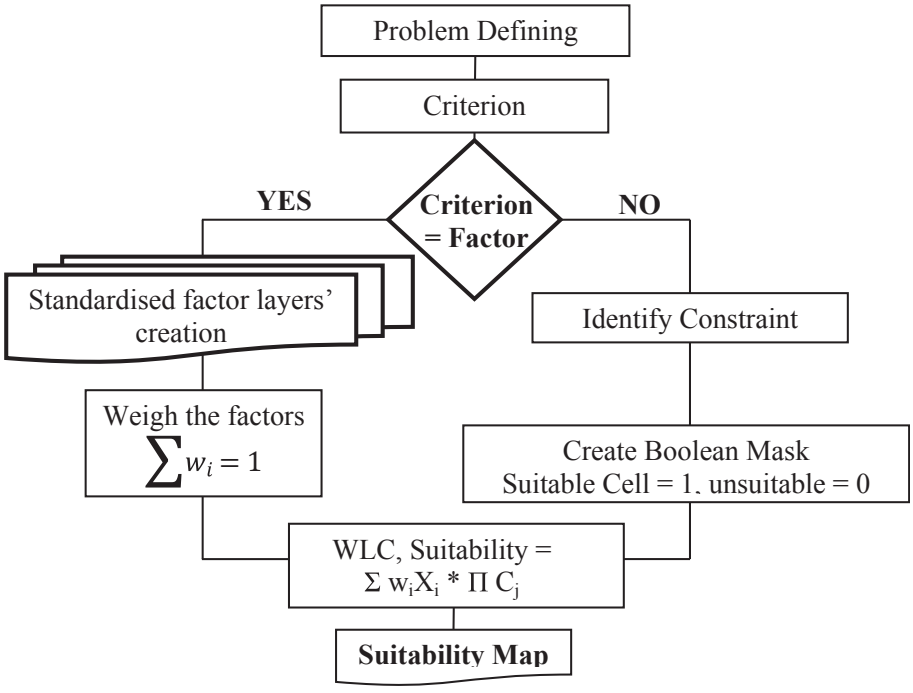

Fig. 1. Diagrammatic representation of the AHP process.

Table 2
Criteria definitions and optimisation needed for locating offshore wind farms. Where F is a factor and C is a constraint.

Criteria	Description	Unit	Optimisation	Type (F/C)
Wind	Energy of the wind	W/m^2	Identify areas with wind resource, between 45 and 850 W/m^2	F
Water depth	Water depth in selected area of the sea	m	Identify areas with depth between 5 and 60 m	F
Cables	Submerged cable paths.	–	Avoid	C
Oil	–	–	Avoid	C
Parks	Legally protected areas to preserve endangered marine ecosystem	–	Avoid	C
Shipping Routes	Ships/vessels movement routes	–	Avoid	C
National Grid	Length between the cell and national grid.	m	Choose places closer to the grid	F
Military Areas	Identified by military defence authorities.	–	Avoid	C
Soil	Determined by borehole tests - status, type and depth of soil	m	Choose sites with sandy sediment layer closer to the seabed.	F
Distance to shore	Distance to shoreline	m	1.5–200 km to shore, to reduce cable cost	F
Fishing areas	Areas determine by the authorities for fishing.	–	Avoid	C

4. Case study: Egypt energy and offshore wind

In order to apply the above approach for offshore wind farm sitting, we have identified Egypt as an appropriate case study. This is due to its unique location between two inner seas, its huge need for renewable energy, and wind data availability (Egypt is the only country in the Middle East that has a detailed wind atlas).

4.1. Energy needs in Egypt

Egypt has approximately 3000 km of coastal zones situated on the Mediterranean Sea and the Red Sea (Fig. 2). Approximately 1150 km of the coast is located on the Mediterranean Sea, whilst 1200 km is bordered by the Red Sea with 650 km of coast located on the Gulf of Suez and Aqaba [24]. According to the 2014 census, the population of Egypt was estimated to be around 90 million, 97% of which live permanently in 5.3% of the land mass area of Egypt [25]. Egypt's electricity consumption is increasing by around 6% annually [26]. Within a five-year period, the consumption has increased by 33.7%, which was delivered by a 27% increase in capacity for a population increase of only 12% during this period (Table 3). Until 1990, Egypt had the ability to produce all its electricity needs from its own fossil fuel and hydropower (High Aswan Dam) plants. However, in recent years, due to a combination of population increase and industrial growth, the gap between production and consumption has widened greatly [27].

The Egyptian New and Renewable Energy Authority (NREA) estimates that energy consumption will be double by 2022 due to population increase and development [29]. The Egyptian government is currently subsidising the energy supply system to make electricity affordable to the mostly poor population [27]. Such subsidies create an additional burden on the over-stretched Egyptian economy. The budget deficit in 2014/2015 was 10% of GDP accompanied by a "high unemployment rate, a high poverty rate, and a low standard of living" [30]. The projected increase in energy consumption will undoubtedly lead to more pollution such as CO_2 emissions, as increased capacity will be derived from greater consumption of fossil fuels.

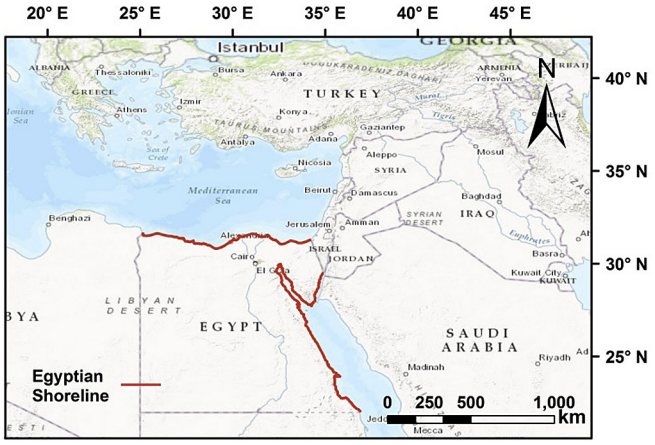

Fig. 2. Study area map, Egypt is shaded in red, the map adopted from Ref. [28].

Wind and solar resources are the main and most plentiful types of renewable energy in Egypt. In 2006, and in order to persuade both the public and the public sectors to invest in renewable energy, NREA conducted a study which emphasised that Egypt is a suitable place for wind, solar, and biomass energy projects [29]. The study urged the Egyptian government to start building wind farms, and the private sector to develop smaller projects to generate solar and biomass energy [29]. Egypt aims to produce 20% of its electricity needs from renewable energy by 2020 with approximately 12% derived from wind energy. Onshore wind currently supplies only 1.8% of the Egyptian electrical power and there are no offshore wind farms. Without more and urgent investments in wind energy, there is an increased possibility that the 2020 target will be pushed back to 2027 [26].

The first action taken by the Egyptian government towards generating electricity from wind was the creation of the Egyptian Wind Atlas [31]. This was followed by installation of the Za'afarana onshore wind farm, which has 700 turbines and a total capacity of 545 MW. The monthly average wind speed at this farm is in the range 5–9 m/s. The government is now planning to develop three more wind farms at different sites in Egypt [32]. As indicated earlier, all wind energy in Egypt is currently generated onshore, and the emphasis now is to scale up capacity from the current 1 GW–7.5 GW by 2027 [33], by going offshore where the wind resource is much higher.

Due to its geographical location, Egypt (for its size) has one of the largest offshore wind potentials in the world [34]. The Red Sea region has the best wind resource, with a mean power density, at 50 m height, in the range 300–800 W/m^2, at mean wind speed of 6–10 m/s. Egypt's offshore wind potential in the Mediterranean Sea is estimate to be around 13 GW. For a relatively small land footprint, this resource is large when compared with, for example, the estimated total offshore wind resource for much larger countries such as the USA with 54 GW potential [35].

As previously indicated, Egypt is currently experiencing serious electricity shortages due to ever-increasing consumption and the lack of available generation capacity to cope with demand [29]. In many instances, power blackouts occur many times a day [30]. In order to cope with the demand and provide sustainable energy, the Egyptian government embarked on a programme to produce electrical power from onshore wind. To date, however, only a small number of wind farms are in production with a total capacity of

Table 3
Egypt Yearly Peak Load (YPL) [26], population [25], and electricity consumption [26].

Year	2008	2009	2010	2011	2012	2013	2014	2015	2016
YPL (GW)	19.74	21.33	22.75	23.47	25.71	27.00	26.14	28.02	29.2
Population (millions)	77.4	79.1	81.7	83.3	85.9	88.1	92.8	96.3	99.8
Consumption (TWh)	106.6	111.7	118.9	125.2	134.1	140.3	143.6	146.7	149.2

around 1 GW, which is not sufficient to support the ever-increasing demand [29]. In order to alleviate power shortages, offshore wind can play a major part in this respect as the resource is vast and its exploitation will increase capacity thereby alleviating shortages. Investment in offshore wind will also benefit economic development of the country and will reduce pressure on land areas where wind speeds are high but are of greater commercial importance for recreation and tourism [34].

4.2. Previous wind energy studies in Egypt

To date and to the authors' knowledge, there have been no detailed studies conducted to explore offshore wind energy potential in Egypt. The only available literature consists of few studies on onshore wind. For example, the economic and the environmental impact of wind farms was assessed by Ref. [36] using a Cost-Benefits Ratio. It concluded that Za'afarana along the Red Sea coast was the most suitable site in Egypt for onshore wind farms. A "road map for renewable energy research and development in Egypt" was produced by Ref. [37], which emphasised that wind energy is the most suitable renewable energy source for Egypt particularly for technology positioning and market attractiveness. The first survey to assess the wind energy potential in Egypt used 20-year old data from 15 different locations to estimate the wind energy density at 25 m height and the mean wind power density [38]. It estimated the magnitude of the wind energy density to be in the range 31–500 kWh/m^2/year and the power density in the range of 30–467 W/m^2. The study concluded that the Red Sea and the Mediterranean Sea, plus some interior locations (Cairo, Aswan, El-Dabah, and El-Kharga) were the most suitable locations for onshore wind farms.

Many studies presented a set of analyses that covered the land areas adjacent to the Red Sea and the Mediterranean Sea coasts [33,39–43], as well as some interior locations around Cairo and Upper Egypt [44,45]. Small size (100–200 kW capacity) wind farms are a suitable solution for the isolated communities in the Red Sea coast and 1 MW capacity farms are appropriate for the northern Red Sea coast area which could be linked to the Egyptian Unified Power Network [46]. The "Wind Atlas of Egypt", which took nearly 8 years to complete, was the only institutional effort [31].

As can be seen from the above, there is a gap in addressing the wind renewable energy resource in Egypt, and especially offshore wind. Our additional aim is to address this gap through systematic analysis based on well-understood approaches developed for other global sites.

5. Analysis

In order to establish a pathway for exploiting the offshore wind resource, systematic analysis for such exploitation is needed and this is one of the reasons Egypt was used as the case study for the methodology. Additionally, the work will also address the paucity of knowledge on offshore wind energy in Egypt. In order to test our proposed methodology outlined above, the analysis for the case study will investigate the wind energy potential, specify appropriate locations of high resources with no imposed restrictions and generate suitability maps for offshore wind energy exploitation. It will also identify the needed criteria that govern offshore wind farms spatial siting.

5.1. Criteria identifying

In accordance with Egyptian conditions, all criteria that affect the cost will be considered, in addition to two added environmental restrictions. All criteria in Table 2 are included except for fishing areas constraints. According to Egyptian law 124 (1983) the allowed depth for large fishing vessels is more than 70 m [47]. In addition, fishing using simple techniques noted unlikely to interfere with offshore-submerged cables [48]. Hence fishing activities around Egypt will have no effect on OWF locations which will operate at maximum depths of 60 m.

5.2. Spatial data accumulation and processing

A map layer in ArcGIS was created for each the criterion using the available and relevant spatial data. Wind power data was derived from the "Wind Atlas for Egypt" [31]. A shape file of the land cover of Egypt was created and was used as a base map. To represent the wind power map as a layer in the ArcGIS, the Georeferencing Tool using geographical control points was used to produce a map image. The power density areas contours were then entered as a shape features. Finally, the shape feature was converted to a raster file with cell size (x, y) = (0.8, 0.8) km, the Geographic Coordinate System used was "GCS_WGS_1984", (Fig. 3).

The bathymetry data (in raster form) for both the Red and Mediterranean Seas was adopted from the British Oceanographic Data Centre [49]. Fig. 4 shows the topography of Egypt raster map in meters. Later on, we will apply a Boolean mask to eliminate levels above −5 m. In Egypt, tunnels exist only in Cairo, and beneath the Suez Canal, according to the National Authority for Tunnels [50]. Therefore there is no need to account for tunnel data in the sea. Undersea cables locations were extracted from the Submarine Cable Map web [51]. Fig. 5 shows the raster map for these cables and additionally depicts other parameter determined by the analysis.

In Egypt, Law number 20 (1976) [52], permits the establishment of offshore structures in areas preserved for future excavation or mining but for safety reasons, a restricted buffer zone of 1 km was created around present and future offshore oil and gas wells. Data for these areas and restrictions adopted from Ref. [53] are shown in Fig. 5. Under Law number 102 (1983) [48], 30% of the Egyptian footprint, encompassing 30 regions, were declared as Nature Reserves. The Sea Marine Nature Reserves represent nine such areas with seven located in the Red Sea, and the others located in the Mediterranean Sea. The locations and dimensions of the reserves were established from the official web site of the Egyptian Environmental Affairs Agency [48]. The data processing was conducted in the same way as the wind power density layer and the resultant raster map is shown in Fig. 5.

The shipping routes around Egypt were determined from the ship density maps of marine traffic for the period 2013-14 [54]. Ports and approach channels areas were identified from the Marine Traffic and Maritime Transport Authority of Egypt [55]. The GIS

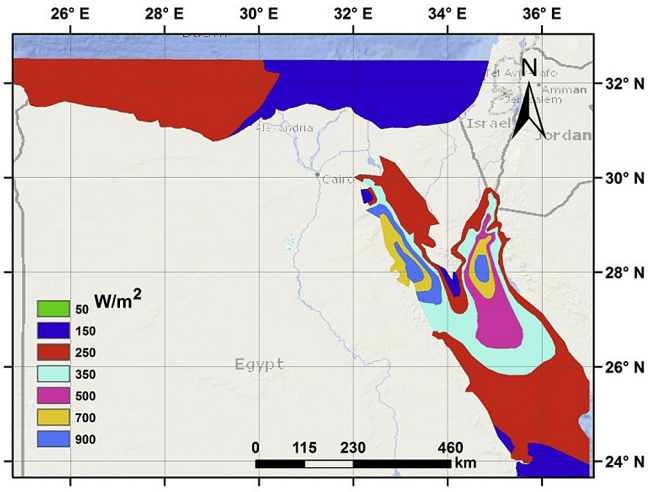

Fig. 3. Digitized map layer of the wind power density over the sea 'areas only, the wind power density was calculated over a 50 m height.

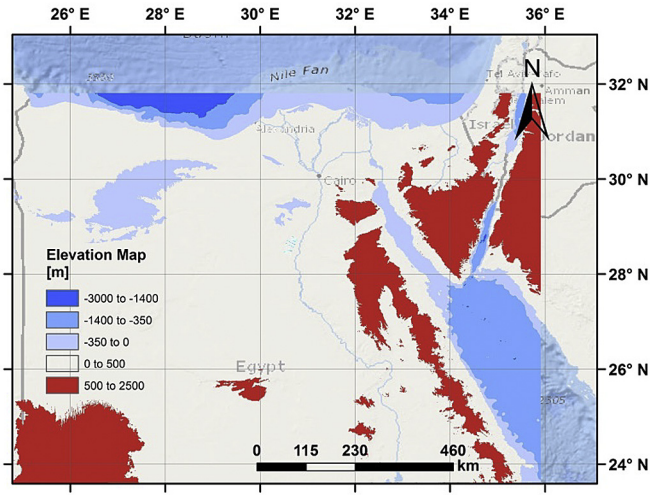

Fig. 4. Topography and bathymetry raster map of Egypt.

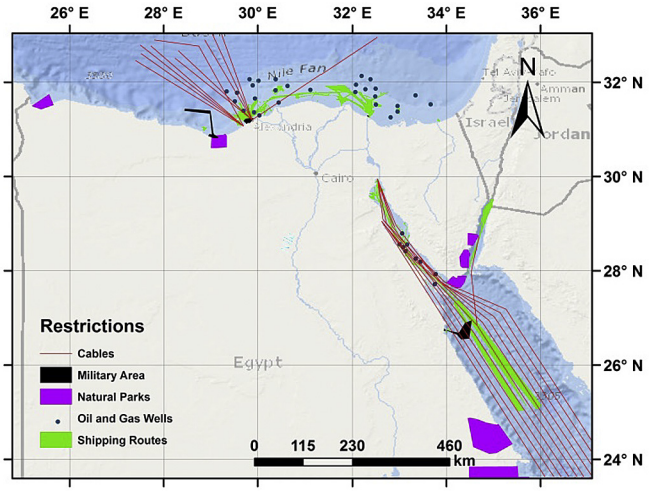

Fig. 5. All constrains layers of our study, coloured areas will take a value of 0, and other areas will take a value of 1.

representation of these areas is shown Fig. 5.

The Egyptian power network from which it is possible to identify appropriate grid connections to high wind resource sites [56]. The Euclidean Distance Tool in ArcGIS was used to estimate the distance from each electricity grid line to the sites and the raster layer results are in Fig. 6.

To ascertain and assess the proximity of military exercise areas to the high wind resource regions, data used was gathered from the official website of Ministry of Defence and Military Production [57] and these areas were excluded from our analysis as shown in the layers in Fig. 5. The coastline of Egypt was drawn to calculate the distance from the sea to the shoreline, applying the Euclidean Distance Tool, and the results are shown in Fig. 7. In terms of ground conditions, most of the seabed adjacent to the Egyptian coast has a medium to coarse sandy soil [58–60]. Hence, all cells in the modelling within the sea will have a score of 1.

6. Results and discussion

In our analysis, the factor spatial layer was ranked using the scale from Ref. [9], assuming that wind power density has the same importance as the total cost of the project and as such was given the same weight. The other factors comprise the major items for calculating the total cost. Data obtained from Ref. [21] was used to compare factors and to identify the different elements of costs of OWF. It should be noted that the cost values were estimated as an average from the cost of offshore wind projects in the UK spanning the period 2010 to 2015 [21]. Table 4 gives the cost of the various components for a wind farm including turbine foundation, cabling cost and their percentage of the total cost [21].

Table 5 takes into account the importance of the various scales assigned to "intensity of importance" to identify the impact between pairs. For example, wind power density factor was assigned a score of 3 compared to 1/3 assigned to the depth factor, as the latter represents about 1/3 of the project total cost (Table 4) and according to the pairwise comparison rules (see Section 3).

The comparison matrix of the calculated factors' weights is given in Table 6. This was determined by dividing each cell in Table 5 by the sum of its column. The values of the CI, RI, λ_{max} and CR were found to be 0.039, 1.12, 5.16 and 0.04 respectively; CR value is much less than 0.10, indicating that the assumptions and the calculations are valid.

Fuzzy function describes the relationship between the increases in a factor's magnitude as compared to overall cost appreciation/reduction. Such an assessment also depends on the experience and the knowledge about the factors. The data from Ref. [1] indicates that the relationships for the major factors (wind, distance to shore, and water depth) are linear.

The Fuzzy Membership tool in ArcGIS was applied to produce a new standardised layer for each factor. Table 7 shows the factor membership type and its limitations, which was adapted from Table 2. Some factors need another Boolean mask to conduct their limitations, these were, distance to shore and water depth for more than the maximum value limit.

Boolean mask was created to exclude the restricted cells by giving them value 0 or 1 (Table 8), which was adopted from the constraints shown in Table 2. Finally, all these constraints were gathered in one layer, using Raster Calculator tool, and shown in Fig. 8. All criteria were aggregated to create the suitability map of OWF in Egypt. The WLC equation was used to conduct the aggregation. The standardised layers were first multiplied by its weights, then summed together, using Weighted Sum tool in ArcGIS. Finally, the Weighted Sum layer was multiplied by the Boolean Mask layer, using the Raster Calculator tool. The final Suitability Map layer is shown in Fig. 9.

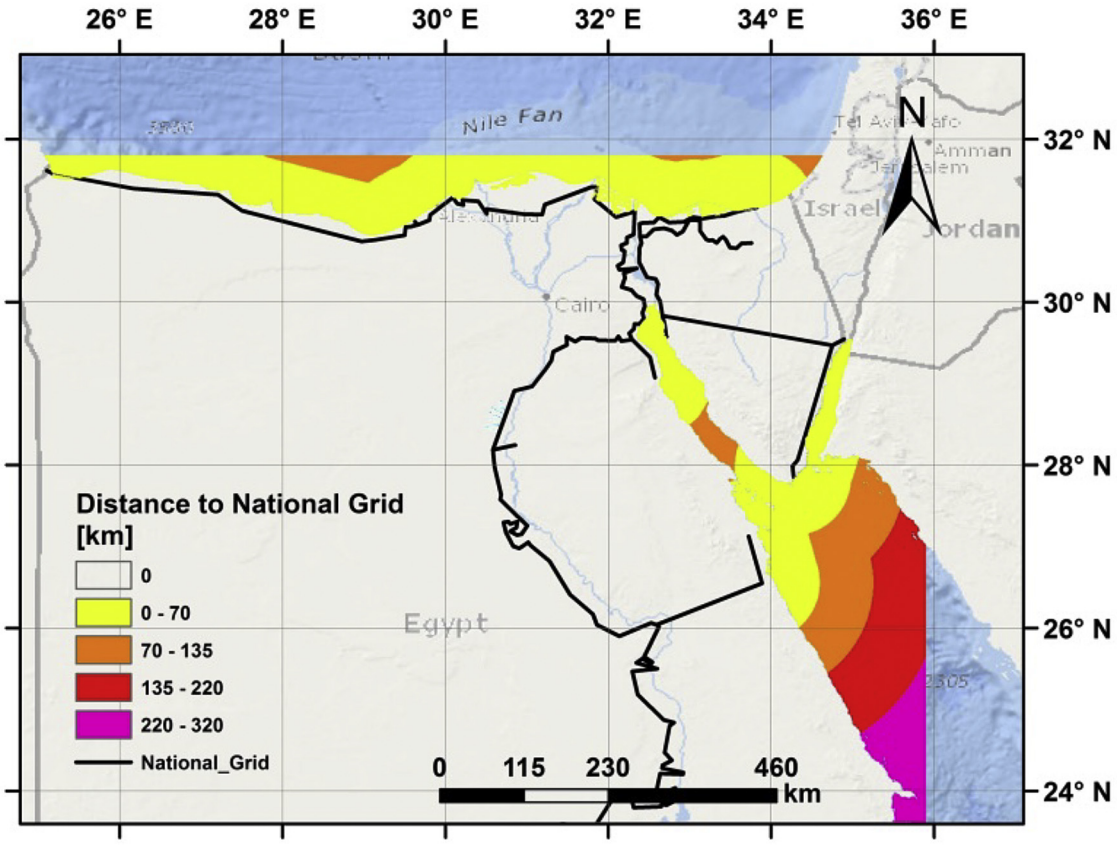

Fig. 6. Map showing distance from sites to national grid.

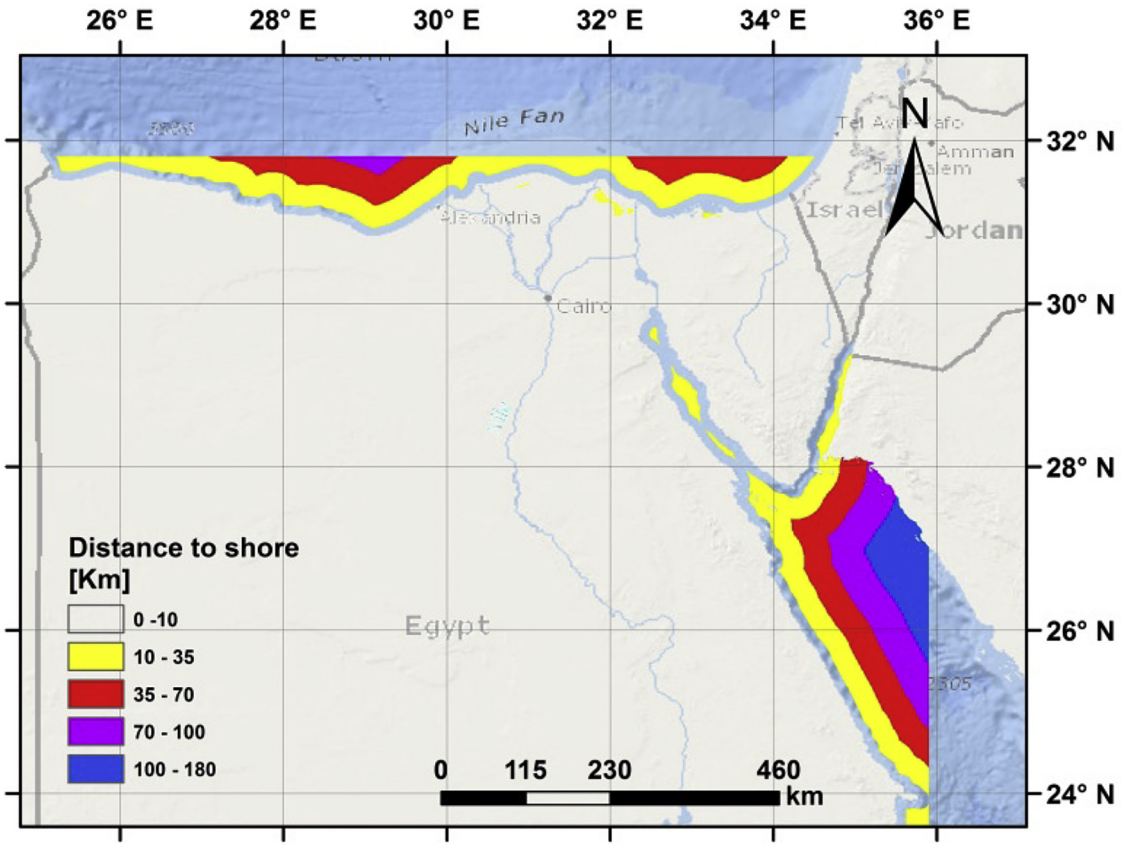

Fig. 7. Distance to the Egyptian's shore.

Table 4
Average cost and % to total cost estimated from UK OWF costs [21].

Factor		Cost £m/MW	%
Foundation	Depth	0.50	27
	Soil Properties	0.23	12
Connecting to the National Grid		0.16	5
Distance from shoreline (Under water cables)		0.29	9
Installation and substations		0.67	21
Total		1.85	100
Total including the turbine		3.2	–

Table 5
Pairwise Comparison matrix.

Factor	F1	F2	F3	F4	F5
Wind power density (F1)	1	3	8	9	6
Depth (F2)	1/3	1	4	5	3
Soil Properties (F3)	1/8	1/4	1	2	1/2
Distance to National Grid (F4)	1/9	1/5	1/2	1	1/3
Distance from shoreline (F5)	1/6	1/3	2	3	1
Sum	1.74	4.78	15.5	20.0	10.8

Table 6
Normalised matrix and weight determination.

Factor	F1	F2	F3	F4	F5	Weight	λ_{max}
F1	0.58	0.63	0.52	0.45	0.55	0.54	0.95
F2	0.19	0.21	0.26	0.25	0.28	0.24	1.13
F3	0.07	0.05	0.06	0.10	0.05	0.07	1.04
F4	0.06	0.04	0.03	0.05	0.03	0.04	0.88
F5	0.10	0.07	0.13	0.15	0.09	0.11	1.16
Sum	1.00	1.00	1.00	1.00	1.00	1.00	5.16

In our analysis, an area with a value of 1 was found inland in the Boolean mask layer, circled in red (Fig. 8). The reason for this confliction is that the area considered has an altitude less than −5 m below mean sea level and corresponds to the *Qattara Depression*, located in the north west of Egypt. This is "the largest and deepest of the undrained natural depressions in the Sahara Desert", with the lowest point of −134 m below mean sea level [61]. Identifying such areas gives further confidence in the robustness of the analysis and these points were excluded from the suitability map.

The total number of high suitability areas for OWF is approximately 3200 cells which represent about 2050 km^2, while the moderate suitability area is approximately 21650 cells which represent about 13860 km^2. These numbers are promising when compared with, for example, the 122 km^2 of the world's largest OWF, the London Array, which has a capacity of 630 MW [16]. The areas that are unsuitable for OWF are equal to 16403 km^2. In our work, the cell dimensions are 800 m by 800 m, which represent an area of 0.64 km^2.

Zooming into specific areas to obtain a finer grain of suitable locations in the suitability map given in Fig. 10, we arrive at the most suitable locations for OWF in Egypt, which are shown circled (in red colour the figure). Locations 1 and 2 are in the Egyptian territorial waters, while location 3 is situated between Egypt and Saudi Arabia. Location 1, 2, and 3 contain 1092, 2137, 969 km^2 of high suitable areas for OWF, respectively.

In order to estimate the potential wind energy capacity of these areas, we use the method described in Refs. [62,63] which estimates the effective footprint per turbine (array spacing) using the expression: *Array Spacing = (rotor diameter)^2 × downwind spacing factor × crosswind spacing factor.* However, we adopted the E. ON data for the turbine spacing of 5–8 times rotor diameter (to reduce turbulence between turbines) and used an average wind speed of 10 m/s [31]. Hence, for a 5 MW turbine of 126 m rotor diameter, a one square kilometre of the chosen areas would yield ~7.9 MW of installed capacity. Following these considerations, Table 9 gives our estimated power for the three locations shown in Fig. 10. The total wind power capacity of all these sites is around 33 GW.

From the final suitability map (Fig. 9), it is clear that most of the high suitability cells are concentrated in areas that have wind power density > 600 W/m^2, which reflects the strong influence of wind power criterion on the cells' ranks. This is reasonable because the wind power has a relative importance of more than 50%. The second factor is water depth which it has a 24% share of the total weight, and this explains the long, wide area with moderate suitability which can be seen adjacent to the northern coast of Egypt (shown as yellow areas within the black rectangle in Fig. 9). Despite an average mean power density of less than 200 W/m^2 in these areas, their slope is mild (shallow) approximately less than 1:800 for more than 50 km away from the sea [49].

7. Conclusions

A new methodology to model and identify suitable areas for offshore wind sites is introduced which addresses a gap in knowledge in the offshore wind energy field. The methodology can be easily utilised in other regions by applying the four steps summarised in Section 3 and the process depicted in Fig. 1. There are some assumptions, requirements, and limitations related to the proposed methodology. The model is limited to national or regional scales requiring a wide knowledge and data (wind speed and bathometry) when considering these scales. The model was built on the assumption that cost related criteria are higher in weight than those assigned to the environmental aspect of the site to be exploited.

Table 7
Fuzzy membership functions of the factors and its limitations.

Factor	Membership Type	Max Value = 1.0	Min Value = 0.0	More than Max	Less than Min
Wind	Linear	850 W/m^2	45 W/m^2	1.0	0.0
Depth	Linear	5.0 m	60.0 m	0.0	0.0
Sandy soil level	Linear	5.0 m	21.0 m	1.0	0.0
National Grid	Linear	1 km	450 km	1.0	0.0
Distance to shore	Linear	1.5 km	200 km	0.0	0.0

Table 8
Constraints definition and limitation.

Constraint	0	1
Depth	Depths <5.0 m or >60.0 m	Else
Distance from shore	Distance <1.5 km or >200.0 km	Else
Military Areas	Military areas as shown in Fig. 5	Else
Shipping Routes	Areas as shown in Fig. 5	Else
Oil & Gas Areas	Areas as shown in Fig. 5	Else
Cables and tunnels	Lines as shown in Fig. 5	Else
Nature Reserves	Marine parks as shown in Fig. 5	Else

Table 9
Estimate wind power capacity per considered area (Fig. 10).

Location in Fig. 10	Area (km^2)	Estimated power (GW)
Red Circle 1	1092	8.6
Red Circle 2	2137	16.8
Red Circle 3	969	7.6
Total (GW)		33.0

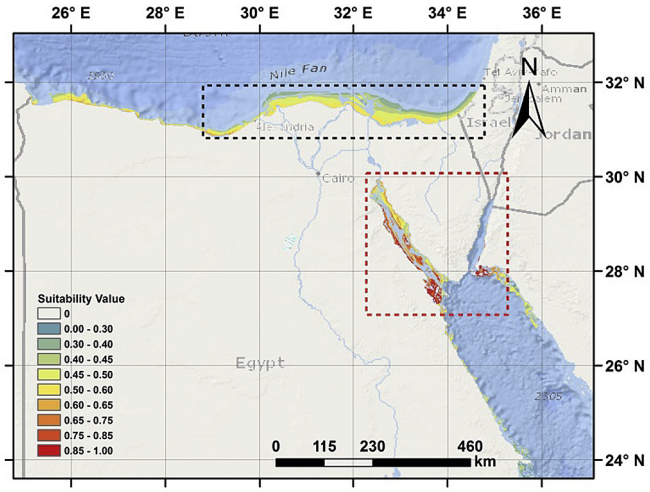

Fig. 9. Final Suitability Map for offshore wind in Egypt, where the legend indicates the weights of suitability where 0 = least suitable and 0.99 = most suitable. Black and red rectangles represent areas of moderate and high suitability respectively.

The approach presented was successful in providing a suitability map for offshore wind energy in Egypt. The applied model is capable of dealing with the conflicting criteria that govern the spatial planning for offshore wind farms. The spatial analysis was undertaken at a medium resolution (800 m by 800 m), which is confined to the cell size of the bathymetry map data availability.

Five factors and seven constraints were applied using MCDM and GIS models for Egypt as the case study area. The analysis was conducted at large scale covering the whole of Egypt and its surrounding waters and hence has implications for renewable energy policies in Egypt and, to some extent, Saudi Arabia. The study transcends different conditions present in two seas – the Red Sea and the Mediterranean Sea, and hence is of wider applicability in these regions. To our knowledge, no detailed studies have been conducted either onshore or offshore, that have considered such a footprint, provided spatial planning examination of appropriate sites.

The final results indicate that Egypt could potentially benefit from around 33 GW, achieved by only considering installations at the high suitability offshore wind sites available. This significant amount of green renewable energy could provide a solution to the electricity shortage in Egypt; furthermore, the offshore wind solution has no effect on important tourist resort lands around the chosen sites. This outcome confirms the huge offshore wind energy potential in Egypt. In addition, as the fuel from wind electrical power production is free, exploitation of offshore wind could positively contribute to the country's Gross domestic product (GDP) and budgets balances, reducing dependence on imported fuels

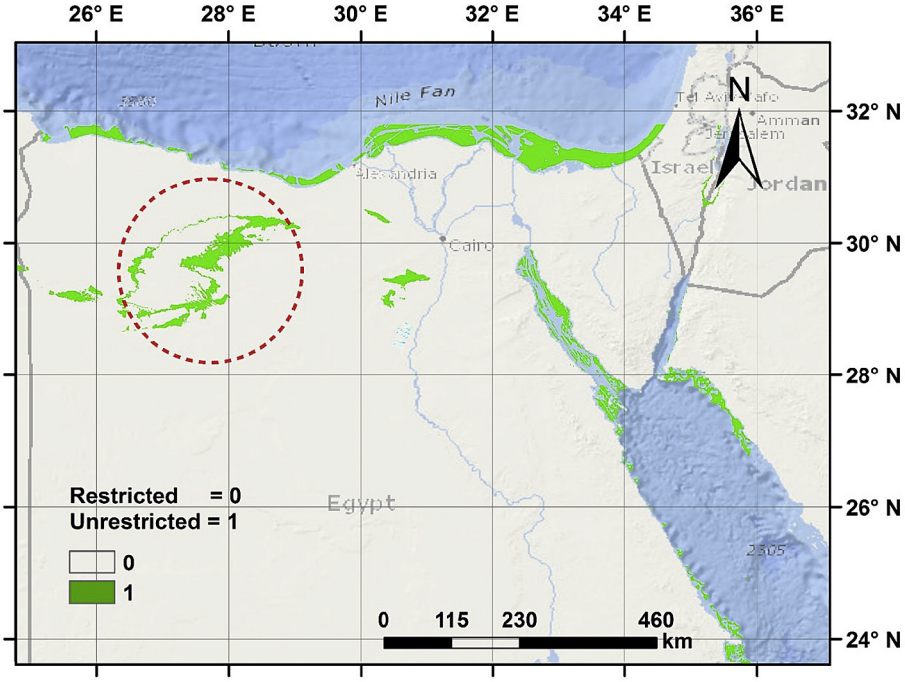

Fig. 8. Final Boolean mask layer – The red circle showing the Qattara Depression (see text under results).

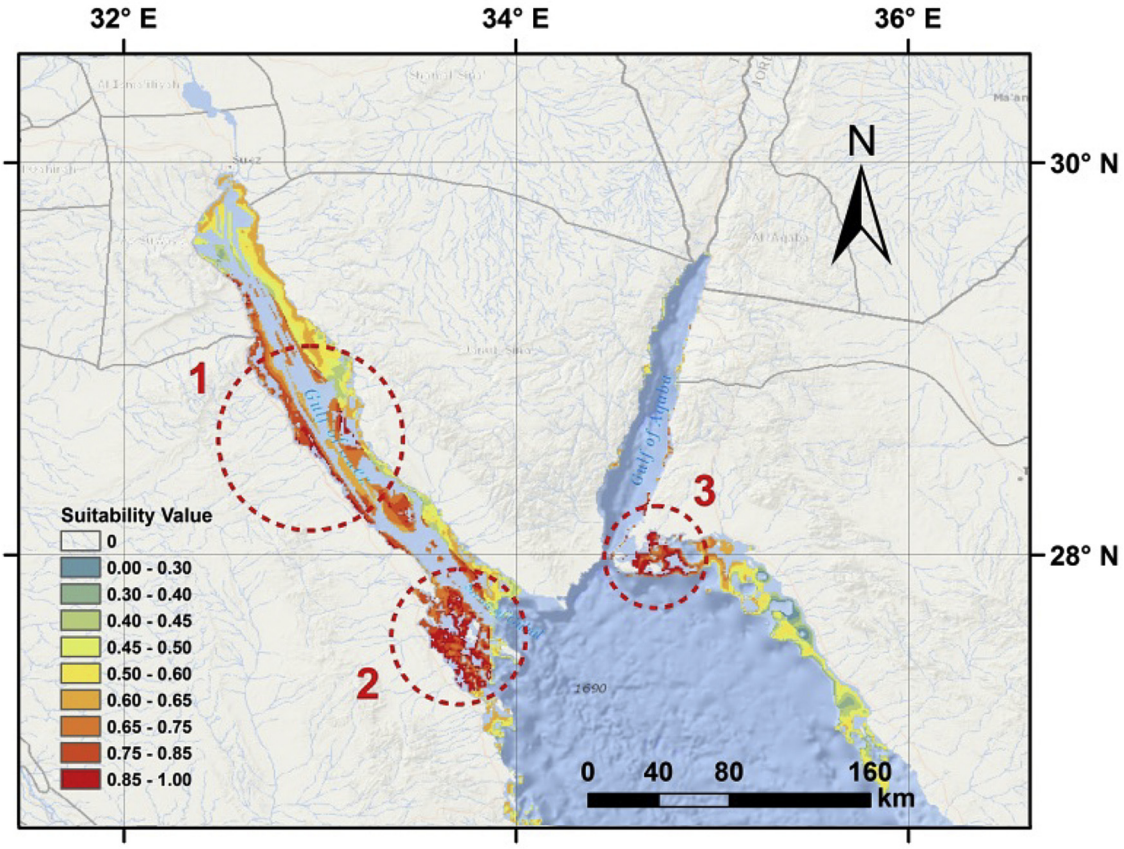

Fig. 10. The Suitability Map for offshore wind farms around the southern coast of Sinai Peninsula, Red Sea, Egypt. The encircled area areas show high wind energy potentials.

whilst providing a cleaner and more sustainable approach to electricity production in Egypt. Nevertheless, a coherent policy coupled with capacity building would be needed to allow such exploitation to occur.

This case study provides the needed evidence to establish an appropriate programme to exploit the offshore wind energy resource in Egypt and will contribute to the country energy mix so that it can cope with its ever-increasing energy demand. In essence, the work presented here not only plugs a knowledge gap but also provides realistic evaluation of the Egyptian offshore wind potential which can form the basis of the needed blueprint for developing the appropriate policies for its exploitation. The existence of vast commercial experience in offshore wind is more than likely to consider such a resource and can be marshalled to support it exploitation in Egypt.

Lastly, the scope and methodology of this study addressed a knowledge gap in the development of renewable energy systems, particularly that of offshore wind. The methodology used here provides a robust offshore spatial siting analysis that can be applied in different locations around the world.

Acknowledgment

This work is part of the activities of the Energy and Climate Change Division and the Sustainable Energy Research Group at the University of Southampton (www.energy.soton.ac.uk). The research is also part of a PhD programme sponsored by the Faculty of Engineering, PortSaid University, Egypt. We would also like to show our gratitude to Mr. Ahmed Elghandour for his support in securing some of the data used in the research.

References

[1] R. Green, N. Vasilakos, The economics of offshore wind, Energy Policy 39 (2011) 496–502.
[2] M.D. Esteban, J.J. Diez, J.S. López, V. Negro, Why offshore wind energy? Renew. Energy 36 (2011) 444–450.
[3] J. Kaldellis, M. Kapsali, Shifting towards offshore wind energy—recent activity and future development, Energy Policy 53 (2013) 136–148.
[4] J. Kaldellis, M. Kapsali, E. Katsanou, Renewable energy applications in Greece—what is the public attitude? Energy Policy 42 (2012) 37–48.
[5] M. Bilgili, A. Yasar, E. Simsek, Offshore wind power development in Europe and its comparison with onshore counterpart, Renew. Sustain. Energy Rev. 15 (2011) 905–915.
[6] H. Jiang, J.R. Eastman, Application of fuzzy measures in multi-criteria evaluation in GIS, Int. J. Geogr. Inf. Sci. 14 (2000) 173–184.
[7] M.N. DeMers, Fundamentals of Geographic Information Systems, John Wiley & Sons, 2008.
[8] K.P. Yoon, C.-L. Hwang, Multiple Attribute Decision Making: an Introduction, Sage Publications, 1995.
[9] T.L. Saaty, Decision making with the analytic hierarchy process, Int. J. Serv. Sci. 1 (2008) 83–98.
[10] J.R. Eastman, H. Jiang, J. Toledano, Multi-criteria and multi-objective decision making for land allocation using GIS, in: Multicriteria Analysis for Land-use Management, Springer, 1998, pp. 227–251.
[11] D. Latinopoulos, K. Kechagia, A GIS-based multi-criteria evaluation for wind farm site selection. A regional scale application in Greece, Renew. Energy 78 (2015) 550–560.
[12] N.Y. Aydin, E. Kentel, S. Duzgun, GIS-based environmental assessment of wind energy systems for spatial planning: a case study from Western Turkey, Renew. Sustain. Energy Rev. 14 (2010) 364–373.
[13] H.S. Hansen, GIS-based multi-criteria analysis of wind farm development, in: ScanGIS 2005: Scandinavian Research Conference on Geographical Information Science, 2005, pp. 75–87.
[14] L.C. Rodman, R.K. Meentemeyer, A geographic analysis of wind turbine placement in Northern California, Energy Policy 34 (2006) 2137–2149.
[15] S.M. Baban, T. Parry, Developing and applying a GIS-assisted approach to locating wind farms in the UK, Renew. energy 24 (2001) 59–71.
[16] The Crown Estate, Round 3 Offshore Wind Site Selection at National and Project Levels, 2012.

[17] C. Schillings, T. Wanderer, L. Cameron, J.T. van der Wal, J. Jacquemin, K. Veum, A decision support system for assessing offshore wind energy potential in the North Sea, Energy Policy 49 (2012) 541–551.
[18] C. Ntoka, Offshore Wind Park Sitting and Micro-sitting in Petalioi Gulf, Greece, Aalborg University, Denmark, 2013, p. 77.
[19] J. Waewsak, M. Landry, Y. Gagnon, Offshore wind power potential of the Gulf of Thailand, Renew. Energy 81 (2015) 609–626.
[20] M. Argin, V. Yerci, Offshore wind power potential of the Black Sea region in Turkey, Int. J. Green Energy 14 (10) (2017).
[21] S. Cavazzi, A. Dutton, An Offshore Wind Energy Geographic Information System (OWE-GIS) for assessment of the UK's offshore wind energy potential, Renew. Energy 87 (2016) 212–228.
[22] J.R. Eastman, Idrisi Para Windows: Version 2.0, Enero 1997. Tutorial Exercises, Clark University, 1997.
[23] T.L. Saaty, A scaling method for priorities in hierarchical structures, J. Math. Psychol. 15 (1977) 234–281.
[24] The Annual Report of the Ministry of Environment, Minister of State for Environmental Affairs, 2016.
[25] Population, Egypt State Information Service, 2017.
[26] Annual Report of the Authority of the Egyptian Electricity Holding Company, The Ministry of Electricity and Energy of Egypt, 2016.
[27] G. Bahgat, Egypt's energy outlook: opportunities and challenges, Mediterr. Q. 24 (2013) 12–37.
[28] The ArcGIS Help Library, esri, 2012.
[29] New and Renewable Energy Authority, Study No. (IMC/PS), in, 2006.
[30] D.S. Abdou, Z. Zaazou, The Egyptian revolution and post socio-economic impact, Top. Middle East. Afr. Econ. 15 (2013) 92–115.
[31] N.G. Mortensen, U.S. Said, J. Badger, Wind Atlas of Egypt, RISO National Laboratory, New and Renewable Energy Authority, Egyptian Meteorological Authority, 2006.
[32] Annual Report of the Authority of the New and Renewable Energy in Arabic, The Ministry of Electricity and Energy of Egypt, 2013.
[33] A. Lashin, A. Shata, An analysis of wind power potential in Port Said, Egypt, Renew. Sustain. Energy Rev. 16 (2012) 6660–6667.
[34] N.G. Mortensen, J.C. Hansen, J. Badger, B.H. Jørgensen, C.B. Hasager, U.S. Paulsen, O.F. Hansen, K. Enevoldsen, L.G. Youssef, U.S. Said, Wind atlas for Egypt: measurements, micro-and mesoscale modelling, in: Proceedings of the 2006 European Wind Energy Conference and Exhibition, February, 2006. Athens, Greece.
[35] G. Gaudiosi, Offshore wind energy in the world context, Renew. Energy 9 (1996) 899–904.
[36] M.A. El-Sayed, Substitution potential of wind energy in Egypt, Energy Policy 30 (2002) 681–687.
[37] A.K. Khalil, A.M. Mubarak, S.A. Kaseb, Road map for renewable energy research and development in Egypt, J. Adv. Res. 1 (2010) 29–38.
[38] A. Mayhoub, A. Azzam, A survey on the assessment of wind energy potential in Egypt, Renew. Energy 11 (1997) 235–247.
[39] A.S. Ahmed, Investigation of wind characteristics and wind energy potential at Ras Ghareb, Egypt, Renew. Sustain. Energy Rev. 15 (2011) 2750–2755.
[40] A.S. Ahmed, Electricity generation from the first wind farm situated at Ras Ghareb, Egypt, Renew. Sustain. Energy Rev. 16 (2012) 1630–1635.
[41] A.S. Ahmed Shata, R. Hanitsch, Evaluation of wind energy potential and electricity generation on the coast of Mediterranean Sea in Egypt, Renew. Energy 31 (2006) 1183–1202.
[42] A.S. Ahmed Shata, R. Hanitsch, Electricity generation and wind potential assessment at Hurghada, Egypt, Renew. Energy 33 (2008) 141–148.
[43] A.A. Shata, R. Hanitsch, The potential of electricity generation on the east coast of Red Sea in Egypt, Renew. Energy 31 (2006) 1597–1615.
[44] A.S. Ahmed, Analysis of electrical power form the wind farm sitting on the Nile River of Aswan, Egypt, Renew. Sustain. Energy Rev. 15 (2011) 1637–1645.
[45] A.S. Ahmed, Potential wind power generation in South Egypt, Renew. Sustain. Energy Rev. 16 (2012) 1528–1536.
[46] H. Ahmed, M. Abouzeid, Utilization of wind energy in Egypt at remote areas, Renew. energy 23 (2001) 595–604.
[47] Fishing Regulation Laws, The General Authority for Fish Resources Development, 2009.
[48] Protectorates: Natural Protectorates and Biological Diversity, The Egyptian Environmental Affairs Agency, 2015.
[49] The GEBCO_2014 Grid, The British Oceanographic Data Centre, 2014.
[50] The Home Page in English, National Authority for Tunnels (NAT), 2015.
[51] Submarine Cable Map, TeleGeography Company, 2015.
[52] Mining Laws in Egypt, Ministry of Petroleum and Mineral Resources, 2015.
[53] Map of the Gas and Oil Wells in Egypt, The Egyptian Natural Gas Holding Company (EGAS), 2015.
[54] Ship Density Maps, The MarineTraffic, 2015.
[55] Egyptian Ports, Maritime Transport Sector, 2015.
[56] The Ministry of Electricity and Energy of Egypt, Egyptian Unified Power Network, 2016.
[57] The Offical Website, Ministry of Defence and Military Production, 2015.
[58] W.S. El Diasty, S. El Beialy, A.A. Ghonaim, A. Mostafa, H. El Atfy, Palynology, palynofacies and petroleum potential of the upper Cretaceous–Eocene Matulla, Brown Limestone and Thebes formations, Belayim oilfields, central Gulf of Suez, Egypt, J. Afr. Earth Sci. 95 (2014) 155–167.
[59] A.I. Ghaly, A.E. Khalil, A.A. Mahmoud, Stratigraphic analysis and petroleum exploration, offshore, Nile Delta, Egypt, Seismic Stratigr. Seismic Geomorphol. 1 (1) (2013).
[60] Geological Report for Dikheila Port in Alexandria, Egypt, MAS Consultant Office, 2005.
[61] C.C. Albritton, J.E. Brooks, B. Issawi, A. Swedan, Origin of the Qattara depression, Egypt, Geol. Soc. Am. Bull. 102 (1990) 952–960.
[62] E. ON, Offshore Wind Energy Factbook, E. ON Climate & Renewables GmbH, 2012.
[63] B. Sheridan, S.D. Baker, N.S. Pearre, J. Firestone, W. Kempton, Calculating the offshore wind power resource: robust assessment methods applied to the US Atlantic Coast, Renew. Energy 43 (2012) 224–233.

OFFSHORE WIND ENERGY POTENTIAL AROUND THE EAST COAST OF THE RED SEA, KSA

Mostafa Mahdy [1*], AbuBakr S. Bahaj [1] and Abdulsalam S Alghamdi [2]

[1] Sustainable Energy Research Group, Energy & Climate Change Division (www.energy.soton.ac.uk), Faculty of Engineering and the Environment, University of Southampton SO17 1BJ, Southampton (United Kingdom)

[2] Electrical Engineering Department, King Abdulaziz University, Jeddah (Saudi Arabia)

[*] Corresponding author, E-mail: m.mahdy@soton.ac.uk

Abstract

Under its Vision 2030, the Kingdom of Saudi Arabia (KSA) announced an ambitious strategy to diversify their economy from oil dependency. One of the goals of the vision is an initial target to produce 9.5 GW of electricity from renewable energy sources. Offshore wind energy conversion is considered to be mature technology with more than 12 GW of installed capacity globally. Offshore wind has advantages when compared with onshore wind, such as, higher wind speed, reduced turbulence, minimal visual and noise impacts. KSA has two shorelines, one is laying on the Arabian Gulf and the other is on the Red Sea. The work presented here evaluates offshore wind potentials in in the East Coast of the Red Sea in KSA which was chosen due minimum restrictions and has no close oil extraction facilities. The evaluation was based on a Boolean Mask model linked coupled analysis undertaken in Geographical Information System developed for the Red Sea area.

Using the UK's London Array wind farm as a minimum required area for offshore wind farms, the work identifies ten different locations as possible areas for the first offshore wind farms in KSA. The analysis considered the deployment of two types of turbine of capacities 3.6MW and 5MW. The results for the higher capacity turbine indicate that over 12.3 GW of offshore wind power can be generated from the identified sites. These results and the produced location maps could be used to help stakeholders in KSA in planning for the exploitation of offshore wind energy in KSA. Thus providing a pathway to contribute to achieving the 9.5 GW national target.

Keywords: Wind energy, offshore wind, GIS, Boolean Mask, Red Sea, KSA

1. Introduction

Offshore wind energy is considered mature technology with over 12 GW of installed capacity globally. The recent contract for difference (CfD) announcement in the UK showed halving the cost per MWh to £57.5 compared to the previous round (CB, 2017). Onshore wind on the other hand is further ahead in terms of economics, however, it has some disadvantages, such as the value of the land areas, noise, high vibrations, visual impacts, bird paths hazards, and shadow flicker effect. Shadow flicker effect that is an infrequent event, which could happen, when the sun's light is at horizon. Shadow flicker could be responsible for photo-induced seizures or photosensitive epilepsy and other disturbance to humans near the turbines (Knopper & Ollson, 2011). Offshore wind on the whole does not suffer from these disadvantages, and has two extra advantages: the average wind speed is larger than over onshore areas and the turbulence wind effect is minimized when compared to installation over land. The latter is important as fatigue stress encountered is smaller enhancing offshore wind turbines life.

The Kingdom of Saudi Arabia (KSA) has a total area of 2.2 million km^2, and a population of more than 30 million. KSA lies between latitude of 17.5 °N and 31 °N and longitude of 36.6 °E and 50 °E (Bahakeem, 2015). The west coastline of KSA is more than 1800 km in length and is situated around the Red Sea and the Gulf of Aqaba with a boundary between Haql to the north and Jazan to the south (Fig.1).

The energy consumption of KSA has been on rapid rise to cope with the growing demand of the industrial, water

doi:10.18086/swc.2017.38.02 Available at http://proceedings.ises.org

and building sectors. Most of this energy is derived from fossil fuels leading to high carbon emissions. This dependence is as a result of the vast oil resources in KSA estimated to be more than 250 billion barrels of oil reserves or one-fifth of total known global reserves (Bahakeem, 2015). Hence there is an urgent need for KSA to move towards low carbon renewable energy production.

In order to decrease its reliance on fossil fuels and balance its economy, KSA has developed the Vision 2030 programme under which it plans to generate 9.5 gigawatts of electricity from renewable energy sources (Gazette, 2016). This is more likely to be derived from solar energy and wind energy. Hence, this work is directed towards the latter, but concentrated on offshore wind around the Sea Area of KSA where we will identify suitable locations for offshore wind farms (OWF) and evaluate their potential. To our knowledge, only one article was found that considers the offshore wind resources in KSA but the study was focused on the east coast of the country (Rehman, 2005).

In summary, the aims of this work is to identify the suitable areas in KSA for offshore wind focusing on the the Red Sea regions, estimate the electrical power potential form the identified sites and provide suitability maps for these locations.

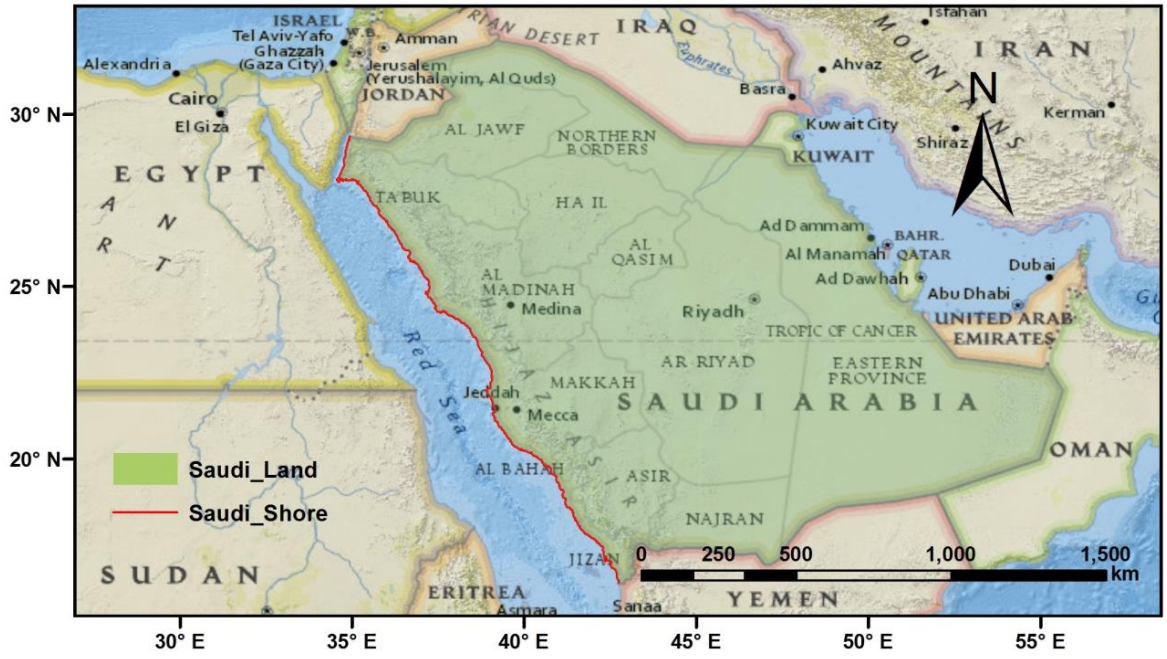

Fig.1: Study area map, KSA is shaded with light green, the Red Sea east shoreline is the red line, adopted from (esri, 2012).

2. Methodology

In this work the required outcome is a spatial siting of the wind farms. Such a problem comprises a large number of suitable alternatives and multiple constraints to choose the alternative with zero constraint. Both the constraints and alternatives can be determined or evaluated and weighted by stockholders, or scholars based on their knowledge and experience (Estoque, 2011).

The map of the study region is divided to grid as an equal size, the smallest part of such grid is called a cell, which corresponds to one of the feasible alternative. For instant, to decide the suitable cell for offshore wind energy in the Red sea, wind speed, water depth, distance to shore, distance to the electricity grid, shipping routes, military areas, cables paths, and reserved natural parks, are the constraints to be considered in the analysis and before taking a final decision. Fig.2 provides a flow chart summarising the whole assessment process, under the Boolean Mask technique utilised in this study to solve the problem.

Boolean Mask (overlay), is used to locate sites with no restrictions (constrains). Boolean relations [and, or, and not] are used, from which the name has been derived.The created map layer has two colours (boundaries), one represents areas that has a value of 1 (the unrestricted areas) and the other represents areas of value 0 value (restricted areas). Boolean mask is a powerful tool for simple and quick spatial decisions (Jiang & Eastman, 2000).

In this work, we need to create a primary map for suitable offshore wind farms in the Red Sea, around the KSA coast, and evaluate the potential electrcila power from these farms. The **Constraints** can be explained as a tool to eliminate alternatives (cells). The limitations or restrictions of the constraints are defined as a (true/false) relationship. For example, if the commercial wind power development becomes feasible around wind speed greater than 3 m/s, so all areas with wind speed less than this threshold (3 m/s) will be given 0 value, while other areas will take the value of 1.

The equation used to calculate the Boolean Map is adopted from (Eastman, Jiang, & Toledano, 1998), and is given by:

$$Boolean\ Mask = \left(\prod_{j=1}^{l} C_j\right) \qquad \text{(eq. 1)}$$

Where:

C_j is the constraint j (Boolean Mask j),

Π is the product of constraints, and

ℓ is the number of constraints.

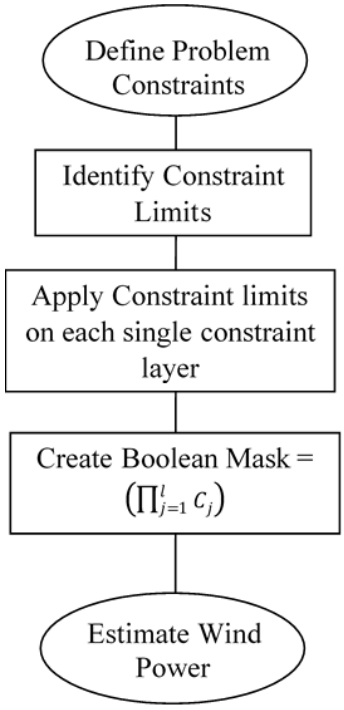

Fig.2: Flow chart summarising the whole assessment process, under the Boolean Mask technique utilised in this work.

3. Analysis

To satisfy the conditions of the sites around the Red Seas in KSA coasts, nine constraints were considered, and are summarised in Table 1. In addition, the table also provides the two limits for each constraint, where only two values are identified; zero value, which is the undesirable areas (cells) according to the constraint definitions, while the value of one is assigned the other areas (cell).

3.1 Relevant Data

A map layer in ArcGIS was created for each constraint, using the available and relevant spatial data. The bathymetry data for the Red Sea around the shores of KSA was adopted from (The British Oceanographic Data Centre, 2014), the source file of water depth data was in raster form, with a sell size of 800 x 800 m, and the file "GCS_WGS_1984" is the Geographic Coordinate System used. Due to the source file cell size and the coordinating system type, all constraints layers were confined to same cell size and GCS_WGS_1984 coordinate system. Fig.3, shows the water depth map for the Red Sea, which has a range from 0 to -3000 m. The areas with the required depth for offshore wind farm are concentrated in the South West part of the KSA. Wind speed data was adopted from the "Wind Atlas for Egypt" (Mortensen et al., 2006) and from the Global Atlas for Renewable Energy (Kieffer & Couture, 2015). The map layer in Fig.4 shows the average wind speed in [m/s] at a height of 10 m over a flat and uniform sea, which has a range between 3 and 7 m/s. Locations with desirable wind speed are centred in the North West part of the KSA.

Fig.5 shows all constraints in the study area, KSA has only two maritime reserved parks in the Red Sea named "Umm al-Qamari Islands" and "Farasan Islands". Locations and shape dimensions of these parks were taken from the official web site of the Saudi Wildlife Authority (SWA, 2017). Shipping Routes in the Red Sea adjacent to the KSA coast line were identified using the data available from ship density maps of Marine Traffic website (The MarineTraffic, 2015). Submerged undersea cable locations and paths were extracted from the submarine cable map of (TeleGeography Company, 2015). Marine military restricted areas was assessed from Royal Saudi Navy Forces official website (RSNF, 2017). According to Saudi Aramco (Aramco, 2017), all petrol oil extraction areas are located on the Arabian Gulf, so the oil extraction constraint was excluded.

Table 1: Constraints 0, and 1 definitions and data source data.

Constraint	Symbol	0 description and data source	1
Wind Speed (m/s)	W_B	Areas with wind speed less than 3.0 m/s **or** more than 25.0 m/s at a height of 10 m over a flat and uniform sea (Archer & Jacobson, 2005), wind speed data were adopted from (Mortensen, Said, & Badger, 2006) and (Kieffer & Couture, 2015).	Else
Water Depth (m)	D_B	Depths less than 5.0 m **or** more than 60.0 m, the bathymetry data was adopted from British Oceanographic Data Centre (BODC) (The British Oceanographic Data Centre, 2014).	Else
Distance to the shore (km)	S_B	Distance less than 1.5 km or more than 200.0 km, the distances data was adopted and processed using ArcGIS Program (esri, 2012).	Else
Distance to the Grid (km)	G_B	Distance more than 250.0 km, the distances data was adopted and processed using ArcGIS Program (esri, 2012).	
Military Practice & Exercise Areas	M_B	Locations were adopted from (RSNF, 2017)..	Else
Shipping Routes	R_B	Shipping areas adopted from (The MarineTraffic, 2015)	Else
Maritime Boundaries	B_B	Boundaries were adopted and processed using ArcGIS Program (esri, 2012)..	Else
Nature Reserves	N_B	Places in the sea area protected by the power of law to reserve the endangered marine ecosystem species, marine parks were adopted from (SWA, 2017).	Else
Under Sea Cables	U_B	Locations of the submerged sea cables (TeleGeography Company, 2015).	Else

Fig.6 shows the map layer of the National Electricity Transmission Grid of KSA (the grid is drawn as a line network in a black colour), which was adopted from the Global Energy Network Institute (GENI, 2017). The Euclidean Distance Tool was deployed to calculate the distance between nearest electricity line to each cell, (Fig.6). Fig.7 shows the coastline of the Red Sea of KSA in km and was drawn using data from (esri, 2012). Euclidean Distance Tool within the ArcGIS programme was applied to create a map shown in Fig.7, which illustrates the distance from each cell to the coastline of KSA.

3.2 Boolean Mask

A Boolean mask was created to eliminate restricted cells, constraint cell value = 0, and unrestricted cell value = 1, see Fig.5. The Raster Calculator tool was used to produce the final Boolean Mask, and is shown in Fig.8. The below equation was used:

$$\text{Boolean Mask} = W_B \times D_B \times S_B \times G_B \times M_B \times R_B \times B_B \times N_B \times U_B \quad \text{(eq. 2)}$$

Where: W_B, D_B, S_B, G_B, M_B, R_B, B_B, N_B, and U_B are defined in Table 1 above.

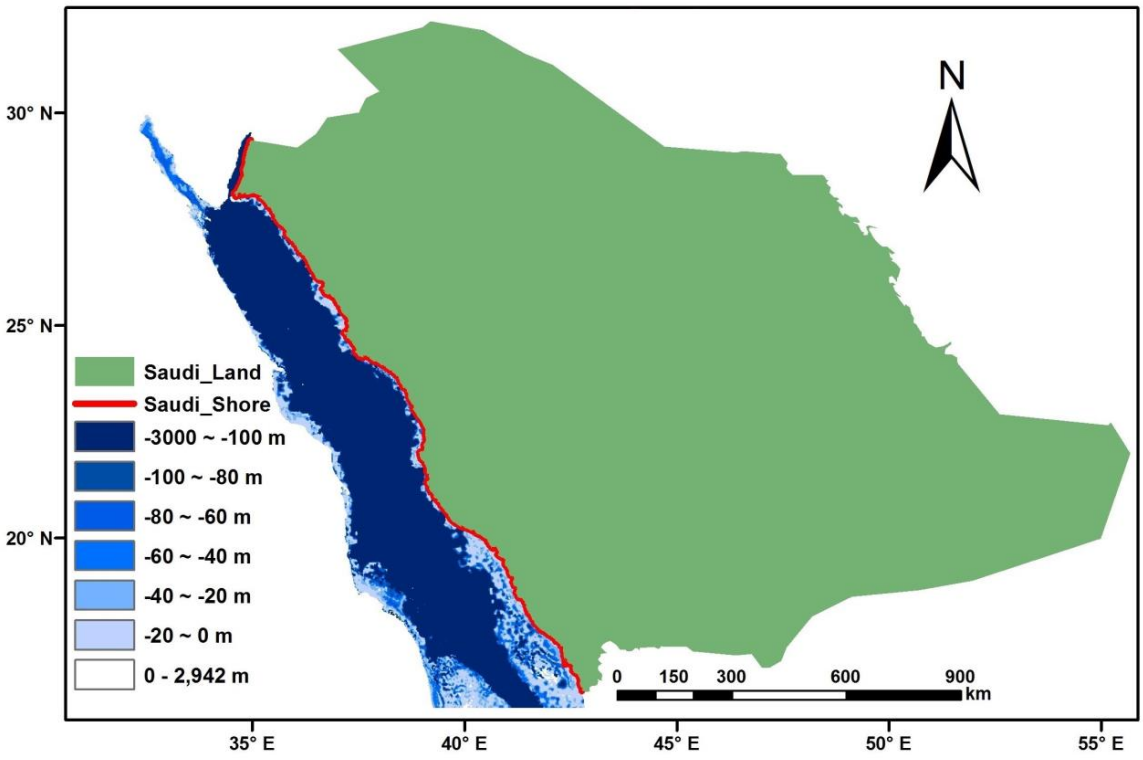

Fig.3: Bathometry map of the Red Sea.

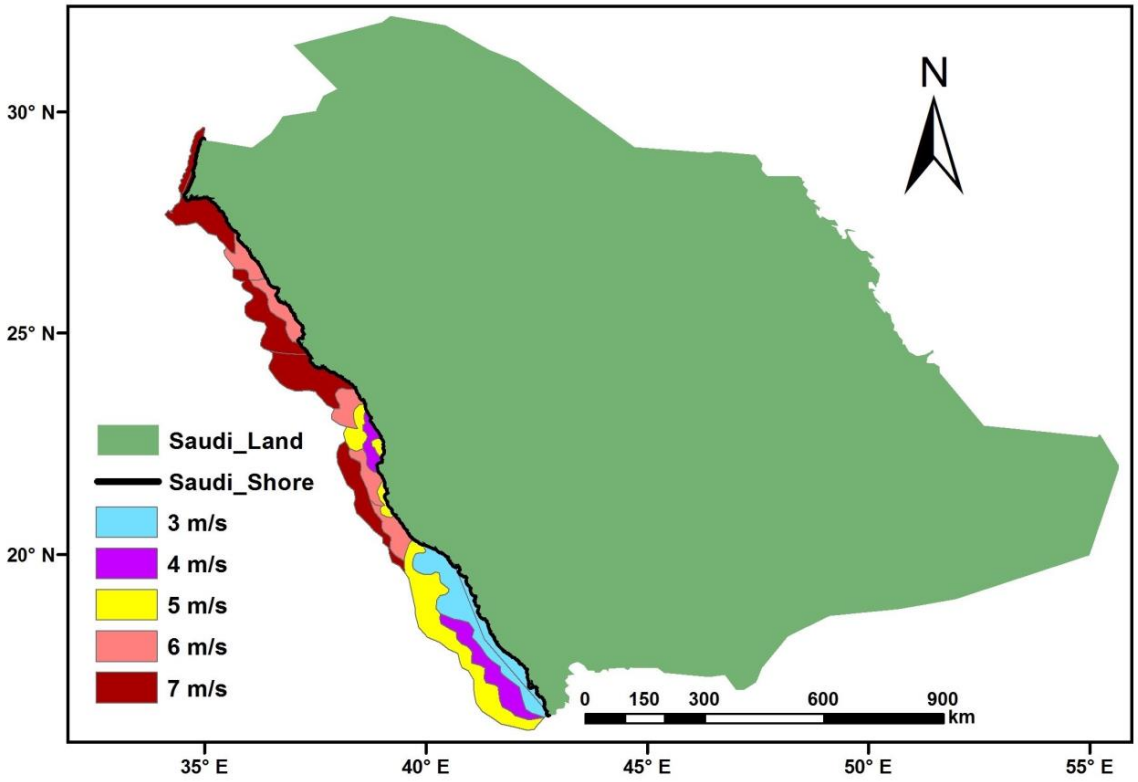

Fig. 4: Wind Speed [m/s] map around the Red Sea coastline of KSA.

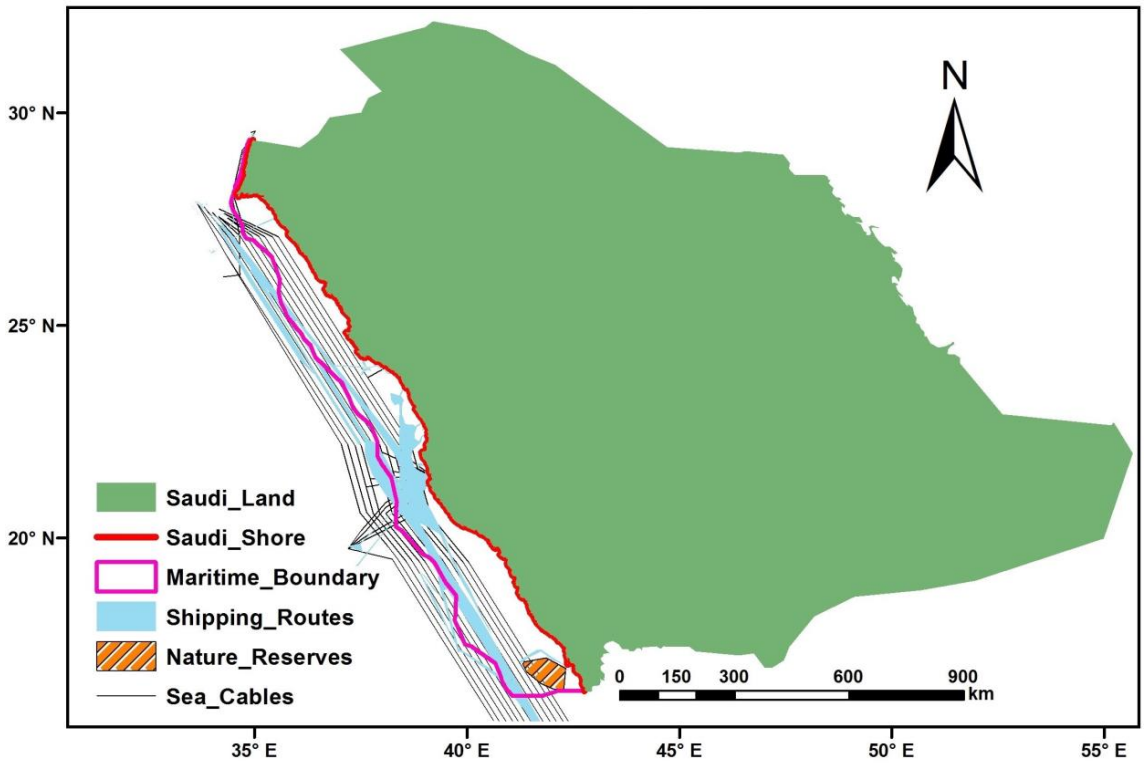

Fig. 5: Raster layer for the all restricted areas around the Red Sea region of KSA.

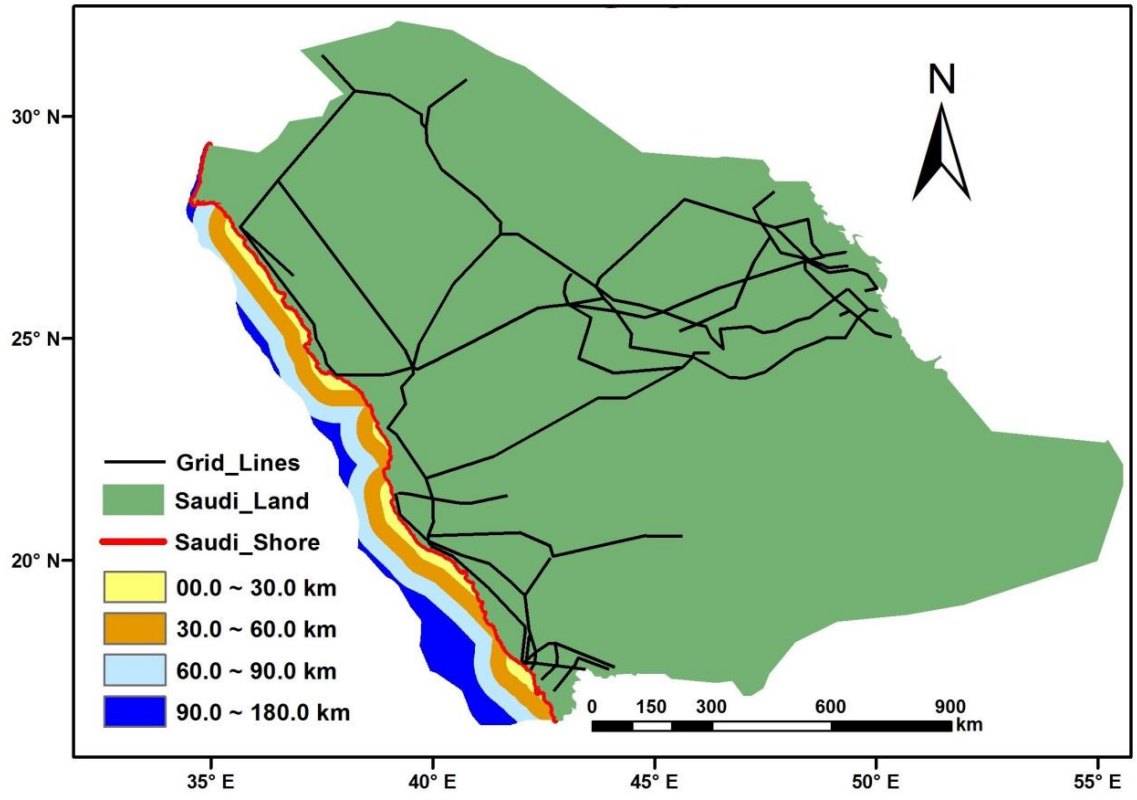

Fig. 6: KSA electricity grid lines for and the distance between cells and the grid near the Red Sea region of KSA.

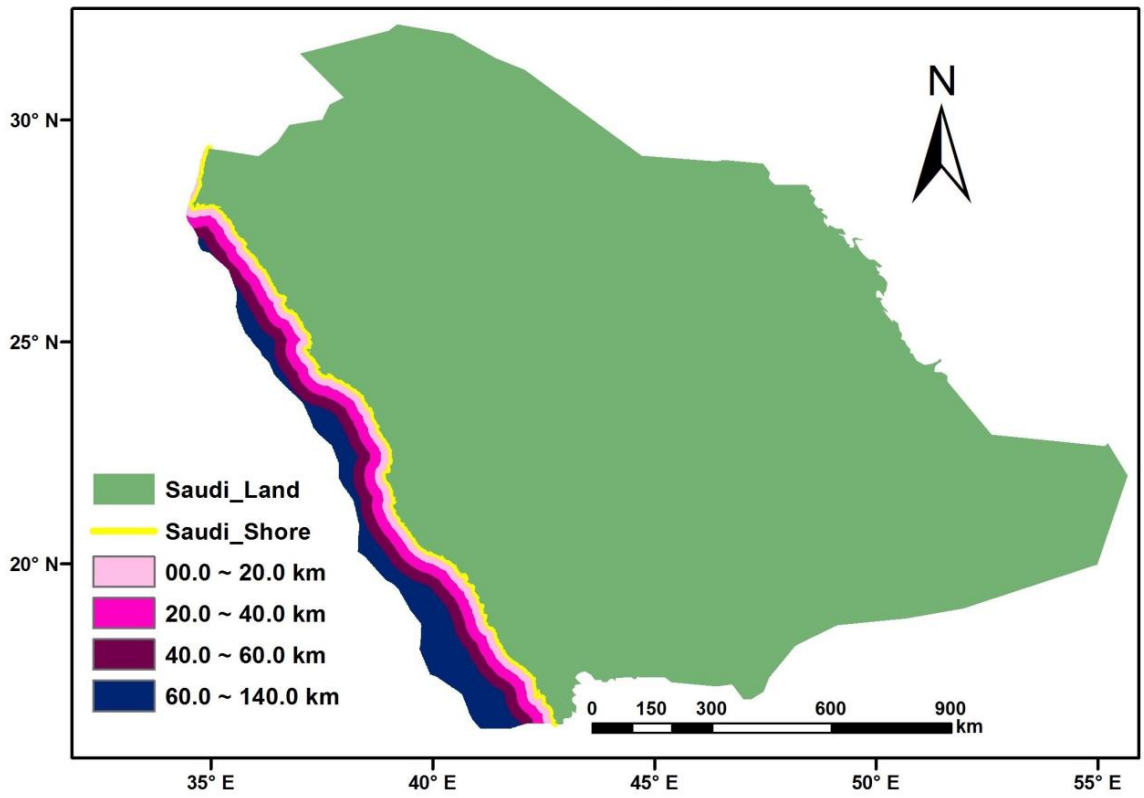

Fig. 7: Layer map of the distance between cells and shoreline around the Red Sea region of KSA.

4. Results, Discussion and Conclusions

The results shown here were based on analysis undertaken for the wind energy potential for the offshore Red Sea region of KSA. The analysis is based on a the development of a Geographical Information System (GIS) encompassing Boolean Mask technique through which a model was developed to create a map for offshore wind farm locations in the Red Sea, KSA. The developed model to solve the spatial sitting for offshore wind farms is efficient and was successful to deal with the conflicting constraints.

Using the UK's London Array wind farm which has an area of 122 km^2 (The Crown Estate, 2012) as a minimum required area (threshold) for offshore wind farms, the analysis was set to identify different locations as possible areas for offshore wind farms in KSA. Ten different locations which conform to the London array threshold were identified using the Boolean Mask map as shown in Fig.8.As can be seen from the figure, the largest locations can be found in the middle part of the coastline stretch, which is due to the main two constraints (wind speed and water depth), which are centred in two different directions of the map, see Fig.3, 4, and also the results in Fig.9.

To estimate the offshore wind power potential for the identified sites, we use the analysis to estimate the array spacing between offshore wind turbines developed by (Sheridan, Baker, Pearre, Firestone, & Kempton, 2012) given by Equation 3 below.

$$S = R_d^2 \times L_d \times L_c \qquad \text{(eq. 3)}$$

Where:

S is the array spacing between offshore wind turbines

R_d is rotor diameter

L_d is the downwind spacing factor

L_c is the crosswind spacing factor

Furthermore, and according to E.ON data (E.ON, 2012), to reduce turbulence interaction between turbines, the ideal turbine spacing is 5 to 8 times rotor diameter. In our analysis we confine the turbine capacities to a 5 MW and 3.6MW turbines to estimate offshore wind power for the identified sites. The 5 MW turbine has a 126m rotor diameter and the characteristics of the turbine were adapted from (Jonkman, Butterfield, Musial, & Scott, 2009). The 3.6 MW turbine has a 107m rotor diameter and the characteristics of the turbine were adapted from (Ajayi, Fagbenle, & Katende, 2011).

Table 2 shows the area for each possible location for offshore wind farm. The two dimensions a, and b are length and width of the rectangular of the locations measured in ArcGIS. The power in GW represent the full power captured by the turbines and was calculated for both 5MW, and 3.6MW using Equation 3. While the last two columns of the table show the estimated actual power assuming a capacity factor, C_f, of equal 0.4 and 0.5. The Capacity Factor which also known as the Load Factor ranges from 0.32 to 0.43 for 80m – 107m rotor diameter, and from 0.40 to 0.50 for turbines with rotor diameter more than 120m (Estate, 2017).

Table 2: Estimate offshore wind power for the chosen sites, where a, and b are the length and width of the rectangles of the location shown in Fig.9.

Location, see Fig. 10	a [km]	b [km]	Area [km^2]	Power (GW)		Estimated Power for	
						C_f = 0.40	C_f = 0.50
				3.6MW turbine	5.0MW turbine	3.6MW turbine	5.0MW turbine
Location 1	11.8	27.8	328.0	1.7	2.6	0.7	1.3
Location 2	7.2	33.0	237.6	1.2	1.9	0.5	0.9
Location 3	7.2	24.6	177.1	0.9	1.4	0.4	0.7
Location 4	9.2	18.5	170.2	0.9	1.3	0.4	0.7
Location 5	5.3	26.9	142.6	0.7	1.1	0.3	0.6
Location 6	14.3	24.1	334.6	1.8	2.7	0.7	1.4
Location 7	11.8	33.2	391.8	2.0	3.1	0.8	1.5
Location 8	18.6	47.6	885.4	4.6	7.0	1.8	3.5
Location 9	7.3	38.0	277.4	1.4	2.2	0.6	1.1
Location 10	7.7	21.8	167.9	0.9	1.3	0.3	0.7
Total			3122.5	16.1	24.6	6.4	12.3

As can be seen form Table 2, the total estimated wind power for the identified sites is around 6.4 GW and 12.3 GW for the 3.6MW and 5MW turbines, respectively. These results confirm that offshore wind energy conversion can play a major role in the short and long term plan for the renewable energy expansion in KSA. For instant, utilising the 5MW turbine route would more than satisfy the 9.5 GW target stipulated in the KSA Vision 2030. Hence this work can be used to plan for offshore wind expansion in KSA and provide a knowledge platform for stakeholders interested in wind energy deployment.

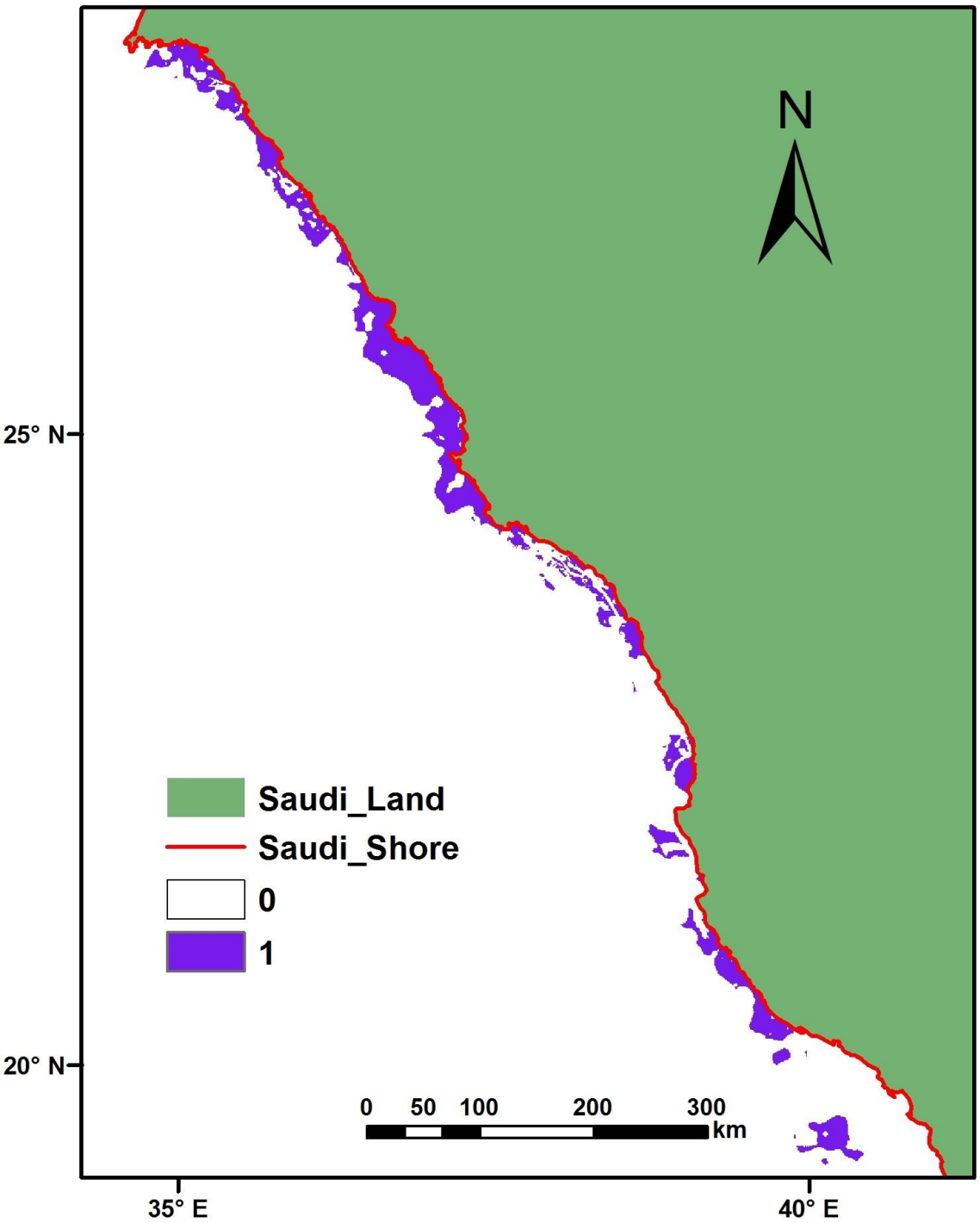

Fig. 8: Final Boolean Mask for offshore wind areas around the Red Sea, KSA.

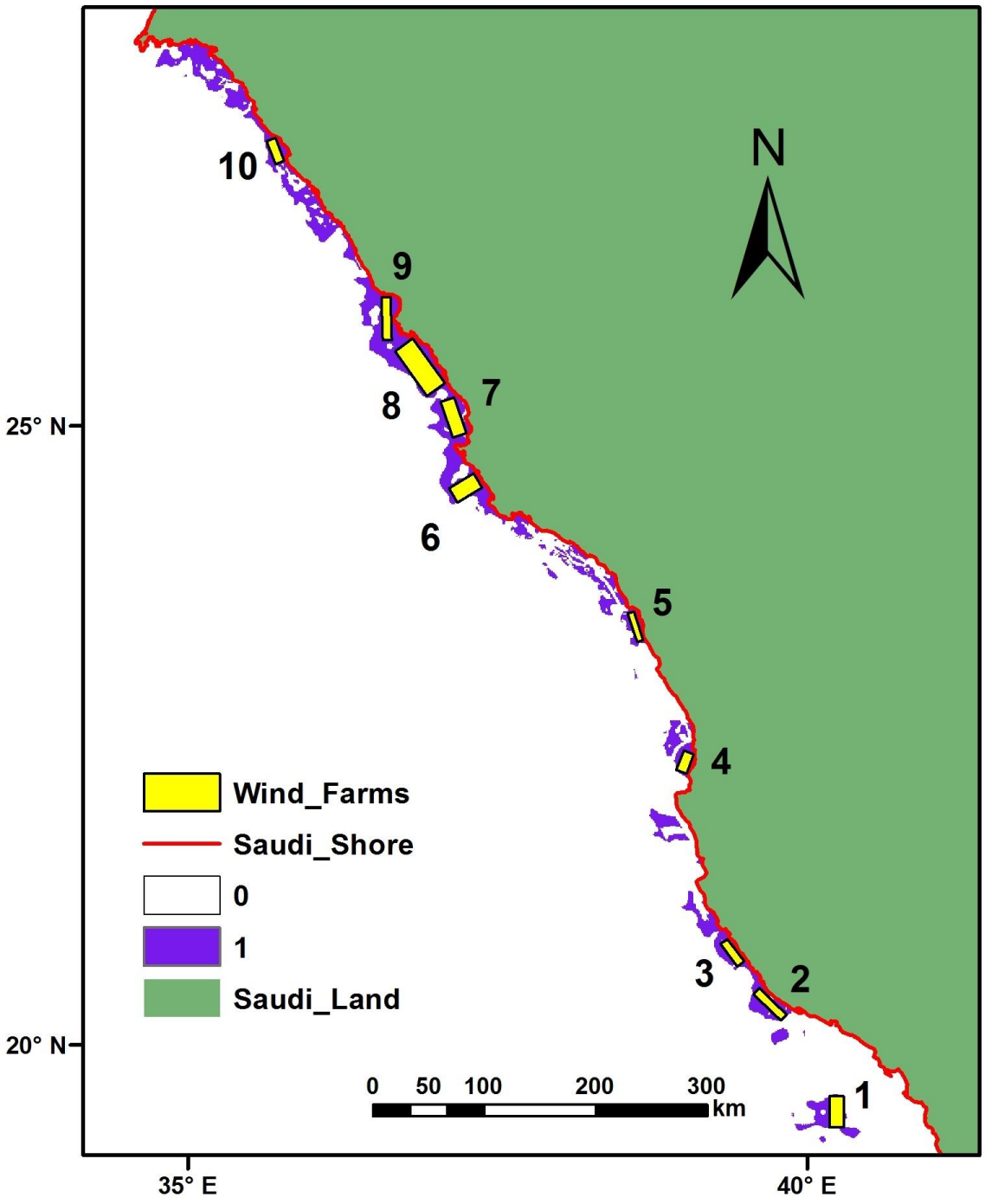

Fig. 9: Locations of the proposed offshore wind farms around the Red Sea region of KSA.

5. Acknowledgment

This work within the activities of the Energy and Climate Change Division and the Sustainable Energy Research Group at the University of Southampton (www.energy.soton.ac.uk) and that of King Salman bin Abdulaziz Chair for Energy Research at King Abdulaziz University (KAU), KSA. The research is part of a PhD programme sponsored by the Faculty of Engineering, Port Said University, Egypt.

6. References

Ajayi, O., Fagbenle, O. R., & Katende, J., 2011. Wind profile characteristics and econometrics analysis of wind power generation of a site in Sokoto State, Nigeria. Energy science and technology, 1(2), 54-66.

Aramco. (2017). Petrol oil extraction map, KSA. Retrieved from http://www.saudiaramco.com/en/home.html

Archer, C. L., & Jacobson, M. Z., 2005. Evaluation of global wind power. Journal of Geophysical Research: Atmospheres, 110(D12).

Bahakeem, A. S., 2015. A Hybrid Renewable Energy Model For Medina City of Saudi Arabia Using Integer Linear Programming. Journal of Electrical and Electronics Engineering (IOSR-JEEE), 9,(5).

CB, S. V., 2017. CfD allocation round two. Retrieved from https://home.kpmg.com/content/dam/kpmg/uk/pdf/2017/09/cfd-allocation-round-two-energy-update.pdf

E.ON., 2012. Offshore Wind Energy Factbook. E. ON Climate & Renewables GmbH.

Eastman, J. R., Jiang, H., & Toledano, J., 1998. Multi-criteria and multi-objective decision making for land allocation using GIS Multicriteria analysis for land-use management (pp. 227-251): Springer.

esri., 2012. The ArcGIS Help Library. Retrieved from http://help.arcgis.com/en/arcgisdesktop/10.0/help/

Estate, T. C., 2017. Offshore wind operational report January – December 2016. Retrieved from https://www.thecrownestate.co.uk/media/1050888/operationalwindreport2017_final.pdf

Estoque, C., 2011. GIS-based multi-criteria decision analysis,(in natural resource management). Ronald, D1–Division of spatial information science, University of tsukuba.

Gazette, S., 2016. Full Text of Saudi Arabia's Vision 2030. Saudi Gazette, 26.

GENI., 2017. National Electricity Transmission Grid of Saudi-Arabia. Retrieved from http://www.geni.org/globalenergy/library/national_energy_grid/saudi-arabia/index.shtml

Jiang, H., & Eastman, J. R., 2000. Application of fuzzy measures in multi-criteria evaluation in GIS. International Journal of Geographical Information Science, 14(2), 173-184.

Jonkman, J., Butterfield, S., Musial, W., & Scott, G. (2009). Definition of a 5-MW reference wind turbine for offshore system development. National Renewable Energy Laboratory, Golden, CO, Technical Report No. NREL/TP-500-38060.

Kieffer, G., & Couture, T., 2015. Renewable energy target setting. IRENA, Masdar.

Knopper, L. D., & Ollson, C. A., 2011. Health effects and wind turbines: A review of the literature. Environmental Health, 10(1), 78.

Mortensen, N. G., Said, U. S., & Badger, J., 2006. Wind Atlas of Egypt: RISO National Laboratory, New and Renewable Energy Authority, Egyptian Meteorological Authority.

Rehman, S., 2005. Offshore wind power assessment on the east coast of Saudi Arabia. Wind Engineering, 29(5), 409-419.

RSNF., 2017. Marine military restricted areas for the Royal Saudi Navy Forces Retrieved from https://www.rsnf.gov.sa/RoyalNavy/Pages/home.aspx

Sheridan, B., Baker, S. D., Pearre, N. S., Firestone, J., & Kempton, W., 2012. Calculating the offshore wind power resource: Robust assessment methods applied to the US Atlantic Coast. Renewable Energy, 43, 224-233.

SWA., 2017. Protected areas map. Retrieved from https://www.swa.gov.sa/en/protected-areas/protected-areas-map

TeleGeography Company., 2015. Submarine Cable Map. Retrieved from http://www.submarinecablemap.com/

The British Oceanographic Data Centre., 2014. The GEBCO_2014 Grid Retrieved from www.gebco.net

The Crown Estate., 2012. Round 3 Offshore Wind Site Selection at National and Project Levels. Retrieved from

The MarineTraffic., 2015. Ship Density Maps. Retrieved from https://www.marinetraffic.com/

Selection and Design of Offshore Wind Turbine Foundations for the Red Sea Area - Egypt

MOSTAFA MAHDY[1], DAVID RICHARDS[2], AND ABUBAKR S. BAHAJ[3]

[1] *University of Southampton, SO17 1BJ, United Kingdom, m.mahdy@soton.ac.uk*
[2] *University of Southampton, SO17 1BJ, United Kingdom, djr@soton.ac.uk*
[3] *University of Southampton, SO17 1BJ, United Kingdom, A.S.bahaj@soton.ac.uk*

Abstract: The remarkable growth of offshore wind farms (OWF) coupled with the wide potential of new sites for deploying such farms, will require cost optimised solutions. Foundations and reliable method for select them to match site conditions forms part of such cost optimisation. By the end of 2015, Monopile systems represent more than 80% of the total installed foundations, while the other types such as Gravity Base, Tripods and Jackets represent the rest. Water depth and installation cost are the main criteria to select offshore foundation type. For this work we have selected three different locations in the Red Sea around the southern tip of Saini Peninsula, using Boolean Mask technique. The sites were located less than 20 km from the nearest port in Egypt, and have ample wind resource of speed above 9 m/s, and an average water depth is 25m. This work aims to provide foundation solutions appropriate to these sites.

A Monopile system was designed for the 3 different sites taking into account their conditions – solid type, depth etc. The designs were achieved through a review of current state of art and additional analysis of the different technologies available for Monopile foundations. The results indicate that for the sandy soil type of the three chosen locations, Monopile foundation system (8 cm wall thickness, 6 m diameter with driven depths ranged from 16 to 24 m) are safe and economical to use for a modelled 5MW offshore wind turbine. All the structural analysis for the foundations in three sites was accomplished using ABAQUS software programme. A cost benefit analysis was conducted to update the outdated Monopile cost estimation providing relevance to sites selected. The results indicate that the achieved Monopile foundation designs are capable of supporting a 5 MW wind turbine for water depths in the range 20 m to 24 m pile depth Our economic analysis indicate that such foundations will have a of £4.9 million which compares well with published data.

Keywords: Offshore wind, Foundation, cost, ABAQUS, Monopile.

1. INTRODUCTION

Red Sea of Egypt is located between 24º53`E, 34º33`E and 22º03`N, 31º41`N, and has approximately 1850 km of coastal line. The costline extended from Taba in the north to Hala`ib Triangle in the southeast, 650 km of its shoreline are located on the Gulf of Suez and Aqaba (Minister of State for Environmental Affairs 2013), see Figure 1. Wind speed around the El-Zaafarana area exceeds 10 m/s (measured at 80m above the MSL) blowing from one direction all over the year (Mortensen, Said et al. 2006). Soil conditions are also significant with bearing capacity (modules of elasticity) more than 30 MPa, medium to dense sandy soil, which is significantly robust to deploy offshore wind foundation.

Electricity consumption in Egypt is increasing annually by around 6% (The Ministry of Electricity and Energy of Egypt 2014). Over the last five years due to a population increase of 12%, electricity consumption has increased by 33.5 % and in an attempt to meet demand, a 27% increase in generating capacity was built during this period(The Ministry of Electricity and Energy of Egypt 2014). However, for the same period, the gap between production and consumption has , widened, due to population increase and industrial growth (Bahgat 2013: 12-37).

Offshore wind energy is starting to have a significant presence in the renewable energy sector. In 2016, over 2.2GW of offshore wind capacity was installed, bringing the worldwide cumulative installed capacity to over 14GW (European Wind Energy Association 2016). For the UK only, offshore wind currently contributes about 5% of the annual electricity demand, which is expected to grow to 10% by 2020 (European Wind Energy Association 2016). One of the main capital cost of offshore wind is that for the foundation. The main parameter to reduce offshore foundation cost is to choose and design suitable foundation taking into account site conditions such as water depth, climate, and soil conditions.

Offshore foundation selection depends mainly on water depth and their installation cost. These two parameters seem to be the most important in the selection process which is geared to minimise overall wind energy farm cost and hence the cost of energy. Most of the work undertaken on offshore wind farms considered only Monopile foundations where the cost is deemed mainly dependent on water depth, with some consideration being given to soil type conditions. In this work, we explore the different offshore wind turbine foundations and present a framework for the selection and design of appropriate foundation types based on site location, water depth, cost, and past and current state of art of the designs.

The paper has two main parts, the first covers the determination of suitable sites for offshore wind farms in the Red Sea, and this step is done using Boolean Mask technique. The second part deals with offshore foundation design and selection using the ABAQUS the 3-D finite element structural software program. Foundation types and specification are also discussed in the final part of the paper.

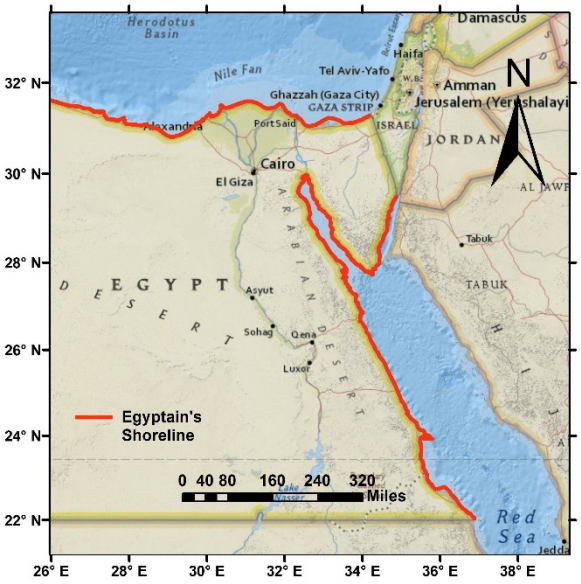

Figure 1: Study area map, the map generated using ArcGIS library maps (esri 2012).

2. OFFSHORE WIND TURBINE (OWT) FOUNDATION

Operating in the sea, offshore wind farms (OWF) creates additional challenges in relation to design of turbine foundations. The design has to be robust to withstand turbine loads to seabed floor as well as the impact of sea conditions. Support system for the offshore wind turbine (OWT) is an important factor in the design and installation process and cost of foundations represent about 25 to 34% of the total cost of OWT (Bhattacharya 2014).

OWT consist of four parts, rotor-nacelle, tower, sub-structure, and foundation (Figure 2). **Rotor** is a rotating propeller typically, consists of three blades, turns around its horizontal axes, converting the kinetic energy of wind to a mechanical power. The **nacelle** contains the power take-off including the shaft, brakes and generator, power electronics etc., which receives the mechanical power from the rotor, transforming it to electricity. **Tower** is a steel cylinder, which connects the nacelle to the sub-structure. **Sub-structure** is the part that connect between the tower and the foundation, sub-structure could be a monopod, which is a cylinder (see A, C in Figure 2), or a tripod (see b in Figure 2). **Foundation** is a structure, which transfers vertical and lateral loads to the seabed or the sea floor.

Figure 2, also shows the main three concepts of OWT foundations. A **Monopile** foundation, which is a hollow steel pipe driven into the seabed, (Figure 2-A). The three legs of the tripod are laying on a three short piles in the **Tripile**

foundation, (Figure 2-B). **Gravity Base** foundation is simplest type of OWT foundation, consisting of a large pre-cast reinforced concrete block, (Figure 2-C). More details and literature review of OWT foundation is given below.

Foundation type selection depend mainly on OWT installation depth. While Monopile type is used widely around the world in shallow waters (5~30m), the Tripod is used for deep water (30~60m). For depths more than 60m, floating foundation could be used. Table 1 shows the world's largest OWF built the mid of 2017. The table, also give the number of turbines, turbine electrical capacity, foundation type and cost, and maximum deployment depth. According to the European Wind Energy Association 80% of the foundations are Monopile, 9.1% are Gravity Base, and Tripods account for 5.3% of the 3,313 OWT deployed in European seas until the end of 2015, (European Wind Energy Association 2016),.

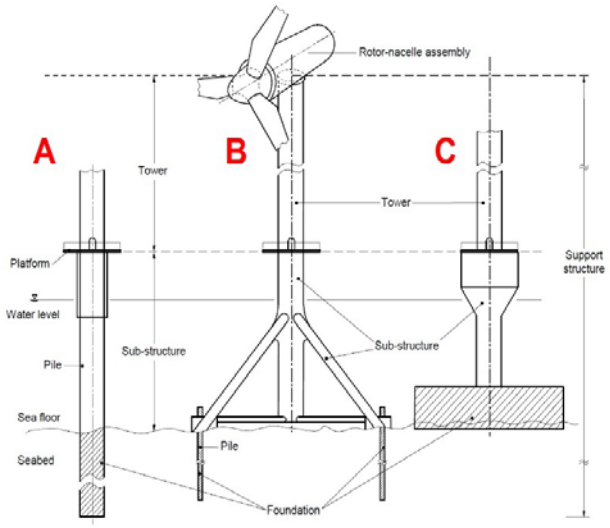

Figure 2: The main three concepts of OWT foundations and its different parts, adopted from (Commission 2009).

Reviewing the foundation technologies used or announced for OWF up to the year 2020, the main foundation type used is Monopile, and Tripod in the second place with a significant difference away from Monopile. The majority of OWF, which are online, under construction or consented around the world, is in transition water between 10 to 30 meter water depths. All these projects are using Monopiles as a foundation support (Arapogianni, Genachte et al. 2013). The max depth (only one consented project) was 50 meter. According to (Arapogianni, Genachte et al. 2013), all attempts to lunch commercial floating OWF are still under development and design, normally all floating OWF projects consist of one turbine with 2 to 7 MW capacity. The final conclusion is that Monopile still the main foundation system around the world. In addition, moving toward deeper water depths, more than 50 meter to gain more energy, still under consideration, it needs more time for the floating foundation solution to move towards the commercial scale.

Gravity base foundations are used for OWT in shallow water less than 15m. The foundation is made of large reinforcement concert block, see Figure 2-C. The foundation resist lateral and rotational displacement depending on its heavy weight. Around 303 out of 3,313 of OWT foundations in Europe are Gravity base (European Wind Energy Association 2016).

Monopile is a simple design structure, which is a cylindrical steel pipe that support a Monopod wind turbine, see Figure 2-A. The pile depth depends on soil conditions and the depth of sand soil layer. It is subjected to a large lateral displacement, vibration, and torsion due to significant values of lateral loads and bending moment. The Monopile is widely used in offshore wind farms, 80%, or 2,653 out of 3,313 of OWT foundations in Europe are Monopiles at the end of 2015, while it represents 97% of the installed foundation in the year 2015 (European Wind Energy Association 2016). Nine out of eleven top largest OWF support structure are Monopile for water depths ranged between 19 and 32 m, see Table 1. A 5 to 7.5 m diameter piles are needed to support 5MW turbine in shallow waters in the range 15 to 30 m depth. Piles of these sizes are needed to enhance the bearing capacity to resist high lateral loads from wind and sea waves (Achmus, Kuo et al. 2009: 725-735). A Monopile is designed with consideration to two types of stress. First, is the ultimate stresses that pile can reach due different load combination (static loads), and the second is the fatigue stress due to cyclic loading (dynamic loads).

The Tripile OWT foundation structure is a three-legged pile (cylindrical steel tubes) to support the Tripod sub-structure, which carries the turbine tower, see Figure 2-B. It is used for depths between 30 and 50m. Despite the fact that the first Tripile was deployed in 2008, 175 out of 3,313 of OWT foundations in Europe are Tripod (European Wind Energy Association 2016). Two of the largest OWF around the world is using Tripile, (European Wind Energy Association 2016). The floating foundations are used for OWTs with sea depth more than 60m, the concept of floating foundation is to fix the OWT on a floating stage and connect the stage to the sea bed using steel flexible wires, the wires then fixed to piles or heavy concrete base. The technology of floating OWT is still under research and development.

Table 1: Largest OWF around the world until the mid of 2017 (European Wind Energy Association 2016, Offshore 2017).

	Park	Region	Year	OWT no	OWT rate [MW]	Capacity [MW]	Max depth [m]	Foundation type	Foundation cost [MM£]
1	London aray	UK	2013	175	3.6	630	25	Monopile	4.2
2	Gemini	Netherland	2017	150	4	600	34	Monopile	5.4
3	Gwynt y Môr	UK	2015	160	3.6	576	28	Monopile	4.2

4	Greater Gabbard	UK	2011	140	3.6	504	32	Monopile	4.7
5	BARD offshore 1	Germany	2013	80	5	400	40	Tripile	10.6
6	Global Tech I	Germany	2015	80	5	400	41	Tripile	6.1
7	Anholt	Denmark	2013	111	3.6	399.6	19	Monopile	3.7
8	Duddon Sands	UK	2014	108	3.6	388.8	23	Monopile	4.1
9	Sheringham Shoal	UK	2013	88	3.6	316.8	22	Monopile	4.4
10	Borkum Riffgrund 1	Germany	2015	78	4	312	29	Monopile	4.7
11	Thanet	UK	2010	100	3	300	25	Monopile	3.2
12	Nordsee Ost	Germany	2015	48	6.15	295.2	25	Jacket	7.6
13	Amrumbank West	Germany	2015	80	3.6	288	25	Monopile	3.3
14	Butendiek	Germany	2015	80	3.6	288	22	Monopile	4.4
15	DanTysk	Germany	2015	80	3.6	288	21	Monopile	4.3
16	EnBW Baltic2	Germany	2015	80	3.6	288	20	Monopile	4.2
17	Sandbank	Germany	2017	72	4	288	31	Monopile	4.9
18	Meerwind Sud/Ost	Germany	2014	80	3.6	288	22	Monopile	4.4
19	Lincs	UK	2013	75	3.6	270	15	Monopile	4.7
20	Burbo Bank Ext	UK	2017	32	8	256	17	Monopile	8.8
21	Humber Gateway	UK	2015	73	3	219	16	Monopile	3.5
22	Northwind	Belgium	2014	72	3	216	23	Monopile	3.4
23	Westermost Rough	UK	2015	35	6	210	25	Monopile	8.7
24	Horns Rev 2	Denmark	2010	91	2.3	209.3	13	Monopile	1.5
25	Rødsand 2	Denmark	2010	90	2.3	207	9	Gravity	1.5
26	Trianel Bokum I	Germany	2015	40	5	200	33	Tripile	6.3

3. BOOLEAN MASK

Boolean overlay, is widely used to locate sites with no restrictions (constrains). Boolean relationships are known as the (And, OR, or Not) relations. These relations are applied to achieve a specific decision with valid or not invalid as a result value. The resulted map has only two colours (boundaries), one is for the unrestricted areas and the other represents restricted areas. Boolean mask is suitable for simple and quick spatial decisions, such as which offshore areas are not restricted and can be developed (Jiang and Eastman 2000: 173-184). **Constraint** can be defined as a criterion that eliminate alternatives; alternatives in our study are the pixel cells on the ArcGIS map. It accomplishes the limitations or restrictions of the constraint, so it is a (true/false) relationship. For instance, if the law prohibited constructing offshore projects in the sea military areas, these areas will be excluded as a possible solution. Constraints have the same priority, applied using Boolean logic, “0 or 1”. Zero values are when the constraints are true, and vice versa.

Table 2: Constrains 0, and 1 definitions and data source data.

Constrain	0 description and data source	1
Wind Power	Areas with wind speed between 3 and 25 m/s, wind speed data were adopted from New and Renewable Energy Authority, Egyptian Meteorological Authority (Mortensen, Said et al. 2006).	Else
Water Depth	Depths less than 5.0 m or more than 60.0 m, the bathymetry data was adopted from British Oceanographic Data Centre (BODC) (The British Oceanographic Data Centre 2014).	Else
Distance to the shore	Distance less than 1.5 km or more than 200.0 km, the distances data was adopted and processed using ArcGIS Program (esri 2012).	Else
Military Practice and Exercise Areas	locations were adopted from Ministry of Defence and Military Production (Ministry of Defence and Military Production 2015).	Else
Shipping Routes	Shipping areas adopted from TeleGeography company web site (TeleGeography Company 2015).	Else
Oil & Gas Wells	Areas data were adopted from Egyptian Natural Gas Holding Company (EGAS) (The Egyptian Natural Gas Holding Company (EGAS) 2015).	Else
Nature Reserves	Places in the sea area protected by the power of law to reserve the endangered marine ecosystem species, marine parks were adopted from the Egyptian Environmental Affairs Agency (The Egyptian Environmental Affairs Agency 2015)	Else
Sandy soil layer level	Sites with sandy sediment layer closer to the seabed (less than 20m), data were adopted from different sources (MAS Consultant Office 2005, Ghaly, Khalil et al. 2013, El Diasty, El Beialy et al. 2014: 155-167).	Else

A Boolean mask was created to exclude the restricted cells by giving them 0 value, and 1 value to the others cells, see Table 2, which describes constraints limits. A Raster Calculator tool was used to gather all these constrains

layers in one layer, see Figure 3. Boolean overlay produced by multiplying all the constraints layers together, the resultant map is called the Boolean Mask Map. The equation used to calculate the Mask Map is given by:

$$Suitability = \left(\prod_{j=1}^{l} C_j\right) \quad (1)$$

Where: C_j = constraint j (Boolean Mask j), Π = product of constraints, ℓ = number of constraints.

4. SOIL PROPERTIES FOR THE CHOSEN SITES

Three sites were located using Boolean Mask methodology. The locations are not very far of each other (Figure 3), but the soil characteristic are different as shown in Table 3. The soil properties considered here in terms of: friction angle (φ) in degrees, submerged unit weight (γ_{sub}) in kN/m^3, Young's modules / modules of elasticity (E_s) in MPa, Poisson's ratio (v), dilation angle (ψ) in degrees, and maximum yield stress (f_y) in kPa. Table 3, shows the soil properties for the chosen sites in the Red Sea and is used to design offshore foundation for each location.

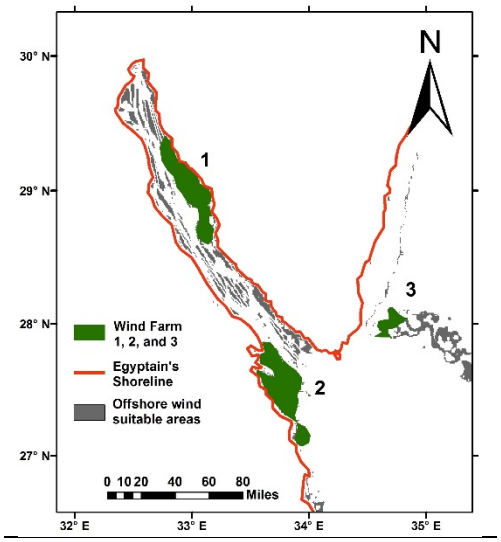

Figure 3: Boolean overlay map, proposed offshore sites are in green colour.

Soil **angle of friction** (ϕ) is driven from the Mohr-Coulomb failure circle, it describes the shear friction resistance between small particles of soil under a normal effective stress. **Poisson's ratio** (v) is the ratio between horizontal strain to the vertical strain under a stress within the elastic stat of the soil. **Modules of elasticity** (E_s), called also as Young's modules, which is the soil stress to its strain, also within the elastic stat of the soil. The **dilation angle** (ψ) "controls an amount of plastic volumetric strain developed during plastic shearing and is assumed constant during plastic yielding" (Bartlett 2010). For sandy soil as a non-cohesive soil, the dilation angle (ψ) relays on the friction angle (ϕ) of the soil. For sand with ϕ >30° the value of the dilation angle can be estimated as ψ =φ-30°, ψ = 0 in case of negative values of dilation angle (Bartlett 2010).

Table 3: Soil properties for the three chosen sites in Egypt

	Unit	Site 1: El-Zaafarana	Site 2: El-Gouna	Site 3: Nabq Bay
Soil Type	-	Medium Sand	Medium Sand	Dense Sand
ϕ	Degree °	30	34	39
γ_{sub}	kN/m^3	9	9.5	11
E_s	MPa	32	44	70
v	-	0.3	0.3	0.3
ψ	°	0	0	0
f_y	kPa	0.001	0.001	0.001
Source	-	(HIDELECCO Construction company 2010)	(ORASCOM Construction Limited 2012)	(Redcon Construction 2007)

5. SERVICEABILITY STEADY STATE LOADS

The chosen offshore wind turbine is that specified by the USA National Renewable Energy Laboratory (NREL) of capacity 5MW. Table 4 display the 5MW NREL wind turbine characteristic, including the tower hub Height, nacelle mass, and rotor diameter and blade angles. The loads combinations used for both the ultimate and serviceability limit stats. Six components were calculated in each limit state, which are F_x (Perpendicular load in x direction), F_y (Perpendicular load in y direction), F_z (vertical load), M_x, M_y, and M_z (moments rotate around x, y, and z axis respectively) For three load combination which are 6C, 3C, and 2C, (Figure 4).

Table 4: 5MW NREL wind turbine characteristic adopted from (Jonkman, Butterfield et al. 2009).

Parameter	Value
Rating	5 MW
Rotor Orientation, Configuration	Upwind, 3 Blades
Control	Variable Speed, Collective Pitch
Drive train	High Speed, Multiple-Stage Gearbox
Rotor, Hub Diameter, Hub Height	126 m, 3 m, 90m
Cut-In, Rated, Cut-Out Wind Speed	3 m/s, 11.4 m/s, 25 m/s
Cut-In, Rated Rotor Speed	6.9 rpm, 12.1 rpm
Rated Tip Speed	80 m/s
Rotor Mass	110,000 kg
Nacelle Mass	240,000 kg
Tower Mass	347,460 kg

Wind loads in the Serviceability Steady State loads, were adopted from NREL's report, which was done utilising FAST (Fatigue, Aerodynamics, Structures, and Turbulence) simulations programme, where they neglected the aerodynamic loads affecting the wind turbine tower before calculating the loads (Jonkman, Butterfield et al. 2009). Neglecting these loads on the tower was because they such loads are very small relative to those of the rotor trust loads. Using (Jonkman, Butterfield et al. 2009)'s charts and (Mortensen, Said et al. 2006)'s wind speed data, the rotor thrust is estimated to be 750 kN and the Rotor torque is 4100 kN.m. Therefore, the final loads from wind in steady state is F_y= 750kN and M_x = 4100 kN.m.

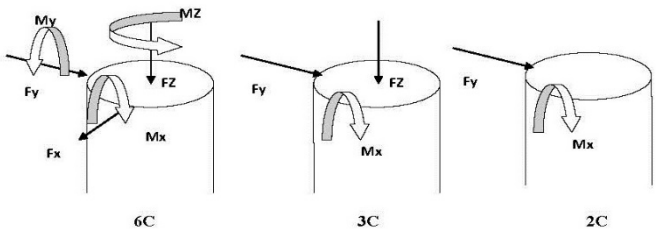

Figure 4: Different load combinations applied at MSL (mean sea level), adopted from (Abdelkader 2015).

The wave properties used to calculate the loads that affect the wind turbine tower are (Fery, Bruss et al. 2012: 446-455): Max Significate Wave Height (H_s) = 4 m, Mean Wave Time Period (T) = 7 s, Average Water Depth (d) = 25m. The next equations adopted from (Manual 1984) are used to calculate the wave force acting on the proposed Monopile system:

$$L = \frac{g\,T^2}{2\pi} * \tanh\frac{2\pi d}{L} \qquad (2),$$

$$P = \rho g * \frac{H_s}{2} * \cos\theta * \frac{\cosh\frac{2\pi\,(z+d)}{L}}{\cosh\frac{2\pi d}{L}} \qquad (3)$$

Where: L is the wave length [length], g is the gravitational acceleration [length/time^2], P is the pressure at any distance below the fluid surface [force/length^2], ρ is the mass density of salt water = 1,025 [kg/m^3], θ is the principal (central) direction for the spectrum measured counter clockwise from the principal wave direction [degree], and z is the water depth below the MSL [length].

Using charts the site conditions data listed above, and using equations from (Manual 1984), the estimated wave load is equal to 850 kN and acting in the y direction. The final OWT weight force was calculated using data from Table 4 to be 6800KN. Therefore, the final forces affecting the wind tower will be: **F_y= 1600kN, F_z= 6800 kN**, and **M_x = 4100 kN.m**, these 2 components will be applied at MSL (mean sea level).

6. ULTIMATE STATE LOADS

The ultimate loads, six load component (three forces and three moments) were obtained from (Abdelkader 2015). Load values were concluded using scale model (1:150), as shown in Figure 5. The force and moment loads were calculated at the base of the scaled turbine model, which was robust (no-displacements were allowed at the base of the prototype) and light-weighted (Abdelkader 2015). The applied the extreme wind and wave values, were extracted by Abdelkader from (Jonkman and Musial 2010: 275-3000) where the results were measured in a parked rotor position (the wind turbines rotors are normally parked during the extreme events). The results were conducted using different "blade configuration scenarios with wind coming from all possible directions" (Abdelkader 2015), see Figure 5, **B, and C**. Then, Abdelkader compared his results with FAST (Fatigue, Aerodynamics, Structures, and Turbulence) programme simulations, which were done by (Jonkman, Butterfield et al. 2009). Finally, he found that his lab results are more creditable than FAST numerical results to be used in offshore wind foundation. The values of the loads are: **F_x= 1750kN, F_y= 1500kN, F_z= 8000 kN**, **M_x = 15E4 kN.m M_y= 15E4 kN.m,** and **M_z = 15E3 kN.m**

Figure 5: Wind Tunnel test configurations: (A) 1:150 5 MW wind turbine prototype with 1:150 scale, (B) rotor angle = (0°-120°-240°) and (C) rotor angle = (60°-180°-300°), adopted from (Abdelkader 2015).

7. FOUNDATION SELECTION

The foundation selection depend on two parameters (water depth and overall cost). The average water depth of the three chosen sites ranged from 20 to 25 meter, so the Gravity base, Tripile, and Floating foundations are neglected. According to Estate the foundation cost is sensitive to steel price, and it represent about 40 to 50% of the total cost of the foundation including installation and transport (Estate 2012).

7.1. Foundation cost

Foundation cost is estimated by considering two elements: manufacturing cost and the cost of transport and installation. Manufacturing cost are determined according to water depth, actual loads (wind and waves), and soil conditions. The simplest way, is to design the offshore foundation for ease of serviceability and environmental loads, then to calculate the actual cost of the proposed design. But for comparison purposes, empirical equations are used to estimate the foundation cost. The next three imperial equations to estimate the Monopile foundation cost were extracted from (Nielsen 2003):

$$C_f = 320P_{WT}\,(1+0.02\,(D-8)) * (1 + 0.08 * 10^{-6}\,(h\,(d/2)^2 - 10^5)) \qquad [k€/turbine] \qquad (4)$$

Where: C_f [k€/MW] is the estimated foundation cost, D [m] represents sea depth, P_{WT} [MW] is the rated power of a single offshore wind turbine, h [m] is hub height, d [m] is rotor diameter.

Applying equation (4) and using the available data form Table 1, the error between the estimated foundation cost and actual cost are more than 50% for all recently installed or announced mega projects. So, a regression analysis was conducted to produce a new foundation cost equation, which has more up to date factors and is much more reliable. This is now given as Equation (5), which was derived using STATA program and the collected data shown in Table 1.

$$C_f = 0.0397P_{WT} * D + 0.939 \qquad [MM£/turbine] \qquad (5)$$

8. FOUNDATION DESIGN

The main challenge of OWT foundation is to deliver all loads resulting from the wind turbine weight and dynamic working to the seabed level without exceeding the allowed deformation. This challenge could be satisfied if a three loading states are considered and assessed (Bhattacharya 2014). First, **Ultimate Limit State** is required to apply the ultimate lateral loads from wind and sea waves, especially in extreme event, such as storms or hurricanes, which could be expressed as the combination of the ultimate moment, lateral and axial loads. In this case the turbine rotor is stopped from moving using brakes to save the turbine from being damaged. Second, **Serviceability Limit State**, which is the state to apply the predicted service wind and waves loads for one year at least of its expected time of the OWT. Last, **Fatigue Limit State**, which requires the modelling to apply the predicted service wind, waves, and also the expected loads from extreme events for a long time period to estimate the life cycle of the OWT foundation.

The maximum allowable pile head rotation after OWT subjected to ultimate and serviceability static load cases is 0.5 degree, and also the maximum cumulative permanent rotation due to cyclic loading over the designed life span of OWT is 0.5 degree (Malhotra 2011). To avoid OWT collapse, the foundation should be designed with frequency more than the tower and water waves frequencies, which force the foundation to be relatively stiff, hence will be more expensive than the flexible foundation (Malhotra 2011). The maximum allowable pile head lateral and vertical displacements are 6 and 10 cm, respectively (Frank 2006: 577-586).

8.1. Foundation system description

The proposed system for a 5MW OWT is Monopile foundation, which contains of two main pieces: First part is a hollow steel pile 8 cm thickness, 6 m diameter, and 40 m length. The first 20 meter of the pile will be driven into the sandy soil of the chosen sites, and the other 20 are submerged by seawater. The second part is the transitional part, which is subjected to tidal range and sea waves. Transitional part used to connect the pile with the OWT tower, and they are connected using a bolted flange connection, see Figure 6.

8.2. Numerical modelling

The numerical analysis to examine the three proposed system was done using the finite element method. The ABAQUS (Hibbett, Karlsson et al. 1998) software programme was applied to model the foundation system and soil as a 3-dimensional nonlinear finite element model. The soil and the Monopile system were modelled using 3-D deformable solid elements with different material models. The different types of soil were simulated with an elastic-

perfectly plastic constitutive model and the Mohr-Coulomb failure criterion. The steel pile was represented using elastic-perfectly plastic model and the Mohr-Coulomb failure criterion with the following steel properties: yield strength, f_y = 240 MPa, Young's Modulus, E_s = 200 GPa and Poisson's ratio, v = 0.3. Interaction properties were applied between different materials to ensure the actual simulation including: tangential behaviour with friction coefficient equal to 0.5 with fraction of characteristic surface dimension equal to 0.005; and normal behaviour using the constraint enforcement method and pressure-overclosure as hard contact with allowing separation after contact.

In order to evaluate the performance of the hybrid system relative to the conventional Monopile system, five different foundation systems were analysed. The different soil properties of the soil were considered using the data from Table 3. In addition, the different load combinations were applied, for the serviceability limit, only the 3C, and the 2C combinations were applied, and for the ultimate limit the 6C, 3C, and 2C load combinations were used, see Figure 4 The boundary size of the soil was: in the horizontal direction was estimated to be three times the pile diameter (3×6m = 18m), measured from the pile toe. In the vertical direction, the soil circle boundary was estimated to be ten times the pile diameter (10×6m = 60m), measured from the centre of the pile. The mesh was developed using the automatic sweep meshing technique and the medial axis algorithm, which is available in the ABAQUS (Hibbett, Karlsson et al. 1998). The circle face of the steel shaft and the soil were divided into 16 part. In addition, the vertical dimension of both of them were divided in 1-meter step.

The boundary conditions of the soil were All nodes of the soil model bottom were fixed from translations in X, Y and Z directions. In addition, all nodes of the vertical boundaries of the soil model were fixed translations in X, and Y directions, so nodes can move only in Z direction. Interaction surfaces were applied at the interfaces between the elements representing the pile and adjacent soil that allow pile slippage and separation, which can properly simulate the tangential and normal behaviour.

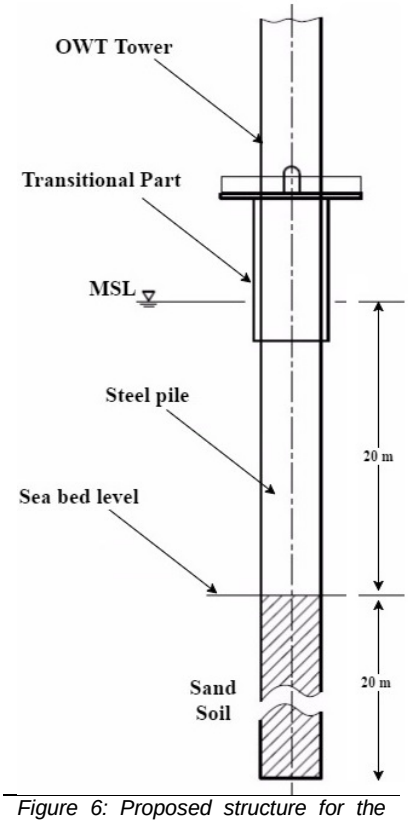

Figure 6: Proposed structure for the Monopile foundation.

9. RESULTS, DISCUSSION AND CONCLUSIONS

The three proposed sites were tested using their soil characteristics, and the results are given in Table 5. The Monopile foundation system with 8 cm thickness, 6 m diameter, and 20 m depth under the sea bed to support 5 MW OWT, was applied in the different locations.

First, the system was modelled under serviceability working loads and subjected to 3C (one horizontal load, one vertical load and one rotating moment) and 2C (one horizontal force and one rotating moment). The results of displacements for the three sites subjected to serviceability limit loads are shown under the column titled "Serviceability limit state" of Tables 5.

Second, the system was modelled using ultimate limit forces and subjected to the following load combinations: 6C (two horizontal forces, one vertical force and three rotating moments), 3C (one horizontal load, one vertical load and one rotating moment) and 2C (one horizontal force and one rotating moment). The values displacements for the three sites subjected to ultimate limit loads are shown in the column entitled "Ultimate limit state" of Table 5.

The maximum allowable displacements for OWT are: a) Lateral displacement at ML [< 6 cm], Pile rotation at ML [< 0.5º], and vertical displacement of the pile [< 10 cm]. By reviewing all serviceability limit state loading displacement for the three sites, all the results are less than the allowable displacement limits, which confirms the foundation system resistance under serviceability limit loads. In addition, the displacement results under ultimate state loading are less than the allowable limits, except for El-Zaafarana site, where lateral displacements at ML are 7 and 6 cm for 6C and 3C loading combination, which are higher than the 5 cm lateral displacement allowable limit. To avoid failure under ultimate state loading at El-Zaafarana site, a 24-meter pile was suggested instead of the 20 meter pile. The 3-D model was modified for the new pile, and the analysis under 6C and 3C ultimate limit state load combinations were applied. The new displacement results were below the allowable limits, Lateral displacement at ML was 5 [cm], and Pile rotation at ML was 0.011º, which confirm the 24 meter pile for El-Zaafarana site.

Floating foundations are still under devolvement and major research is currently being undertaken to support their commercialisation. Hybrid foundations are also still under fundamental research and to our knowledge, there are no plans to build a 1:1 Hybrid foundation prototype in place. However, this is likely to change as we go to deeper water.

Table 5: Displacement results for location Sites 1,2, and 3

Site	Displacement	Serviceability limit state			Ultimate limit state		
		6C	3C	2C	6C	3C	2C
1	Lateral displacement at MSL [cm]	-	18.70	13.30	31	30	20
	Lateral displacement at ML [cm]	-	01.01	00.82	7	6	5
	Pile rotation at ML [degree]	-	0.002	0.001	0.013	0.013	0.009
	Vertical displacement [cm]	-	-4.1	-2.0	-4.3	-4.1	-2.0
2	Lateral displacement at MSL [cm]	-	10.32	09.21	17	19.8	14.9
	Lateral displacement at ML [cm]	-	00.83	00.54	5	4.9	4.1
	Pile rotation at ML [degree]	-	0.001	0.001	0.007	0.007	0.005
	Vertical displacement [cm]	-	-3.9	-1.7	-2.5	-2.7	-1.3
3	Lateral displacement at MSL [cm]	-	09.80	07.94	12	17.2	11.8
	Lateral displacement at ML [cm]	-	00.69	00.48	4.2	4.7	4
	Pile rotation at ML [degree]	-	0.001	0.001	0.005	0.005	0.005
	Vertical displacement [cm]	-	-3.2	-1.3	-1.9	-2.1	-1.1

The structural analysis using ABAQUS program was done to design the selected foundation (Monopile system). The analysis shown that a 24 meter pile is needed to deploy OWT in site 1, a 20 meter pile is suitable for site number 2, and a 16 meter pile could be stable to be used in site 3 (need more investigation). The final estimated foundation cost is 4.9 million pound; the value was calculated using equation 5. C_f = 0.0397x5x20 + 0.939 = 4.9 [MM£/turbine].

Acknowledgment: This work is part of the activities of the Energy and Climate Change Division and the Sustainable Energy Research Group at the University of Southampton. The research is also part of a PhD programme sponsored by the Faculty of Engineering, Port Said University, Egypt. We would also like to show our gratitude to Dr. Ahmed Abdelkader and Mr. Ahmed Elghandour for their support in securing the data used in the research.

10. REFERENCES

Abdelkader, A. R. (2015). Investigation of Hybrid Foundation System For Offshore Wind Turbine. Doctor of Philosophy, The University of Western Ontario, London, Ontario, Canada.

Achmus, M., Y.-S. Kuo and K. Abdel-Rahman (2009). "Behavior of monopile foundations under cyclic lateral load." Computers and Geotechnics **36**(5): 725-735.

Arapogianni, A., A. Genachte, R. M. Ochagavia, J. Vergara, D. Castell, A. R. Tsouroukdissian, J. Korbijn, N. Bolleman, F. Huera-Huarte and F. Schuon (2013). "Deep Water; The next step for offshore wind energy." European Wind Energy Association (EWEA).

Bahgat, G. (2013). "Egypt's Energy Outlook: Opportunities and Challenges." Mediterranean Quarterly **24**(1): 12-37.

Bartlett, S. F. (2010). "Mohr-Coulomb Model."

Bhattacharya, S. (2014). "Challenges in design of foundations for Offshore Wind Turbines." Engineering & Technology Reference **1**(1).

Commission, I. E. (2009). "Wind Turbines—Part 3: Design Requirements for Offshore Wind Turbines." No. IEC61400-3.

El Diasty, W. S., S. El Beialy, A. A. Ghonaim, A. Mostafa and H. El Atfy (2014). "Palynology, palynofacies and petroleum potential of the Upper Cretaceous–Eocene Matulla, Brown Limestone and Thebes formations, Belayim oilfields, central Gulf of Suez, Egypt." Journal of African Earth Sciences **95**: 155-167.

esri. (2012). "The ArcGIS Help Library." Retrieved /14, 2016/07, from http://help.arcgis.com/en/arcgisdesktop/10.0/help/.

Estate, C. (2012). "Offshore wind cost reduction: Pathways study." United Kingdom, May.

European Wind Energy Association (2016). The European offshore wind industry -key trends and statistics 2015.

Fery, N., G. Bruss, A. Al-Subhi and R. Mayerle (2012). Numerical study of wind-generated waves in the Red Sea. Proceedings 4th International Conference of the application of physical modeling to port and coastal protection, Coastlab12, Ghent, Belgium.

Frank, R. (2006). Design of pile foundations following Eurocode 7. Proc. XIII Danube-European Conference on Geotechnical Engineering, Citeseer.

Ghaly, A. I., A. E. Khalil and A. A. Mahmoud (2013). "Stratigraphic Analysis and Petroleum Exploration, Offshore, Nile Delta,Egypt." Seismic Stratigraphy and Seismic Geomorphology.

Hibbett, Karlsson and Sorensen (1998). ABAQUS/standard: User's Manual, Hibbitt, Karlsson & Sorensen.

HIDELECCO Construction company (2010). Geological Report for El-Zaafarana coastal area, Egypt.

Jiang, H. and J. R. Eastman (2000). "Application of fuzzy measures in multi-criteria evaluation in GIS." International Journal of Geographical Information Science **14**(2): 173-184.

Jonkman, J., S. Butterfield, W. Musial and G. Scott (2009). "Definition of a 5-MW reference wind turbine for offshore system development." National Renewable Energy Laboratory, Golden, CO, Technical Report No. NREL/TP-500-38060.

Jonkman, J. and W. Musial (2010). "Offshore code comparison collaboration (OC3) for IEA task 23 offshore wind technology and deployment." Contract **303**: 275-3000.

Malhotra, S. (2011). Selection, design and construction of offshore wind turbine foundations, INTECH Open Access Publisher.

Manual, S. P. (1984). "Coastal Engineering Research Center." Department of the Army, Waterways Experiment Station **1**.

MAS Consultant Office (2005). Geological Report for Dikheila Port in Alexandria, Egypt.

Minister of State for Environmental Affairs (2013). The annual report of the Ministry of Environment.

Ministry of Defence and Military Production. (2015). "The offical website." Retrieved /30, 2016/06, from http://www.mod.gov.eg/.

Mortensen, N. G., U. S. Said and J. Badger (2006). Wind Atlas of Egypt, RISO National Laboratory, New and Renewable Energy Authority, Egyptian Meteorological Authority.

Nielsen, P. (2003). "Offshore wind energy projects, feasibility study guidelines." SEAWIND-Altener project-Feasibility Study Guidelines (EMD).

Offshore, F. (2017). "Global Offshore Wind Farms Database." Blekinge Offshore AB Offshore Wind Farm." www. 4coffshore. com/windfarms/windfarms. aspx.

ORASCOM Construction Limited (2012). Geological Report for El-Gouna Bay, Egypt.

Redcon Construction (2007). Geological Report for Nabq Bay, Egypt.

TeleGeography Company. (2015). "Submarine Cable Map." Retrieved /29, 2016/06, from http://www.submarinecablemap.com/.

The British Oceanographic Data Centre. (2014). "The GEBCO_2014 Grid " Retrieved /25, 2016/03, from www.gebco.net.

The Egyptian Environmental Affairs Agency. (2015). "Protectorates: Natural Protectorates and Biological Diversity " Retrieved /05, 2016/04, from http://www.eeaa.gov.eg/English/main/about.asp.

The Egyptian Natural Gas Holding Company (EGAS). (2015). "Map of the gas and oil wells in Egypt." Retrieved /17, 2016/04, from http://www.egas.com.eg/.

The Ministry of Electricity and Energy of Egypt (2014) "Annual Report of the Authority of the Egyptian Electricity Holding Company in English."

Renewable Energy 152 (2020) 441–457

Contents lists available at ScienceDirect

Renewable Energy

journal homepage: www.elsevier.com/locate/renene

New approach to determine the Importance Index for developing offshore wind energy potential sites: Supported by UK and Arabian Peninsula case studies

AbuBakr S. Bahaj [a, *], Mostafa Mahdy [a], Abdulsalam S. Alghamdi [b], David J. Richards [a]

[a] Energy and Climate Change Division / Sustainable Energy Research Group, School of Engineering, Faculty of Engineering and Physical Sciences, University of Southampton, SO17 1BJ, United Kingdom
[b] Electrical Engineering Department, King Abdulaziz University, Jeddah, Saudi Arabia

ARTICLE INFO

Article history:
Received 6 August 2019
Received in revised form
13 December 2019
Accepted 14 December 2019
Available online 18 December 2019

Keywords:
Offshore wind
GIS/MCDA
Offshore wind constraints
Representative cost ratio
Suitability maps
UK and Arabian Peninsula offshore wind areas

ABSTRACT

A multi-criteria decision-making analysis linked to a Geographical Information System was developed to solve the spatial siting for offshore wind farms taking into account appropriate conflicting factors/constraints. A new approach is presented to solve the conflicting factors by determining the Importance Index (I) for offshore wind farms. This is based on a newly defined parameter *Representative Cost Ratio* (RCR) facilitating the comparison process. The method compares factor pairs and overcomes the issue where the evaluation of "alternatives" and "criteria", conducted by a number of experts result in reduced accuracy, coherence, and making the process time-consuming. The approach is tested through two case studies (i) UK deployed projects and (ii) determining the offshore wind energy potential around the Arabian Peninsula at scale. The presented method circumvents the literature-highlighted shortcomings with the advantage of considering all restrictions/constraints together at the start of the analysis, arriving at a signally combined Boolean Mask. RCR compares factor pairs to interpret the relationship between Importance Index scale (1–9) and its descriptors. Results from both case studies provided excellent outcomes, confirming the robustness of the RCR approach and its global applicability in addressing the spatial planning of offshore wind farms.

1. Introduction

Offshore wind energy is now considered a mature technology with over 19 GW capacity already installed globally [1,2]. In addition, offshore wind energy costs are declining globally. For instance, the UK's Department for Business, Energy and Industrial Strategy (BEIS) recently announced the outcome of its 2018 Contracts for Difference (CfD) scheme which incentivise long term investment for supporting low-carbon electricity generation [3]. For offshore wind projects in the UK, the tenders showed a halving of the cost per MWh to £57.50 (US$80) compared to the cost of the previous round [4]. Onshore wind energy is cheaper compared to offshore wind; however, it has some disadvantages. For instance, the lost value of the land used, noise, high vibrations, visual impact, bird path hazards, and shadow flicker effect. Shadow flicker effect is an infrequent event that occurs when the sunlight is at the horizon. This could be responsible for photo-induced seizures or photo-sensitive epilepsy and other disturbance to people near the turbines [5]. Offshore wind on the other hand, does not suffer these disadvantages and has two other noticeable advantages: (a) offshore wind speeds on average are higher than those onshore and (b) in general, the effect of turbulence is reduced compared to inland projects. Furthermore, turbulences assessment is required when considering intra-array and array-to-array effects, especially under stable atmospheric conditions in offshore wind farms. Reducing turbulence in offshore wind regions could extend the life cycle of wind turbines and reduce the materials used to support the wind turbine, as the fatigue stress is minimised [6]. Furthermore, offshore wind farms need further robust environmental impact assessment around the farm sites. This should include impacts on sea life – such as fish, mammals and birds encompassing noise and vibration etc. Hence, studies to appropriately site offshore wind farms are needed to support technology expansion taking into

* Corresponding author.
E-mail address: a.s.bahaj@soton.ac.uk (A.S. Bahaj).
URL: http://www.energy.soton.ac.uk

https://doi.org/10.1016/j.renene.2019.12.070

account all local and regional constraints.

Offshore wind energy, similar to most of the other renewable sources, has a low power density, for instance, it could occupy 50 times more space than a comparative gas-fuelled electrical power plants, which makes the spatial siting for offshore wind farms a critical process not only in addressing the appropriate data needs but also for optimised decision-making.

Identifying the most suitable locations for offshore wind energy around a region is a spatial siting decision problem. Spatial problems comprise the analysis of a large number of suitable alternatives and multiple criteria that will need appropriate evaluation. Once these criteria are chosen, they are evaluated and weighted by experts - stakeholders, and/or scholars. The evaluation is normally based on knowledge and experience of the appraisers concerning the specific problem to be solved, and the region under consideration [7]. In such cases, Analytic Hierarchy Process (AHP) is used to identify the problem criteria, to weight them, and then to evaluate each alternative [8,9]. Literature for example [10–14] indicates that such *spatial decision problems* are complex and require innovation. This is because the techniques typically involve a large set of feasible alternatives and multiple evaluation criteria, which are often conflicting.

The Analytic Hierarchy Process (AHP) is a well-known multi-criteria decision analysis technique in engineering to solve complex problems including the spatial planning for siting renewable energy projects – such as offshore wind farms [15–17]. AHP is a structured technique for organising and analysing complex decisions, based on mathematics and psychology. This work utilises AHP for siting offshore wind farms promoting a new approach developed to support coherent analysis, which circumvent the current processes, which have reduced accuracy and are time-consuming.

In comparison, AHP was employed to prioritise the highly suitable areas for solar farms of the regional unit Rethymno, Greece [18], where the study used an inverted scale of suitability - a score of four was considered not suitable and a score zero is suitable area. The work used Geographical Information System (GIS) and established four scenarios and ten factors to find sustainable areas to deploy photovoltaics and concentrated solar power farms.

A further study was conducted to test the hypothesis that onshore wind is the cheapest renewable energy in the UK addressing many of the constraints faced in its deployment [19]. The study used a multi-criteria decision analysis (MCDA) and AHP approach which provided what the authors claimed to be accurate estimation for the UK's onshore potentials which was around 5% of previous estimates.

The GIS-based constraints analyses limited to only restrictions, such as government regulations, are not enough to identify the most suitable locations, for offshore wind energy development. In essence, such analysis is most suitable for small-scale study areas as evidenced in the studies [20–25]. In a recent study addressing techno-economic constraints for small regions, especially islands the authors evaluated the offshore wind energy potentials of the Canary Islands, Spain [25]. The work considered both fixed and floating turbines, for two constraints - minimum speed of 6.5 m/s and exclusion of all protected areas. The study used only constraint analysis and no factors were applied. The results showed that the expected electrical power from the wind farm would be more than 20 times that of the annual electricity demand of the islands. Moreover, the levelised cost of electricity is approximately 9%–40% lower than the current electricity tariff in the islands.

To make it widely and fully applicable, one needs to produce suitability maps which requires an AHP analysis to produce factor weights to score the available areas on the maps to *high*, *moderate* and *not suitable* grades. For example, in the UK, the available areas for offshore wind energy are vast, so, stakeholders and investors do not need just the locations of the available areas only; they need to know the most suitable locations. Hence, appropriate analyses will need to create a descending score of the available areas from the highest to the lowest suitability (i.e. suitability maps). Such suitability maps assist stakeholders in targeting investments by exploiting the most suitable areas first and then the moderate areas and so on.

In essence, currently published work needs to find a robust way to compare factor pairs. As indicated earlier, alternatives and criteria are often evaluated by several individuals (decision-makers, managers, stakeholders, interest groups) who most of the time, have conflicting ideas, preferences, objectives, etc. This current practice, which is based on expert surveys and their subsequent analysis, is a long-winded process, requiring: (a) the generation of appropriate succinct questions to be addressed, (b) ethics approval for data collection, (c) identifying a cohort of experts, (d) once identified pooling them with the survey questionnaires and hoping to get robust sample return from the cohort, and (e) analysis for providing judgment and agreement between experts. This could take 6 months or more, [26–32]. This period is evaluated for academic practise only, as compared to experienced industry development teams where such survey may take shorter time frame. In addition, most literature only mentions the Importance Index (I) parameter without a clear explanation of how they arrive at the outcomes [10,20,33–38].

In this work, we addressed these issues heads on, by providing a new and unambiguous way to compare factor pairs. This new approach is on the *Representative Cost Ratio* (RCR) developed to facilitate the comparison process, which, in our view, is an innovative process to circumvent all the shortcomings highlighted above. Unlike previous offshore wind spatial siting research, for example [38–40], our considerations bring all restrictions together from the beginning of the analysis and then combined these in one Boolean Mask. This approach compares factor pairs to interpret the relationship between the Importance Index (I) sometimes referred to as the (Intensity of Importance) scale and its descriptions (see definitions and details in Section 2).

In order to test the above approach, we have applied it to two case studies covering: (i) analysis of the UK's deployed and planned offshore wind energy farms sites (ii) application across the whole process steps needed to quantify the offshore wind renewable energy potential at regional scale around the shores of the Arabian Peninsula (AP). In the following sections, we discuss the methodology, the two case studies, the results and implications of the analysis, followed by the discussion and the conclusions.

2. Methodology

2.1. Consideration for assessing offshore wind energy potential

The cost of a project is determined to be the most critical aspect of offshore wind energy exploitation. As indicated earlier, AHP is normally based on judgement and experience [15,16], where for offshore and onshore wind spatial siting, the cost is considered to link the factor pairs. In order to avoid such judgments and provide a robust way to compare factor pairs, we propose the *Representative Cost Ratio* to link pairs and provide the relative grading in terms of the Importance Index values needed. This innovation circumvents all the shortcomings previously highlighted in the current literature. Furthermore, our considerations have the advantage of bringing all restrictions together at the start of the analysis and then combining these in one Boolean Mask.

2.1.1. AHP process

A Multi-Criteria Decision-Making (MCDM) analysis linked to a Geographical Information System (GIS) model was developed to solve the spatial siting for offshore wind farms in an efficient manner, which takes into account regional and appropriately defined conflicting factors and constraints. Fig. 1 provides a summary of the steps to be undertaken within the whole AHP process including problem definition, identifying criteria and the needed processing [16,41].

The alternatives of spatial siting problem consist of a small unit called "cell or pixel". The study area map is then divided into an equal size grid where each pixel on the grid is a cell/alternative. The criteria of the problem are then divided into factors and constraints, constraints are explained later in Section 2.1.2.

Factors are the weighted criteria that increase or decrease the suitability of the alternatives (most/least cells). For example, the wind speed factor, where high/low wind speed means most/least suitable cell according to this factor [41].

A standardisation (Non-Boolean Standardisation) step is required to facilitate the final accumulation part. Due to the different magnitude and units of the factors, a standardisation process is used to transform them to a similar scale [42]. For instance, the wind speed has a scale ranging from 3 m/s [Min] to 9 m/s [Max], while water depth has a scale ranging from 5 m [Min] to 60 m [Max]. Therefore, to accumulate the two factors together, a standardisation process is applied by converting the two magnitudes of each factor to similar scales namely: 0 [Min] and 1 [Max] scale. This process is carried out using a fuzzy linear function, which is available as a tool in ArcGIS [43]. In addition, factors also have different weights according to their *importance*, so pairwise comparison method is used to weigh these factors as per the method developed in Refs. [15,16].

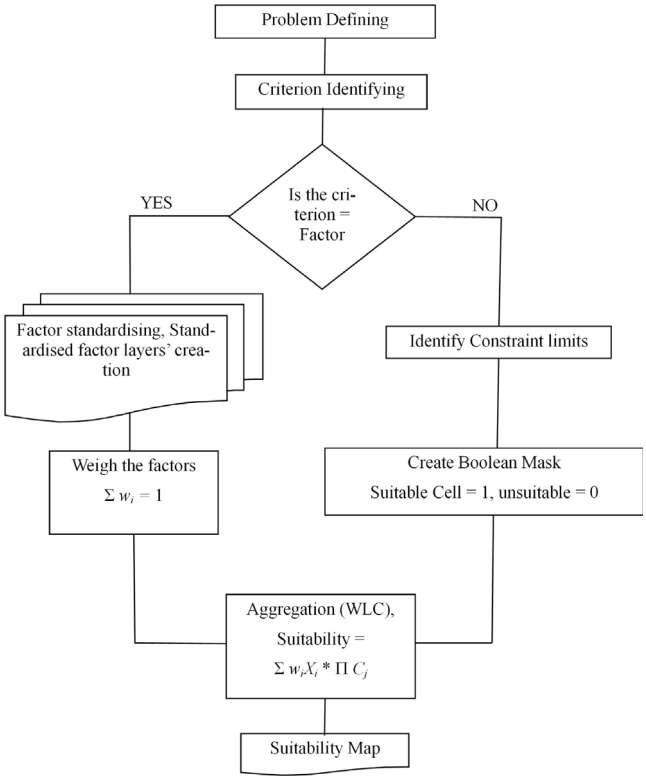

Fig. 1. AHP process stages undertaken including problem definition identifying criteria and the needed processing adopted from Ref. [41].

The required pairwise comparison process is accomplished by building two different matrices. The first matrix is the "pairwise comparison matrix", with an equal number of rows and columns, the number of rows and columns should be equal to the number factors (in this paper, n = 4). The two rules to create the pairwise comparison matrix are given below:

- Rule 1: The matrix element value is equal to the Importance Index value. This is adopted from Table 1, with the condition that the factor named in the left column (A) (Table 2) of the matrix has higher importance compared with the factor named in the top row (B) of the matrix (Table 2).
- Rule 2: Represents the condition when the factor named in the left column (A) of the matrix has lower importance when compared with the factor named in the top row (B) of the matrix (Table 2). In this case, the matrix element is equal to the inverse of the values in Table 1.

Table 1 provides the definitions and descriptions of the Importance Index's scale, which are used to compare factor pairs. The second matrix is the "normalised matrix", which is created by dividing each matrix element by its column sum. The weight of each factor is equal to the average of its row in the new matrix. The total sum of factor weights is one. The final step to complete the pairwise comparison is to validate the comparison assumption, using the following equations adopted from Ref. [15].

$$CR = CI / RI \quad (1)$$

$$CI = (\lambda_{max} - n) / (n - 1) \quad (2)$$

Where, *CR* is the Consistency Ratio having a value less or equal to 0.1 and is used to validate the accuracy of the Importance Index, *I*, values. *CI* is the Consistency Index, *RI* is the Random Consistency Index, with its values adopted from Ref. [15], and λ_{max} is the Principal Eigenvalue. λ_{max} is equal to the products of the factor sum (total) of each column of the pairwise matrix and the determined Factor Weight value.

2.1.2. Restrictions and Boolean Mask

To identify a suitable cell, a Boolean Mask is applied before the aggregation process is conducted, so that restricted cells are eliminated. Constraints are the criteria used in the Boolean Mask, which differentiates between suitable and unsuitable cells. Boolean relations (AND, OR and NOT) are used to sum different constraints into the final Boolean Mask map, see Equation (3).

The government regulations have a role to play in the analysis that will be taken into account by converting the regulations into restrictions in the analysis from the start of site consideration (Boolean Mask). The applied Boolean mask fulfils the role of such regulations, providing a generic approach applicable widely in any jurisdiction. The Boolean mask outcomes are unique outputs that differ from location to location, e.g. UK and Arabian Peninsula models considered in this paper. On the contrary, factors are mostly not affected by government regulations, for example, water depth, distance to grid, distance to shore, and wind speed factors of the offshore wind energy spatial siting are inherent to the sites and therefore represent the technical aspects of the analysis. Further environmental impact assessment is needed after locating the most suitable areas to cover additional government regulation not covered by the analysis. A recent example is the UK offshore wind farm socio/economic/environmental impact statement [44].

The criteria considered as restrictions are oil and gas installations – platforms (OGS), high capacity shipping routes (HCSR), cables paths, maritime natural reverse (MNR), maritime

Table 1
The Importance Index (I) scale adopted from Ref. [16].

Importance Index, *I*	Definition	Description
1	Equal importance	Two activities contribute equally to the objective
2	Weak/slight	
3	Moderate importance	Experience and judgement slightly favour one activity over another
4	Moderate plus	
5	Strong importance	Experience and judgement strongly favour one activity over another
6	Strong plus	
7	Very strong	An activity is favoured very strongly over another
8	Very, very strong	
9	Extreme importance	Evidence favouring one activity over another is of highest possible order

boundaries (MB), military practice and exercises areas (PXEA), fishing zones, existing or planned offshore wind farms (OWF), protected wrecks, and tunnels [33]. A Boolean mask need to be created to eliminate restricted cells, so that constraint cells have a value of zero, and unrestricted cells have a value of one. The final Boolean Mask is produced using Equation (3).

$$Boolean\ Mask = (OGS)\ x\ (HCSR)\ x\ (MNR)\ x\ (MB)\ x\ (PEXA)\ x\ (Fishing)\ x\ (OWF)\ x\ (Wrecks)\ x\ (Tunnels) \quad (3)$$

2.1.3. WLC aggregation process

As indicated in Fig. 1, the final step in the AHP process is the aggregation where the Weighted Linear Combination (WLC) method is used [8]. WLC combines the standardised factors after multiplying each factor by its weight and finally multiply the result map by the Boolean Mask (generated by multiplying all the constraints together). The overall outcome is called the Suitability Map and is estimated using Equation (4).

$$\begin{aligned} Suitability\ of\ any\ cell/alternative &= (Sum\ of\ factors\ weights)\ x\ (score)\ x\ (Boolean\ Mask) \\ &= \left(\sum_{i=1}^{n} W_i X_i\right) \times \left(\prod_{j=1}^{l} C_j\right) \end{aligned} \quad (4)$$

Where, W_i is the weight assigned to factor i, X_i is the criterion score of factor *i*, *n* is the number of factors, C_j is zero or one score of the constraint j, Π is the product of constraints, and *l* is the number of constraints.

2.2. RCR approach

In order to address the importance of the factors used and compare them in pairs, the Importance Index is introduced [16]. The Importance Index is an integer with scale between 1 and 9 and is critical in determining the relationship and importance between factor pairs that govern a project and its cost. The pairwise comparison process is undertaken by linking factor pairs to the Importance Index and its overall parameters. This process is mainly governed by the contribution of the factors to the cost of a project and associated impacts [41]. In this paper, we introduce the new term *Representative Cost Ratio* (RCR) to facilitate the determination of the Importance Index and the evaluation of offshore wind energy projects overcoming current methods which are time-consuming and less robust. The following steps in the methodology will now provide an approach to estimate these relationships and the values for both the Importance Index and RCR.

The relationship is gained through analysis of the literature and their data to assess the onshore wind energy potentials [45–47], as to the authors' knowledge, this work provides the first consideration of offshore wind energy farm siting using AHP and the RCR. A study of such wind energy potential in the South of the UK [47], which was based on the opinion provided by five experts in the wind energy field will be used to estimate the Importance Index. The study used six factors to evaluate the study area, which are wind speed, distance from historically important areas, distance from residential areas, distance from wildlife designations, distance from transport links, and distance from the electrical network connection. The other two studies [45,46] have used their experience and judgment to arrive at an appropriate and relevant Importance Index of each factor pair related to urban studies. These three studies are independent from each other; their work encompassed generic approach for siting of wind farms at different locations (Kozani of Greece, onshore areas of England, and South Central England of the UK) [45–47]. The authors used similar factors (some with more than ten factors) and the same range of the RCR; see Table 2 and Fig. 2. In essence, these three studies, conducted by different scholars, covered different study areas and periods. These authors did not rely on each other's work, yet the authors arrived at the same range of RCR for the different locations considered. Hence, factors could be applied to any locale.

Table 2 is based on data from the aforementioned studies [45–47] which are used to determine the appropriate range (1–9) of RCR for each Importance Index in terms of factor pairs. The factor pairs determined from these studies is shown in column A of Table 2. RCR is the ratio of factor pairs contribution to the final Levelised Cost of Energy (LCOE) of the project. To estimate RCR for this case we use the LCOE given in Table 3, by using the ratio between pairs. For example, the Wind Speed vs. Residential Areas Proximity is 52.2:16.2 giving a value of 3.2 in Table 2 Column C, and so on. In order to determine the values of the Importance Index in Column B, we used the pairwise comparison method mentioned above. The pairwise matrix and the normalised matrix for onshore wind spatial siting are given in Tables 4 and 5 respectively.

To arrive at the range for RCR, we use the interpolation given in Fig. 2 with the results shown in Column D of Table 2. For example, the Importance Index for the Wind Speed vs. Residential Areas Proximity pair is 4 and from Fig. 2 this is in the RCR range of 3–4,

Table 2
Process of obtaining the RCR range from previous onshore wind studies [45–47].

(A) Factor Pair	(B) Importance Index [47]	(C) RCR [48]	(D) Appropriate RCR Range
Wind Speed vs. Residential Areas Proximity	4	52.2/16.2 = 3.2	3–4
Wind Speed vs. Wildlife Designations Proximity	5	52.2/12.8 = 4.1	4–7
Wind Speed vs. Network Connection Proximity	5	52.2/10.3 = 5.1	4–7
Wind Speed vs. Transport Links Proximity	6	52.2/7.3 = 7.2	7–10
Wind Speed vs. Historical Areas Proximity	9	52.2/1.2 = 44	>18
Residential Areas vs. Wildlife Designations	2	16.2/12.8 = 1.3	1–2
Residential Areas vs. Network Connection	2	16.2/10.3 = 1.6	1–2
Residential Areas vs. Transport Links	3	16.2/7.3 = 2.2	2–3
Residential Areas vs. Historical Areas	8	16.2/1.2 = 14	13–18
Wildlife Designations vs. Network Connection	2	12.8/10.3 = 1.5	1–2
Wildlife Designations vs. Transport links	3	12.8/7.3 = 2.1	2–3
Wildlife Designations vs. Historical Areas	7	12.8/1.2 = 11	10–13
Network Connection vs. Transport Links	2	10.3/7.3 = 1.4	1–2
Network Connection vs. Historical Areas	6	10.3/1.2 = 8.5	7–10
Transport links vs. Historical Areas	5	07.3/1.2 = 6.1	4–7
Approaches and data from Refs. [45,46]			
Land Use vs. Road Network Proximity	3	16.2/7.3 = 2.2	2–3
Land use vs. Natural Areas Proximity	2	16.2/12.8 = 1.3	1–2
Natural Areas vs. Road Network Proximity	3	16.2/7.3 = 2.2	2–3
Urban Areas vs. Historic Sites	7	16.2/1.2 = 14	10–13
Roads vs. Historic Sites	6	10.3/1.2 = 8.5	7–10

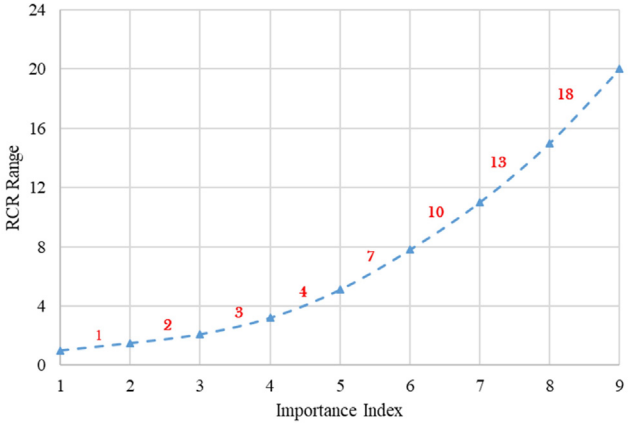

Fig. 2. The interpolation curve to determine the RCR range (red numbers show RCR range).

and so on. It must be noted that the last five rows of Table 2 are from Refs. [45,46] and are included here to illustrate the process of estimating RCR, based on factor pairs representing land use and urban areas, etc.

The Principal Eigenvalue λ_{max} is determined by the product of the factor sum (total) of each column of the pairwise matrix (Table 4) and the Factor Weight value (Table 5) determined earlier. For example, for the wind speed factor, $\lambda_{max} = 1.93 \times 0.512 = 0.99$ and so on for the other values.

In order to ascertain the validity of the assumptions made, the magnitude range of the Consistency Ratio CR (Eq. (1)) should be less than or equal to 0.1. The Consistency Index, *CI*, using Equation (2) has a value of 0.0185 since $\Sigma\ \lambda_{max} = 6.09$ from Table 5 and $n = 6$. The Random Consistency Index, *RI*, for the six factors has a value of 1.24, [15]. Using these values in Equation (1), *CR* has a value of 0.0149, which is < 0.10. Hence, the assumptions in Table 4 are correct [16]. The final range of RCR and the corresponding Importance Index are shown in Table 6, the table will be used later in Section 2.2.1 to calculate the factor weights that control the decision making of offshore wind energy spatial siting.

2.2.1. Offshore wind energy factors weighting

As indicated earlier, using the *Representative Cost Ratio (RCR)* as the new approach to calculate factor weighs will reduce time and

Table 3
The LCOE contribution to a 2.16 MW Land-Based Turbine, adopted from Ref. [48].

	Wind Speed	Residential Area Proximity	Wildlife Proximity	Network Proximity	Transport Links	Historical Sites	Total Cost
LCOE[a] [$/kW]	830	258	116	164	203	19	1590
LCOE [%] = (Factor/Total Cost)	52.2	16.2	7.3	10.3	12.8	1.2	

[a] LCOE [$/kW] = The Redistribution readjustment number to meet the total capital expenditures.

Table 4
The pairwise matrix for onshore wind spatial siting.

	Wind Speed	Residential Area Proximity	Wildlife Proximity	Network Proximity	Transport Links	Historical Sites
Wind Speed	1	4	5	5	6	9
Residential Areas Proximity	1/4	1	2	2	3	8
Wildlife proximity	1/5	1/2	1	2	3	7
Network Proximity	1/5	1/2	1/2	1	2	6
Transport Links	1/6	1/3	1/3	1/2	1	5
Historical Sites	1/9	1/8	1/7	1/6	1/5	1
Sum	1.93	6.46	8.98	10.7	15.20	36.00

Table 5
The normalised matrix for onshore wind spatial siting.

	Wind Speed	Residential Area Proximity	Wildlife Proximity	Network Proximity	Transport Links	Historical Sites	Factor Weight	λ_{max}	Error
Wind Speed	0.52	0.62	0.56	0.47	0.39	0.25	0.512	0.99	0.04
Residential Areas Proximity	0.13	0.15	0.22	0.19	0.20	0.22	0.178	1.15	0.07
Wildlife Proximity	0.10	0.08	0.11	0.19	0.20	0.19	0.135	1.22	0.01
Network Proximity	0.10	0.08	0.06	0.09	0.13	0.17	0.092	0.99	0.05
Transport Links	0.09	0.05	0.04	0.05	0.07	0.14	0.058	0.88	0.01
Historical Sites	0.06	0.02	0.02	0.02	0.01	0.03	0.024	0.88	0.02
Sum	1.00	1.00	1.00	1.00	1.00		1.00	6.09	

Note: Average Error is 0.01.

Table 6
The Importance Index and the corresponding RCR range.

Importance Index (Definition and description in Table 1)	1	2	3	4	5	6	7	8	9
RCR Range	(0–1):1	(1–2):1	(2–3):1	(3–4):1	(4–7):1	(7–10):1	(10–13):1	(13–18):1	18>:1

effort to rank the criteria for offshore wind spatial siting. Table 7 identifies the Importance Index, *I*, of each possible factor pair, using the definition given in Table 1 and the RCR range in Table 6. The selected values for the Importance Index are chosen based on the contribution to the final Levelised Cost of Energy (LCOE) as shown in Table 6 [40,41]. In these published articles, the contribution to the LCOE for wind speed is 50%, water depth is 20% and distance to shoreline is 5% and distance to grid is 2% [40,41] (Table 7). To arrive at the RCR value the contribution of these pairs in relation to each other will need to be established.

That is, the Wind Speed (WS) will need to be paired with other factors (Water Depth (WD), Distance to Shore (DS) and Distance to the Grid (DG)) and so on. Hence, the Importance Index score will be dependent on these combined contributions and the range of RCR given in Table 6, also shown in Table 7 for the specific RCR. For example, the Importance Index (I) for Wind Speed compared to Water Depth is determined by their contribution to the LCOE as follows: WS:WD = 50%:20% = 2.5 this falls in the RCR range to 2–3:1 (Table 6) and hence was given a value of 3 (Table 7). Similarly, WS:DG = 50%:2% = 25, this falls in the RCR range 18>:1 (Table 6) and hence *I* given is 9 (Table 7) and so on.

The values in Table 7 were then used to establish the pairwise comparison matrix (Table 8), using the two rules discussed earlier. The normalised matrix (Table 9) is determined by dividing each matrix element of Table 8 by its column sum (described above). For instance, the wind speed value in the normalised matrix is determined by $1 \div 1.59 = 0.63$ and so on for the other values. The Factor Weight values in Table 9 are the average of all values determined in the row for each factor.

The Principal Eigenvalue λ_{max} is determined by the product of the factor sum (total) of each column of the pairwise matrix (Table 8) and the Factor Weight value (Table 9) determined earlier. For example, for the wind speed factor, $\lambda_{max} = 1.59 \times 0.58 = 0.93$ and so on for all other values.

In order to ascertain the validity of the assumptions made, the magnitude range of the Consistency Ratio CR (Eq. (1)) should be less than or equal to 0.1. The Consistency Index, *CI*, using Equation (2) has a value of 0.077 since $\Sigma\ \lambda_{max} = 4.23$ from Table 9 and $n = 4$. The Random Consistency Index, *RI*, for the four factors has a value of 0.9, [15]. Using these values in Equation (1), *CR* has a value of 0.085, which is < 0.10. Hence, the assumptions in Table 7 are correct [16].

In order to apply the above analysis to the two case studies, a consideration of the membership limitations for the factors to be used in each study area is needed. These limitations are depicted in Table 10. A Fuzzy Membership tool will be applied to produce a new linear standardised layer for each factor. Such a process will be accomplished for each case study separately.

3. Analysis and results

This section provides analysis to test the methodology and its resilience through application to two case studies undertaken for siting offshore wind energy farms sites. The first case study (Section 3.1) addresses the UK wind energy programme where most of the projects are already in place or being commissioned. The UK is at the forefront of offshore wind energy and most of the analysis undertaken is for the UK projects at their specific sites. These projects were funded under the various UK mechanisms (called "Rounds") for offshore wind energy deployments [33]. The second case study was geared to test and provide the outcomes from the methodology at a regional scale. This considers seven countries covering an area of approximately 3.1 million km^2 and coastline stretch of 9180 km. To the authors' knowledge, this is the largest scale considered by any study in the offshore wind energy field.

3.1. Case study 1: UK offshore wind energy round projects

The UK has an ambitious programme for offshore wind. This is normally managed through the Crown Estate, which is an independent authority, with responsibility of overseeing the seabed of the UK including the promotion and the exploitation of the resources around and within the UK's shores. For offshore wind energy, such exploitation was undertaken through a process called "leasing rounds" or "Rounds" for short. The Crown Estate utilised a Marine Resource System (MaRS) tools based on a GIS database to identify potential offshore wind areas under various government investments stages to support each Round. There are three Rounds - 1 to 3 - where offshore wind farm projects are tendered for deployment at various locations around the UK [33]. It must be noted that Rounds 1 and 2 have already been deployed whilst Round 3 is in partial deployment.

The UK's Round 3, announced in mid-2008 covered an approximate area of 27,000 km^2 and aimed to exploit more than 32 GW of offshore wind energy. However, by the end of 2018 only 30% of this area has been exploited. Nevertheless, this represents 49% of Europe's gross offshore wind installed capacity in 2018, with the UK representing the highest installed capacity in the world [49].

For the development of these projects, the Crown Estate has only published the location maps for the three Rounds and has not disclosed details of the methodology used for the spatial siting of the wind farms in the selected locations [33,50–53]. However, their reports state the criteria and the scenarios/iterations considered

Table 7
Importance Index *I* of each possible factor pair, using definition given in Table 1 and RCR range in Table 6.

Contribution to LCOE, %	*Representative Cost Ratio* (RCR) = (Contribution to LCOE/other pair contribution)		Importance Index, *I*									Contribution to LCOE, %
			Equal Importance	Weak or slight	Moderate importance	Moderate plus	Strong importance	Strong plus	Very strong	Very, very strong	Extreme importance	
			1	2	3	4	5	6	7	8	9	
50	2.5	Wind Speed (WS)			x							Water Depth (WD) 20
	10								x			Distance to Shoreline (DS) 5
	25										x	Distance to Grid (DG) 2
20	4	Water Depth (WD)					x					Distance to Shoreline (DS) 5
	10							x				Distance to Grid (DG) 2
5	2.5	Distanced to Shoreline (DS)			x							2

when approving projects [33,50–53]. Such considerations are useful to allow us to undertake analysis to compare the effectiveness of our methodology with that of the results achieved through the Crown Estate considerations.

The Factor Weight values in Table 9, which were calculated using the introduced *Representative Cost Ratio* approach, were used to create a suitability map for the UK's offshore regions. The UK has the rights to exploit their shores out to 200 miles of the seabed for renewable energy power generation. In this section, we provide the analysis undertaken which is geared to check the appropriateness and validity of our proposed methodology and its assumption. This is accomplished by applying it to assess the suitability of the locations of the UK offshore wind farms' ongoing deployments.

Four suitability factor maps were produced using the available information from the Crown Estate Maps and their GIS Data website, which was updated in 2019 [53]. The source shape files of the water depth, grid connection, wind speed, and shoreline were converted to a raster format, with a cell size of 200 × 200 m, and its Geographic Coordinate System was "WGS 1984 UTM Zone 31N". The data for different factors were established in different dimensions (wind speed, water depth, distance to shore, and distance to grid – referred to as layer) and scales of values. Therefore, to arrive at the Weighted Linear Combination (WLC) step (last step in Fig. 1 as we already have the information for the previous steps in Fig. 1 from the Crown Estate published data), linear fuzzy limits were applied to unify their scales and dimensions to a scale from (1–0) (see methodology). These new layers called factor suitability maps represent: (a) Water depth factor, (b) Distance to electricity grid line, (c) Distance to UK shorelines, and (d) Wind speed factor. The four maps are processed using the Fuzzy-membership Tool in ArcGIS programme with the resulting suitability maps for these four factors shown in Fig. 3.

The Boolean mask was not used in this analysis as the Crown Estate had already eliminated the constraints criteria from the mapping of the three Rounds. The four suitability maps shown in Fig. 3 were integrated using ArcGIS Raster Calculator Tool, applying Equation (3), (Weighted Linear Combination (WLC) method). The final UK suitability score for each map cell equals [0.28 x water depth suitability + 0.05 x distance to grid suitability + 0.09 x distance to shorelines suitability + 0.58 x wind speed suitability], where the factors weight values are those given in Table 9.

These considerations resulted in the offshore wind suitability map for the UK shown in Fig. 4. The suitability score shown in Fig. 4 ranged from 0 (least suitability) to 1 (highest suitability). The results indicate that around 26% of the UK's offshore areas have high suitability (Fig. 4 legend range - 0.6 to 1.0) for offshore wind and that these areas are concentrated in the East of England and most of Scottish waters.

To validate the new approach, the suitability of the operational and planned UK's offshore wind farms under Rounds 1, 2 and 3, were identified using their original locations and boundaries derived from Crown Estate maps, which were superimposed onto the newly generated UK offshore wind suitability map. The appropriate validation is to ascertain whether all the cells identified by the Crown Estate to develop the offshore wind energy Rounds through the last two decades, coincide within the high and moderate suitability areas generated through our methodology, shown in Fig. 4.

Fig. 5 shows the locations of three Rounds of the UK's offshore wind energy farms superimposed on our resultant analysis of Fig. 4. Fig. 5 is the same as Fig. 4 but enlarged to show more details. The Clipping Tool in ArcGIS was used to clip the suitability map of the UK resulting in the outlines shown in the figure covering three sets: (i) Round 1 and 2 operating wind farms (shown in grey), and (ii) Round 3 operational wind farms areas outlined in red and (iii)

Table 8
Pairwise comparison matrix.

A	B			
	Wind Speed	Water Depth	Distance to Shoreline	Distance to Grid
Wind Speed	1	3	7	9
Water Depth	1/3	1	5	6
Distance to Shoreline	1/7	1/5	1	3
Distance to Grid	1/9	1/6	1/3	1
Total (Σ)	1.59	4.37	13.33	19

Table 9
Normalised matrix and final factors weight value.

	Wind Speed	Water Depth	Shoreline	Grid	Factor Weight	λ_{max}
Wind Speed	0.63	0.69	0.53	0.47	0.58	0.93
Water Depth	0.21	0.23	0.38	0.32	0.28	1.23
Shoreline	0.09	0.05	0.08	0.16	0.09	1.23
Grid	0.07	0.04	0.03	0.05	0.05	0.84
Σ	1.00	1.00	1.00	1.00	1.00	4.23

Round 3 under construction or planned shown dotted. It is clear from the results in Fig. 5 that the UK offshore wind Rounds are within the high and medium suitability areas generated by our analysis.

In order to estimate the suitability percentage distribution for the three sets, (i), (ii) and (iii) mentioned above, the Attribute Table which identifies the geographic feature of an ArcGIS Layer for each set was used to arrive at the number of cells for every suitability score range (0–1). The Attribute Table and the scores for these sets are given in appendix A. Table 11, depicts the suitability percentages for all the three Rounds of the UK offshore wind projects. The table shows the estimated areas for each Round as well as the predicted suitability determined by the methodology presented here. The cell suitability distribution in Table 11 is divided into three ranges - unsuitable cells (0.0–0.39 score), moderately suitable cells (0.4–0.59), and highly suitable (0.6–1.0). As can be seen from the results in Table 11, all the UK's operational or planned offshore wind locations are in moderate and high suitability ranking. For Rounds 1

Table 10
Fuzzy membership limitations and related values.

Factor	Max	Min	Condition	Value	Condition	Value
Wind Speed	7 m/s	3 m/s	> Max	1.0	< Min	0.0
Water Depth	- 60.0 m	- 5.0 m	< Max	0.0	> Min	0.0
Distance to Shoreline	140 km	5.0 km	> Max	1.0	< Min	0.0
Distance to the Grid	180 km	10.0 km	> Max	0.0	< Min	1.0

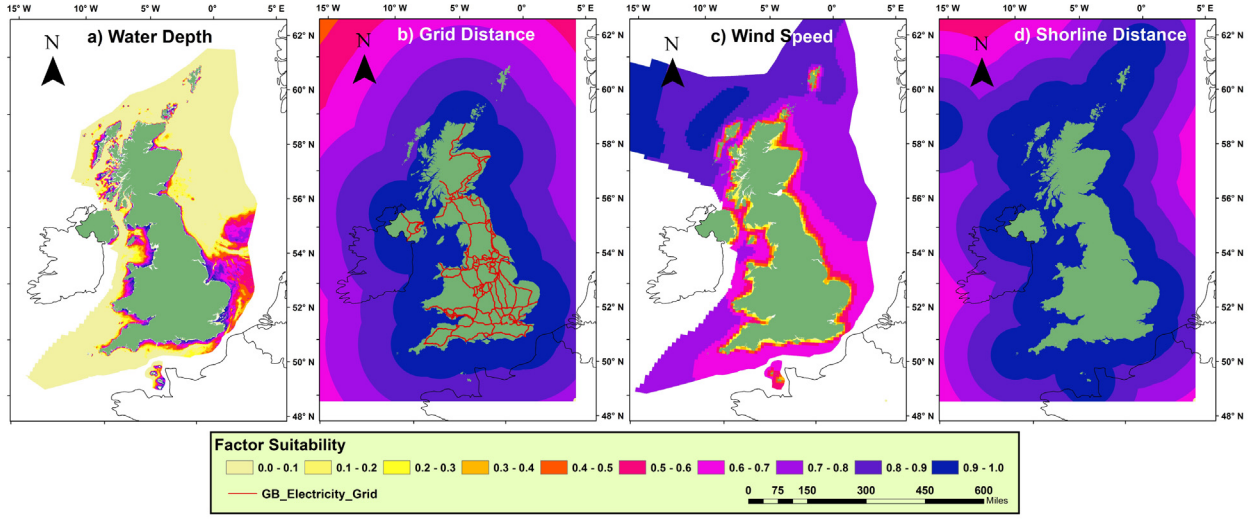

Fig. 3. The suitability maps for the four considered factors: (a) Water depth factor, (b) Distance to electricity grid line, (c) Distance to UK shorelines, and (d) Wind speed factor.

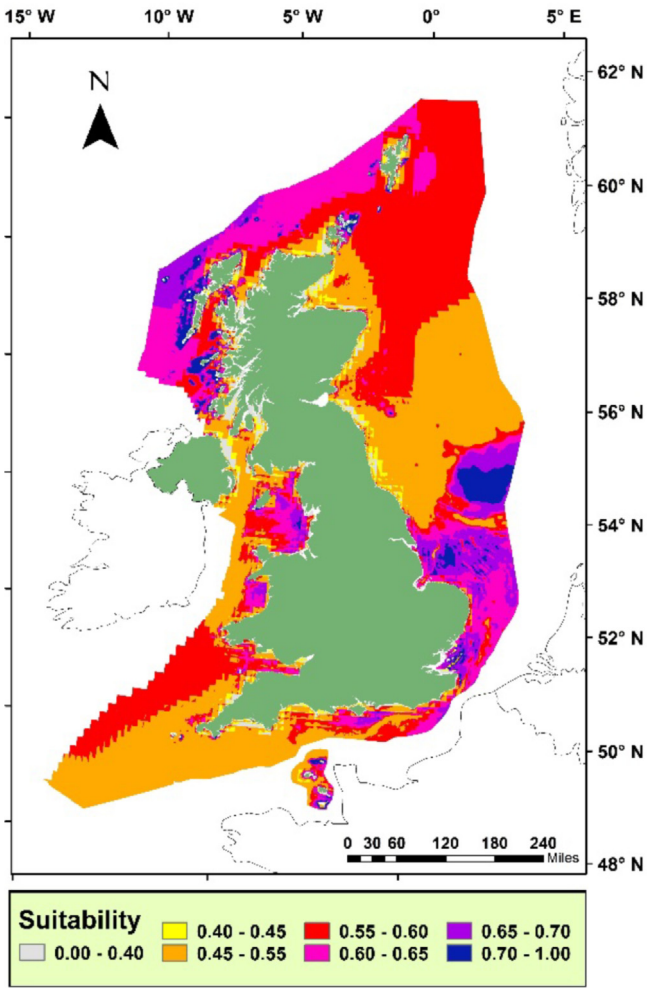

Fig. 4. UK's offshore wind suitability map produced by the methodology presented here. The suitability score is ranged from 0 (least suitability) to 1 (highest suitability). The results in the figure is also duplicated in Fig. 5 opposite where it is enlarged to allow more details to be shown including superimposing the 3 Rounds of the current and future offshore wind farms.

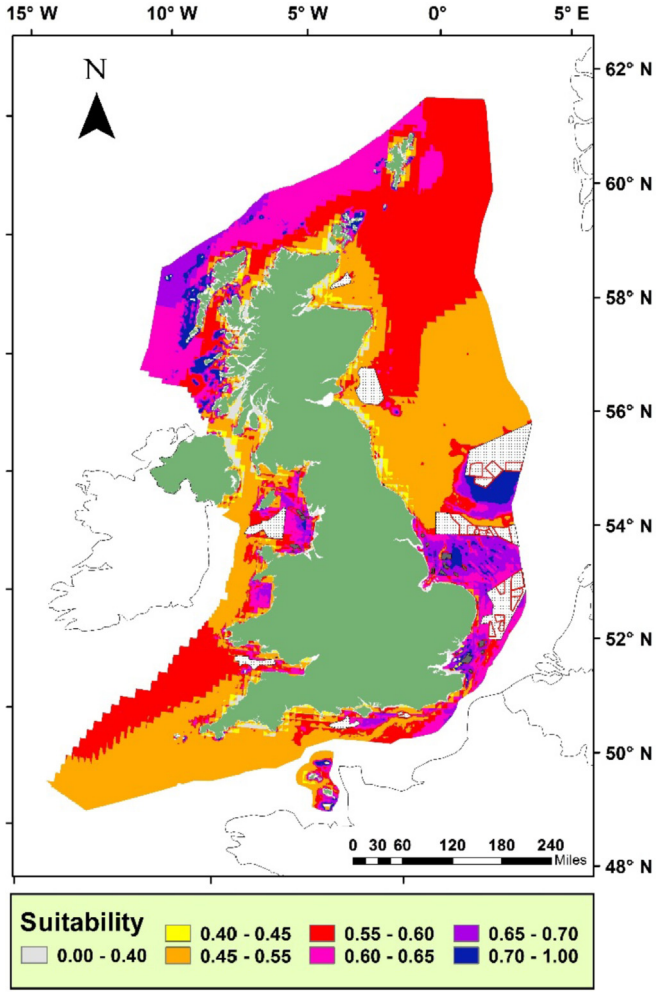

Fig. 5. Same suitability distribution map as Fig. 4. However here we also show the UK 3 Rounds – Rounds 1 and 2 in grey and Round 3 dotted areas with current wind farms outlines in red.

and 2, 92.4% of the farms were found to be in the high suitability areas with an estimated area of 1342 km^2. While for operational farms in Round 3, 85.8% were in high suitability areas, with an estimated area of 8565 km^2. For under construction or planned farms in Round 3 only 64.2% are within highly suitable areas, while the remaining (35.8%) areas are in moderately suitable areas, covering an estimated area of 27,039.9 km^2. The reason for this split is the high water depth average that exceeds 39.4 m, which will reduce the percentage of high suitability cells for the wind farms planned in Round 3.

The spatial siting verification was performed using the pre-planned UK offshore wind energy projects announced under Rounds 1 to 3. As can be seen from the results, the verification proved that the new *Representative Cost Ratio* (RCR) approach is very accurate as all of the cells of these farms are located in either moderate or high suitability categories (Table 11). Furthermore, this verification is significant, as we have simulated the data used by the UK, the country with highest installed capacity of offshore wind farms coupled with unmatched experience in planning, financing, and constructing such farms globally.

Considering that, the UK's Crown Estate is spending around £90k per MW for the cost of the offshore wind spatial planning process alone [40], which means that their commissioned maps are highly precise and accurate. The proposed new approach will save on such expenditure and reduce the time and effort needed to achieve the optimal spatial siting plan decision. We, therefore, conclude, that the results given in Figs. 4 and 5 and Table 11 confirm the quality of the different assumptions and calculation of the new RCR approach to accurately estimate the suitability of offshore wind energy farms. This approach will now be tested further by applying it to the analysis of the potential for offshore wind energy at a regional scale, in un-investigated areas around the shores of the Arabian Peninsula.

3.2. Case study 2: Arabian Peninsula

The Arabian Peninsula (AP) is bounded between 10°N and 35°N latitude and 35°E and 60°E longitude with a spatial extent, which includes the offshore areas of the Red Sea, the Gulf of Aden, the Arabian Gulf, and the northern part of the Arabian Sea. AP encompasses the countries of Bahrain, Kuwait, Oman, Qatar, Kingdom of Saudi Arabia (KSA), United Arab Emirates (UAE), and Yemen. Most of these countries rely on fossil fuel for their electricity supply. Table 12 depicts various characteristics of the AP including areas, population, and installed fossil fuel power capacities. The Gulf Cooperation Council (GCC) countries sit on more than 500 billion

Table 11
Percentages of suitability distribution for the UK offshore wind projects.

Round/[Location Source]	Estimated Area (km^2)	Installed Capacity (GW)	Predicted Suitability Distribution [%][a]		
			Unsuitable	Moderate	High
Round 1 and 2/[54]	1342.4	7.5	0	7.6	92.4
Round 3 operating wind farms until the end of 2018/[53]	8565.8	10.1	0	14.2	85.8
Round 3 under construction/planned/[37]	27039.9	32	0	35.8	64.2

[a] Cell scores: Unsuitable < 0.39; Moderate 0.4 to 0.6; High > 0.6 (suitability maps Figs. 4 and 5).

Table 12
Some characteristic of the Arabian Peninsula countries (GCC and Yemen) adopted from the references shown, power derived from fossil fuels.

Country/[Reference]	Area (10^6 km^2)	Coastline [km]	Population [Million]	Installed Power Capacity [GW]
Bahrain/[56]	0.008	161	1.41	3.93
Kuwait/[57]	0.017	499	2.88	16.0
Oman/[58]	0.310	2092	3.42	7.87
Qatar/[59]	0.012	563	2.31	8.80
KSA/[21,60]	2.148	2640	28.6	69.1
UAE/[61,62]	0.084	1318	6.07	28.9
Yemen/[63]	0.528	1906	28.0	1.50
Total	3.09976	9179	72.69	136.1

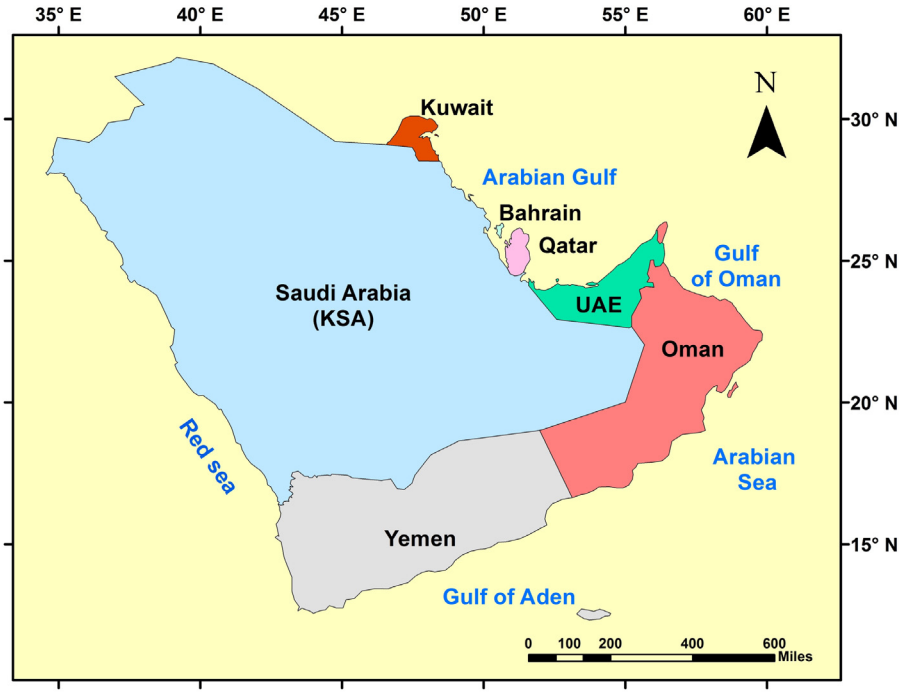

Fig. 6. Arabian Peninsula countries considered in this study, created using ArcGIS programme.

barrels of oil reserves ($^1/_3$ of the total known global reserves), hence most of their electricity is generated using fossil fuels [55].

The Arabian Peninsula is surrounded by water (Fig. 6), where Saudi Arabia has two shorelines; - Arabian (Persian) Gulf and the Red Sea, Bahrain, Kuwait, Qatar and UAE have shorelines on the Arabian Gulf. Oman has shorelines laying on the Arabian Gulf and the Arabian Sea whilst Yemen has shorelines on the Red Sea and the Arabian Sea. Hence, these countries would benefit from identifying the offshore wind energy potential around their shores.

To our knowledge, offshore wind energy potential in the AP region has not been fully investigated. In addition to testing the methodology, the research will also provide the quantification of the potential of offshore renewable wind energy for these countries contributing to both knowledge and understanding. The outcomes of the research based on the optimised methodology applied at scale could also assist in the speedy achievement of the regional renewable energy targets.

The following section outlines the steps undertaken to produce an overall outcome for offshore wind farm spatial siting in the AP region. Due to the wide-area footprint of the region and the different conditions presented by the considered countries, the analysis was conducted using nine criteria. Four of these criteria are factors covering: (i) wind speed (m/s), (ii) water depth in (m), (iii) distance from alternative cells to the shoreline in (km), and (iv) distance to the grid lines in (km). While the constraints used, which were selected due to their appropriateness for the region, are (a)

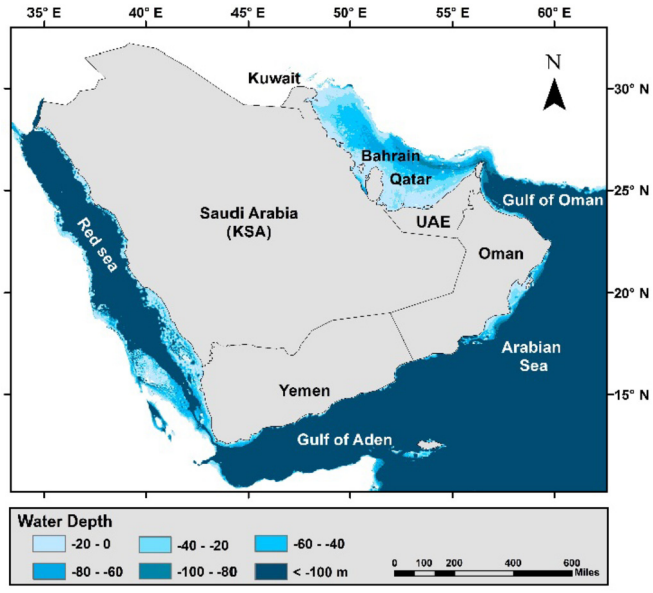

Fig. 7. Bathymetry (water depth) map around the Arabian Peninsula.

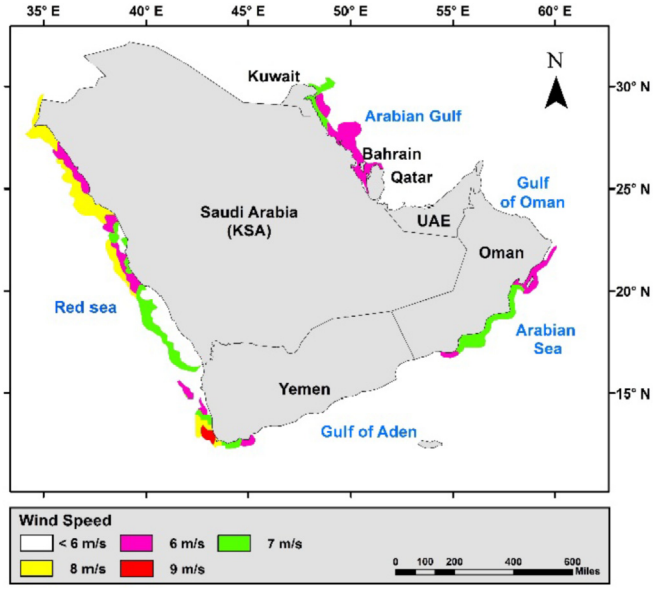

Fig. 8. Wind Speed [m/s] map around offshore areas of the Arabian Peninsula.

maritime boundaries, (b) oil and gas extraction areas, (c) reserved maritime natural parks, (d) shipping routes paths, and (e) underwater (sea) cables paths.

Table 13
Maritime reserved parks for Arabian Peninsula countries.

Country	Park name	Source
Oman	Daymaniyat Islands Nature Reserve, Jabal Samhan Nature Reserve, Ras Al Jinz Turtle Reserve, The Khawrs of the Salalah Coast Reserve	[69]
Yemen, Qatar, UAE, Bahrain, Kuwait	N/A	[70,71]
KSA	Umm al-Qamari Islands Farasan Islands	[72]

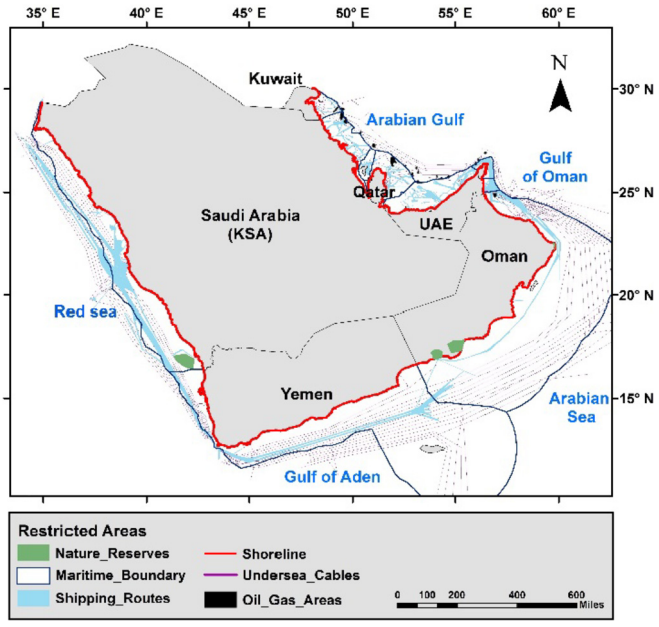

Fig. 9. Restricted areas raster layer around the offshore areas of the Arabian Peninsula.

In order to carry out the analysis, an ArcGIS [43] map layer for each criterion was created utilising available and relevant published spatial data. The bathymetry (water depth) data for the offshore areas around GCC countries and Yemen were adopted from Ref. [64]. The source file of the bathymetry data was created in raster format, with a cell size of 800 × 800 m, and its Geographic Coordinate System was "GCS_WGS_1984". The results for the water depth for the considered countries are shown in Fig. 7. It must be noted that all other criteria layers were also confined to the same cell size and coordination system type as that of the bathymetry source file.

Wind speed data was adopted from the "Wind Atlas for Egypt" [65] and from the Global Atlas for Renewable Energy [66]. The

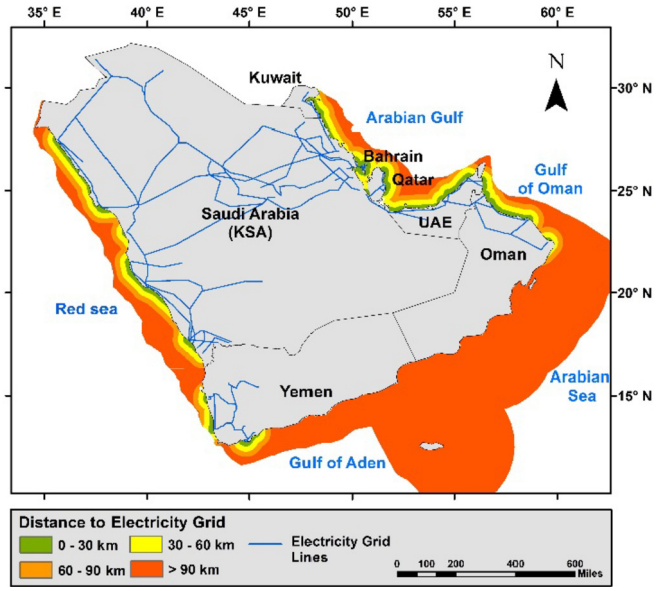

Fig. 10. Distance between representative cells of the offshore wind resources and electricity grid lines.

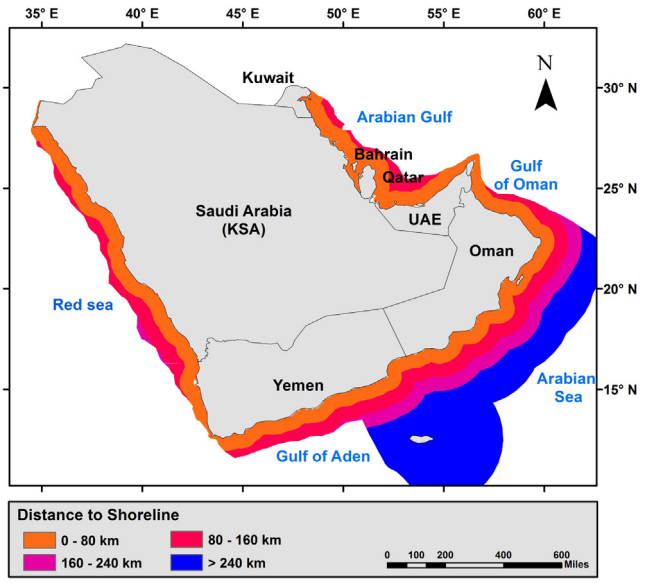

Fig. 11. Layer map of the distance between representative cells of the offshore wind resources and shoreline.

determined values were then verified using data available from Refs. [67,68]. The map layer in Fig. 8 shows the results of the average wind speed in [m/s] at a height of 50m over a flat and uniform sea.

All layers for area restrictions were adopted from different sources. Locations, shapes, dimensions of maritime reserved parks were taken from the official websites of different Wildlife Authorities of these countries, as documented in Table 13. All oil extraction areas are located on the Arabian Gulf, according to data from Saudi Aramco [73]. Shipping Routes within the study area were identified using the data available from ship density maps of the Marine Traffic website [74]. Undersea submerged cable locations and paths were extracted from the submarine cable map given in Ref. [75].

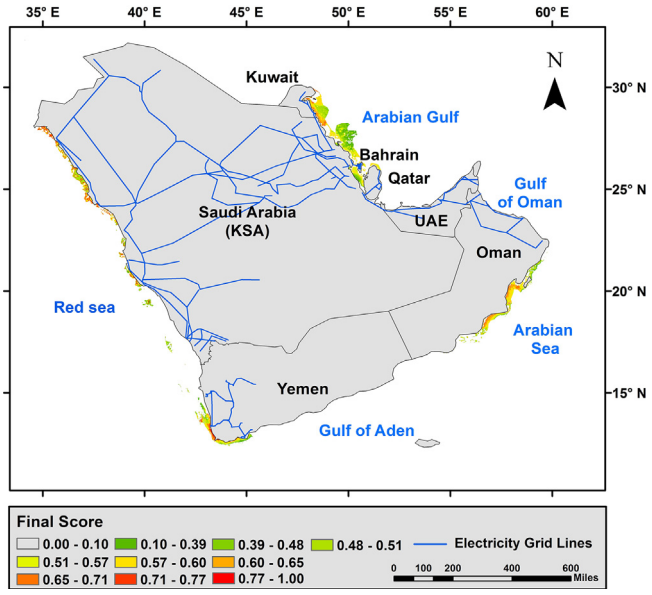

Fig. 12. Offshore wind energy Suitability Map around the Arabian Peninsula. Where 0.0 score is not a suitable area, while a score of 1.00 represents areas of the highest possible suitability. Grid availability, blue line.

Fig. 9 maps the overall results of restrictions for the region covering: natural reserves, oil and gas areas, shipping routes and undersea cables.

Fig. 10 shows the results map layer of the National Electricity Transmission Grid of the GCC and Yemen. The data were adopted from the Global Energy Network Institute [76] and the GCC Interconnection Authority [77]. The Euclidean Distance Tool in ArcGIS [43] was deployed to calculate the distance between the nearest electricity line to each cell, and the results are depicted in Fig. 10. Fig. 11 illustrates the results of the distance from each cell considered in the analysis to the coastline utilising data from Ref. [43].

A Boolean mask was created to eliminate restricted cells, so that constraint cells have a value of zero, and unrestricted cells have a value of one. The Raster Calculator tool in ArcGIS was used to produce the final Boolean Mask given by Equation (3).

All considered criteria were aggregated using Weighted Linear Combination (WLC) given by Equation (3), to create the final suitability map for offshore wind for the AP case study. Four standardised layers were first multiplied by their Factor Weight from Table 9 (Section 2.2.1), then summed together, using the Raster Calculator tool in ArcGIS by applying Equation (3). Finally, restricted cells were removed from the WLC layer using the Boolean Mask layer.

As indicated earlier, the modelling was undertaken using an 800 × 800 m cell size confined to the source file of the bathymetry map. Four factors and five constrained criteria were chosen to evaluate the alternatives/cells around the countries of the Arabian Peninsula. The model solved the spatial siting for offshore wind farms dealing with the chosen conflicted factors and constraints efficiently.

The suitability map for the studied area (Fig. 12) represents the cells around the shores of the AP where the cells final scores and their corresponding areas are graded as follows:

(i) 0.0 < Cell Score < 0.39 - not suitable. This represents 20,935 km^2 of the studied regions (the 0 score assigned by the Boolean Mask is not accounted in this area).
(ii) 0.4 < Cell Score < 0.59 - moderately suitable. This represents 23,080 km^2 of the studied regions.
(iii) Cell Score > 0.6 – highly suitable. This represents around 3251 km^2 of the studied regions.

The results for the overall suitability map of the Arabian Peninsula is shown in Fig. 12 with high resolution details of the regional sites given in Fig. 13. It must be noted that in the final suitability map, the UAE has no suitable cells (due to low wind speeds and dense shipping routes as indicated by Figs. 8 and 9 respectively), while Qatar and Bahrain have moderate suitability cells and no high suitable cells. In addition, the suitable areas for Yemen and Oman are centred on one area of their shoreline due to the lack of wider electricity grids provisions, (see Fig. 10). Yemen, Kuwait, Oman, and KSA have the most suitable sites for offshore wind, with KSA having the highest suitable areas in the region (due to high wind speeds in the Red Sea).

4. Discussion

A mathematical approach including the utilisation of an Analytic Hierarchy Process (AHP) was developed to solve the spatial siting for offshore wind farms. This is achieved by reducing the conflict between factors and constraints (restrictions) as follows:

(a) A Boolean Mask is produced to eliminate the restricted areas at the start of the analysis where the Mask is different for different locations, e.g. UK and Arabian Peninsula.

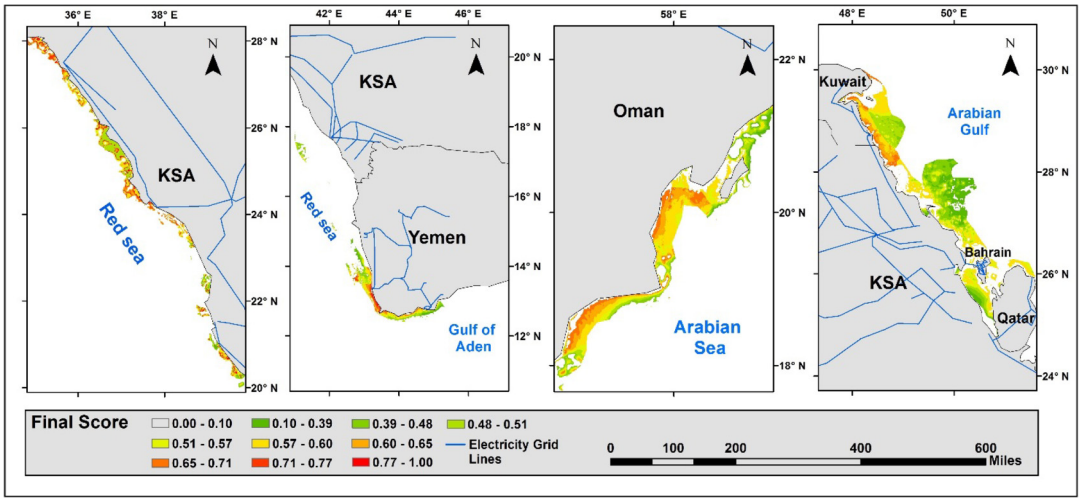

Fig. 13. High-resolution offshore wind energy Suitability Map for the countries with highest offshore wind energy potential - KSA, Yemen, Oman, Qatar, Bahrain, and Kuwait - around the AP. Where a 0.0 score indicates areas which are not suitable, while a score of 1.00 represents areas of the highest possible suitability.

(b) In the methodology, an appropriate Representative Cost Ratio (RCR) was introduced to reduce time, cost, and complexity encountered in previous approaches to analyse offshore wind energy potential.
(c) This new approach was validated using the actual UK offshore wind energy location maps, and the methodology and our analysis predicted this with high accuracy. Furthermore, the methodology also identified future regions of offshore wind energy potential in the UK which are currently being considered for commercialisation.
(d) The methodology can be applied at large scale as evidenced by the outcome for offshore wind energy potential around the Arabian Peninsula.

The methodology and its resilience were tested through application to two case studies. The first case study considered the matured UK wind energy programme where most of the projects are already in place/being commissioned or sites to be utilised (Section 3.1). The methodology and our analysis predicted this with high accuracy. Furthermore, the methodology also identified future regions of offshore wind energy potential in the UK which are currently being considered for commercialisation.

The second case study provided outcomes at regional scale of the Arabian Peninsula (AP) covering an area ~3.1 million km^2 and coastline of 9180 km with Fig. 13 showing the results map for offshore wind energy potential in the region. The outcomes in the figure is used to estimate the suitability distribution for the seven countries in the AP as shown in Table 14. As can be seen from Table 14, the KSA has more than 25,000 km^2 of unrestricted areas, which represents 54% of the total available area for offshore wind energy potential in the Arabian Peninsula region. Despite the high wind potentials in KSA around the Red Sea region (Fig. 8), less than 3.5% of the total available area of the region is considered to be of high suitability. This is due to the fact that most of the Red Sea region of the KSA has a water depth of 60m or more (Fig. 7) which is beyond current turbine foundations technologies. So to extend suitability, it is feasible for the KSA to consider investigating floating offshore wind turbines, which are more suitable for deeper water.

Oman's share of the total available area of the region is around 18%, and only 8.7% of that is highly suitable for offshore wind, which is surprising at it has a shoreline of 2092 km, which is not too dissimilar to that of the KSA (Table 12). Despite this, Oman has a significant average wind speed on the Arabian Sea, but unfortunately, this is remote, located over 90 km from the nearest electricity grid in the area. Nevertheless, Oman does, however, have a well-established national power grid near the Gulf of Oman (Fig. 10), but the wind speed in this location is less than desirable. Kuwait has around 14% of the total available unrestricted area, with a similar percentage of the highly suitable area within the region. These numbers are relatively high when compared to its short shoreline (around 5% of the total coastlines of the region considered). Kuwait has high offshore wind potentials compared to its footprint since it has minimum restriction on the Arabian Gulf (Fig. 9), average wind speed of 6.2 m/s (Fig. 8), and a shallow water depth range of 35m (Fig. 7).

Yemen's offshore wind potential and grid proximity are concentrated in the same area (Figs. 8 and 10), which justifies its 441 km^2 of high suitability areas, despite its current poor infrastructure when compared to others in the Gulf States. Qatar and

Table 14
Suitability distribution for the Arabian Peninsula countries offshore wind sites.

	Unsuitable Suitable Area (km^2)	Moderate Suitable Area (km^2)	High Suitable Area (km^2)	Total Available Area (km^2)
KSA	14732	9204	1586	25522
Oman	493	7410	769	8672
Kuwait	2800	3319	455	6574
Yemen	2742	2843	441	6026
Qatar	162	220	0	382
Bahrain	6	84	0	90
UAE	0	0	0	0
Total	20935	23080	3251	47266

Table 15
National installed electrical power capacities in Arabian Peninsula countries compared with estimated power capacity achieved from offshore wind high suitability sites from an 8 MW capacity turbine in these countries.

	National installed capacity (GW) [81]	High Suitable Area (km^2)	Estimated offshore wind Capacity (GW)	No. of turbines	Potential offshore wind contribution to capacity (%)
KSA	69.1	1586	17.06	2125	24.7
Oman	7.87	769	8.28	1031	105.2
Kuwait	16.0	455	4.90	610	30.6
Yemen	1.5	441	4.75	591	316.5
Qatar	8.8	*0*	–	–	–
Bahrain	3.93	*0*	–	–	–
UAE	28.9	0	0.00	0	0.0
Total	136.1	3555	35	4765	25.7

Bahrain have no high suitable offshore wind areas. UAE has more than 23 seaports; seven of them are mega container ports, resulting in a high volume shipping route density (Fig. 9) and hence zero availability for offshore wind.

To estimate the offshore wind power potential for the investigated sites, one needs to provide a spatial siting of the turbines and their inter turbine spacing in an array or farm. To estimate the array spacing between offshore wind turbines, Equation (5) developed in Ref. [78] was used:

$$S = (R_d)^2.\ L_d.\ L_c \tag{5}$$

Where S is the array spacing giving the footprint for each offshore wind turbine in an array, R_d is the rotor diameter, L_d is the downwind spacing, L_c is the crosswind spacing.

To reduce turbulence interaction between turbines, the ideal turbine spacing is in the range of 5–8 times the turbine rotor diameter [79]. In our analysis, L_c was given the value 5 and L_d the value 8. Hence a wind turbine footprint $S = 5 \times 8 \times 164^2$ for an 8 MW turbine (rotor diameter 164 m [80]). The estimated number of wind turbines for 8 MW configuration given in Table 15, is derived by dividing the Suitable Area (km^2) by S for the turbine size used.

The estimated offshore wind power capacities for each country using the turbine type in combination with Equation (5) are shown in Table 15. The table also provides details of the Arabian Peninsula countries currently installed power capacity and the percentage contribution from the estimated offshore wind capacities established here.

As can be seen from Table 15, the estimated overall total cumulative capacity of offshore wind power contribution (from the high suitability areas only) to these countries is approximately 35 GW for an 8 MW turbine capacity. The results indicate that for the 8 MW turbine case around 25.7% of the overall Arabian Peninsula countries power capacity can be achieved from offshore wind. In terms of country, specific offshore wind capacity potential determined in this study, Saudi Arabia has 17 GW, Oman 8 GW, Kuwait 4.9 GW, and Yemen 4.8 GW. Bahrain and Qatar have moderate offshore wind energy capacities of 2.37 GW and 0.9 GW respectively. The United Arab Emirates (UAE) has small forefront to the sea and has many restrictions especially around shipping lanes (Dubai being a world commercial centre). When combined with the limited wind resources around its shores the analysis indicates that UAE has very limited suitable areas and hence negligible wind power potential. This latter outcome provides more rigorous analysis providing stronger evidence than [82], where only two factors were used to select a suitable site for offshore wind around Abu Dhabi, only in the UAE.

It must be noted that the markets, especially in Europe, are now leaning towards the 8 MW capacity turbine with some developers now upgrading these turbines to 9.5–10 MW and are thinking about 12 MW turbines in the next two years with research now being directed towards 13–15 MW turbines [83]. In the case of the countries studied here, it is imperative that any development of the sites highlighted should bear these developments in mind. In our view, the 8 MW option seems to be the most sensible option to go for at this stage.

However, it must be noted that in this new approach the cost ratios need to be updated constantly, and that in some cases some of the factors cannot be easily costed, for example, environmental impacts (if considered as a factor).

Spatial siting models are sensitive to the data quality and availability for the analysis. In this case, factor layers needed to be available at 500–1000 m resolution (cell size). Hence, the spatial siting investigations accuracy is dependent on the data availability and quality. The analysis has considered cost-related criteria as factors, while other criteria, such as environmental and social impacts were considered as restrictions.

Unlike other studies, the presented approach considered more factors in its designed methodology. These included the main four factors (requiring appropriate weights) affecting the offshore siting process, which are wind speed, water depth, distance to land, and distance to the electricity grid. These are augmented by constraints criteria affecting the offshore areas such as Marine Protected Areas, Marin Boundaries, Undersea Cables, Shipping Routes, Military Restricted Areas, and Oil and Gas Extraction Areas, which are combined in one Boolean Mask. Other studies tend to use one or two factors to identify the suitable areas.

This new approach is quick and less complex. It was validated using the actual UK offshore wind energy location maps, and the methodology and predicted outcomes matched well with the "costly mapping" determined by the Crown Estate for their projects for the three UK's Rounds. Furthermore, the methodology also identified future regions of offshore wind energy potential in the UK which are currently being considered for commercialisation. This gives confidence that the RCR approach is accurate as all of the cells for these projects are located in either moderate or high suitability categories determined by this study.

The final suitability maps produced by the methodology provide stakeholders (e.g. governments) the suitable zones for offshore wind energy exploitation. Development of such zones will require further in-depth detail study to address local issues.

The paper introduced the new parameter termed the "Representative Cost Ratio" (RCR) to support the quantification (weighing) of the spatial siting of offshore wind potential areas. This parameter coupled with the approach are also applicable to other renewable energy sources spatial planning. However, it should be noted that the weighting process is to distinguish between compatible zones

within the site(s) considered – defining the most/least suitable areas for renewable energy conversion technologies. This weighting must take into account the type of energy and the territory where it is applied. Thus, for example, if all study areas have enough wind to install wind power plants, the wind factor, in this case, is not applicable, and therefore only the other factors should be weighted. Furthermore, when conducting detailed studies, local expertise will be needed to address regional specificity and characteristic to support the study.

In summary, due to the nature of the problem, the work integrates modelling and engineering approaches coupled with regional considerations. The proposed new approach (i) overcomes many of the shortcoming of previous studies (ii) has been verified by the UK offshore wind programme projects and (iii) has predicted the sites and capacities of the Arabian Peninsula offshore wind potential at a large scale. However, it is not tested, as it cannot be compared with previous analysis.

5. Conclusions

Multiple-criteria decision-making (MCDM) analysis coupled with AHP are widely used to solve complex renewable energy spatial planning problems. Here we proposed a new approach to use the *Representative Cost Ratio* (RCR) to assist in the rapid and accurate determination of offshore wind energy potential areas. This approach was quantified through a robust methodology and was used in two case studies to support its applicability and usefulness. The spatial results obtained for the UK offshore wind programme matched well with the "costly mapping" determined by the Crown Estate for their projects (£90k/MW) for the three Rounds [40]. This gives confidence that the RCR approach is accurate as all of the cells for these projects are located in either moderate or high suitability categories determined by this study.

In the second case study, we consider the regional area of the Arabian Peninsula to test the methodology across the whole process (Fig. 1) and to provide detailed indication of the offshore wind energy potential in this region. The analysis and modelling covered seven countries, for which final suitability maps were generated using appropriate factors and weights of relevance to the region's countries. The identified sites were analysed in terms of potential power capacities based on an 8 MW wind turbine which now seems to be the standard capacity being deployed in Europe and elsewhere. The results shown in Table 15 indicate a cumulative regional capacity of up to 35 GW for the turbine capacity selected. This Middle East region has not seen any significant or meaningful development to exploit its offshore wind energy potential and this work and its outcomes has also addressed this gap in knowledge. To the authors' knowledge, the outcomes represent the first detailed assessment of the offshore wind energy potential for the Arabian Peninsula countries. This work will contribute to the stimulation of interest in the region of the importance of offshore wind as part of a regional energy mix.

It must be noted that this work does not compare the various attributes of the available renewable energy resources in the region, but provides seminal work for understanding the offshore wind energy potential. The outcomes also show the effective aspect of the presented methodology and its utilisation at such a large regional scale.

In summary, the proposed new approach has been verified by the UK offshore wind programme projects and has predicted the sites and capacities of the Arabian Peninsula offshore wind potential at a large scale. The use of the *Representative Cost Ratio* to assist in the rapid and accurate determination of offshore wind energy potential regions will save money and reduce the time and effort taken to achieve the optimal spatial siting decisions for offshore wind energy farms.

Author contributions

The authors contributed to the paper as follows:

AbuBakr S Bahaj designed, led and directed the overall research of the paper and subsequent revisions; Mostafa Mahdy, obtained essential research data, modelling, design and analysis;

Abdulsalam S. Alghamdi contributed to the KSA side of the research and.

David Richards contributed to the editing and critiquing of manuscript.

All authors contributed to the writing, proof reading, and revisions of the manuscript.

Data accessibility

The datasets supporting this article have been implemented as part of the main manuscript.

Declaration of competing interest

The authors declare that they have no known competing financial interests or personal relationships that could have appeared to influence the work reported in this paper.

Acknowledgements

This work is part of the activities of the Energy and Climate Change Division and the Sustainable Energy Research Group in the Faculty of Engineering and Environment at the University of Southampton (www.energy.soton.ac.uk), UK. It is also part of the work of the King Salman bin Abdulaziz Chair for Energy Research within King Abdulaziz University, KSA. It is also supported by EPSRC grants including EP/K012347/1, and the International Centre for Infrastructure Futures (ICIF) and EP/R030391/1 Fortis Unum: Clustering Mini-Grid Networks to Widen Energy Access and Enhance Utility Network Resilience. The research is also part of a PhD programme sponsored by the Faculty of Engineering, Port Said University, Egypt.

Appendix A

Table A
Attribute tables for the three sets of the UK's offshore wind areas.

set a. Round 1 and 2			Set b. Round 3 all operating			Set c. Round 3		
ID	Suitability Value [x 100]	Cells Count	ID	Suitability Value [x 100]	Cells Count	ID	Suitability Value [x 100]	Cells Count
1	41	140	1	40	215	1	42	163
2	42	129	2	41	429	2	43	236
3	44	49	3	42	314	3	44	417
4	45	110	4	43	297	4	45	471
5	46	882	5	44	438	5	46	675
6	47	61	6	45	240	6	47	423
7	48	354	7	46	1081	7	48	113
8	49	65	8	47	240	8	49	380
9	50	81	9	48	267	9	50	1244
10	51	23	10	49	104	10	51	2981
11	52	44	11	50	396	11	52	5343
12	53	4	12	51	664	12	53	7656
13	54	109	13	52	887	13	54	23030
14	56	106	14	53	727	14	55	38889
15	57	7	15	54	2190	15	56	37240
16	59	389	16	55	5117	16	57	43640
17	60	617	17	56	4553	17	58	42704
18	61	1120	18	57	3542	18	59	36686
19	62	1264	19	58	4324	19	60	32195
20	63	1020	20	59	4672	20	61	42883
21	64	1002	21	60	4692	21	62	43159
22	65	2052	22	61	6844	22	63	44510
23	66	2854	23	62	8619	23	64	62563
24	67	3736	24	63	13518	24	65	54082
25	68	3165	25	64	26100	25	66	32675
26	69	5418	26	65	35765	26	67	46389
27	70	3887	27	66	11893	27	68	13139
28	71	1798	28	67	12573	28	69	10860
29	72	1117	29	68	8702	29	70	13526
30	73	781	30	69	10447	30	71	19247
31	74	529	31	70	12728	31	72	17132
32	75	652	32	71	16562	32	73	1347
			33	72	13023			
			34	73	1703			
	Moderate Suitability		35	74	185			
	High Suitability		36	75	95			

References

[1] W. Council, World Energy Resources 2016, World Energy Council, London, UK, 2016.
[2] The Global Wind Energy Council, Offshore wind power, 2018, http://gwec.net/global-figures/global-offshore/, 2018. (Accessed 5 July 2018).
[3] Department for Business & Energy & Industrial Strategy UK, Contracts for difference (CFD) second allocation round results. https://goo.gl/5EquUC, 2018. (Accessed 6 September 2018).
[4] C.B. Simon Virley, CfD Allocation Round Two, 2017.
[5] L.D. Knopper, C.A. Ollson, Health effects and wind turbines: a review of the literature, Environ. Health 10 (1) (2011) 78.
[6] A.M.M. Ismaiel, S. Yoshida, ISNN, Study of Turbulence Intensity Effect on the Fatigue Lifetime of Wind Turbines, Evergreen, 2018, 2189-0420.
[7] C. Estoque, GIS-based Multi-Criteria Decision Analysis,(in Natural Resource Management), Ronald, D1–Division of Spatial Information Science, University of tsukuba, 2011.
[8] J.R. Eastman, H. Jiang, J. Toledano, Multi-criteria and Multi-Objective Decision Making for Land Allocation Using GIS, Multicriteria analysis for land-use management, Springer, 1998, pp. 227–251.
[9] J. Eastman, Multi-criteria evaluation and GIS, Geographical information systems 1 (1999) 493–502.
[10] H.S. Hansen, GIS-based Multi-Criteria Analysis of Wind Farm Development, ScanGIS 2005, Scandinavian Research Conference on Geographical Information Science, 2005, pp. 75–87.
[11] H. Jiang, J.R. Eastman, Application of fuzzy measures in multi-criteria evaluation in GIS, Int. J. Geogr. Inf. Sci. 14 (2) (2000) 173–184.
[12] R. Lesslie, Mapping Our Priorities—Innovation in Spatial Decision Support, Innovation for 21st century conservation, 2012, pp. 156–163.
[13] J.S. Dodgson, M. Spackman, A. Pearman, L.D. Phillips, Multi-criteria Analysis: a Manual, 2009.
[14] M. Dell'Ovo, S. Capolongo, A. Oppio, Combining spatial analysis with MCDA for the siting of healthcare facilities, Land Use Policy 76 (2018) 634–644.
[15] T.L. Saaty, A scaling method for priorities in hierarchical structures, J. Math. Psychol. 15 (3) (1977) 234–281.
[16] T.L. Saaty, Decision making with the analytic hierarchy process, Int. J. Serv. Sci. 1 (1) (2008) 83–98.
[17] M.Z. Siddiqui, J.W. Everett, B.E. Vieux, Landfill siting using geographic information systems: a demonstration, J. Environ. Eng. 122 (6) (1996) 515–523.
[18] M. Giamalaki, T. Tsoutsos, Sustainable siting of solar power installations in Mediterranean using a GIS/AHP approach, Renew. Energy 141 (2019) 64–75.
[19] M. Harper, B. Anderson, P. James, A. Bahaj, Assessing socially acceptable

locations for onshore wind energy using a GIS-MCDA approach, Int. J. Low Carbon Technol. 14 (2) (2019) 160–169.
[20] C. Ntoka, Offshore Wind Park Sitting and Micro-sitting in Petalioi Gulf, Greece, Aalborg University, Denmark, 2013, p. 77.
[21] M. Mahdy, A.S. Bahaj, A.S. Alghamdi, Offshore Wind Energy Potential Around the East Coast of the Red Sea, KSA, Solar World Congress 2017, UAE, Abu Dhabi, 2017.
[22] B. Farhan, A.T. Murray, Siting park-and-ride facilities using a multi-objective spatial optimization model, Comput. Oper. Res. 35 (2) (2008) 445–456.
[23] T. Jäger, R. McKenna, W. Fichtner, The feasible onshore wind energy potential in Baden-Württemberg: a bottom-up methodology considering socio-economic constraints, Renew. Energy 96 (2016) 662–675.
[24] S.H. Siyal, U. Mörtberg, D. Mentis, M. Welsch, I. Babelon, M. Howells, Wind energy assessment considering geographic and environmental restrictions in Sweden: a GIS-based approach, Energy 83 (2015) 447–461.
[25] J. Schallenberg-Rodríguez, N.G. Montesdeoca, Spatial planning to estimate the offshore wind energy potential in coastal regions and islands. Practical case: the Canary Islands, Energy 143 (2018) 91–103.
[26] T. Lirn, H. Thanopoulou, M.J. Beynon, A.K.C. Beresford, An application of AHP on transhipment port selection: a global perspective, Marit. Econ. Logist. 6 (1) (2004) 70–91.
[27] Ž. Stević, S. Vesković, M. Vasiljević, G. Tepić, The Selection of the Logistics Center Location Using AHP Method, University of Belgrade, Faculty of Transport and Traffic Engineering, LOGIC, Belgrade, 2015, pp. 86–91.
[28] D. Dalalah, M. Hayajneh, F. Batieha, A fuzzy multi-criteria decision making model for supplier selection, Expert Syst. Appl. 38 (7) (2011) 8384–8391.
[29] M. Aruldoss, T.M. Lakshmi, V.P. Venkatesan, A survey on multi criteria decision making methods and its applications, American Journal of Information Systems 1 (1) (2013) 31–43.
[30] H. Martin, G. Spano, J. Küster, M. Collu, A. Kolios, Application and extension of the TOPSIS method for the assessment of floating offshore wind turbine support structures, Ships Offshore Struct. 8 (5) (2013) 477–487.
[31] E. Lozano-Minguez, A. Kolios, F.P. Brennan, Multi-criteria assessment of offshore wind turbine support structures, Renew. Energy 36 (11) (2011) 2831–2837.
[32] N. Akbari, C.A. Irawan, D.F. Jones, D. Menachof, A multi-criteria port suitability assessment for developments in the offshore wind industry, Renew. Energy 102 (2017) 118–133.
[33] The Crown Estate, Round 3 Offshore Wind Site Selection at National and Project Levels, 2012.
[34] N.Y. Aydin, E. Kentel, S. Duzgun, GIS-based environmental assessment of wind energy systems for spatial planning: a case study from Western Turkey, Renew. Sustain. Energy Rev. 14 (1) (2010) 364–373.
[35] J.-J. Wang, Y.-Y. Jing, C.-F. Zhang, J.-H. Zhao, Review on multi-criteria decision analysis aid in sustainable energy decision-making, Renew. Sustain. Energy Rev. 13 (9) (2009) 2263–2278.
[36] A. Mostafaeipour, Feasibility study of offshore wind turbine installation in Iran compared with the world, Renew. Sustain. Energy Rev. 14 (7) (2010) 1722–1743.
[37] D. Flood, Round 3 Offshore Wind Farms. UK Future Energy Scenarios Seminar 2012, Forewind Report, 2012.
[38] T. Kim, J.-I. Park, J. Maeng, Offshore wind farm site selection study around Jeju Island, South Korea, Renew. Energy 94 (2016) 619–628.
[39] D. Lande-Sudall, T. Stallard, P. Stansby, Co-located offshore wind and tidal stream turbines: assessment of energy yield and loading, Renew. Energy 118 (2018) 627–643.
[40] S. Cavazzi, A. Dutton, An Offshore Wind Energy Geographic Information System (OWE-GIS) for assessment of the UK's offshore wind energy potential, Renew. Energy 87 (2016) 212–228.
[41] M. Mahdy, A.S. Bahaj, Multi Criteria Decision Analysis for Offshore Wind Energy Potential in Egypt, Renewable Energy, 2017.
[42] J.R. Eastman, Idrisi Para Windows: Version 2.0, Enero 1997, Clark University, 1997. Tutorial Exercises.
[43] Esri, The ArcGIS help library. http://help.arcgis.com/en/arcgisdesktop/10.0/help/, 2012. (Accessed 14 July 2016).
[44] B. Durning, M. Broderick, Development of cumulative impact assessment guidelines for offshore wind farms and evaluation of use in project making, Impact Assess. Proj. Apprais. 37 (2) (2019) 124–138.
[45] D. Latinopoulos, K. Kechagia, A GIS-based multi-criteria evaluation for wind farm site selection. A regional scale application in Greece, Renew. Energy 78 (2015) 550–560.
[46] S.M. Baban, T. Parry, Developing and applying a GIS-assisted approach to locating wind farms in the UK, Renew. Energy 24 (1) (2001) 59–71.
[47] J.J. Watson, M.D. Hudson, Regional Scale wind farm and solar farm suitability assessment using GIS-assisted multi-criteria evaluation, Landsc. Urban Plan. 138 (2015) 20–31.
[48] T. Stehly, D. Heimiller, G. Scott, Cost of Wind Energy Review, National Renewable Energy Laboratory, 2016.
[49] WindEurope, Offshore Wind in Europe: Key Trends and Statistics 2017, 2018.
[50] The Crown Estate, Offshore Wind Cost Reduction: Pathways Study, United Kingdom, 2012. May.
[51] The Crown Estate, Offshore Wind Operational Report, 2014.
[52] The Crown Estate, Offshore Wind Operational Report January – December 2016, 2017.
[53] The Crown Estate, Offshore Wind Shapefiles, 2019. United Kingdom.
[54] D. Lambkin, J. Harris, W. Cooper, T. Coates, Coastal Process Modelling for Offshore Wind Farm Environmental Impact Assessment: Best Practice Guide, COWRIE Limited, London, 2009.
[55] V. UNFCCC, Adoption of the Paris Agreement, I: Proposal by the President (Draft Decision), vol. 32, United Nations Office, Geneva (Switzerland), 2015 s.
[56] H.A. Buflasa, D. Infield, S. Watson, M. Thomson, Wind resource assessment for the Kingdom of Bahrain, Wind Eng. 32 (5) (2008) 439–448.
[57] S. Munawwar, H. Ghedira, A review of renewable energy and solar industry growth in the GCC region, Energy Procedia 57 (2014) 3191–3202.
[58] H.A. Kazem, Renewable energy in Oman: status and future prospects, Renew. Sustain. Energy Rev. 15 (8) (2011) 3465–3469.
[59] A.-H. Marafia, H.A. Ashour, Economics of off-shore/on-shore wind energy systems in Qatar, Renew. Energy 28 (12) (2003) 1953–1963.
[60] S. Rehman, Offshore wind power assessment on the east coast of Saudi Arabia, Wind Eng. 29 (5) (2005) 409–419.
[61] O. Nematollahi, H. Hoghooghi, M. Rasti, A. Sedaghat, Energy demands and renewable energy resources in the Middle East, Renew. Sustain. Energy Rev. 54 (2016) 1172–1181.
[62] A. Mostafaeipour, N. Mostafaeipour, Renewable energy issues and electricity production in Middle East compared with Iran, Renew. Sustain. Energy Rev. 13 (6) (2009) 1641–1645.
[63] M.A.H. Mondal, D. Hawila, S. Kennedy, T. Mezher, The GCC countries RE-readiness: strengths and gaps for development of renewable energy technologies, Renew. Sustain. Energy Rev. 54 (2016) 1114–1128.
[64] The British Oceanographic Data Centre, The GEBCO_2014 grid. www.gebco.net, 2014. (Accessed 25 March 2016).
[65] N.G. Mortensen, U.S. Said, J. Badger, Wind Atlas of Egypt, RISO National Laboratory, New and Renewable Energy Authority, Egyptian Meteorological Authority, 2006.
[66] G. Kieffer, T. Couture, Renewable Energy Target Setting, IRENA, Masdar, 2015.
[67] C.M.A. Yip, U.B. Gunturu, G.L. Stenchikov, High-altitude wind resources in the Middle East, Sci. Rep. 7 (1) (2017) 9885.
[68] C.M.A. Yip, U.B. Gunturu, G.L. Stenchikov, Wind resource characterization in the arabian Peninsula, Appl. Energy 164 (2016) 826–836.
[69] Ecotravelworldwide, NATIONAL PARKS OF OMAN. https://www.nationalparks-worldwide.com/oman.htm, 2017.
[70] Ecotravelworldwide, NATIONAL PARKS OF YEMEN. https://www.nationalparks-worldwide.com/yemen.htm, 2017.
[71] Ecotravelworldwide, NATIONAL PARKS OF THE UNITED ARAB EMIRATES. https://www.nationalparks-worldwide.com/united_arab_emirates.htm, 2017.
[72] SWA, Protected Areas Map, 2017. https://www.swa.gov.sa/en/protected-areas/protected-areas-map. (Accessed 9 August 2017).
[73] Aramco, Petrol Oil Extraction Map, KSA, 2017. http://www.saudiaramco.com/en/home.html. (Accessed 4 August 2017).
[74] The MarineTraffic, Ship Density Maps, 2015. https://www.marinetraffic.com/. (Accessed 4 July 2016).
[75] TeleGeography Company, Submarine Cable Map, 2015. http://www.submarinecablemap.com/. (Accessed 29 June 2016).
[76] GENI, National, Electricity Transmission Grid, 2017. http://www.geni.org/globalenergy/library/national_energy_grid. (Accessed 24 December 2017).
[77] A. Al-Mohaisen, S. Sud, Update on the Gulf Cooperation Council (GCC) electricity grid system interconnection, in: Power Engineering Society General Meeting, 2006, IEEE, 2006, p. 6. IEEE.
[78] B. Sheridan, S.D. Baker, N.S. Pearre, J. Firestone, W. Kempton, Calculating the offshore wind power resource: robust assessment methods applied to the US Atlantic Coast, Renew. Energy 43 (2012) 224–233.
[79] Offshore wind energy factbook report, E.ON Climate & Renewables GmbH, Http://Www.eon.com/Content/Dam/Eon-Content-Pool/Eon/Company-Asset-Finder/Company-Profiles/Ecr/2012_09_11_EON_Offshore_Factbook_en_pdf_%20final.pdf, 2012 (2012).
[80] C. Desmond, J. Murphy, L. Blonk, W. Haans, Description of an 8 MW reference wind turbine, IOP Publishing, J. Phys. Conf. Ser. (2016), p. 092013.
[81] C. Factbook, The world factbook. https://www.cia.gov/library/publications/the-world-factbook, 2018.
[82] N. Saleous, S. Issa, J. Al Mazrouei, GIS-BASED WIND FARM SITE SELECTION MODEL OFFSHORE ABU DHABI EMIRATE, UAE, international archives of the photogrammetry, Remote Sensing & Spatial Information Sciences 41 (2016).
[83] T. Jimichi, M. Kaymak, R.W. De Doncker, Design and experimental verification of a three-phase dual-active bridge converter for offshore wind turbines, in: 2018 International Power Electronics Conference (IPEC-Niigata 2018-ECCE Asia), IEEE, 2018, pp. 3729–3733.

List of References

4C OFFSHORE 2017. Global Offshore Wind Farms Database. *Blekinge Offshore AB Offshore Wind Farm." www. 4coffshore. com/windfarms/windfarms. aspx*.

4C OFFSHORE LTD. 2018. *Offshore Wind Farms Informations* [Online]. Available: www.4coffshore.com/windfarms [Accessed 2018].

ABDALLAH, A. 2014. Monitoring Environmental Changes in El-Ain El-Sokhna Area, Gulf of Suez, Egypt.

ABDEL-AZIZ, N. E., GHOBASHI, A. E., DORGHAM, M. M. & EL-TOHAMI, W. S. 2007. Qualitative and quantitative study of copepods in damietta harbor, egypt.

ABDELKADER, A. 2015. *Investigation of Hybrid Foundation System For Offshore Wind Turbine.* Doctor of Philosophy, The University of Western Ontario, London, Ontario, Canada.

ABDOU, D. S. & ZAAZOU, Z. 2013. The Egyptian Revolution and post Socio-economic impact. *Topics in Middle Eastern and African Economies,* 15**,** 92-115.

ABPMER 2018. Atlas of UK Marine Renewable Energy Resources.

ACHMUS, M., KUO, Y.-S. & ABDEL-RAHMAN, K. 2009. Behavior of monopile foundations under cyclic lateral load. *Computers and Geotechnics,* 36**,** 725-735.

ACKER, T. & CHIME, A. H. 2011. Wind modeling using WindPro and WAsP software. *Norther Arizon University, USA,* 1560000.

AFEWERKI, S., KARLSEN, A. & MACKINNON, D. 2018. Configuring floating production networks: A case study of a new offshore wind technology across two oil and gas economies. *Norsk Geografisk Tidsskrift-Norwegian Journal of Geography***,** 1-12.

AHMED, H. & ABOUZEID, M. 2001. Utilization of wind energy in Egypt at remote areas. *Renewable energy,* 23**,** 595-604.

AKBARI, N., IRAWAN, C. A., JONES, D. F. & MENACHOF, D. 2017. A multi-criteria port suitability assessment for developments in the offshore wind industry. *Renewable Energy,* 102**,** 118-133.

AL-MAAMARY, H. M., KAZEM, H. A. & CHAICHAN, M. T. 2017. Renewable energy and GCC States energy challenges in the 21st century: A review. *International Journal of Computation and Applied Sciences IJOCAAS,* 2**,** 11-18.

AL-MOHAISEN, A. & SUD, S. Update on the Gulf Cooperation Council (GCC) electricity grid system interconnection. Power Engineering Society General Meeting, 2006. IEEE, 2006. IEEE, 6 pp.

ALBRITTON, C. C., BROOKS, J. E., ISSAWI, B. & SWEDAN, A. 1990. Origin of the Qattara depression, Egypt. *Geological Society of America Bulletin,* 102**,** 952-960.

ALFADHLI, B. H. 2018. Boundaries and Territorial Disputes in the GCC States.

ALNASER, W. & ALNASER, N. 2011. The status of renewable energy in the GCC countries. *Renewable and Sustainable Energy Reviews,* 15**,** 3074-3098.

AMERICAN PETROLEUM INSTITUTE 1989. *Recommended practice for planning, designing, and constructing fixed offshore platforms*, American Petroleum Institute.

ARAMCO. 2017. *Petrol oil extraction map, KSA* [Online]. Available: http://www.saudiaramco.com/en/home.html [Accessed 04/08/2017].

ARANY, L., BHATTACHARYA, S., MACDONALD, J. & HOGAN, S. 2017. Design of monopiles for offshore wind turbines in 10 steps. *Soil Dynamics and Earthquake Engineering,* 92**,** 126-152.

ARAPOGIANNI, A., GENACHTE, A., OCHAGAVIA, R. M., VERGARA, J., CASTELL, D., TSOUROUKDISSIAN, A. R., KORBIJN, J., BOLLEMAN, N., HUERA-HUARTE, F. & SCHUON, F. 2013. Deep Water; The next step for offshore wind energy. *European Wind Energy Association (EWEA)*.

ARGIN, M. & YERCI, V. 2017. Offshore Wind Power Potential of the Black Sea Region in Turkey. *International Journal of Green Energy*.

ARULDOSS, M., LAKSHMI, T. M. & VENKATESAN, V. P. 2013. A survey on multi criteria decision making methods and its applications. *American Journal of Information Systems,* 1**,** 31-43.

ASGARI, N., HASSANI, A., JONES, D. & NGUYE, H. H. 2015. Sustainability ranking of the UK major ports: Methodology and case study. *Transportation research part E: logistics and transportation review,* 78**,** 19-39.

AWAD, A. H. A. 2002. Environmental Study in Subway Metro Stations in Cairo, Egypt. *Journal of Occupational Health,* 44**,** 112-118.

AYDIN, N. Y., KENTEL, E. & DUZGUN, S. 2010. GIS-based environmental assessment of wind energy systems for spatial planning: A case study from Western Turkey. *Renewable and Sustainable Energy Reviews,* 14**,** 364-373.

B. J. GRIBBEN, N. W., D. RANFORD 2010 Offshore Wind Farm Layout Design - A Systems Engineering Approach *Ocean Power Fluid Machinery.*

BABAN, S. M. & PARRY, T. 2001. Developing and applying a GIS-assisted approach to locating wind farms in the UK. *Renewable energy,* 24**,** 59-71.

BADRAN, M. & EL-HAGGAR, S. 2006. Optimization of municipal solid waste management in Port Said–Egypt. *Waste Management,* 26**,** 534-545.

BAHAKEEM, A. S. 2015. A Hybrid Renewable Energy Model For Medina City of Saudi Arabia Using Integer Linear Programming. *Journal of Electrical and Electronics Engineering (IOSR-JEEE),* 9,.

BAHGAT, G. 2013. Egypt's Energy Outlook: Opportunities and Challenges. *Mediterranean Quarterly,* 24**,** 12-37.

BARTLETT, S. F. 2010. Mohr-Coulomb Model.

BASEER, M., REHMAN, S., MEYER, J. P. & ALAM, M. M. 2017. GIS-based site suitability analysis for wind farm development in Saudi Arabia. *Energy,* 141**,** 1166-1176.

BHATTACHARYA, S. 2014. Challenges in design of foundations for Offshore Wind Turbines. *Engineering & Technology Reference,* 1.

BILGILI, M., YASAR, A. & SIMSEK, E. 2011. Offshore wind power development in Europe and its comparison with onshore counterpart. *Renewable and Sustainable Energy Reviews,* 15**,** 905-915.

BIRDLIFE INTERNATIONAL. 2018. *Soaring Bird Sensitivity Map* [Online]. Available: http://migratorysoaringbirds.undp.birdlife.org/en/sensitivity-map [Accessed].

BODANSKY, D. 2016. The Paris climate change agreement: a new hope? *American Journal of International Law,* 110**,** 288-319.

BOND, A. J., HIGHT, D. & JARDINE, R. 1997. *Design of Piles in Sand in the UK Sector of the North Sea*, HSE Books.

BROWER, M. C. & ROBINSON, N. M. 2012. The openWind deep-array wake model: development and validation. *AWS Truepower*.

BROWN, M. C. 2006. *Hacking google maps and google earth*, Wiley Pub.

BRUNS, B., KUHN, C., STEIN, P., GATERMANN, J. & ELMER, K.-H. The new noise mitigation system'Hydro Sound Dampers': History of development with several hydro sound and vibration measurements. INTER-NOISE and NOISE-CON Congress and Conference Proceedings, 2014. Institute of Noise Control Engineering, 4915-4923.

BUFLASA, H. A., INFIELD, D., WATSON, S. & THOMSON, M. 2008. Wind resource assessment for the Kingdom of Bahrain. *Wind Engineering,* 32**,** 439-448.

CARSWELL, W., ARWADE, S., DEGROOT, D. & MYERS, A. 2016. Natural frequency degradation and permanent accumulated rotation for offshore wind turbine monopiles in clay. *Renewable Energy,* 97**,** 319-330.

CAVAZZI, S. & DUTTON, A. 2016. An Offshore Wind Energy Geographic Information System (OWE-GIS) for assessment of the UK's offshore wind energy potential. *Renewable Energy,* 87**,** 212-228.

CHEN, Y., YU, J. & KHAN, S. 2010. Spatial sensitivity analysis of multi-criteria weights in GIS-based land suitability evaluation. *Environmental modelling & software,* 25**,** 1582-1591.

CHEN, Y., YU, J., SHAHBAZ, K. & XEVI, E. A GIS-based sensitivity analysis of multi-criteria weights. Proceedings of the 18th World IMACS/MODSIM Congress, Cairns, Australia. Citeseer, 2009. 13-17.

CHOU, C.-C. 2007. A fuzzy MCDM method for solving marine transshipment container port selection problems. *Applied Mathematics and Computation,* 186**,** 435-444.

CLAYTON, C. R. 1995. *The standard penetration test (SPT): methods and use*, Construction Industry Research and Information Association.

COUNCIL, W. 2016. World energy resources 2016. *World Energy Council, London, UK*.

DALALAH, D., HAYAJNEH, M. & BATIEHA, F. 2011. A fuzzy multi-criteria decision making model for supplier selection. *Expert systems with applications,* 38**,** 8384-8391.

DELL'OVO, M., CAPOLONGO, S. & OPPIO, A. 2018. Combining spatial analysis with MCDA for the siting of healthcare facilities. *Land use policy,* 76**,** 634-644.

DEMERS, M. N. 2008. *Fundamentals of geographic information systems*, John Wiley & Sons.

DESMOND, C., MURPHY, J., BLONK, L. & HAANS, W. Description of an 8 MW reference wind turbine. Journal of Physics: Conference Series, 2016. IOP Publishing, 092013.

DICORATO, M., FORTE, G., PISANI, M. & TROVATO, M. 2011. Guidelines for assessment of investment cost for offshore wind generation. *Renewable Energy,* 36**,** 2043-2051.

DNV-GL 2016. SUPPLY CHAIN, PORT INFRASTRUCTURE AND LOGISTICS STUDY.

DNV, G. 2014. Design of Offshore Wind Turbine Structures. Offshore Standard DNV-OS-J101. *DNV GL AS, Høvik (Norway)*.

DODGSON, J. S., SPACKMAN, M., PEARMAN, A. & PHILLIPS, L. D. 2009. Multi-criteria analysis: a manual.

DOHERTY, P. & GAVIN, K. 2011. Laterally loaded monopile design for offshore wind farms. *Proceedings of the ICE-Energy,* 165**,** 7-17.

E.ON 2012. Offshore Wind Energy Factbook. *E. ON Climate & Renewables GmbH*.

EASTMAN, J. 1999. Multi-criteria evaluation and GIS. *Geographical information systems,* 1**,** 493-502.

EASTMAN, J. R. 1997. *Idrisi Para Windows: Version 2.0, Enero 1997. Tutorial Exercises*, Clark University.

EASTMAN, J. R. 2006. IDRISI Andes tutorial. *Clark Labs, Worcester, MA*.

EASTMAN, J. R., JIANG, H. & TOLEDANO, J. 1998. Multi-criteria and multi-objective decision making for land allocation using GIS. *Multicriteria analysis for land-use management.* Springer.

ECOTRAVELWORLDWIDE. 2017a. *NATIONAL PARKS OF OMAN* [Online]. Available: https://www.nationalparks-worldwide.com/oman.htm [Accessed].

ECOTRAVELWORLDWIDE. 2017b. *NATIONAL PARKS OF THE UNITED ARAB EMIRATES* [Online]. Available: https://www.nationalparks-worldwide.com/united_arab_emirates.htm [Accessed].

ECOTRAVELWORLDWIDE. 2017c. *NATIONAL PARKS OF YEMEN* [Online]. Available: https://www.nationalparks-worldwide.com/yemen.htm [Accessed].

EEA 2009. Europe's onshore and offshore wind energy potential.

EED, M. A. A. M. 2012. Monitoring of Oil Spills along Suez-Ain Sokhna Coastal Zone, Using Remote Sensing Techniques.

EGYPT STATE INFORMATION SERVICE. 2017. *Population* [Online]. Available: http://www.sis.gov.eg/En/ [Accessed /03 2016/08].

EL-GEZIRY, T. M., ABD ELLAH, R. & MAIYZA, I. A. 2007. bathymetric chart of alexandria wastern harbor.

EL-SAYED, M. A. 2002. Substitution potential of wind energy in Egypt. *Energy Policy,* 30**,** 681-687.

EL-SHIMY, M. 2010. Optimal site matching of wind turbine generator: Case study of the Gulf of Suez region in Egypt. *Renewable Energy,* 35**,** 1870-1878.

EL DIASTY, W. S., EL BEIALY, S., GHONAIM, A. A., MOSTAFA, A. & EL ATFY, H. 2014. Palynology, palynofacies and petroleum potential of the Upper Cretaceous–Eocene Matulla, Brown Limestone and Thebes formations, Belayim oilfields, central Gulf of Suez, Egypt. *Journal of African Earth Sciences,* 95**,** 155-167.

ELKINTON, C. N., MANWELL, J. F. & MCGOWAN, J. G. 2008. Algorithms for offshore wind farm layout optimization. *Wind Engineering,* 32**,** 67-84.

ELLIOTT, D., HOLLADAY, C., BARCHET, W., FOOTE, H. & SANDUSKY, W. 1987. Wind energy resource atlas of the United States. *NASA STI/Recon Technical Report N,* 87.

ELMER, K.-H. & SAVERY, J. New Hydro Sound Dampers to reduce piling underwater noise. INTER-NOISE and NOISE-CON Congress and Conference Proceedings, 2014. Institute of Noise Control Engineering, 5551-5560.

EMBABI, N. S. 2018. Geographic Regions of Egypt. *Landscapes and Landforms of Egypt.* Springer.

ENERGYNUMBERS. 2019. *UK offshore wind capacity factors* [Online]. Available: http://energynumbers.info/uk-offshore-wind-capacity-factors [Accessed 16/12/2019].

ERICKSON, W. P., JOHNSON, G. D. & DAVID JR, P. A summary and comparison of bird mortality from anthropogenic causes with an emphasis on collisions. In: Ralph, C. John; Rich, Terrell D., editors 2005. Bird Conservation Implementation and Integration in the Americas: Proceedings of the Third International Partners in Flight Conference. 2002 March 20-24; Asilomar, California, Volume 2 Gen. Tech. Rep. PSW-GTR-191. Albany, CA: US Dept. of Agriculture, Forest Service, Pacific Southwest Research Station: p. 1029-1042, 2005.

ESRI. 2012. *The ArcGIS Help Library* [Online]. Available: http://help.arcgis.com/en/arcgisdesktop/10.0/help/ [Accessed /14 2016/07].

ESSA, K. S., EMBABY, M. & MARROUF, A. 2007. Feasibility study of electrical generation by wind energy on the Red-Sea Coast in Egypt. *Wind Engineering,* 31**,** 293-301.

ESTEBAN, M., COUÑAGO, B., LÓPEZ-GUTIÉRREZ, J., NEGRO, V. & VELLISCO, F. 2015. Gravity based support structures for offshore wind turbine generators: Review of the installation process. *Ocean Engineering,* 110**,** 281-291.

ESTEBAN, M., LOPEZ-GUTIERREZ, J. S., DIEZ, J. & NEGRO, V. 2011a. Methodology for the design of offshore wind farms. *Journal of Coastal Research***,** 496.

ESTEBAN, M. D., DIEZ, J. J., LÓPEZ, J. S. & NEGRO, V. 2011b. Why offshore wind energy? *Renewable Energy,* 36**,** 444-450.

ESTOQUE, C. 2011. GIS-based multi-criteria decision analysis,(in natural resource management). *Ronald, D1–Division of spatial information science, University of tsukuba*.

EUROPEAN WIND ENERGY ASSOCIATION 2016. The European offshore wind industry - key trends and statistics 2015.

FACTBOOK, C. 2018. The world factbook. *See also: https://www.cia.gov/library/publications/the-world-factbook*.

FARHAN, B. & MURRAY, A. T. 2008. Siting park-and-ride facilities using a multi-objective spatial optimization model. *Computers & Operations Research,* 35**,** 445-456.

FERY, N., BRUSS, G., AL-SUBHI, A. & MAYERLE, R. Numerical study of wind-generated waves in the Red Sea. Proceedings 4th International Conference of the application of physical modeling to port and coastal protection, Coastlab12, Ghent, Belgium, 2012. 446-455.

FIJN, R., GYIMESI, A., COLLIER, M., BEUKER, D., DIRKSEN, S. & KRIJGSVELD, K. 2012. Flight patterns of birds at offshore gas platform K14. *Flight intensity, flight altitudes and species composition in comparison to OWEZ. Report***,** 11-112.

FJELLANGER, E. M. 2016. *Wind Farm Layout Optimization-A case study on maximizing the annual energy production in Creyke Beck B.* The University of Bergen.

FLOOD, D. 2012. Round 3 offshore wind farms. UK Future Energy Scenarios seminar 2012. Forewind Report.

FOOD & AGRICULTURE ORGANIZATION OF THE UNITED NATIONS 2015. FAO GEONETWORK. Rome, Italy: FAO.

FRAILE, D. & MBISTROVA, A. 2018. Wind in Europe 2017-Annual combined onshore and offshore wind energy statistics. *Wind Europe, Φεβ*.

FRANK, R. Design of pile foundations following Eurocode 7. Proc. XIII Danube-European Conference on Geotechnical Engineering, 2006. Citeseer, 577-586.

GALAL, A. 2017. Seaports as a Tool for the Urban & Economic Development in Egyptian Coastal Cities.

GAUDIOSI, G. 1996. Offshore wind energy in the world context. *Renewable Energy,* 9**,** 899-904.

GAYTHWAITE, J. W. Design of marine facilities for the berthing, mooring, and repair of vessels. 2004. American Society of Civil Engineers.

GENERAL AUTHORITY FOR FISH RESOURCES DEVELOPMENT. 2009. *Fishing regulation laws* [Online]. Available: http://www.gafrd.org/ [Accessed /20 2016/04].

GENI. 2017. *National Electricity Transmission Grid* [Online]. Available: http://www.geni.org/globalenergy/library/national_energy_grid [Accessed 24/12/2017].

GHALY, A. I., KHALIL, A. E. & MAHMOUD, A. A. 2013. Stratigraphic Analysis and Petroleum Exploration, Offshore, Nile Delta,Egypt. *Seismic Stratigraphy and Seismic Geomorphology*.

GIELEN, D. 2012. Renewable energy technologies: cost analysis series–wind power. *IRENA working paper.* International Renewable Energy Agency (IRENA).

GL-ENERGY, D. 2014. WindFarmer Theory Manual. *GL Garrad Hassan,* 843.

GREEN, R. & VASILAKOS, N. 2011. The economics of offshore wind. *Energy Policy,* 39**,** 496-502.

GUY, E. & URLI, B. 2006. Port selection and multicriteria analysis: An application to the Montreal-New York alternative. *Maritime Economics & Logistics,* 8**,** 169-186.

HADŽIĆ, N., KOZMAR, H. & TOMIĆ, M. 2014. Offshore renewable energy in the Adriatic Sea with respect to the Croatian 2020 energy strategy. *Renewable and Sustainable Energy Reviews,* 40**,** 597-607.

HAMADA, H., SAGAWA, Y. & YAMAMOTO, D. Influence of seawater mixing and curing on strength characteristics and porosity of ground granulated blast-furnace slag concrete. IOP Conference Series: Materials Science and Engineering, 2017. IOP Publishing, 012070.

HAMBURG WIND ENERGY 2018. Conference on Technical Surfaces.

HANSEN, H. S. GIS-based multi-criteria analysis of wind farm development. ScanGIS 2005: Scandinavian Research Conference on Geographical Information Science, 2005. 75-87.

HARPER, M., ANDERSON, B., JAMES, P. A. & BAHAJ, A. S. 2019. Onshore wind and the likelihood of planning acceptance: Learning from a Great Britain context. *Energy Policy,* 128**,** 954-966.

HIBBETT, KARLSSON & SORENSEN 2010. *ABAQUS/standard: User's Manual*, Hibbitt, Karlsson & Sorensen.

HIDELECCO CONSTRUCTION COMPANY 2010. Geological Report for El-Zaafarana coastal area, Egypt.

INTERNATIONAL ELECTROTECHNICAL COMMISSION 2009. Wind Turbines—Part 3: Design Requirements for Offshore Wind Turbines. *No. IEC61400-3*.

INTERNATIONAL ENERGY AGENCY 2017. *Key World Energy Statistics*, OECD Publishing.

IRENA 2016. Renewable Energy Market Analysis: The GCC Region. *In:* AGENCY, I. R. E. (ed.) *International Renewable Energy Agency.* International Renewable Energy Agency.

ISMAIEL, A. M. M. & YOSHIDA, S. 2018. Study of turbulence intensity effect on the fatigue lifetime of wind turbines. *Evergreen ISNN***,** 2189-0420.

ISMAIL, N., ISKANDER, M. & EL-SAYED, W. 2012. Assessment of Coastal Flooding at Southern Mediterranean with Global Outlook for Lowland Coastal Zones. *Coastal Engineering Proceedings,* 1**,** 83.

JÄGER, T., MCKENNA, R. & FICHTNER, W. 2016. The feasible onshore wind energy potential in Baden-Württemberg: A bottom-up methodology considering socio-economic constraints. *Renewable energy,* 96**,** 662-675.

JANKOWSKI, P., NYERGES, T. L., SMITH, A., MOORE, T. & HORVATH, E. 1997. Spatial group choice: a SDSS tool for collaborative spatial decisionmaking. *International journal of geographical information science,* 11**,** 577-602.

JIANG, H. & EASTMAN, J. R. 2000. Application of fuzzy measures in multi-criteria evaluation in GIS. *International Journal of Geographical Information Science,* 14**,** 173-184.

JIMICHI, T., KAYMAK, M. & DE DONCKER, R. W. Design and Experimental Verification of a Three-Phase Dual-Active Bridge Converter for Offshore Wind Turbines. 2018 International Power Electronics Conference (IPEC-Niigata 2018-ECCE Asia), 2018. IEEE, 3729-3733.

JONKMAN, J., BUTTERFIELD, S., MUSIAL, W. & SCOTT, G. 2009. Definition of a 5-MW reference wind turbine for offshore system development. *National Renewable Energy Laboratory, Golden, CO, Technical Report No. NREL/TP-500-38060*.

JONKMAN, J. & MUSIAL, W. 2010. Offshore code comparison collaboration (OC3) for IEA task 23 offshore wind technology and deployment. *Contract,* 303**,** 275-3000.

JOOS, M. & STAFFELL, I. 2018. Short-term integration costs of variable renewable energy: Wind curtailment and balancing in Britain and Germany. *Renewable and Sustainable Energy Reviews,* 86**,** 45-65.

JUNG, S., KIM, S.-R. & PATIL, A. 2015. Effect of monopile foundation modeling on the structural response of a 5-MW offshore wind turbine tower. *Ocean Engineering,* 109**,** 479-488.

KAHLERT, J., PETERSEN, I. K., FOX, A. D., DESHOLM, M. & CLAUSAGER, I. 2004. Investigations of birds during construction and operation of Nysted offshore wind farm at Rødsand-Annual status report 2003: Report request. Commissioned by Energi E2 A/S.

KAISER, M. 2009. Environmental changes, remote sensing, and infrastructure development: The case of Egypt's East Port Said harbour. *Applied Geography,* 29**,** 280-288.

KALDELLIS, J., APOSTOLOU, D., KAPSALI, M. & KONDILI, E. 2016. Environmental and social footprint of offshore wind energy. Comparison with onshore counterpart. *Renewable Energy,* 92**,** 543-556.

KALDELLIS, J. & KAPSALI, M. 2013. Shifting towards offshore wind energy—Recent activity and future development. *Energy Policy,* 53**,** 136-148.

KALDELLIS, J., KAPSALI, M. & KATSANOU, E. 2012. Renewable energy applications in Greece—What is the public attitude? *Energy Policy,* 42**,** 37-48.

KAZEM, H. A. 2011. Renewable energy in Oman: Status and future prospects. *Renewable and Sustainable Energy Reviews,* 15**,** 3465-3469.

KHALIL, A. K., MUBARAK, A. M. & KASEB, S. A. 2010. Road map for renewable energy research and development in Egypt. *Journal of Advanced Research,* 1**,** 29-38.

KIEFFER, G. & COUTURE, T. 2015. Renewable energy target setting. *IRENA, Masdar*.

KIM, T., PARK, J.-I. & MAENG, J. 2016. Offshore wind farm site selection study around Jeju Island, South Korea. *Renewable energy,* 94**,** 619-628.

KNOPPER, L. D. & OLLSON, C. A. 2011. Health effects and wind turbines: A review of the literature. *Environmental Health,* 10**,** 78.

KUSIAK, A. & SONG, Z. 2010. Design of wind farm layout for maximum wind energy capture. *Renewable energy,* 35**,** 685-694.

LAM, J. S. L. & DAI, J. 2012. A decision support system for port selection. *Transportation Planning and Technology,* 35**,** 509-524.

LAMBKIN, D., HARRIS, J., COOPER, W. & COATES, T. 2009. Coastal process modelling for offshore wind farm environmental impact assessment: best practice guide. *COWRIE Limited, London*.

LASHIN, A. & SHATA, A. 2012. An analysis of wind power potential in Port Said, Egypt. *Renewable and Sustainable Energy Reviews,* 16**,** 6660-6667.

LATINOPOULOS, D. & KECHAGIA, K. 2015. A GIS-based multi-criteria evaluation for wind farm site selection. A regional scale application in Greece. *Renewable Energy,* 78**,** 550-560.

LAVANCHY, D. 2011. Evolving epidemiology of hepatitis C virus. *Clinical Microbiology and Infection,* 17**,** 107-115.

LESSLIE, R. 2012. Mapping our priorities—innovation in spatial decision support. *Innovation for 21st century conservation***,** 156-163.

LI, Y., ONG, M. C. & TANG, T. 2018. Numerical analysis of wave-induced poro-elastic seabed response around a hexagonal gravity-based offshore foundation. *Coastal Engineering,* 136**,** 81-95.

LIRN, T., THANOPOULOU, H., BEYNON, M. J. & BERESFORD, A. K. C. 2004. An application of AHP on transhipment port selection: a global perspective. *Maritime Economics & Logistics,* 6**,** 70-91.

LOZANO-MINGUEZ, E., KOLIOS, A. & BRENNAN, F. P. 2011. Multi-criteria assessment of offshore wind turbine support structures. *Renewable Energy,* 36**,** 2831-2837.

MAHDY, M., BAHAJ, A. S. & ALGHAMDI, A. S. 2017. Offshore Wind Energy Potential around the East Coast of the Red Sea, KSA. *Solar World Congress 2017.* Abu Dhabi, UAE

MALHOTRA, S. Design Considerations for Offshore Wind Turbine Foundations in the United States. The Nineteenth International Offshore and Polar Engineering Conference, 2009. International Society of Offshore and Polar Engineers.

MALHOTRA, S. 2011. *Selection, design and construction of offshore wind turbine foundations*, INTECH Open Access Publisher.

MANUAL, S. P. 1984. Coastal Engineering Research Center. *Department of the Army, Waterways Experiment Station,* 1.

MARAFIA, A.-H. & ASHOUR, H. A. 2003. Economics of off-shore/on-shore wind energy systems in Qatar. *Renewable Energy,* 28**,** 1953-1963.

MARITIME TRANSPORT SECTOR. 2015. *Egyptian Ports* [Online]. Available: http://www.mts.gov.eg/ [Accessed /08 2016/04].

MARTIN, H., SPANO, G., KÜSTER, J., COLLU, M. & KOLIOS, A. 2013. Application and extension of the TOPSIS method for the assessment of floating offshore wind turbine support structures. *Ships and Offshore Structures,* 8**,** 477-487.

MAS CONSULTANT OFFICE 2005. Geological Report for Dikheila Port in Alexandria, Egypt.

MATLOCK, H. & REESE, L. C. 1960. Generalized solutions for laterally loaded piles. *Journal of the Soil Mechanics and foundations Division,* 86**,** 63-94.

MATLOCK, H. & REESE, L. C. Foundation analysis of offshore pile supported structures. Proc. Of 5th Int. Conf. On Soil Mechanics and Foundation Engineering, Paris, 1961. 91-97.

MAYHOUB, A. & AZZAM, A. 1997. A survey on the assessment of wind energy potential in Egypt. *Renewable Energy,* 11**,** 235-247.

MINISTER OF STATE FOR ENVIRONMENTAL AFFAIRS 2016. The annual report of the Ministry of Environment.

MINISTRY OF DEFENCE AND MILITARY PRODUCTION. 2015. *The offical website* [Online]. Available: http://www.mod.gov.eg/ [Accessed /30 2016/06].

MINISTRY OF PETROLEUM AND MINERAL RESOURCES. 2015. *Mining Laws in Egypt* [Online]. Available: http://www.petroleum.gov.eg/en/pages/default.aspx [Accessed /15 2016/06].

MONDAL, M. A. H., HAWILA, D., KENNEDY, S. & MEZHER, T. 2016. The GCC countries RE-readiness: Strengths and gaps for development of renewable energy technologies. *Renewable and Sustainable Energy Reviews,* 54**,** 1114-1128.

MORATÓ, A., SRIRAMULA, S., KRISHNAN, N. & NICHOLS, J. 2017. Ultimate loads and response analysis of a monopile supported offshore wind turbine using fully coupled simulation. *Renewable Energy,* 101**,** 126-143.

MORTENSEN, N. G., HANSEN, J. C., BADGER, J., JØRGENSEN, B. H., HASAGER, C. B., PAULSEN, U. S., HANSEN, O. F., ENEVOLDSEN, K., YOUSSEF, L. G. & SAID, U. S. Wind atlas for Egypt: measurements, micro-and mesoscale modelling. Proceedings of the 2006 European Wind Energy Conference and Exhibition, Athens, Greece, February, 2006a.

MORTENSEN, N. G., SAID, U. S. & BADGER, J. 2006b. *Wind Atlas of Egypt*, RISO National Laboratory, New and Renewable Energy Authority, Egyptian Meteorological Authority.

MOSTAFAEIPOUR, A. 2010. Feasibility study of offshore wind turbine installation in Iran compared with the world. *Renewable and Sustainable Energy Reviews,* 14**,** 1722-1743.

MOSTAFAEIPOUR, A. & MOSTAFAEIPOUR, N. 2009. Renewable energy issues and electricity production in Middle East compared with Iran. *Renewable and Sustainable Energy Reviews,* 13**,** 1641-1645.

MTS. 2018. *Commercial Ports in Egypt: Specifications and Maritime Characteristics* [Online]. Available: http://www.emdb.gov.eg [Accessed].

MUNAWWAR, S. & GHEDIRA, H. 2014. A review of renewable energy and solar industry growth in the GCC region. *Energy Procedia,* 57**,** 3191-3202.

NASR, P. & SMITH, E. 2006. Simulation of oil spills near environmentally sensitive areas in Egyptian coastal waters. *Water and Environment Journal,* 20**,** 11-18.

NATIONAL AUTHORITY FOR TUNNELS (NAT). 2015. *The home page in English* [Online]. Available: http://www.nat.org.eg/english/index.html [Accessed /26 2016/06].

NEHLS, G., BETKE, K., ECKELMANN, S. & ROS, M. 2007. Assessment and costs of potential engineering solutions for the mitigation of the impacts of underwater noise arising

from the construction of offshore windfarms. *BioConsult SH report, Husum, Germany. On behalf of COWRIE Ltd*.

NEMATOLLAHI, O., HOGHOOGHI, H., RASTI, M. & SEDAGHAT, A. 2016. Energy demands and renewable energy resources in the Middle East. *Renewable and Sustainable Energy Reviews,* 54**,** 1172-1181.

NEW AND RENEWABLE ENERGY AUTHORITY 2019. Study No. (IMC / PS).

NIELSEN, P. 2003. Offshore wind energy projects, feasibility study guidelines. *SEAWIND-Altener project-Feasibility Study Guidelines (EMD)*.

NTOKA, C. 2013. *Offshore wind park sitting and micro-sitting in Petalioi Gulf, Greece.* Master in science, Aalborg University, Denmark.

OH, K.-Y., NAM, W., RYU, M. S., KIM, J.-Y. & EPUREANU, B. I. 2018. A review of foundations of offshore wind energy convertors: Current status and future perspectives. *Renewable and Sustainable Energy Reviews,* 88**,** 16-36.

ORASCOM CONSTRUCTION LIMITED 2012. Geological Report for El-Gouna Bay, Egypt.

PARK, J. & LAW, K. H. 2015. Layout optimization for maximizing wind farm power production using sequential convex programming. *Applied Energy,* 151**,** 320-334.

PEIRE, K., NONNEMAN, H. & BOSSCHEM, E. 2009. Gravity base foundations for the thornton bank offshore wind farm. *Terra et Aqua,* 115**,** 19-29.

PÉREZ-ARJONAA, I., ESPINOSAA, V., PUIGA, V., ORDÓÑEZA, P., SOLIVERESA, E., POVEDAB, P., RAMISB, J., DE LA GÁNDARAC, F. & CORTD, J. L. 2014. Effects of offshore wind farms operational noise on bluefin tuna behaviour.

PETERSEN, T. U. 2014. *Scour around offshore wind turbine foundations.* Technical University of Denmark. Department of Mechanical Engineering.

PETERSEN, T. U., SUMER, B. M., FREDSØE, J., RAAIJMAKERS, T. C. & SCHOUTEN, J.-J. 2015. Edge scour at scour protections around piles in the marine environment—Laboratory and field investigation. *Coastal Engineering,* 106**,** 42-72.

REDCON CONSTRUCTION 2007. Geological Report for Nabq Bay, Egypt.

REESE, L. C., COX, W. R. & KOOP, F. D. 1974. Analysis of laterally loaded piles in sand. *Offshore Technology in Civil Engineering Hall of Fame Papers from the Early Years***,** 95-105.

REHMAN, S. 2005. Offshore wind power assessment on the east coast of Saudi Arabia. *Wind Engineering,* 29**,** 409-419.

ROBERTS, H. H. & MURRAY, S. P. 1988. Gulfs of the Northern Red Sea: Depositional settings of abrupt siliciclastic-carbonate transitions. *Developments in sedimentology.* Elsevier.

RODMAN, L. C. & MEENTEMEYER, R. K. 2006. A geographic analysis of wind turbine placement in Northern California. *Energy Policy,* 34**,** 2137-2149.

SAATY, T. L. 1977. A scaling method for priorities in hierarchical structures. *Journal of mathematical psychology,* 15**,** 234-281.

SAATY, T. L. 2008. Decision making with the analytic hierarchy process. *International journal of services sciences,* 1**,** 83-98.

SALEOUS, N., ISSA, S. & AL MAZROUEI, J. 2016. GIS-BASED WIND FARM SITE SELECTION MODEL OFFSHORE ABU DHABI EMIRATE, UAE. *International Archives of the Photogrammetry, Remote Sensing & Spatial Information Sciences,* 41.

SCHALLENBERG-RODRÍGUEZ, J. & MONTESDEOCA, N. G. 2018. Spatial planning to estimate the offshore wind energy potential in coastal regions and islands. Practical case: The Canary Islands. *Energy,* 143**,** 91-103.

SCHILLINGS, C., WANDERER, T., CAMERON, L., VAN DER WAL, J. T., JACQUEMIN, J. & VEUM, K. 2012. A decision support system for assessing offshore wind energy potential in the North Sea. *Energy Policy,* 49**,** 541-551.

SEED, H. B. & DE ALBA, P. Use of SPT and CPT tests for evaluating the liquefaction resistance of sands. Use of in situ tests in geotechnical engineering, 1986. ASCE, 281-302.

SHATA, A. 2010. Wind energy as a potential generation source at Ras Benas, Egypt. *Renewable and Sustainable Energy Reviews,* 14**,** 2167-2173.

SHATA, A. 2011a. Analysis of electrical power form the wind farm sitting on the Nile River of Aswan, Egypt. *Renewable and Sustainable Energy Reviews,* 15**,** 1637-1645.

SHATA, A. 2011b. Investigation of wind characteristics and wind energy potential at Ras Ghareb, Egypt. *Renewable and Sustainable Energy Reviews,* 15**,** 2750-2755.

SHATA, A. 2012a. Electricity generation from the first wind farm situated at Ras Ghareb, Egypt. *Renewable and Sustainable Energy Reviews,* 16**,** 1630-1635.

SHATA, A. 2012b. Potential wind power generation in South Egypt. *Renewable and Sustainable Energy Reviews,* 16**,** 1528-1536.

SHATA, A. & HANITSCH, R. 2006a. Evaluation of wind energy potential and electricity generation on the coast of Mediterranean Sea in Egypt. *Renewable Energy,* 31**,** 1183-1202.

SHATA, A. & HANITSCH, R. 2006b. The potential of electricity generation on the east coast of Red Sea in Egypt. *Renewable Energy,* 31**,** 1597-1615.

SHATA, A. & HANITSCH, R. 2008. Electricity generation and wind potential assessment at Hurghada, Egypt. *Renewable Energy,* 33**,** 141-148.

SHAWON, M., EL CHAAR, L. & LAMONT, L. 2013. Overview of wind energy and its cost in the Middle East. *Sustainable Energy Technologies and Assessments,* 2**,** 1-11.

SHEREET, S. 2009. Pollution of petroleum hydrocarbon in the New Damietta Harbor, Egypt. *Emirates J. Engineering Research,* 14**,** 65-71.

SHERIDAN, B., BAKER, S. D., PEARRE, N. S., FIRESTONE, J. & KEMPTON, W. 2012. Calculating the offshore wind power resource: Robust assessment methods applied to the US Atlantic Coast. *Renewable Energy,* 43**,** 224-233.

SIDDIQUI, M. Z., EVERETT, J. W. & VIEUX, B. E. 1996. Landfill siting using geographic information systems: a demonstration. *Journal of environmental engineering,* 122**,** 515-523.

SIMON VIRLEY CB 2017. CfD allocation round two.

SIYAL, S. H., MÖRTBERG, U., MENTIS, D., WELSCH, M., BABELON, I. & HOWELLS, M. 2015. Wind energy assessment considering geographic and environmental restrictions in Sweden: A GIS-based approach. *Energy,* 83**,** 447-461.

SØRENSEN, S. P. H. & IBSEN, L. B. 2013. Assessment of foundation design for offshore monopiles unprotected against scour. *Ocean Engineering,* 63**,** 17-25.

SOVACOOL, B. K., LINDBOE, H. H. & ODGAARD, O. 2008. Is the Danish wind energy model replicable for other countries? *The Electricity Journal,* 21**,** 27-38.

STATACORP, L. 2007. Stata data analysis and statistical Software. *Special Edition Release,* 10**,** 733.

STEHLY, T., HEIMILLER, D. & SCOTT, G. 2016. Cost of Wind Energy Review. *National Renewable Energy Laboratory*.

STEVIĆ, Ž., VESKOVIĆ, S., VASILJEVIĆ, M. & TEPIĆ, G. 2015. The selection of the logistics center location using AHP method. *University of Belgrade, Faculty of Transport and Traffic Engineering, LOGIC, Belgrade***,** 86-91.

SWA. 2017. *Protected areas map* [Online]. Available: https://www.swa.gov.sa/en/protected-areas/protected-areas-map [Accessed 09/08/2017].

TELEGEOGRAPHY COMPANY. 2015. *Submarine Cable Map* [Online]. Available: http://www.submarinecablemap.com/ [Accessed /29 2016/06].

THE BRITISH OCEANOGRAPHIC DATA CENTRE. 2014. *The GEBCO_2014 Grid* [Online]. Available: www.gebco.net [Accessed /25 2016/03].

THE CROWN ESTATE 2012a. Offshore wind cost reduction: Pathways study. *United Kingdom, May*.

THE CROWN ESTATE 2012b. Round 3 Offshore Wind Site Selection at National and Project Levels.

THE CROWN ESTATE 2014. Offshore wind operational report.

THE CROWN ESTATE 2017. Offshore wind operational report January – December 2016.

THE CROWN ESTATE. 2019. *Offshore Wind shapefiles*. United Kingdom.

THE EGYPTIAN ENVIRONMENTAL AFFAIRS AGENCY. 2015. *Protectorates: Natural Protectorates and Biological Diversity* [Online]. Available: http://www.eeaa.gov.eg/English/main/about.asp [Accessed /05 2016/04].

THE EGYPTIAN NATURAL GAS HOLDING COMPANY (EGAS). 2015. *Map of the gas and oil wells in Egypt* [Online]. Available: http://www.egas.com.eg/ [Accessed /17 2016/04].

THE MARINETRAFFIC. 2015. *Ship Density Maps* [Online]. Available: https://www.marinetraffic.com/ [Accessed /07 2016/04].

THE MINISTRY OF ELECTRICITY AND ENERGY OF EGYPT. 2011. Annual Report (2010/2011) of the Egyptian Electricity Holding Company. Available: http://www.nrea.gov.eg/annual2012-2013.pdf.

THE MINISTRY OF ELECTRICITY AND ENERGY OF EGYPT. 2013. Annual Report of the Authority of the New and Renewable Energy in Arabic. Available: http://www.nrea.gov.eg/annual2012-2013.pdf.

THE MINISTRY OF ELECTRICITY AND ENERGY OF EGYPT. 2016. *Egyptian Unified Power Network* [Online]. Available: http://www.moee.gov.eg/english_new/ [Accessed /27 2016/03].

THE MINISTRY OF ELECTRICITY AND ENERGY OF EGYPT. 2017. Annual Report (2016/2017) of the Egyptian Electricity Holding Company. Available: http://www.nrea.gov.eg/annual2012-2013.pdf.

TOMAZOS, K. 2017. Egypt's tourism industry and the Arab Spring.

UGBOMA, C., UGBOMA, O. & OGWUDE, I. C. 2006. An analytic hierarchy process (AHP) approach to port selection decisions–empirical evidence from Nigerian ports. *Maritime Economics & Logistics,* 8**,** 251-266.

UKPABI, D., OLALEYE, S., MOGAJI, E. & KARJALUOTO, H. 2018. Insights into online reviews of hotel service attributes: A cross-national study of selected countries in Africa. *Information and Communication Technologies in Tourism 2018.* Springer.

UNFCCC, V. 2015. Adoption of the Paris Agreement. *I: Proposal by the President (Draft Decision), United Nations Office, Geneva (Switzerland)*.

VAN WIJNGAARDEN, M. 2013. Concept design of steel bottom founded support structures for offshore wind turbines.

VERITAS, D.-D. N. 2010. DNV-OS-J101 offshore standard. *Design of offshore wind turbine structures*.

WAEWSAK, J., LANDRY, M. & GAGNON, Y. 2015. Offshore wind power potential of the Gulf of Thailand. *Renewable Energy,* 81**,** 609-626.

WALLACE, J. M. & HOBBS, P. V. 2006. *Atmospheric science: an introductory survey*, Academic press.

WANG, J.-J., JING, Y.-Y., ZHANG, C.-F. & ZHAO, J.-H. 2009. Review on multi-criteria decision analysis aid in sustainable energy decision-making. *Renewable and Sustainable Energy Reviews,* 13**,** 2263-2278.

WATSON, J. J. & HUDSON, M. D. 2015. Regional Scale wind farm and solar farm suitability assessment using GIS-assisted multi-criteria evaluation. *Landscape and Urban Planning,* 138**,** 20-31.

WEBER, R. O. 1999. Remarks on the definition and estimation of friction velocity. *Boundary-Layer Meteorology,* 93**,** 197-209.

WINDEUROPE 2018. Offshore Wind in Europe: key trends and statistics 2017.

WINDEUROPE 2019. Offshore Wind in Europe: key trends and statistics 2018.

WINDPRO, W. I. 2015. WindPRO/Energy.

WOODMAN, B. & FITCH-ROY, O. 2019. Auctions for the support of renewable energy in the UK: updated results and lessons learnt.

WORLD BANK 2018. *World development indicators*, World Bank.

YIP, C. M. A., GUNTURU, U. B. & STENCHIKOV, G. L. 2016. Wind resource characterization in the Arabian Peninsula. *Applied energy,* 164**,** 826-836.

YIP, C. M. A., GUNTURU, U. B. & STENCHIKOV, G. L. 2017. High-altitude wind resources in the Middle East. *Scientific reports,* 7**,** 9885.

YOON, K. P. & HWANG, C.-L. 1995. *Multiple attribute decision making: an introduction*, Sage Publications.

ZALLA, T. & FAWZY, M. A. 2000. *Availability and quality of agricultural data for the new lands in Egypt*, USAID.

ZAVADSKAS, E. K., TURSKIS, Z. & BAGOČIUS, V. 2015. Multi-criteria selection of a deep-water port in the Eastern Baltic Sea. *Applied Soft Computing,* 26**,** 180-192.

ZHU, B., WEN, K., KONG, D., ZHU, Z. & WANG, L. 2018. A numerical study on the lateral loading behaviour of offshore tetrapod piled jacket foundations in clay. *Applied Ocean Research,* 75**,** 165-177.

ZUR MINDERUNG, E. V. H. H. 2016. Offshore Test of Hydro Sound Dampers at'London Array'.